Durham E-Theses

Processing and modelling of seismic reflection data acquired off the Durham coast

Francis Jifon

How to cite:

Use policy

PROCESSING AND MODELLING OF SEISMIC REFLECTION DATA
ACQUIRED OFF THE DURHAM COAST.

by

Francis Jifon

A thesis submitted for the degree of
Doctor of Philosophy in the University of Durham.

Graduate Society   January 1985

ABSTRACT

Off the Durham coast, the Permian succession above the Coal Measures contains limestones and anhydrite bands with high seismic velocities and reflection coefficients. The consequent reduction in penetration of seismic energy makes it difficult to determine Coal Measures structure by the seismic reflection method. Seismic data sets acquired from this region by the National Coal Board in 1979 and 1982 are used to illustrate that satisfactory results are difficult to achieve. Synthetic seismograms, generated for a simplified geological section of the region, are also used to study various aspects of the overall problem of applying the seismic technique in the area.

Standard and non-standard processing sequences are applied to the seismic data to enhance the quality of the stacked sections and the results are discussed. This processing showed that in the 1979 survey, in which a watergun source and a 600m streamer were used, some penetration was achieved but Coal Measures resolution on the final sections is poor. The 1982 data set, shot along a segment of the 1979 line using a sleeve exploder source and a 150m streamer, showed no Coal Measures after processing.

Synthetic seismograms, generated using the reflectivity method and a broadband source wavelet, are processed to confirm that a streamer with a length of 360 to 400m towed at a depth of 5-7.5m will be optimal for future data acquisition in the area. It is also shown that the erosion of the surface of the limestone lowers the horizontal resolution of the Coal Measures. Scattering

from erosional features will be greater for high frequencies, so it will be necessary to use a broadband source which generates significant energy below 50 Hz. However, even when acquisition and processing methods are optimised, seismic reflection data from this area will still be difficult to interpret for Coal Measures structure.

CONTENTS.

ABSTRACT.

ACKNOWLEDGMENTS.

ACKNOWLEDGMENTS

use on this machine and I am grateful to him for his help. The aid offered to me by the staffs of the University's Science Library, the University's Computer Unit and the technicians of the Department of Geophysics is gladly acknowledged. Advice from Dr. Charles Ofoegbu is also greatly appreciated.

My parents, brothers and sisters and Mary Y. Njowir missed me as much as I missed them while I was away. I am very grateful to them for their patience and their fervent prayers on my behalf.

C H A P T E R 1

INTRODUCTION

1.1   Scope of Study.

The costs of coal mining can be extremely sensitive to the geological structure of the coal bearing strata. In addition to drilling boreholes and logging them, seismic reflection surveying is now used as a standard technique to determine the nature and location of major structural features in the U.K. coalfields.

Up to 80% of the coal produced in the U.K. is mined by the method of longwall mining which has been described by Ziolkowski (1979). This method permits a much higher percentage of extraction of coal at depths which are uneconomic to mine by the bord and pillar methods. It has no disadvantage so long as the coal seam is continuous in the direction of advance of the coalface. Sometimes the seam's continuity is broken either by faulting, buried sandstone channels, seam splitting or geological washouts. When this happens, all the coalface machinery (which can weigh over 1000 tonnes and cost over 2 million pounds) is stuck in a narrow underground tunnel where it cannot be easily manoeuvred and where it can no longer pay for itself by mining coal. Without adequate spare capacity, which in itself is expensive to ensure, this situation can and frequently does cause a significant loss of production.
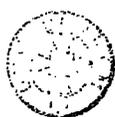
In areas where modern deep underground coal mining can be carried out, it is necessary to confirm the existence of convenient areas of undisturbed coal for continuity of production. The means of ensuring this is by identifying areas with a low intensity of structural disturbance. Two complementary methods are available for this purpose; drilling boreholes and seismic reflection surveying. Both are applicable on land and offshore.

Since it is very expensive to drill boreholes offshore (each borehole costs hundreds of thousands of pounds), a more economic approach to the exploration problem of identifying continuous undisturbed Coal Measures is to do a seismic reflection survey tied in to just a few boreholes, which are essential to determine seam development and stratigraphy. The seismic reflection method has been primarily developed for the exploration of oil and gas. It has to be scaled down if it is to be successfully used in the mapping of Coal Measures which are generally at shallower depths (less than 1.5 km) than the oil and gas targets. The maximum source-receiver distance which can be used in seismic reflection surveying is approximately equal to the target depth (Ziolkowski, 1979). This means that the field recording geometry must be appropriately reduced. Particular care must be taken in the acquisition and processing of the data because of the need to resolve very small scale structures (e.g. faults of only a few meters throw). The elimination of multiple reflections in marine data, and also the removal of ground roll and correct application of static corrections to land data, are crucial. The seismic

reflection technique has been successfully applied for coal exploration.

Mining activity in Durham coalfields currently extends about six miles out from the coast under the North Sea. Seismic reflection surveying was carried out in this region for the purpose of delineating Coal Measures structures and led to the acquisition of data for the National Coal Board (N.C.B.) in 1979 and 1982 respectively. One line of each data set together with some borehole data were used in this project.

The geology of this area presents some problems for the acquisition, processing, and interpretation of seismic reflection data for the purposes outlined above. They are discussed in detail later on in this chapter.

Clarke et al. (1961) published the results of a marine seismic survey of the offshore coalfields of Northumberland, Cumberland and Durham, and concluded that those over the greater part of the offshore coalfields of Durham are disappointing due to the 'masking' effect of the fissured Permian Magnesian Limestone. Ruter and Schepers (1978) and Hughes and Kennett (1982) have studied the seismic response of coal seams embedded in relatively higher velocity country rock both for normal incidence and finite offset situations respectively. In the present study, the effect of the post-Carboniferous layers on the delineation of Coal Measures in the region off the coast of Durham has been considered by using deterministic methods and synthetic seismograms (chapter 3). Samples of the real seismic reflection data acquired from this region have been processed by using both

standard and non-standard methods (chapter 4). A forward modelling procedure has been carried out in order to test propositions of acquisition parameters that may lead to a better delineation of the Coal Measures through standard processing (chapter 5).

In section 1.2, the data sets that were used are presented. In section 1.3, a summary of the geology of the Permian and post-Permian strata of the Wearmouth region is given. The 1979 and 1982 surveys for the N.C.B. were carried out in this area.

In chapter 2, a review of the problems of seismic noise in general and multiple reflections in particular is presented. Some of the processing techniques that have been used in the total or partial suppression of these multiples are discussed and those that have been applied in this project are reviewed both theoretically and illustratively.

1.2 Seismic Reflection Data Sets acquired off the Coast of Durham.

Figure 1.0 shows a map of the area off the coast of Durham and the region over which seismic reflection data were acquired is indicated. The map only displays the area of interest in this work. The entire area over which the surveys were carried out extends both southwards and eastwards.

4

Figure 1.0 . A map of the region off the coast of Durham.
The hatched offshore area shows the region over
which seismic reflection data were acquired in
1979.
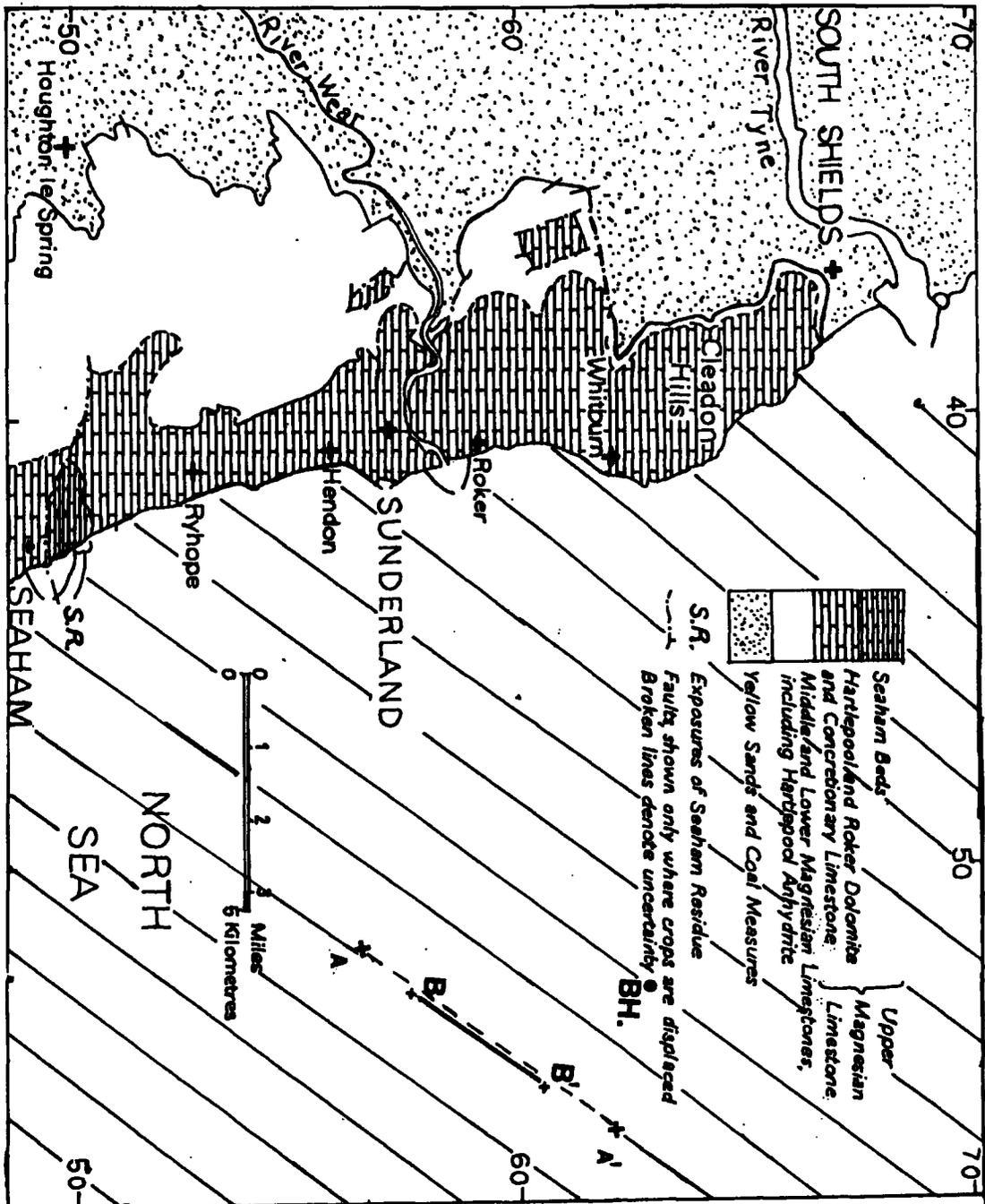
(a) The 1979 Data Set

The data were acquired for the N.C.B. by Horizon Exploration Limited. They used a 24-channel streamer with a hydrophone group length of 25 m thus giving a 600 m long streamer. Each hydrophone group had 16 elements. The distance between each shot and the first hydrophone group (near-trace offset) was 45 m. A shot separation of 12.5 m was maintained thus giving 24-fold common mid-point (CMP) coverage.

The source type used was the SODERA MICAT water gun (SODERA = Societé pour le developpement de la reserche appliquée) and an array of eight 80 cu. inch guns was used per shot. The source depth was 5m .

The data used in this study were acquired along the line that has been marked as AA' on Figure 1.0. The data were transmitted to Durham as trace sequential 24-fold CMP gathers on magnetic tape in Standard SEG'Y' format. The line extends from CMP 26 to CMP 535, a total subsurface distance of about 6 km . Each trace has a length of 1.5 sec and is sampled at 1 msec intervals. The recording filter settings were 27 Hz and 248 Hz for the low-cut and high-cut frequencies respectively.

5

(b) The 1982 Data set

After the 1979 data were processed by the N.C.B., the results showed Coal Measures but the sections were not satisfactory from the point of view of interpretation. It was deemed worthwhile to have another test survey carried out in the region, this time with some control from the results of the 1979 survey. In 1982, a set of lines of seismic reflection data were acquired from this region but a different source and a shorter streamer were used.

The data were acquired by FAIRFIELD AQUATRONICS LIMITED. The cable had 24-channels and a hydrophone group length of 6.25m, thus giving a streamer of about 150 m long. There were 8 elements per group of hydrophones and the near-trace offset was 10 m. The shot separation was maintained at 12.5 m so that a 6-fold CMP coverage was obtained.

The source was the Fairflex sleeve exploder. It was expected to inject more power at high frequencies into the earth than the water guns that were used in 1979. The source depth was 0.76m .

The 1982 data were collected along the line BB' that has been marked on Figure 1.0 . The data were transmitted to Durham as trace sequential 6-fold CMP gathers on magnetic tape in Standard SEG'Y' format. The line extends from CMP 26 to CMP 852. Each trace has a length of 2.0 sec and is sampled at 1 msec intervals. The recording filter settings were the same as those of 1979.

These two data sets have been used for testing various

algorithms and have been processed by both standard and non-standard methods. The results are not a dramatic improvement to those that were obtained by the N.C.B. . A forward modelling approach was used in order to support a suggestion that was made for alternative parameters for the future acquisition and processing of seismic reflection data from this region for the purpose of yielding a subsurface areal image of the Coal Measures structure.

1.3 Permian Geology of the area off the Coast of Durham.

In this section, a summary is given of the post-Carboniferous geology of the region. The facts have been collated from papers by Smith and Francis (1967), Smith (1970), Magraw et al. (1963), Magraw (1975) and Magraw (1978) which were published on borehole data acquired both offshore and onshore. The post-Carboniferous succession is predominantly of Permian age. The Permian beds are overlain by a thin layering of Quaternary sediments. There are no horizons of Mesozoic or Tertiary age in this area.

For the region off the coast of north-east Durham, we follow the sub-division of the Permian strata from Magraw (1978), which is based on data that were acquired up to 1976 and predominantly between 1974 and 1976. The classification is given on Table 1.1. Figure 1.1 (adapted from Smith, 1971) shows the study area. It lies off the coast of Durham extending southwards and eastwards from the Wearmouth area to the area offshore Seaham. The data

TABLE 1.1.

The Stratigraphy of the Permian strata of the Durham offshore area. (following Magraw, 1978)

AGE	FORMATION AND DETAILS	APPROXIMATE THICKNESS IN M
UPPER **PERMIAN**	**UPPER PERMIAN MARLS** ******************* Red-brown marl, Dolomitic limestone, marl with gypsum. Sandy marl and sandstone.	5-90
	UPPER MAGNESIAN LIMESTONE ************************** UPPER NODULAR BEDS (Magraw 1975,fig.1) (?) Limestone, grey to grey-brown,crystall-ine with irregular nodules;originally thinly bedded. Calcite-lined cavities with radial recrystallisation.	15-20
	HARTLEPOOL AND ROKER DOLOMITE (Smith in Magraw et al. 1963; Magraw 1975. fig 1) Dolomitic limestone generally cream- coloured; often soft and powdery; ooli-tic or pisolitic beds present. Some beds of Dolomite 'sand'.	61-67
	CONCRETIONARY LIMESTONE (Magraw,1975 fig. 1) . Limestone, grey to dark grey-brown, generally thinly-bedded to laminated. Black bituminous partings with charact-eristic smell when struck. Recrystalli-sed in several forms- Radial (cannon-ball) and pencil-like or honey-comb segregation structures (See PLATE 4, fig. 1, Magraw 1978).	55-61
	FLEXIBLE LIMESTONE (Magraw 1978) (?) Limestone grey to dark-grey, thinly bedded with black silty argillaceous partings.	2
	MIDDLE MAGNESIAN LIMESTONE **************************** HARTLEPOOL ANHYDRITE (SEAWARD) NORTH MARSDEN BAY LIMESTONE (SHOREWARD) VELVET BEDS LIMESTONES AND BRECCIAS (Magr-aw, 1975) ALGAL BED Limestone, irregularly laminated with small nodules.	0-122 0-72 0.15
	LOWER MAGNESIAN LIMESTONE ************************** Limestone generally regularly bedded, variable in colour and lithology with the tendency for beds of grey and grey-brown mottled limestone sometimes indicating incipient concretions in upper part; Some beds with gypsum.	18-32
	PASSAGE BEDS ************* Alternations of grey limestone and calci-tic or dolomitic siltstone becoming less conspicuous from north to south.	THIN
	MARL SLATE ********** Siltstone ,dark-grey ,laminated ,flecked. Calcitic or dolomitic.	THIN OR ABSENT
LOWER **PERMIAN**	**BASAL PERMIAN (YELLOW) SANDS AND BRECCIAS** *** Sandstone, blue-grey or brown, bi-modal with beds of poorly cemented 'millet seed' grains; Breccias in certain areas. Brown mudstone intercalation in some cases. (Magraw , 1978) U N C O N F O R M I T Y Coal Measures.	0-69

Figure 1.1 . A map of the region off the coast of Durham showing
the lines AA' (1979) and BB' (1982).
The position BH. of the borehole (drilled in 1983)
is marked.
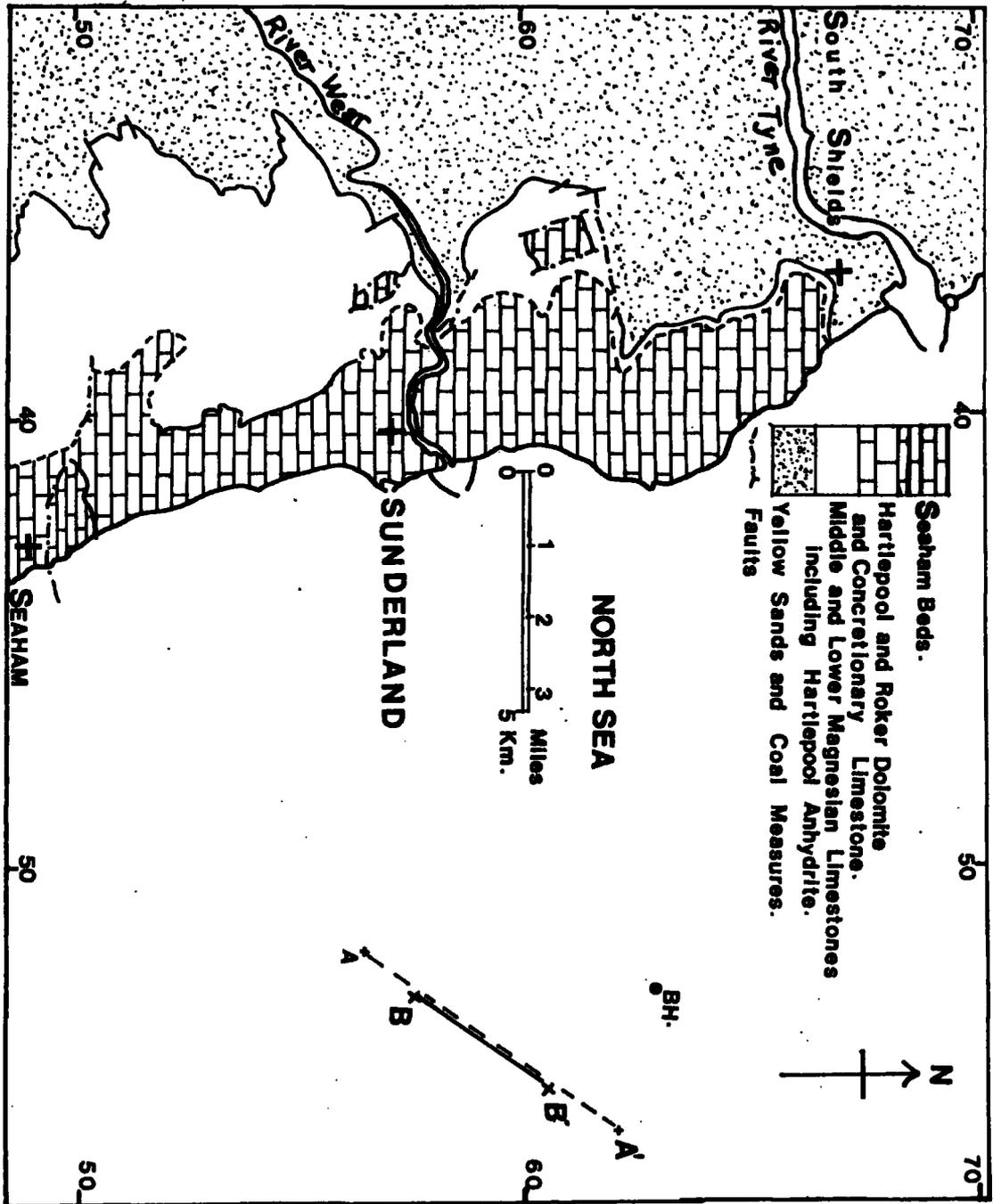
that were used in this project were acquired along the line AA'
and we had lithological information from a recent borehole that
was drilled for the N.C.B. at the position marked BH. (Figure
1.1). The lithological data derived from this borehole are summa-
rized on Figure 1.2. It was not possible to separate the Magne-
sian Limestones into its three broad classes as indicated on
Table 1.1 because of the limited amount of information available.
The blank interval at a depth of about 200 m within the Magnesian
Limestone (Figure 1.2) represents a column in which it is not
certain - because of poor recovery - whether or not there are
anhydrite bands present. An approximate correspondence can be
observed between Table 1.1 and Figure 1.2 .

The Permian deposits unconformably overlie the Coal Measures
at a depth of about 340 m below the seabed. They can be broadly
classed as the Lower Permian strata which comprise the Yellow
Sands and breccias, and are sharply succeeded by the Upper
Permian beds which are made up of six different types of strata
namely the Marl Slate, the Passage Beds (Magraw, 1978), the
Lower, Middle, and Upper Magnesian Limestones and the Upper
Permian Marls respectively. The Permian deposits are overlain by
the Quaternary beds of mainly Boulder Clay.

LOWER PERMIAN DEPOSITS

Yellow Sands and breccias

Evidence from boreholes and shafts in the north of Durham
(Magraw, 1975) indicates that the Coal Measures were eroded from

8

0   **55·3 m**
          (sea bed)

Boulder Clay·

0

Quaternary

50m

Upper Permian
Marls·

100

Upper

Magnesian

Wearmouth OB

Limestones·

No. WM 7A. (1983)

200

Permian

Marl Slate·

300

Yellow Sands·

Base of Permian
at 338·0 m

Lower Permian

Coal Measures·

Carboniferous

400

500

BASE OF HOLE 506·79m
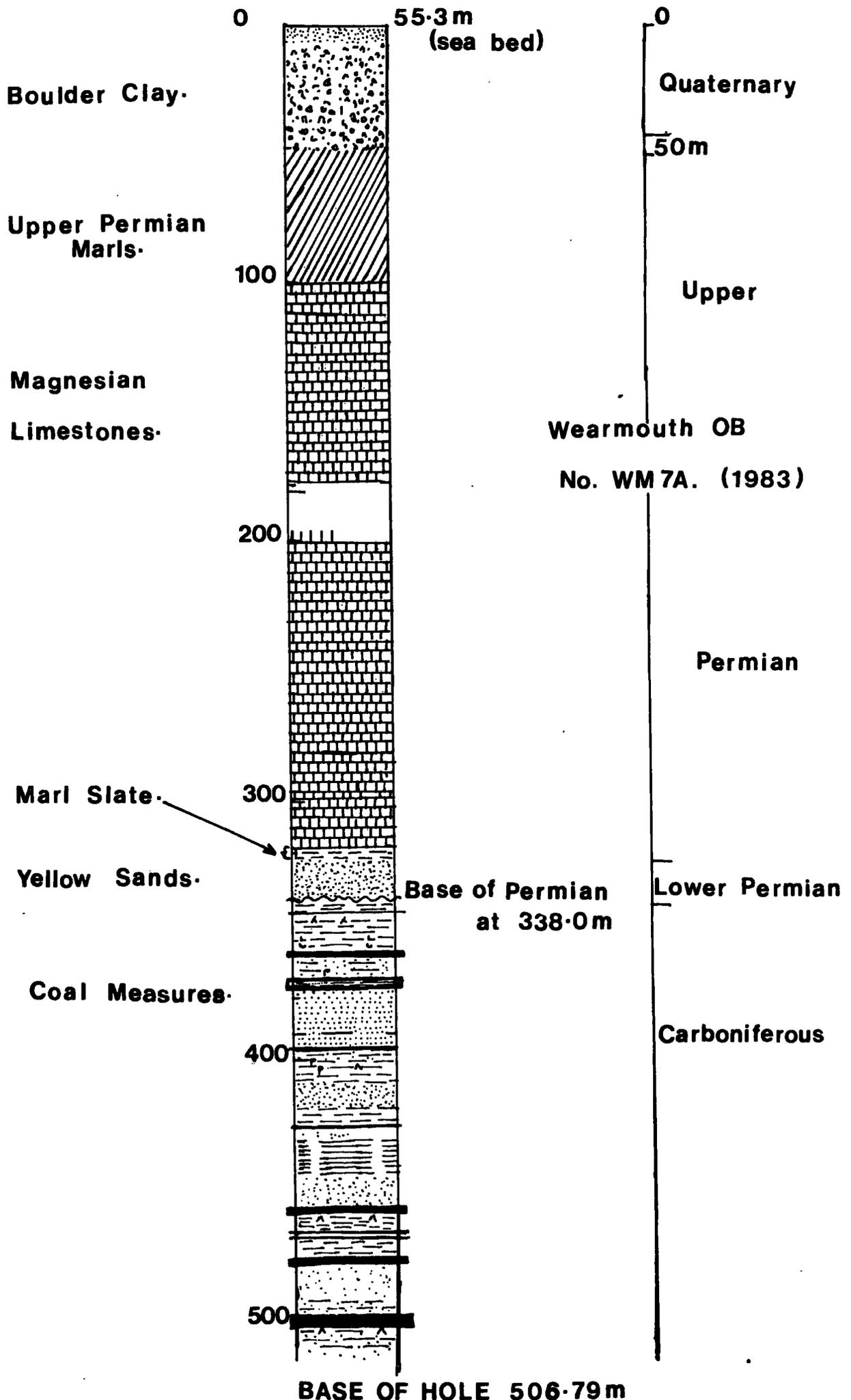
Figure 1.2 . A summary of the lithology off the borehole BH.
drilled in 1983.

parts of North Durham following Hercynian uplift and prior to the deposition of the basal Permian (Yellow) Sands. This late Carboniferous and early Lower Permian erosion reduced large areas of north-east Durham to a broad rolling peneplain sloping gently to the east (Smith, 1970). The first layer to be laid on this land surface was the Yellow Sands which are of early Lower Permian age. Mainly aeolian sand deposits are present in this succession. The series of bedded sands together with breccias of variable thicknesses separate marine Permian strata from the plain of the unconformity. The Yellow Sands range in thickness from 0 to 69 m . The formation has been studied and described by Smith and Francis (1967), Smith (1970) (following Hodge, 1932 and Davies and Rees, 1944) and also by Magraw (1975). The breccias largely consist of limestone, sandstone, siltstone and mudstone fragments. They are of variable but generally small thickness.

UPPER PERMIAN DEPOSITS

We can consider the Upper Permian deposits as made up of three primarily distinct formations which are shown on Figure 1.2 and consist of Marl Slate and Passage Beds, Magnesian Limestones (Lower, Middle, and Upper) and the Upper Permian Marls. The details of the compositions of these layers are given on Table 1.1 .

Marl Slate and Passage Beds.

The Marl Slate formation is a thin argillaceous marine bed. It is not present in the entire region. Where it occurs, its thickness is only up to 6 m (Magraw, 1978). It consists of laminated calcitic or dolomitic siltstone. The Passage Beds are more predominant off the coast of South Northumberland and consist of beds of finely micaceous siltstone or silty sandstone. They are not well developed (Magraw, 1978) in the area of this study.

Magnesian Limestones.

The Marl Slate is mostly overlain by Magnesian Limestones which consist of a thick sequence of carbonates and evaporites formed as a result of cyclic sedimentation. The Magnesian Limestones comprise three major divisions, the oldest of which is the Lower Magnesian Limestone.

Lower Magnesian Limestone.

Two main units of the formation have been identified by Magraw et al. (1963). The lower part is more calcarous and the upper part is predominantly dolomitic and less regularly bedded. There is evidence (Smith, 1970) of limited submarine slumping and sliding within it, confined to a thin group of beds. This evidence supports the views held about the basin floor: namely that it sloped gently either to the east or to the north-east before Permian times. The formation has an average thickness of about 23 m .

Middle Magnesian Limestone.

The Middle Magnesian Limestone comprises Reef Limestones, Hartlepool Anhydrite and equivalent beds (Magraw, 1978). The limestones probably bear some secondary gypsum together with interbedded dolomite in the deeper part of the basin. This was not recovered from the borehole (Figure 1.2) and is thought to be very thin or absent. In general, the anhydrite is thickest in an area which is due south and west of the coast of Hartlepool. The band thins northwards and westwards from this area and incorporates a greater percentage of interbedded dolomite. This northwards thinning probably explains the uncertainty of its presence in the region of Figure 1.1 in general and at the position BH. in particular. Figure 1.3 (from Magraw, 1978) shows the anhydrite band at its area of maximum accumulation and how it thins due north. The Middle Magnesian Limestone has an average thickness of 80 m .

Upper Magnesian Limestone.

The Upper Magnesian Limestone consists of the Flexible Limestone (Woolacott (1912), Trenchman (1925) and Magraw (1975)), Concretionary Limestone, Hartlepool and Roker Dolomites and the Seaham Beds (Smith, 1970) or the Upper Nodular Beds (Magraw, 1978). The Upper Magnesian Limestone has an average thickness of about 140 m . There is evidence on some seismic sections shown in chapter 4 of this thesis, that the upper surface of this formation is not smooth but rough and erosional and some karst
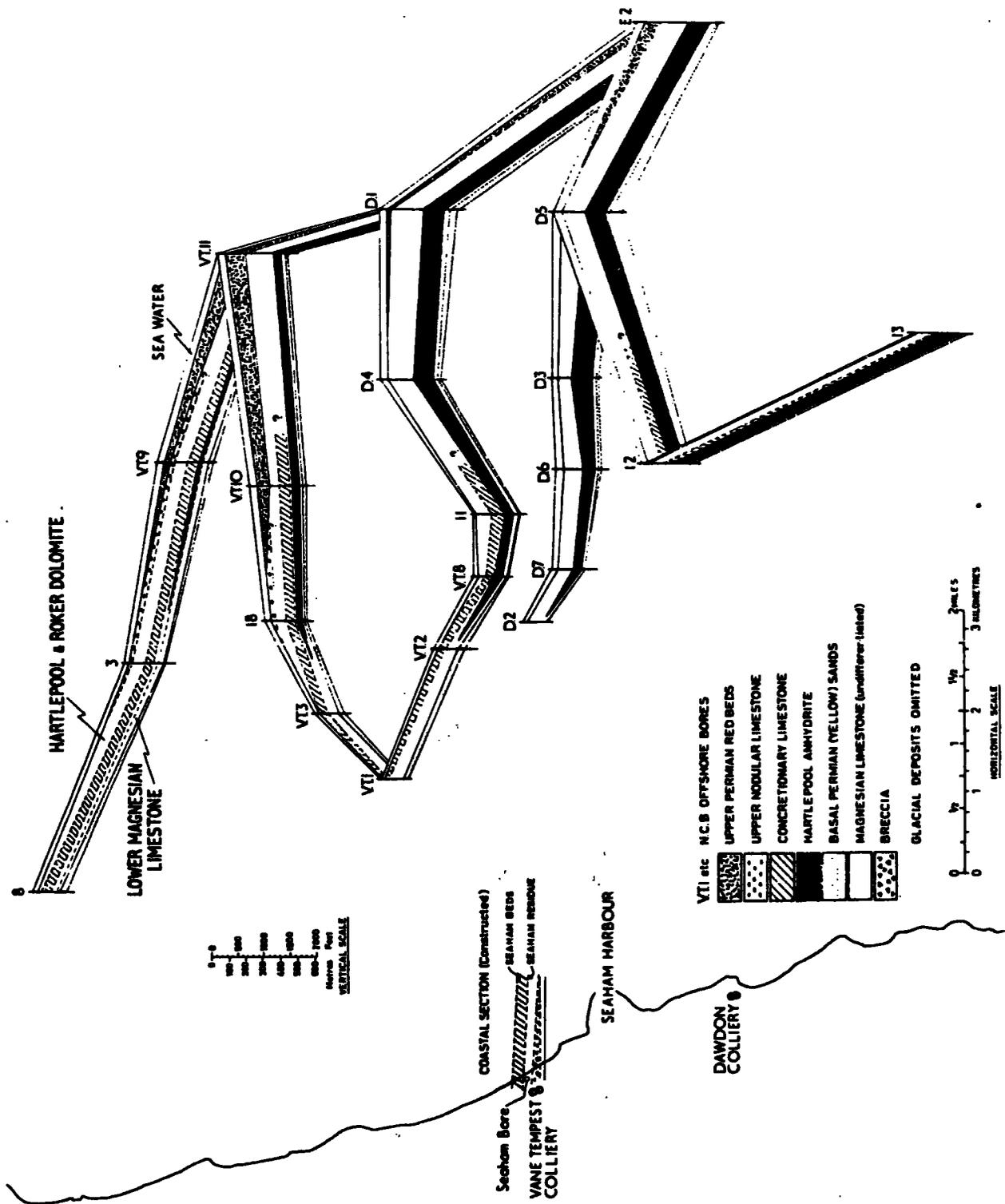
Figure 1.3 . A map showing the northwards thinning of the
Hartlepool Anhydrite. (after Magraw, 1978).
The borehole BH. is about 15 km north-east of
the Seaham bore.

development may have occurred.

Upper Permian Marls.

The Upper Permain Marls consist of mainly red marls or mudstone with subsidiary beds of gypsum and red sandstone. A variation in thickness of these beds and the thickness of the underlying Upper Magnesian Limestone above the top of the Hartlepool Anhydrite suggests that the red beds may be transgressive. Some evidence for this has been found in the presence of badly weathered remnants of apparently bedded red marls in the southern offshore area.

POST-PERMIAN DEPOSITS

Boulder Clay

There are no Mesozoic or Tertiary beds in this area. The Upper Permian Marls are succeeded by a layer of Quaternary sediments mainly Boulder Clay with an average thickness of about 50 m (Figure 1.2). Along the line AA' (Figure 1.1) the depth of the sea water is about 52 m .

1.3.1 Some Problems to be expected during Seismic Reflection Surveying for Coal in this area.

The seismic reflectivity sequence and the problems to be faced during seismic reflection surveying in this area are determined by the geology that is outlined above. (Van Riel, 1965)

Coal has a very low seismic velocity (about 2.2 km/s) and a relatively low density compared to that of other rocks. Geologically, the Coal Measures are a collection of thin coal seams embedded in shales and sandstones which have an average seismic velocity of 3.0 km/s. The Coal Measures are thus characterized in the reflectivity sequence by strong alternately positive and negative reflection coefficients separated by short time intervals. Such a sequence of seams (Ruter and Schepers 1978) acts on the reflected seismic signal as a high-pass filter and on the transmitted seismic signal as a low-pass filter, the cut-off frequencies being determined by the average thickness of the seams. Furthermore, with increasing travel time observed reflections are primarily dominated by short-lag multiples such that the primary reflections comprise an insignificant part of the response.

The Yellow Sands and breccias at the base of the Permian constitute a formation with a seismic velocity of about 3.0 km/s and so the seismic reflection from the unconformity with the Coal Measures is generally expected to be weak. The same is true of the base of the Marl Slate where the acoustic impedance contrast with the Yellow Sands is not significant.

13

The Magnesian Limestones have been considered as a single formation, probably bearing bands of anhydrite in its middle part. The seismic velocities in limestones and evaporites are high (greater than 4.0 km/s and 5.5 km/s respectively) relative to other geological rock types. Their densities are relatively high as well. Besides the strong reflectivities at the top and base of the limestones, the presence of a band or many bands of anhydrite embedded in the Middle Magnesian Limestone would produce another interval of very high coefficients in the reflectivity sequence of this region. These coefficients, together with the seabed reflection coefficient (which is usually strong) and the sea surface, give rise to reverberations of the seismic waves within the layers that are bounded by these interfaces. The reverberations have got unusually high amplitudes such that they overlap and obscure the reflections from the Coal Measures.

In particular, the multiple reflections that arise within the limestone formation and arrive at about the same time as the primary reflections from the Coal Measures have average stacking velocities that are almost equal to those of these primary reflections, and thus possess small differential moveout with the latter. This makes multiple suppression by common mid-point stacking less effective.

Prediction-error deconvolution is much better to rely on for the suppression of these multiples, but in these geological circumstances some of the primaries would tend to be suppressed as well. This is explained by the fact that a few strong primary

events within the Permian and Quaternary, and also within the Carboniferous, contribute more to the autocorrelation function of the seismic trace at non-zero lags than the multiples, which the technique is intended to suppress. In other words, the primary reflection sequence is not white, and not stationary. Special considerations have therefore to be made if the technique is to be effective.

The entire limestone formation is probably fissured (Clarke et al. 1961) and its upper surface is not smooth but rough and erosional. These, coupled with the likely presence of reefs, karst development and vugs within it, results in some scattering of the seismic waves. There is a consequent reduction in the amplitudes of the higher frequency components of the reflected seismic waveform (Kennett, 1983).

The Upper Permian Marls have a lower seismic velocity such that the critical angle at the top of the Magnesian Limestones is very small, and high-energy, wide-angle reflected waves and refracted waves emanate from this surface. The choice of the shooting geometry and the cable configuration is critical for minimising the interference of these waves on the seismic section. Conventional seismic sources can therefore be hampered to some extent by an inability to 'penetrate' these Permian Limestones as suggested by Walker (1980).

The acoustic impedance contrast at the base of the Quaternary is low but the seabed/Boulder Clay interface is a strong reflector and the strong seabed multiples only amplify the problems discussed above.

In summary, a brief account of the post-Carboniferous succession in this region has been given. Some of the difficulties that are likely to be encountered during seismic surveying for coal in this region have been discussed. In particular, the Magnesian Limestone formation sets some constraints on the application of this technique. It is expected to pose major problems which are worsened if there are any anhydrite bands immersed in its matrix. Unfortunately, the permeable Permian strata must be cased off during drilling so no wireline logs are run over the Permian section.

A summary of the computer programs that were developed or used in this project is given in Appendix C of this thesis.

C H A P T E R 2

A Review of Seismic Noise Problems and some Data Processing Techniques that are used in Multiple Suppression.

2.1   **Seismic Noise Problems.**

The purpose of this review is to isolate multiple problems as far as possible from the general context of noise problems and to discuss some of the approaches that are adopted during data processing in order to attenuate them. Some of these techniques have been applied in the course of this work and this will be indicated when they are encountered in the later sections of this chapter. In this thesis, the term 'seismic section' refers to a set of processed, stacked seismic traces. The term 'seismic record' refers to a recorded seismogram that has not been processed.

The object of a seismic survey is to detect subsurface geological horizons to which the investigator has no direct access. A seismic source waveform is injected into the earth, whose response is recorded at different distances from the source point (offsets). After appropriate manipulations and processing have been carried out on the records, the final results are plotted in the form of a seismic section. The section can then be analysed and interpreted in terms of the geology of the region from which the original data were acquired. The success of this procedure primarily depends on the quality of the original data

and on the choice and application of different processing techniques.

Every event that appears on a seismic record or seismic section does not represent a genuine primary reflection from a geological interface. Reflections of purely geological significance are often swamped by events of random and/or non-geological origin. Data quality depends on the quantity of this undesirable information that is present in the seismic records. Seismic data quality varies tremendously from areas of excellent reflection information to those in which hardly any useful events can be identified. All seismic records require some form of processing in order to turn them into seismic sections that contain, as far as possible, only primary reflections. The amount and type of processing that is required for a given data set depends on the quality of the original records. One of the problems that is encountered during the enhancement of data quality by processing arises from multiple reflections. They are seismic reflections that originate when seismic waves reverberate within the subsurface layers. They are considered later in this chapter.

In section 2.1.1, two methods for the assessment of performance for a given processing technique in the enhancement of data quality are given. In the last part of the section, seismic noise in general, seismic signal information, and multiple reflections are distinguished.

In section 2.2, some characteristics of multiple reflections that distinguish them from primary reflections are given. This is

18

followed by a presentation of some techniques that exploit these characteristics of multiples in order to suppress them. Single channel techniques are proposed in section 2.3.1 while multichannel techniques are given in section 2.3.2 . This chapter ends with a summary in section 2.4 .

2.1.1   The Signal-to-Noise ratio (γ) of a Seismic Trace

            and the Autocorrelogram Section.

    A method of assessing an improvement in the quality of data after the application of a given processing technique is by the use of a quantitative parameter known as the signal-to-noise power (S/N) ratio (designated here by γ) of each trace. It is the ratio of the power in the primary reflections (useful signal) to the noise power in a given time window of the trace. There is no straightforward way of measuring this quantity from a seismic trace but it can be estimated (Robinson, 1970, White, 1973 and Rietsch, 1980) from the crosscorrelation of the given trace and others in its suite - for example, in a CMP gather. The S/N ratio is not a stationary parameter and its value depends on which time-gate of the trace it is estimated from.

    If γ is estimated both before and after the application of a processing technique, then the performance of the technique can be judged in terms of whether it (γ) has increased or decreased. This method cannot be used if the processing technique distorts the primary reflections to any extent because the definition of γ then loses its meaning. The method is not

19

usually applied because of the difficulties in the estimation of γ .

Another method is to examine the autocorrelograms. These are straightforward to obtain although the appropriate time window has to be selected. The autocorrelogram (Anstey, 1966, Anstey and Newman, 1966) of a seismic section is made up of the autocorrelation functions of the traces of the given section. The interpretation of an autocorrelogram requires special care. When this is carried out, the method of the assessment of the performance of a technique by inspecting and interpreting the autocorrelogram of the section that results from its application, is cheaper and preferable to the estimation of γ . The method of autocorrelograms has been used more often in this thesis.

2.1.2 Seismic Noise, Seismic Signal and Multiple Reflections.

The term 'seismic signal' is used to refer to all seismic events which are primary reflections from geological interfaces. These primary reflections are often recorded together with other events that arise within the geological layers of the earth. Such events include for example - multiple reflections, diffracted waves and random noise from different sources. Some of these undesirable events have very similar waveforms and frequency spectra as the events which constitute the required signal. They therefore pose immense problems in the interpretation of seismic records or sections. It is appropriate to refer to every aspect of a seismic record or seismic section that is not a primary reflection from a geological interface as 'seismic noise'.

20

Seismic noise encompasses source generated events that are undesired and seismic waves of any other provenance. It is not possible to treat all seismic noise by data processing alone. Tests are usually carried out before a seismic survey in order to establish the characteristics of any dominant noise. The acquisition geometry is then designed in such a way that these modes are reduced, and if possible, cancelled during data acquisition.

Multiples are coherent seismic events that are repeatable and that travel essentially in the vertical direction (Telford et al. 1976). The characteristics of multiples are summarized in the next section.

2.2   **Characteristics of Multiple Reflections.**

The key to suppressing any seismic noise is to identify the characteristics of the noise which distinguish it from the seismic signal. Some of the characteristics that distinguish multiples from primary reflections are:

(1) differences in frequency content,

(2) differences in moveout,

(3) differences in dips on stacked sections,

(4) the tendency for multiples to recur at regular intervals

of time. This time interval is the period of the multiple. It is common to refer to multiples either as short-period or as long-period multiples. Peacock and Treitel (1969) have characterized water reverberations in this way. It was assumed

that the reflectivity sequence is a random sequence in their theory of predictive deconvolution. If the seismogram is corrupted by no other noise but multiples, then those multiples with long periods appear on the autocorrelogram as distinct waveforms which are separated by noticeable quiet zones. The short-period reverberations appear in the form of decaying waveforms which are not separated by any noticeable quiet intervals. This practical criterion is used to distinguish between short-period and long-period multiples depending on their periodicity, the sampling interval of the data and the duration of the basic seismic wavelet.

Some processing techniques that exploit the above differences are given below.

2.3 Some Techniques used in Multiple Suppression.

The techniques that are used for multiple attenuation can be classified into two categories , namely,

(a) single channel techniques, and

(b) multichannel techniques.

Single channel techniques operate in one dimension. This is time in the time domain or frequency in the frequency domain. They deal with one seismic trace at a time, the trace being either a seismic record or a stacked trace. Examples of single channel techniques include frequency filtering, deterministic filtering (Kunetz, 1954, Backus, 1959 and Neidel, 1972), predictive deconvolution (Peacock and Treitel,1969,

22

Ziolkowski, 1980), homomorphic deconvolution (Ulrych, 1971), adaptive deconvolution (Griffiths et al., 1977), maximum entropy deconvolution (Burg, 1967) and others. Some of these techniques are sometimes varied so that the processing of a given trace is not entirely exclusive, for example, a filter that is designed from the near-trace of a CMP gather can be used under appropriate circumstances to process all the traces of the CMP gather.

The use of prediction-error deconvolution and deterministic filtering for multiple suppression is discussed in the next section. The fundamental concepts behind the use of prediction-error deconvolution are summarized in section 2.3.1 (b). A more profound analysis of deterministic methods which includes some examples of their application is given in chapter 3.

Most of the other single channel methods which are used for the same purposes but which are not further considered are variously derived from the same basic assumptions as the predictive technique. Their differences are mainly in the mathematical methods of formulation. Although some of these techniques suppress multiples better than prediction-error filtering when they are applied to particular data sets, prediction-error deconvolution has proved to be the most widely useful technique.

Multichannel algorithms of multiple attenuation deal with more than one trace at a time and they operate in two dimensions. These are time and distance (t-x) in the time-space domain or frequency and wavenumber (f-k) in the frequency-wavenumber domain. Suites of traces are processed together so as to produce

23

one output trace or another set of traces with improved S/N ratio. Examples of such suites are CMP gathers, common shot-point gathers and a set of stacked traces. The correlation of multiple reflections between members of the set is exploited by the algorithms.

The techniques that have been reviewed in this chapter include horizontal stacking (Mayne, 1962), weighted stacking (Robinson,1970) and iterative stacking (Naess, 1979). Examples of these methods are shown in section 2.3.2 . They suppress random noise as well and were applied in the course of this project.

Other multichannel techniques which are not considered include the multichannel prediction and enhancement techniques (Robinson, 1967, Schneider et al., 1964, Schneider et al., 1965, Davies and Mercado, 1968, Treitel, 1970, and Taner, 1980) which predict and suppress periodic and coherent events. They combine optimum multichannel digital filtering and CMP horizontal stacking for the efficient rejection of multiple reflections.

Another technique (and its variants) that is less commonly applied is the 'SOUSTON' technique (Michon et al. 1971) which is useful in cases when strong multiple reflections allow only the efficient estimation of multiple stacking velocities. CMP gathers are stacked with these velocities in order to obtain a multiple model which is scaled and subtracted from each trace that contributed to the stack. Reverse moveout corrections are then performed to get a gather with enhanced primary reflections which is processed as usual. The process is shown on the flow chart of Figure 2.0 .

SOUSTON.

```
        ┌─────────────────────┐
        │  CMP  or  CSP       │
        │     gather          │
        └──────────┬──────────┘
                   │ Multiple NMO corrections
        ┌──────────┴──────────┐
        │ Multiple enhanced   │
        │     gather          │
        └──────────┬──────────┘
                   │
       ┌───────────┴──────────────┐
       │                          │ Stack
       │              ┌───────────┴─────────┐
       │              │   Multiple          │
       │              │     model           │
       │              └───────────┬─────────┘
      +│                          │−
       │                          │
   ┌───┴──────────────────────────┴───┐
   │ Each  trace  of the gather        │
   │           minus                   │
   │ the  multiple  model              │
   │     (decorrections )              │
   └──────────────┬────────────────────┘
                  │
       ┌──────────┴──────────┐
       │ primary enhanced    │
       │ gather   with       │
       │ multiple    NMO     │
       └──────────┬──────────┘
      reverse     │ multiple NMO corrections
       ┌──────────┴──────────┐
       │ CSP  or  CMP        │
       │     gather          │
       └──────────┬──────────┘
                  ▼
           normal processing
```
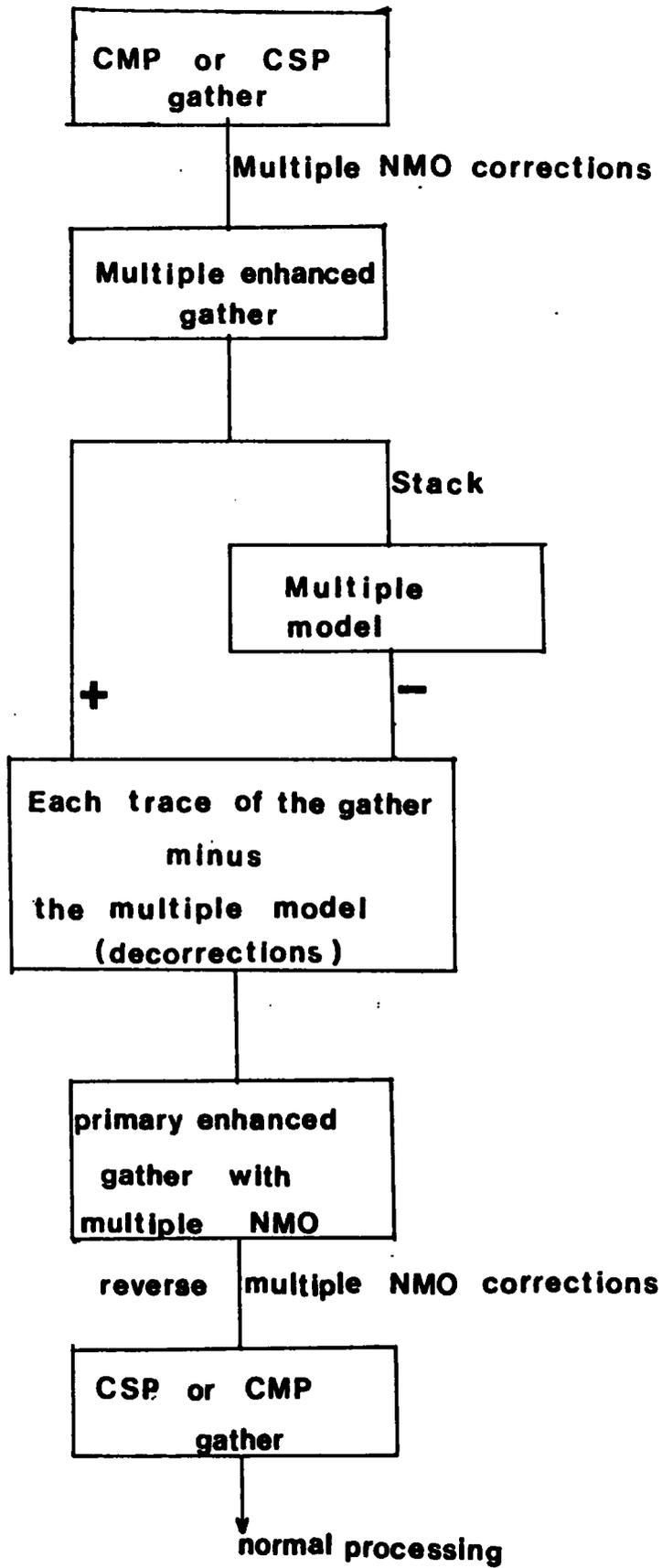
Figure 2.0 . The 'SOUSTON' process of multiple cancellation.

Frequency-wavenumber (f-k) filtering has also been applied for multiple elimination. Dip filters, velocity filters and fan filters (Fail and Grau, 1963, Embree et al., 1963, Schneider et al., 1964, Wiggins, 1965, Treitel et al., 1967, White, 1980, and Ryu, 1982) fall in this category. The filters are designed to suppress events that have dips within a specified range. It is sometimes necessary to perform moveout corrections (as in 'SOUSTON') so that desired and undesired events may assume contrasting dips. They are then easily separated by f-k filtering and the moveout can be retrieved from the result before normal processing proceeds. The efficiency of f-k techniques depends on the amount of differential moveout between primary and multiple reflections and on the S/N ratio of the data.

Velocity filtering was applied in this study in order to suppress seabed multiples before velocity analysis and also as a pre-stack processing step. The results are shown in chapter 4.

2.3.1   Single Channel Methods.

(a) Deterministic Filtering.

Deterministic techniques of seismic reflection data analysis rely on the physical laws that explain the seismic phenomena. The laws are often expressed in the form of mathematical equations.

Deterministic methods seek solutions to these equations which satisfy specified boundary conditions. The adoption of deterministic procedures in seismic reflection multiple problems often results in simple filters (e.g. the three-point filter,

25

Backus, 1959) which can then be applied to the data. They rely on the periodic characteristics of the multiple reflections.

In chapter 3, the deterministic approach is considered in greater detail. It will be shown that the technique is useful for deconvolving synthetic data that are noise-free but that it is too simplistic to be applied to real data.

With such a limited applicability in routine seismic processing, the study of deterministic techniques for the suppression of multiples has not been widespread.

(b) Prediction-error Deconvolution.

The prediction-error technique exploits the fact that multiple reflections within a seismic trace are periodic and therefore predictable. It can be applied either before or after CMP stacking.

Its efficiency when applied before CMP stacking is limited because the multiple reflections within a CMP gather are not ideally periodic. This is illustrated by a simple example on Figures 2.1 (a) and 2.1 (b). A CMP gather obtained by using AIMS (Advanced Interpretive Modelling System, version 3, provided by GeoQuest International Incorporated) is shown on Figure 2.1(a); it is noise-free and has got only one primary reflection P_1 which corresponds to the seabed. The events that are marked as M_1, M_2, and M_3 are the multiple reflections. The prediction-error technique was applied to this gather and the results are shown on Figure 2.1 (b). The strong multiple M_1 has been suppressed but
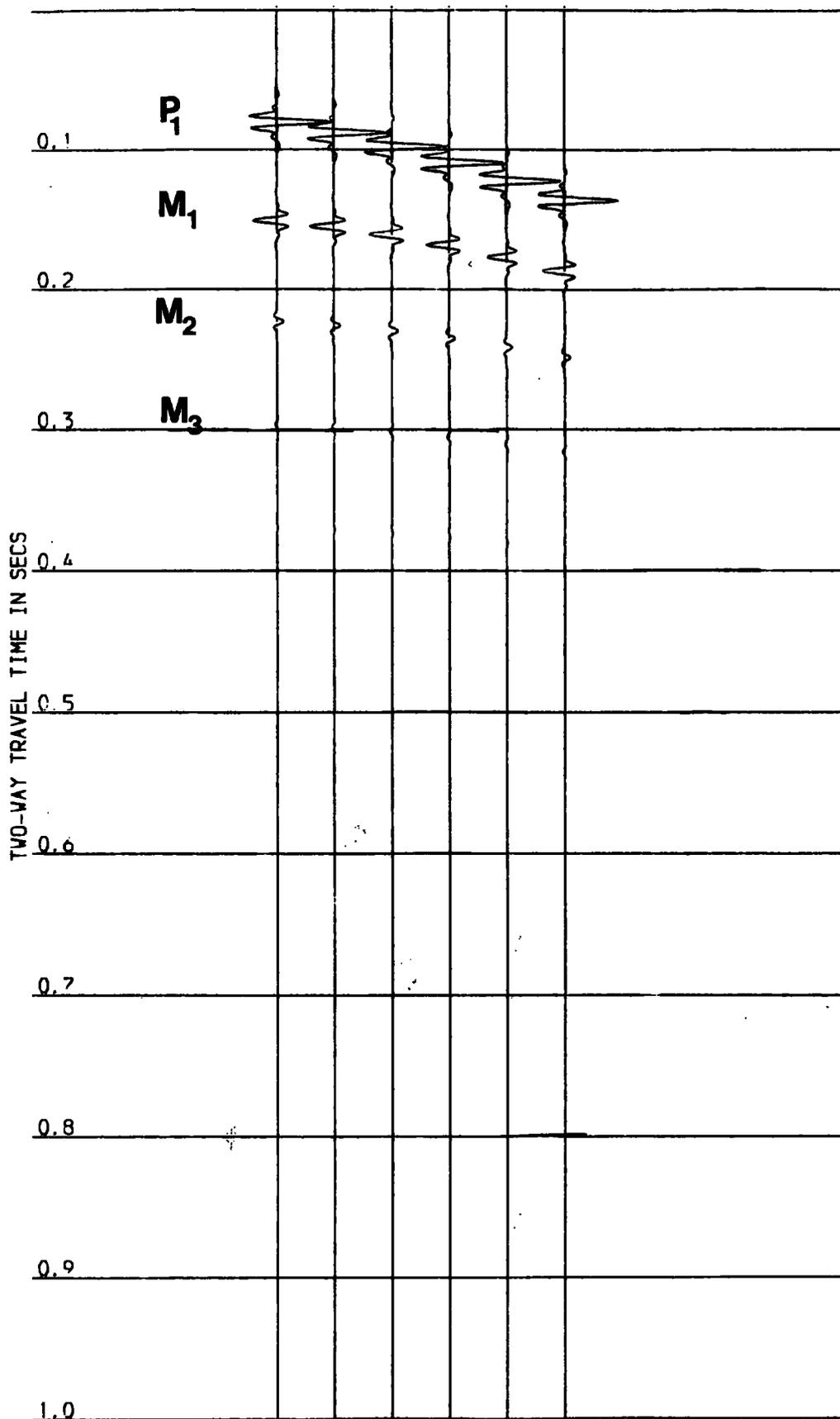
Figure 2.1(a). Common mid-point gather with one primary P_1 and multiples M_1, M_2, and M_3.
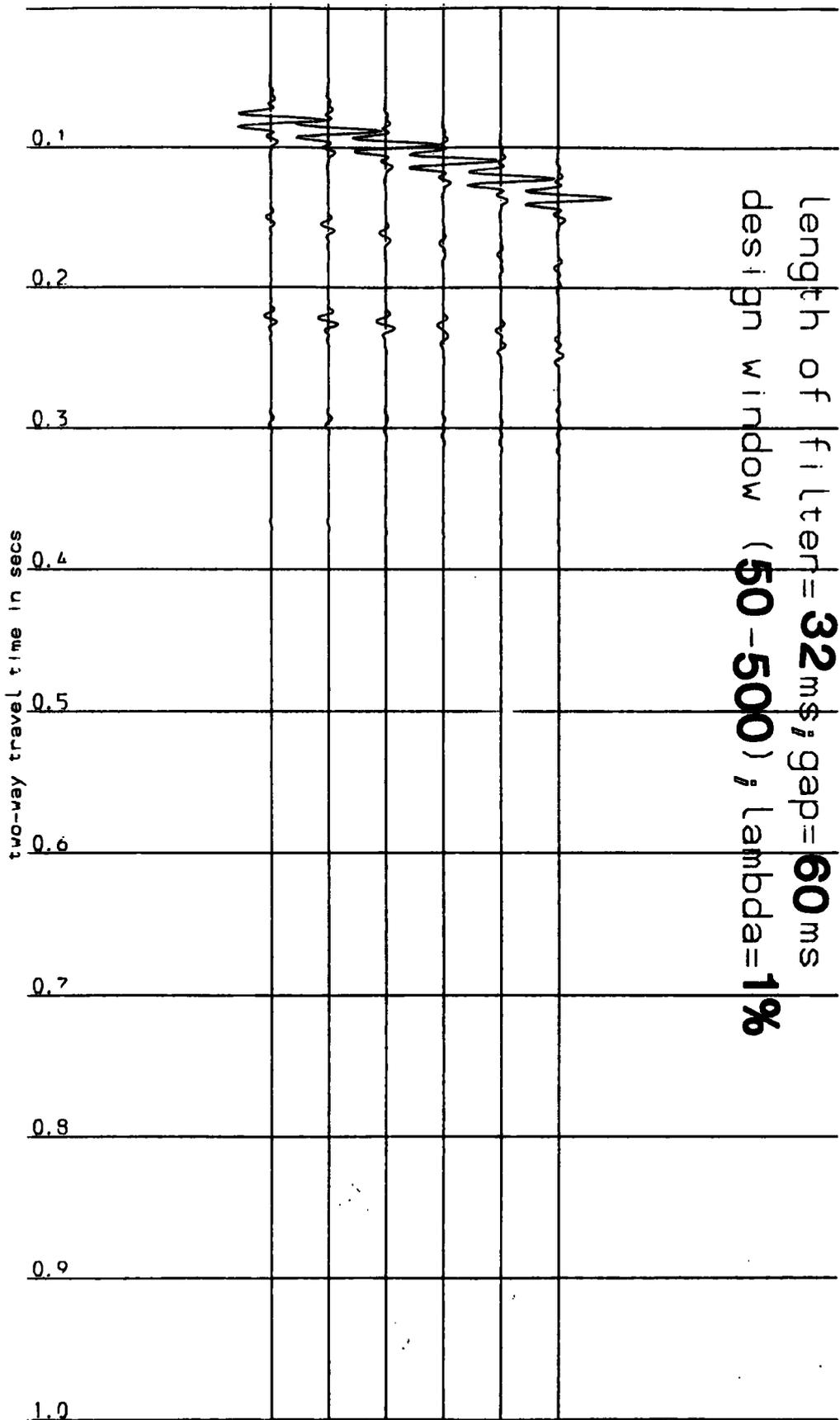
Figure 2.1(b). Common mid-point gather after predictive deconvolution.

not very efficiently in all of the channels. The filter has also introduced noise of various levels on all of the channels. The noise can generally be suppressed during stacking.

However, the pre-stack application of this technique for bubble-pulse elimination (Ziolkowski, 1984), the suppression of ghost reflections (Lindsey, 1960) and for the transformation of seismic wavelets into spikes (spiking deconvolution) is widely used . Spiking deconvolution before stacking also attenuates short-period multiples.

The basis of the prediction-error deconvolution technique is outlined below. The assumptions that are usually made are discussed and its usefulness in the suppression of multiple reflections is highlighted.

The predictive decomposition (now deconvolution) of time series was originated by Robinson, (1957). Many authors have contributed more ideas to the theory and practical application of the technique. Notable publications are those of Peacock and Treitel, (1969), Claerbout, (1976) and Ziolkowski, (1980). This technique is statistical and requires a convenient model of the seismic process.

In the development of this method, the earth is assumed to be made up of a stack of geologically different layers which are linearly elastic to strains with small magnitudes. They possess differing elastic properties and when they are in contact, the interface represents a discontinuity of physical characteristics. This is the acoustic impedance in the case of the propagation of longitudinal waves within the earth, and in general an elastic

wave impedance.

The analytical solution of the wave equation at such a boundary shows that part of the energy in an incident wave will be reflected and that the rest will be transmitted - both processes being possibly accompanied by wave-mode conversion. The reflected energy is eventually propagated back to the surface where the wave that carries it is detected and recorded.

The entire process can be mathematically represented by a discrete, linear, time-invariant system (Habibi-Ashrafi, 1978). The response of this system y(k) to a forcing signal s(k) takes the form of a convolution with the impulse response of the layered earth μ(k); that is,

$$y(k) = \sum_{i=1}^{k} \mu(i)s(k-i) \qquad \text{.. (1)}$$

In this discretized representation, the sampling intervals of all the entities are taken to be one unit of time (that is, $\Delta t = 1$ so that absolute time $t = k\Delta t = k$ where k is an integer).

The response y(k) is the convolutional model (Robinson, 1957) and it is always recorded together with some random noise so that the observed seismogram becomes

$$z(k) = y(k) + v(k)$$
$$= \mu(k) * s(k) + v(k) \qquad \text{.. (2)}$$

where v(k) represents the random noise. In the theory of predictive deconvolution, it is convenient to start with equation (2) as the mathematical representation of the seismic record or

seismic trace.

If it is assumed that the reflection coefficients of the layered medium are small so that their products of the third and higher orders are negligible compared to the ambient noise amplitudes, then the impulse response, $M(k)$, of the earth can be shown (Robinson, 1979) to be a convolution of the normal incidence reflection coefficient sequence r(k) with a~~section~~ multiple train m(k). This leads to a one-dimensional convolutional model of the seismic trace (Robinson, 1979) as

$$z(k) = r(k) * m(k) * s(k) + v(k) \quad .. \quad (3)$$

Equation (3) is only approximate for these purposes.

Useful aspects of z(k) in connection with predictive deconvolution are are that

   (1) it is a time sequence

   (2) m(k) is periodic.

These make it possible at any moment k, to represent the sequence z(k) in terms of its own observable past history (a prediction), plus an unpredictable random-like innovation (Robinson, 1957). Two additional assumptions are usually made in order to implement the predictive deconvolution procedure in a convenient mathematical way. These are that

   (i) the observation z(k) is a realization of a stationary process (so that the estimate of the autocorrelation function $\phi_{zz}(\tau)$ of z(k) will be the same (consistent) when it is estimated from any time window of z(k)).

   (ii) the reflectivity sequence r(k) is a white, stationary

29

sequence (so that $\phi_{zz}(\tau)$ will be the same as the auto-correlation function $\phi_{ss}(\tau)$ of the seismic wavelet except for a scale factor and possible perturbations caused by correlations of the multiple component m(k) of equation (3).)

The decomposition of z(k) can lead to the primary reflections r(k)* s(k) (in practice with some filtered noise) which is the desired signal. The extraction of this term from the z(k) relies on the accuracy of predicting future values of z(k) from the past and present values. If there is little change in the structure of the layered system (that is, in r(k)), then the prediction is accurate and the prediction errors are small. When the geological structure undergoes change, the prediction becomes disturbed and inaccurate and the prediction errors are large. Prediction errors therefore give a measure of the strengths and locations of the primary reflections. The prediction-error deconvolution technique works in two steps. Firstly, the prediction is carried out by using a prediction filter and secondly, the predicted value is subtracted from the observed value to get the desired prediction error. These two steps are often reduced to a single procedure in practice. A prediction filter is evaluated and then used to design a prediction-error filter which is applied to the data to predict and subtract at once.

The efficient design of this filter is controlled by the choices of a predictive distance (gap or lag) α, the length of the prediction filter N, the data window of length T sec (in

practice $T \geqslant 10\alpha(\Delta t)$ and possibly a stabilizing parameter λ. It is often necessary to examine and interprete the autocorrelation functions of the original data before choosing α and N (and hence T). Theoretically, if the S/N ratio of the data is not too low there will be no limit, except for the length of the data that is available, to the choice of N. The larger the value of N, the more cumbersome will become the computation of the prediction operator as it involves the inversion of an N X N matrix of real numbers. The matrix has got the Toeplitz form (Wiggins et al. 1965, Robinson, 1980, pp. 229) which means that the inversion can be performed more efficiently. The determination of the parameters α and N has been discussed by Peacock and Treitel (1969) and more extensively by Ziolkowski (1980).

The prediction filter is a Wiener filter (Wiener, 1942) which is calculated from the estimate of the autocorrelation function of the chosen window of the data. The autocorrelation function can be estimated in a variety of ways (Claerbout, 1976, pp. 136) and in each case a different prediction-error filter will be produced (Habibi-Ashrafi, 1978). The stability of the Wiener filter component is assured by adding a little white noise to the data before the design by means of the prewhitening parameter λ (Ziolkowski, 1980, Treitel and Lines, 1982) which also evens out the statistical distribution of the filtered noise.

In practice, some problems are faced in the application of the prediction-error filtering technique. If the input data have a poor S/N ratio, then the output may even be noisier (Ziolkowski, 1980). This is nevertheless not entirely

31

detrimental because the gain in the resolution of genuine geological events relative to the noise is more significant.

Another of the problems in the application of the method is that there is a danger of accidentally predicting and suppressing primary reflections. This can happen if the reflectivity sequence is not white and not stationary. The operator predicts and suppresses periodic events with periods in the range [α ,α+ N]. If two primary events correlate at a lag which falls within this interval, the filter will not be capable of realizing that it is not multiples that are correlating and the later primary will be predicted from the earlier and suppressed. A careful choice of the window of the input trace from which the autocorrelation function is to be estimated for the design of the filter may alleviate the danger. In real conditions, one cannot expect r(k) to be strictly white and stationary and there is always a likelihood of this accidental suppression of late primaries.

Real seismic traces are not statistically stationary because of geometric spreading and absorption losses and this violates a basic assumption of the predictive technique. Each trace is often scaled with an appropriate time-ramp function in order to correct for the overall decay in amplitude before the autocorrelation function is estimated for filter design. Failure to take this precaution may result in a poorer output.

Sometimes the prediction-error technique is used to suppress specific multiple events before CMP stacking in the hope that the latter will suppress the rest of the multiples or that prediction-error deconvolution after CMP stacking can be applied

to improve the primary-to-multiple energy ratio. This is the situation when prediction-error deconvolution is applied before CMP stacking in order to attenuate strong seabed multiples. Here, the problem of periodicity persists but when the parameters α and N are chosen correctly, the technique may be useful. Multiple reflections that have periods which are shorter than α or longer than α + N can be suppressed during CMP stacking or after it.

It has been assumed thus far that the source wavelet s(k) has a constant, unchanging shape within the seismic trace. This is not true in reality because of various non-linear propagation effects, for example, absorption losses and dispersion. (Kennett, 1983). Sometimes there is a need to correct for these effects. Spectral factorization techniques are usually used for this purpose. Most of the techniques (Burg, 1972, and Claerbout, 1976, pp. 49) are variants of prediction-error deconvolution. A requirement that the seismic wavelet should be minimum delay is sometimes necessary. Prediction-error deconvolution for multiple attenuation does not require that the wavelet be minimum delay although the resolution of the results is improved if the waveform is minimum delay (Robinson, 1980).

Figure 2.2(a) shows the section obtained from the stacking of the CMP gather in Figure 2.1(a) with prediction-error deconvolution applied. Figure 2.2(b) shows the section obtained from the stacking of the CMP gather in Figure 2.1(a) with prediction-error deconvolution applied both before and after stack. In each case the trace has been plotted six times. It is obvious that prediction-error deconvolution after CMP stacking
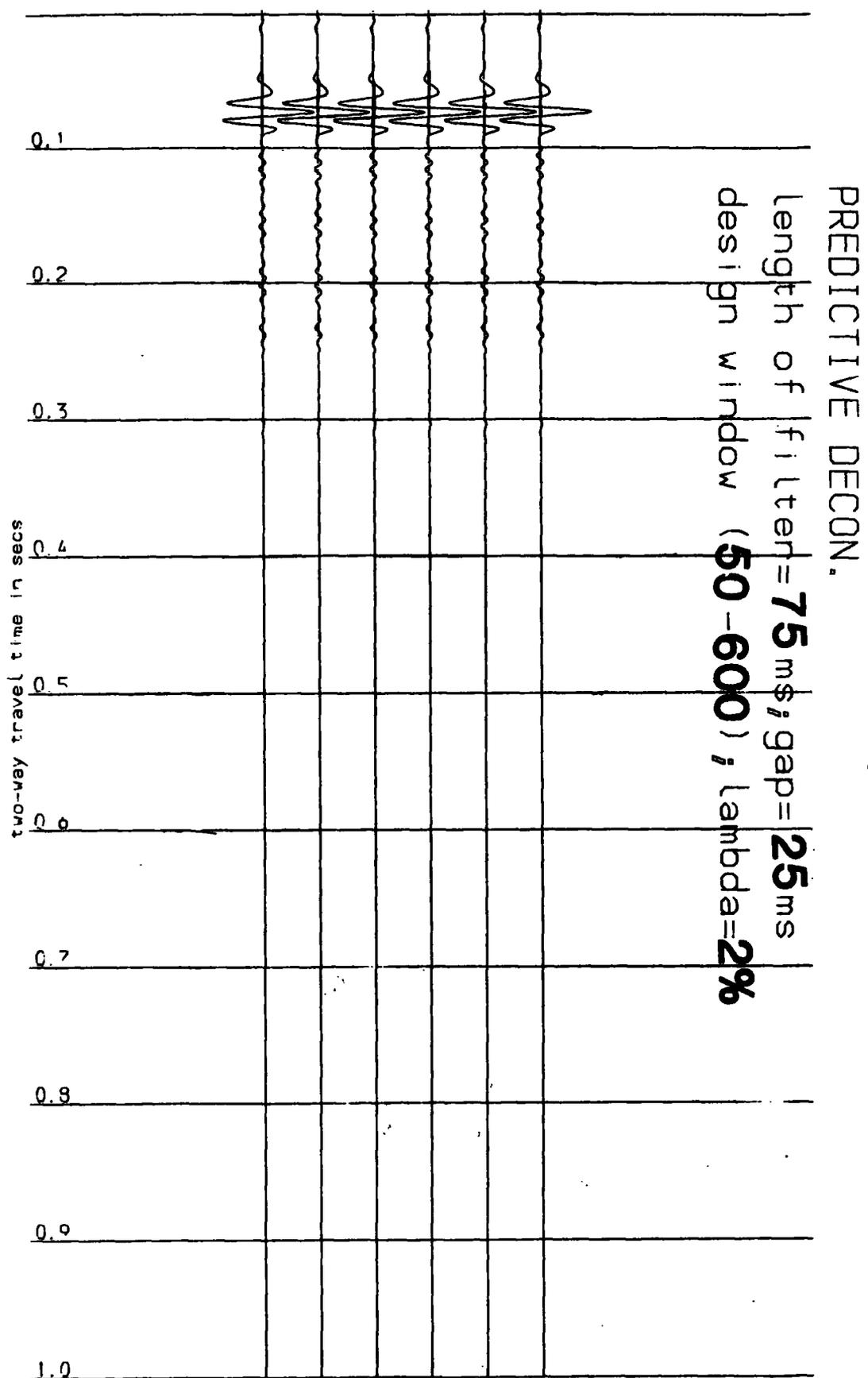
Figure 2.2(a). Stack of Figure 2.1(a) with deconvolution after stack.

PREDICTIVE DECON.

length of filter= **75**ms; gap=**25**ms
design window (**50 - 600**); lambda=**2%**
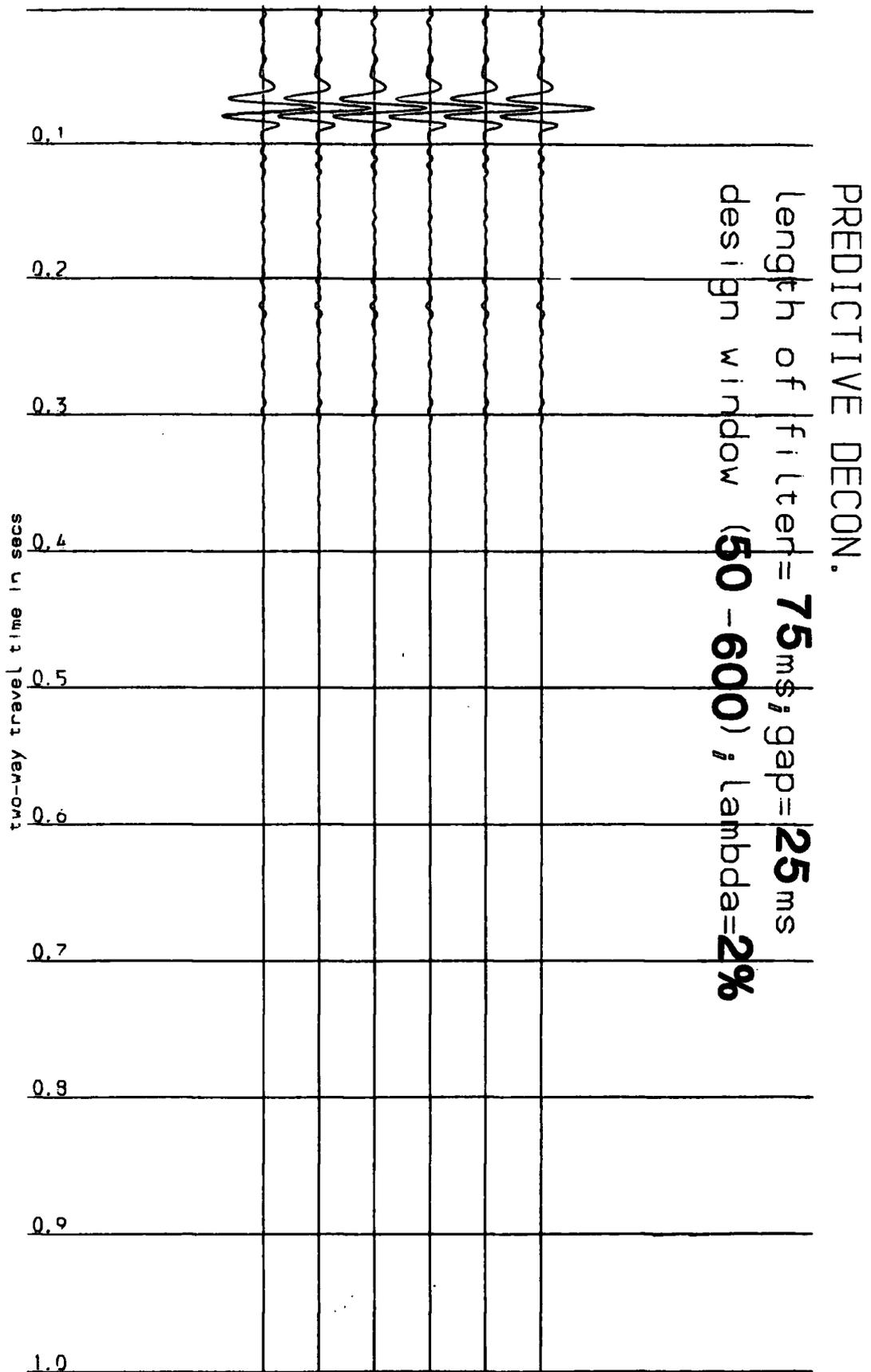
Figure 2.2(b). Stack of Figure 2.1(b) with deconvolution after stack.

has worked better in the case where prediction-error filtering was applied before stack (Figure 2.2 (b)).

The prediction-error deconvolution technique was used in the rest of this study for multiple suppression.

2.3.2   Multichannel Methods.

Multichannel techniques of multiple attenuation require suites of seismic traces or records as input data. These can either be CMP gathers, common-receiver gathers or a set of stacked traces. Figure 2.3 shows the gathers and a stacking chart to illustrate how they are collected. The multichannel techniques that have been applied in this study require normal moveout (NMO) corrected CMP gathers as input.

The CMP gathers that are obtained after the sorting of seismic reflection data have traces which correspond to the same surface mid-point between the source and the receiver. If the subsurface layers are horizontal and if lateral velocity changes are negligible, the reflecting interfaces have 'common reflection points' (Figure 2.4). These subsurface reflection points are laterally displaced when the reflecting interfaces are not horizontal and they spread apart as the structures grow more complicated. Most geometrical structures cause only a small dispersion of the common reflection point (CRP) (Taner et al., 1970, May and Hron, 1978) and the assumption of a stable CRP is usually made.

As shown on Figure 2.4, seismic reflections on successive

TRACE GATHERS

② COMMON-SOURCE ① COMMON-OFFSET

X
Z

③ COMMON- **MID**,-POINT ④ COMMON-RECEIVER

Normal incidence path

STACKING CHART

Direction of seismic line ⟶   Source-receiver midpt.

①   Source
location

②

Schematic ⟶ {
cable
displacement

③   X

④
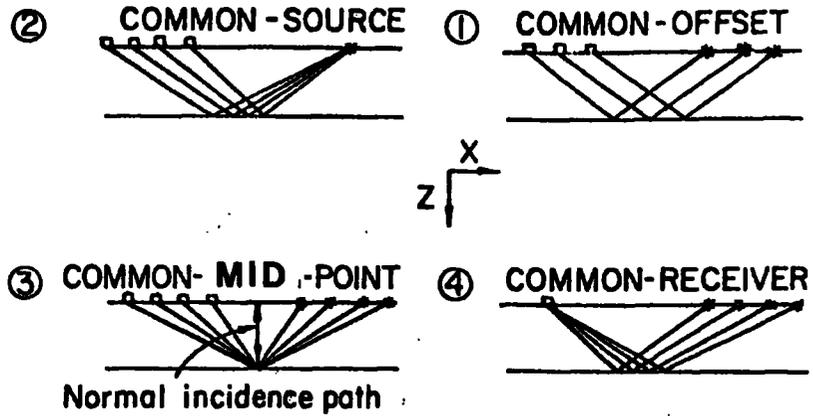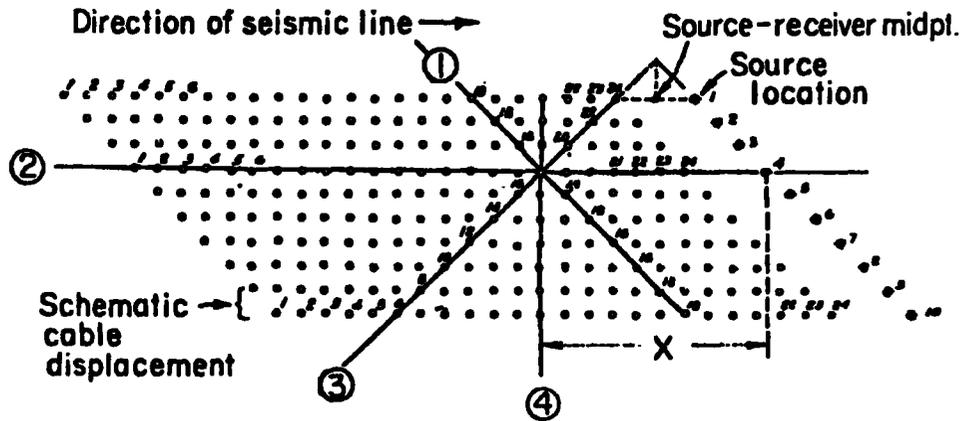
Source and receiver positions corresponding to four principal planes used for sorting seismic traces. X = source-receiver offset distance; Z = depth flow reference plane.

Figure 2.3 . Examples of suites of traces that can be sorted out after CMP data acquisition , (Mayne, 1962). (after Wood, 1982)

$$T_o = \frac{2Z}{V}$$
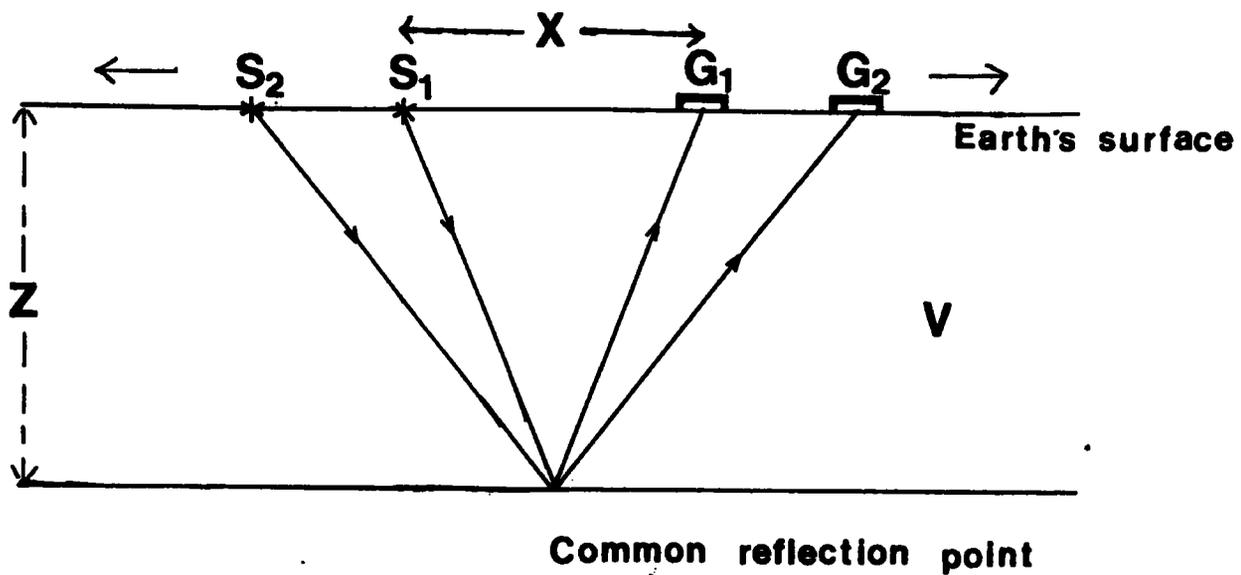
$$T_x^2 = T_o^2 + \frac{X^2}{V^2}$$

Figure 2.4 . The common reflection point and the travel time equation of seismic events.

records from a constant-velocity medium that has a single interface at a depth Z will lie on a hyperbola. If X is the shot-receiver spacing, T_x the travel time and V the seismic velocity, then

$$T_x^2 = T_0^2 + x^2/V^2 \qquad \qquad .. \ (4)$$

following the notation of Figure 2.4 . If there is more than one layer above the reflecting interface, then V becomes approximately a root-mean-square (rms) velocity (Dix, 1955) and depends on the structure above the interface. The travel time T_x would be equal to the two-way normal incidence time T_0 if the source and receiver were at the same location. This is the time at which the events are normally displayed on stacked, unmigrated seismic sections. The events on the CMP gather are out of step because of the geometrical effect ($X \neq 0$) which is referred to as normal moveout (NMO) and which must be corrected for before stacking. The NMO is given by

$$\Delta T = T_x - T_0 \qquad \qquad .. \ (5)$$

or

$$\Delta T = \sqrt{T_0^2 + x^2/\bar{V}^2} - T_0 \qquad \qquad .. \ (6)$$

and

$$\Delta T = (4z^2 + x^2)^{1/2}/\bar{V} - T_0 \qquad .. \ (7)$$

ΔT is the time step between an event on a trace with an offset X and the corresponding event on a hypothetical zero-offset trace. $\bar{V}$ is the rms velocity function defined at X=0.

NMO corrections vary with record time and therefore depend on reflector depth. The time increment ΔT is subtracted from each record time T_x (interpolating where necessary). The purpose of NMO corrections is to align single-bounce 'primary' reflections prior to stacking. Multiples generally travel at lower average velocities than primary reflections with the same arrival times since velocity usually increases with depth; therefore, multiple reflections are misaligned and attenuated during stacking. Efficient NMO corrections require information on the rms velocities (equation 6). These are estimated from CMP gathers by a variety of methods notable among which are the semblance analysis technique (Taner and Koehler, 1969) and the method of velocity scans (Dobrin, 1976, pp. 233). The former technique was applied in chapter four of this study and examples are shown.

Three methods of performing a CMP stack were applied in this work. These are the horizontal (straight) stack, (Mayne, 1962), the weighted stack, (Robinson, 1970) and the iterative stack, (Naess, 1979). The theory and principles are outlined below and examples are given.

The following model for an NMO corrected CMP gather was adopted. The ith trace of the gather is assumed to consist of a signal component (primary reflections) $\{s_j; \ j=1,2...N\}$ and a noise component $\{n_{ij}; \ j=1,2...N\}$ where a time window $N \Delta t$ sec is considered and the fold of cover is M. The following assumptions (Robinson, 1970) are made;

(1) the signal is identical (except for a scale factor) and correlated on all the M traces,

(2) the noise on any trace has got a zero mean value and is statistically independent of the noise on any other trace and of the signal,

(3) the S/N power ratio γ_i of each trace is stationary over this time window. In the rest of this chapter, S/N ratio refers to power ratio unless otherwise stated.

Using these assumptions, equation (3) can be rewritten as

$$z_{ij} = a_i(\ s_j + n_{ij} \ ) \qquad .. \ (8)$$

where a_i, i=1,2....M are signal amplitude scales.

(a) Horizontal (Straight) Stacking

Horizontal (Straight) stacking (Mayne, 1962) consists of the summation of traces of the NMO-corrected gather producing a composited (stacked) trace. The surface location of the stacked trace is the same as the common source-receiver mid-point that is associated with the gather from which it is derived.

Horizontal stacking can improve the rms amplitude level of primary reflections by a factor of $\sqrt{M}$ relative to that of any individual trace that contributes to the stack. This is correct only for the case where the S/N ratios of the M traces are identical and when the signal amplitude scales are equal to each other.

The performance of the straight stack in the elimination of multiples depends on the recording cable geometry, the magnitudes

of the residual moveouts and the range of dominant frequencies in the multiple reflections. It can suppress multiples by as much as 20 dB relative to the enhanced primaries.

From equation (8), the horizontal stack is given by

$$x_j = \sum_{i=1}^{M} (z_{ij}/C) \qquad .. \ (9)$$

j=1,2...N . In general, C is time-variant so that the effects of any data editing (muting or the existence of any 'dead' channels) can be accounted for.

All the amplitudes that contribute to the straight stack (equation 9) have the same weight. It is shown in the next part of this section that such a standard stack is less than optimal.

(b) Weighted Stacking

In horizontal stacking, it is anticipated that there will be an improvement in the S/N ratio of the stacked trace but it may be possible to do better. A calculated weighting of the traces before stacking can improve the S/N ratio of the stack. The best form of weighting is one that would lead to an optimum S/N ratio of the stack and the process is referred to as optimum weighted stacking. Weighted stacking has been treated in the literature (Meyerhoff, 1966, Robinson, 1970 and White, 1977).

The analysis outlined below is based on the model of equation (8). The M-fold weighted stack is given by

$$x_j^{(M)} = \sum_{i=1}^{M} (w_i/C) z_{ij} \qquad \text{.. (10)}$$

where C is a normalization factor and the w_i are the weights. Alternatively, one can consider the terms $\sigma_i = w_i/C$ as the weights. The notation of equation (10) is maintained here since the role of C as a factor which imparts some regularity into the scale of the resulting stack is clearer.

Let the signal energy S_i, the noise energy N_i and the S/N ratio γ_i of the ith trace be respectively defined by

$$S_i = \sum_{j=1}^{N} a_i^2 s_j^2$$

$$= a_i^2 S \, ,$$

$$N_i = N \, E\{a_i^2 n_{ij}^2\}$$

and
$$\gamma_i = S_i/N_i$$

where
$$S = \sum_{j=1}^{N} s_j^2$$

(following Robinson, 1970 but adopting the method of ensemble averages). N is the number of amplitude samples in the time window of the ith trace and E denotes expectation. The following observations can be made:

(i) γ_i is always positive.

(ii) The signal scale a_i may be fixed by setting the signal variance S equal to unity.

(iii) If there is no noise and if each trace is normalized to a unit variance, then $a_i = 1$ for all i.

From equations (8) and (10), we have

$$x_j(M) = \sum_{i=1}^{M} (w_i a_i/C) s_j + \sum_{i=1}^{M} (w_i a_i/C) n_{ij} \quad .. \quad (11)$$

The signal component of the weighted stack (equation 11) will be an unbiased estimate of the actual signal if its expectation is equal to that of the actual signal, that is, if

$$E \left\{ \sum_{i=1}^{M} (w_i a_i/C) s_j \right\} = E \left\{ s_j \right\}$$

which holds only if

$$\sum_{i=1}^{M} (w_i a_i/C) = 1 \quad .. \quad (12)$$

This is also the condition that the signal shall not be distorted by stacking.

When the constraint of equation (12) applies, the signal energy of the weighted stack is S and the noise power N_0 is given by

40

$$N_0 = N \ E\left\{\left[\sum_{i=1}^{M} (w_i a_i / C) n_{ij}\right]^2\right\}$$

which can be shown (see Appendix A) to be

$$N_0 = \sum_{i=1}^{M} (w_i/C)^2 \ N_i \qquad \text{.. (13)}$$

The S/N ratio of the weighted stack is thus

$$\gamma^{(M)} = S \ / \ N_0 \qquad \text{.. (14)}$$

The weights (w_i/C) that are required for an optimum S/N ratio, $\gamma_{opt}^{(M)}$, are obtained by maximizing $\gamma^{(M)}$ of equation (14) subject to the constraint of equation (12). This is done by the method of Lagrange multipliers and we obtain (see Appendix A)

$$w_i/C = \gamma_i/(a_i \ R) \qquad \text{.. (15)}$$

where

$$R = \sum_{i=1}^{M} \gamma_i$$

is the sum of the S/N ratios of the individual traces.

From equations (14), (15) and the definition of γ_i, we have the optimum S/N as

$$\gamma_{opt}^{(M)} = R \qquad \text{.. (16)}$$

The S/N ratio of the optimum weighted stack is the sum of the S/N ratios of the traces that contribute to the stack. When the

weights of equation (15) are used in equation (11), the result is the optimum weighted stack.

If all the traces of the gather have the same S/N ratio, that is , if $\gamma_i = \gamma$ for all i,then the stack will have an optimum S/N ratio given by

$$\gamma_{opt}(M) = M \gamma \qquad \text{.. (17)}$$

If in addition all the traces have got the same amplitude scales, that is, if $a_i = a$ for all i, then the weights become equal to a constant for all i and the optimum weighted stack and the horizontal stack (equation (9)) become identical. Therefore the S/N ratio of an M-fold straight stack can be improved by a factor of M (equation (17)) over any individual trace only if the traces have got identical S/N ratios and identical amplitudes scales. In that case, the straight stack is the same as the optimum weighted stack.   Furthermore, the rms amplitude ratio is given by

$$s_{rms}/n_{rms} = \sqrt{S} /\sqrt{N}$$
$$= \sqrt{\gamma_{opt}(M)}$$

Accordingly, this factor is improved by a factor of $\sqrt{M}$ for optimum weighted stacks if all the traces that contribute to the stack have the same γ ; this is the basis of the well-known standard stack quality enhancement. Only in rare circumstances are the ratios $\gamma_i/(a_i R)$ likely to be equal and therefore the straight stack (equation (9)) has a S/N ratio that is less than optimal.

Implementation.

In order to implement the optimum weighted stack, one must know

(i) the amplitude scales a_i of the signal,

(ii) the S/N ratios γ_i of the traces of the gather,

and (iii) a scheme of fixing the normalization factor C. The third requirement can be easily dealt with.

The estimation of the S/N ratio of a seismic trace by means of the multiple coherence function has been given by White (1973). Some statistical procedures for the estimation of a_i and γ_i have also been presented by Robinson (1970). These depend on the sums of trace cross-products but they are very sensitive to statistical irregularities because they require a statistically independent behaviou̯r of the components of each trace as well as the zero-mean-value assumption of the random noise to be strictly valid. However, more recently Rietsch (1980) has proposed an algorithm for the estimation of the a_i and γ_i when the fold of cover is greater⌃than or equal to three and shows that the estimates improve as the fold increases.

The equations given by Rietsch (loc. cit., see Appendix B) were used for the estimation of these parameters in the illustration of the optimum weight stacking technique at the end of this sub-section.

The above theory does not account for any differences in the noise spectra of the channels i=1,2...M . White (1977) has shown that stacking filters that are derived from a more general version of equation (15), namely

$$w_i(f)/C = \gamma_i(f)/(a_i R(f)), \qquad \qquad \text{.. (18)}$$

in which the parameters w_i, γ_i, and R become frequency dependent, are useful in overcoming this problem.

Other forms of weighted stacking appear in the literature. Examples include the constant energy stack for which

$$w_i/C = 1. \; / \; (\sum_{j=1}^{N} z_{ij}^2 \,)^{1/2} \qquad \text{.. (19)}$$

and the diversity stack for which the weights

$$w_i/C = 1. \; / \; (\sum_{j=1}^{N} z_{ij}^2 \,)^2 \qquad \text{.. (20)}$$

for i=1,2,...M (Nunns, 1980 and Poulter, 1982). In general, these weights may lead to improved stacks over the ordinary straight stack but they are not optimal. In particular, the diversity stack is used to discriminate against ground roll and similar high amplitude wavetrains (Sheriff, 1973).

The main problem in the implementation of the optimum weight stack is that the estimation of the weights can be very difficult. It should be applied only when the data have got very low S/N ratio but this makes the estimation even more inaccurate. Simpler versions of the concept have been found useful in the improvement of the quality of data by multiple and

random noise suppression. Such a version was applied in this study during the processing of the real data (chapter 4).

Illustrations

Examples of the use of straight and weighted stacking in order to attenuate multiples are shown in the following Figures.

Figure 2.5(a) shows an earth model in the form of interval velocity and density versus depth profiles. The geological layers were assumed to be horizontal and isotropic. The AIMS modelling program was used to obtain a 12-fold CMP gather for this model by the method of ray tracing. The near-trace separation was 45 m and the trace spacing was 25 m. Table 2.1 shows the travel times at which the primary reflections arrive. The stacking velocities of these events were obtained from the same program and are shown. Figure 2.5(b) shows the primary reflections only. No random noise was added and a t^2 time-ramp function was applied to each trace in order to enhance the appearance of the late primary events. A zero-phase wavelet with tapered low and high-cut frequencies of 37 Hz and 158 Hz respectively was used.

Figures 2.5(c) and 2.5(d) show a CMP gather that was computed with the inclusion of the first, second and third order seabed multiples for each primary in the downward and upward raypaths respectively. The former shows the computed amplitudes and the latter has a t^2 time-ramp scaling function applied to each trace.

The CMP gather of Figure 2.5(c) was stacked by using three different techniques and the results are presented. The effects

45
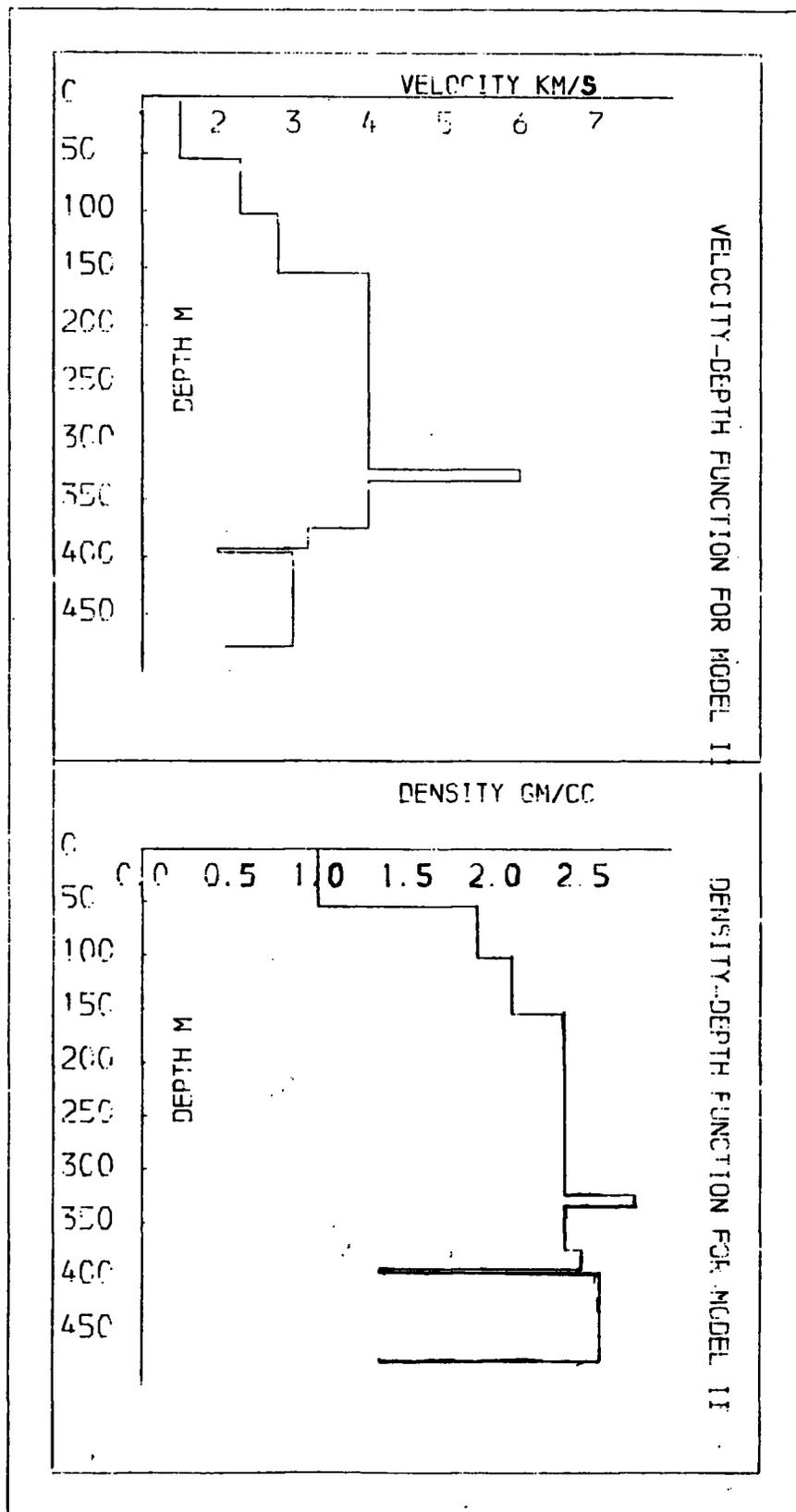
Figure 2.5(a). Velocity-depth and density-depth profiles for the
layered-earth model.

TABLE 2.1

event No.	Arrival time (msec.)	Stacking velocity m/s.
1	073	1500
2	121	2008
3	156	2270
4	237	3028
5	241	3155
6	261	3191
7	272	3181
8	275	3170
9	330	3120
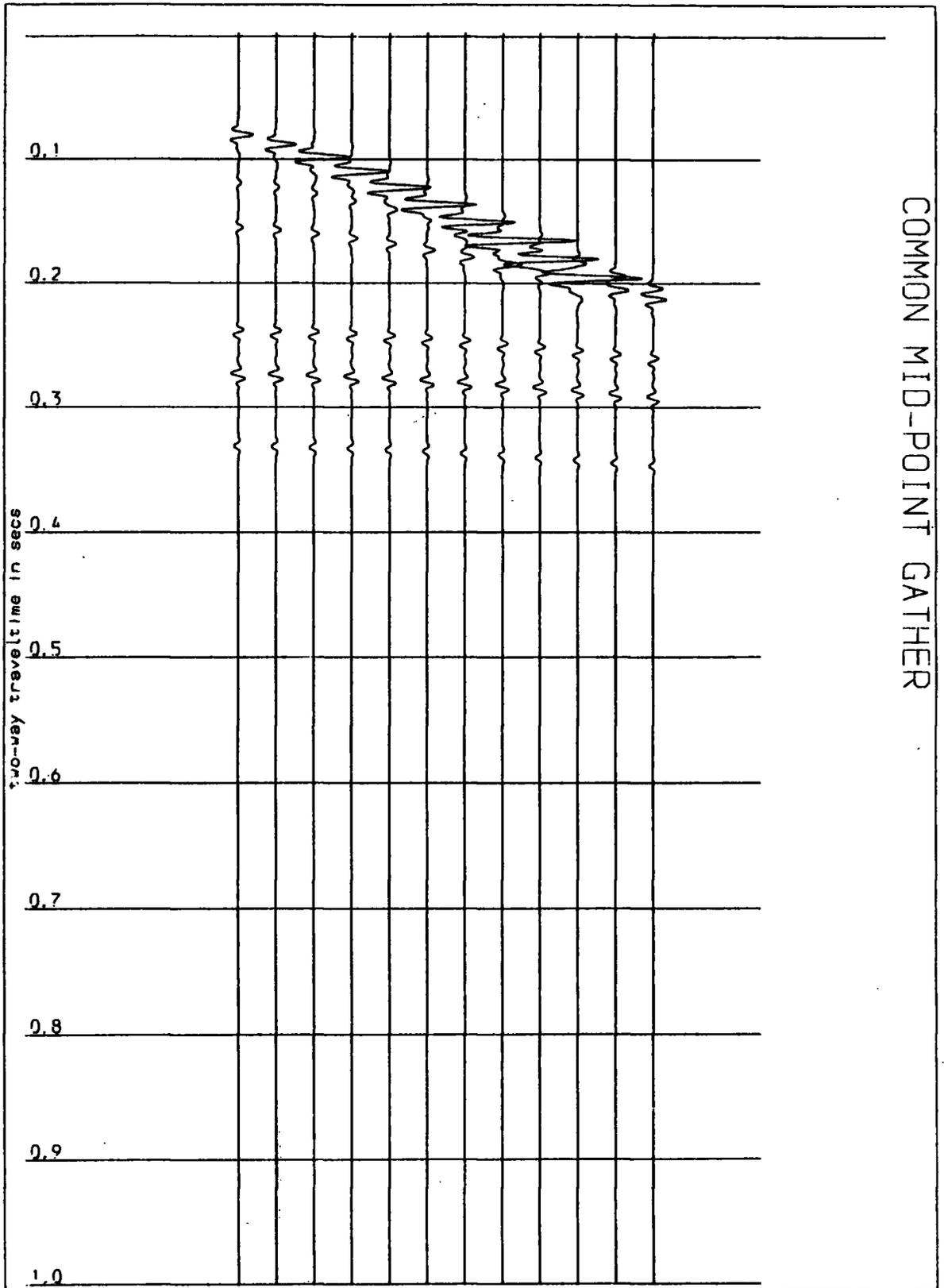
Figure 2.5(b). A 12-fold CMP gather showing primary
reflections only. A t**2 time-ramp function has been
applied to each trace.

COMMON MID-POINT GATHER

two-way travel(time in secs)
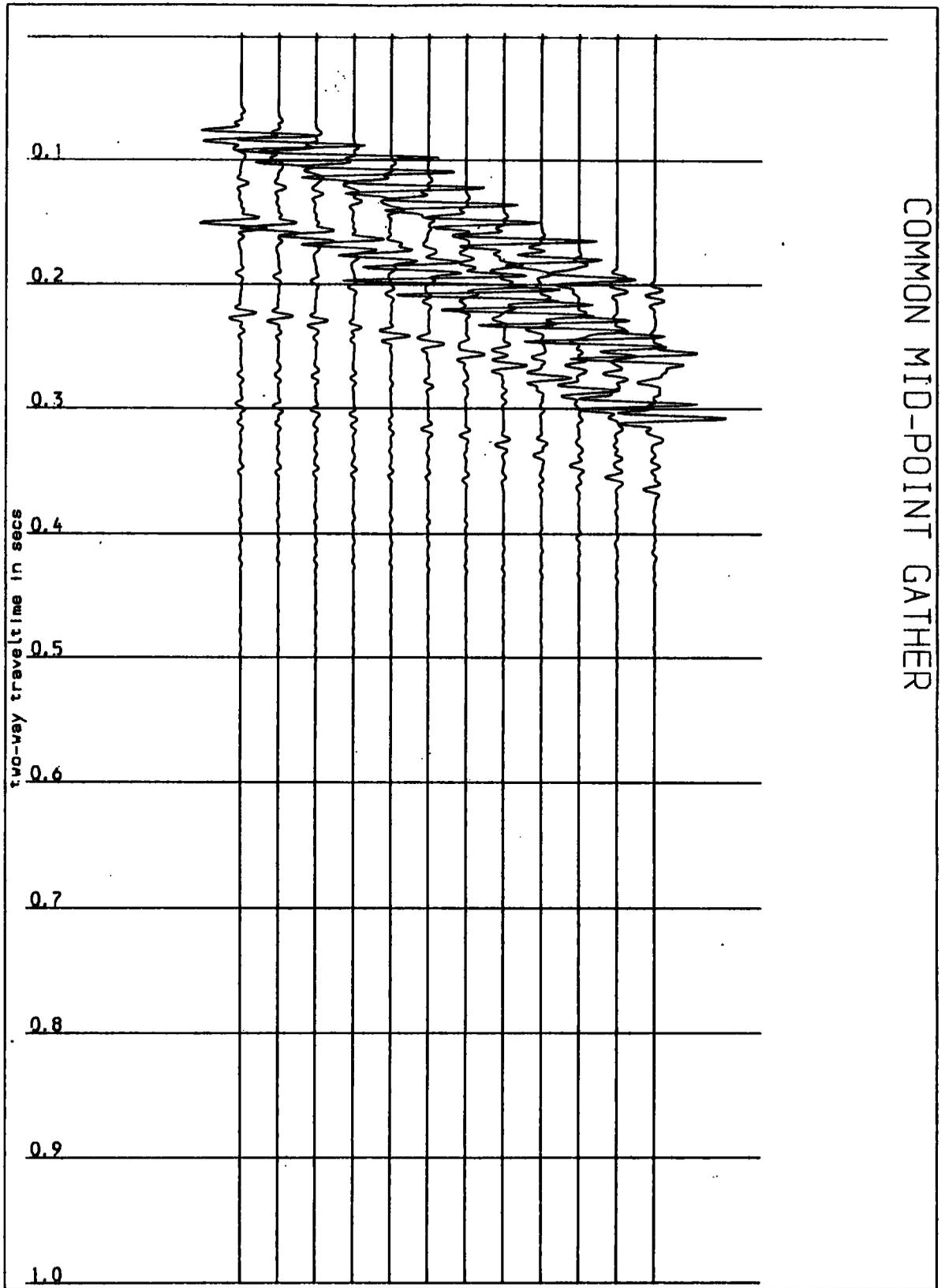
Figure 2.5(c). The 12-fold CMP gather of Figure 2.5(a)
with the first, second and third order seabed multiples
included. No time-ramp function has been applied.

two-way traveltime in secs

0.1
0.2
0.3
0.4
0.5
0.6
0.7
0.8
0.9
1.0
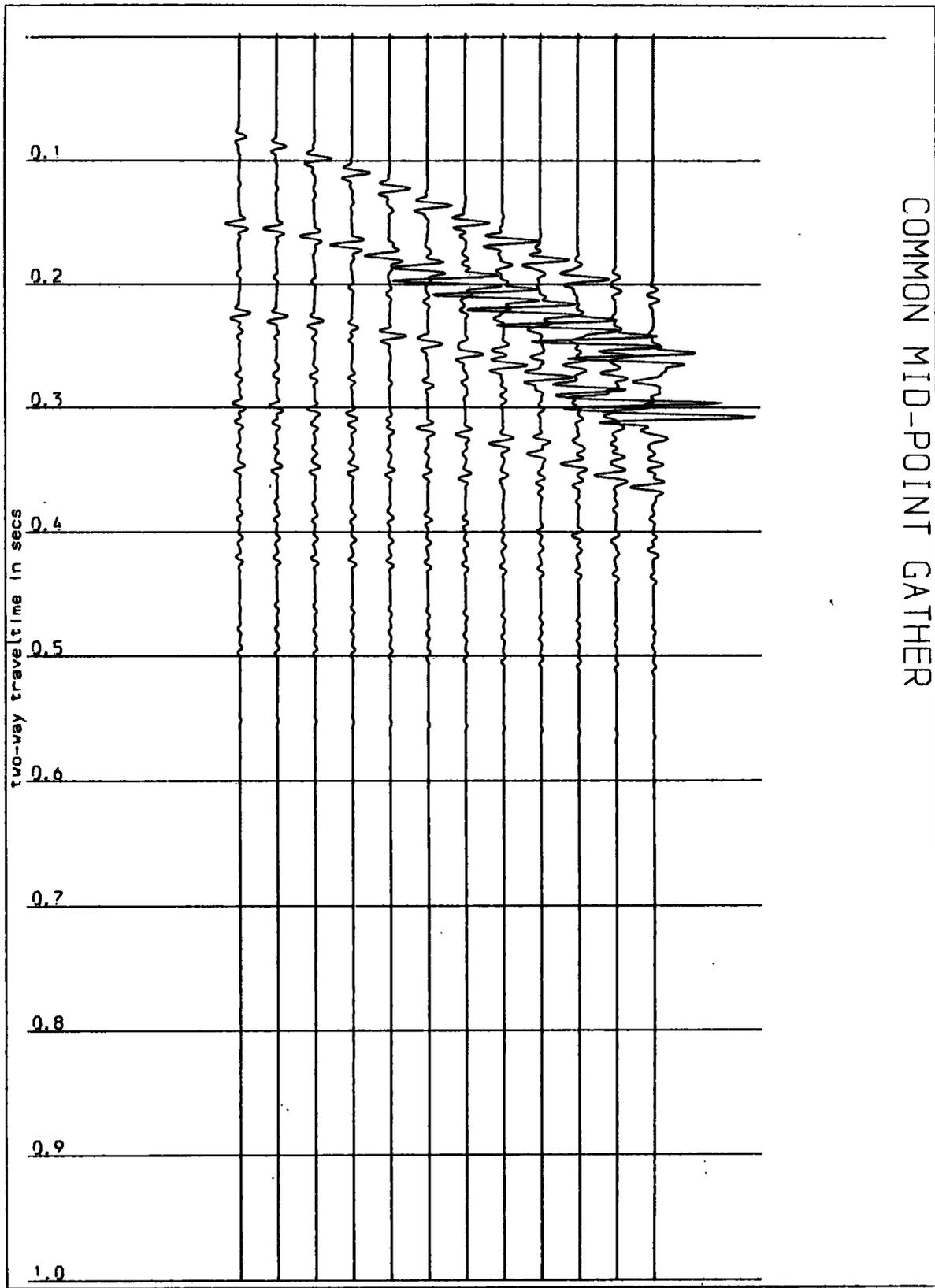
Figure 2.5(d). The 12-fold CMP gather of Figure 2.5(b)
with a t**2 time-ramp function applied to each trace.

of the multiple reflections on the stacked primaries, the extent of the attenuation and the level of the residual noise for each technique are discussed.

Each stacked trace was plotted six times and the resulting plot is loosely referred to as a section. The trace was band-pass filtered (47 Hz - 158 Hz), an AGC (gate of 100 msec) was applied to it and it was normalized to unit amplitude before being plotted. All the sections are plotted with the same gain. The latest primary reflection arrival is at about 330 msec .

<center>(i) The Horizontal Stack.</center>

Figure 2.6 shows a horizontal stack of the CMP gather of Figure 2.5(c). The primary reflections at about 70 msec, 260-270 msec and 330 msec are resolved. Residual direct seabed multiples appear at about 145 msec, 220 msec and 290 msec respectively. Primary events at 120 msec, 156 msec and 235 msec were not obvious because of stacked multiples and noise due to signal stretch during NMO corrections.

The horizontal stack is the standard way in which seismic data are treated and is adequate for most purposes but has been shown to be less than optimal. In cases where a better S/N ratio of the stacked trace is needed, other forms of stacking that take account of the nature of each trace that contributes to the stack can be applied.
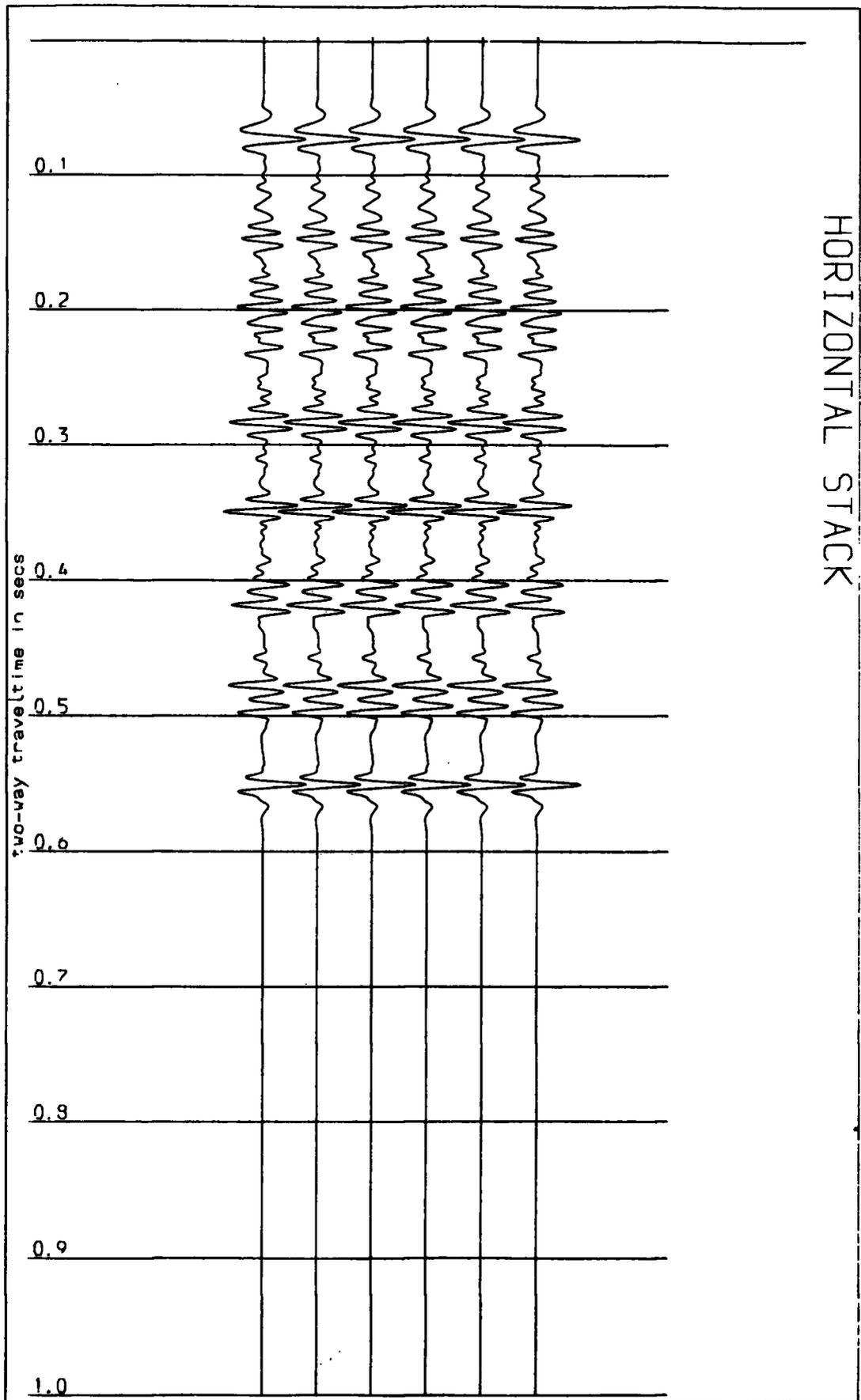
Figure 2.6 . Horizontal (Straight) stack of the CMP gather of Figure
2.5(c) after band-pass filtering, AGC (gate of 100msec)
and normalisation to unit amplitude.

(ii) Weighted Stack.

Figure 2.7 shows the result of an optimum weighted stack of the CMP gather of Figure 2.5(c) . The weights were estimated through equation (15) in which the amplitude factors a_i and the noise energies N_i of each NMO corrected trace were computed from the equations of Rietsch (1980) (Appendix A of this thesis). He applied the equations in weighted stacking of 24-fold split-spread Vibroseis data and obtained a general improvement relative to the straight stack.

For this example, The S/N ratio values and the factors a_i were estimated and the weights were evaluated and applied to each trace before stacking.

The major differences obtained in this stack are for the primary events at 156 msec, 237 msec, and 272 msec. In particular, the character of the event at 156 msec (relative to the seabed reflection) showed that it is predominantly primary energy. The first direct seabed multiple inhibited this resolution during the straight stack. The signal distortion was not so severe and the residual multiple event at about 200 msec was weaker. The primary event at 120 msec was not resolved while the multiple at 310 msec assumed a somewhat higher amplitude although this may partly be due to the effects of the AGC. The multiple at 550 msec appeared stacked up in both cases.

The weights were estimated by using a time gate from 50 msec to 350 msec. They were then applied to the whole trace. In general, this weighted stack resulted in improved resolution of primary events relative to stacked multiples.
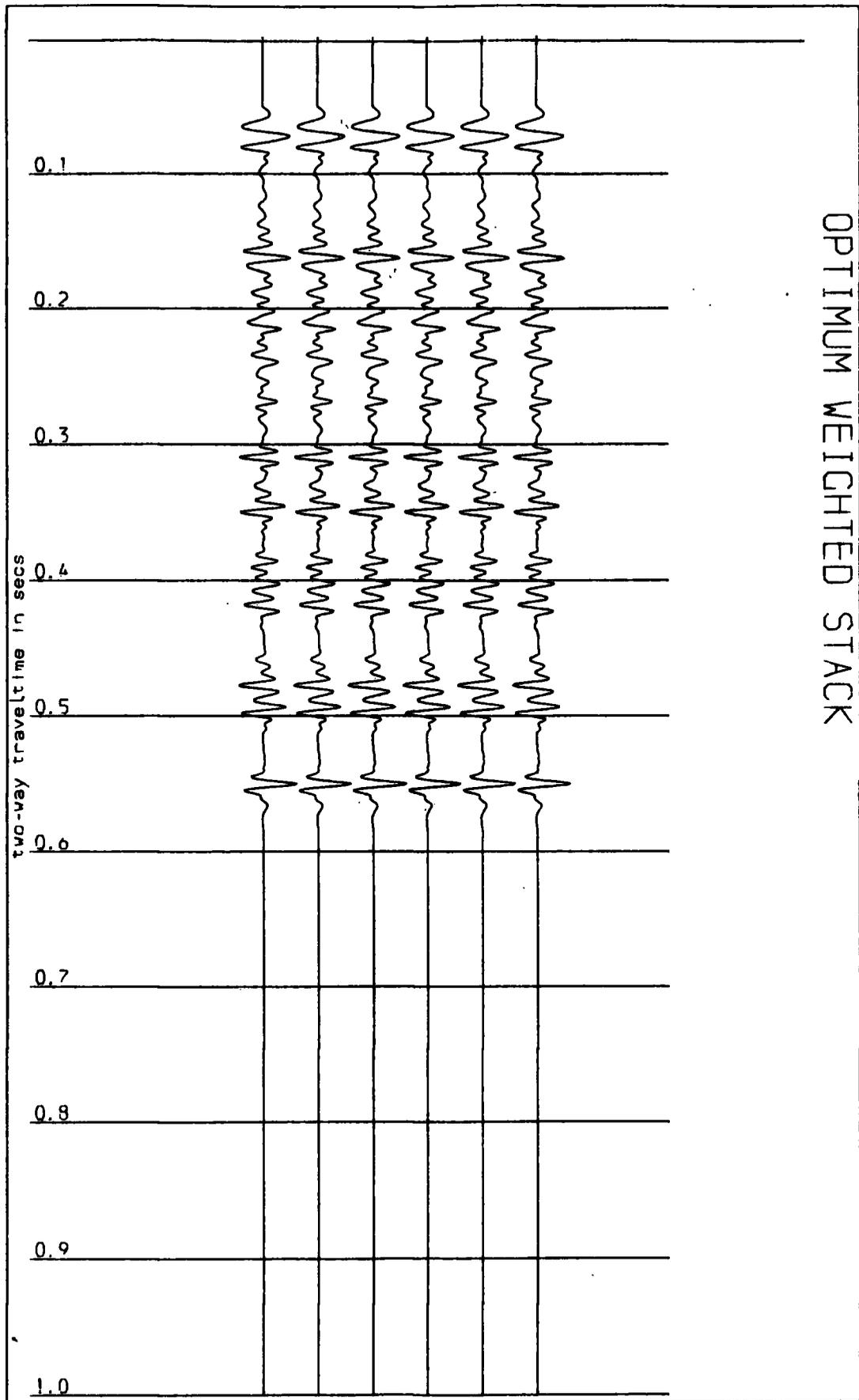
Figure 2.7 . Optimum Weighted Stack of the CMP gather of Figure 2.5(c) after band-pass filtering, AGC (gate of 100 msec) and normalisation to unit amplitude.

(c) Iterative Stacking.

The horizontal stack involves the summation of moveout corrected traces without any regard to the consistency and weighting of the signal. In part (b) it was shown that it is possible to enhance and optimize the performance of this stack by optimum weight stacking (Robinson, 1970, White, 1977 and Rietsch, 1980), but that the problems of implementation are not easy to overcome.

In a horizontal stack, each contributing amplitude has got the same weight. Several small but consistent (coherent) amplitudes may be easily overruled by a few large but inconsistent ones. An example of this occurs when an interfering strong direct water-bottom multiple is unchecked and allowed to participate with its full strength in the stack. It completely masks the primary reflection with which it interferes. Techniques such as the weighted stack and the coherency stack have been proposed in order to reduce these weaknesses of the horizontal stack but they cannot always be relied upon. The coherency stack depends on the coherency criteria that are used.

The iterative stacking algorithm was proposed by Naess (1979) and it takes into account the above-mentioned problems. The assumptions that are made in order to apply the technique and the basis of the algorithm are outlined below and examples are shown to comparatively illustrate the method.

The assumptions required are that

> (1) all the primary reflection amplitudes at a given time level on an NMO-corrected CMP gather are equal in strength

and have the same polarity,

(2) all noise amplitudes show less horizontal consistency
than primary amplitudes.

The second assumption is approximately satisfied for any time
level of a CMP gather after NMO corrections have been applied.
The first assumption is much stronger because it entails that the
a_i of equation (8) should be equal. It would be helpful to carry
out a signal amplitude scale correction before an iterative
stack. This would result in the problems that are encountered in
optimum weight stacking and are being avoided by using an
alternative technique.

Following the assumptions (1) and (2), the algorithm can be
obtained by starting with the z_{ij} of equation (8) and by
considering a unique time level (j). The amplitude of the
horizontal stack is

$$x_j = \sum_{i=1}^{M} (z_{ij}/M) \qquad\qquad .. (21)$$

where the normalization factor C (equation 9) has been considered
constant and equal to M. The index j can be dropped so that at
the end, the procedure can be repeated for all j. If there are m
positive amplitudes and n negative amplitudes contributing to
equation (21) and if they are respectively denoted by $(z_{+i}^{(1)}$,
i=1,2...m) and $(z_{-j}^{(1)}$, j=1,2..n) (j does not designate the time
level anymore; the index i now denotes positive data samples at a
given time level), then equation (21) becomes

49

$$x^{(1)} = x_p^{(1)} + x_n^{(1)} \qquad\qquad .. \ (22)$$

where

$$x_p^{(1)} = (1/M) \ . \ \sum_{i=1}^{m} z_{+i}^{(1)}$$

and

$$x_n^{(1)} = (1/M) \ . \ \sum_{j=1}^{n} z_{-j}^{(1)}$$

Equation (22) is the horizontal stack expressed as a sum of separate polarities $x_p^{(1)}$ (normalized sum of the amplitudes with positive polarity) and $x_n^{(1)}$ (normalized sum of negative amplitudes). It is also the first step of the iterative stack.

The input amplitudes ($z_{+i}^{(1)}$ and $z_{-j}^{(1)}$) are then altered by using the following algorithm (Naess, 1979) in order to obtain another set of amplitudes ($z_{+i}^{(2)}$ and $z_{-j}^{(2)}$);

$$\text{if } z_{+i}^{(1)} > x_p^{(1)} \text{ then } z_{+i}^{(2)} = x_p^{(1)}$$

$$\text{if } z_{+i}^{(1)} \leq x_p^{(1)} \text{ then } z_{+i}^{(2)} = z_{+i}^{(1)} \quad .. \ (23)$$

$$\text{if } /z_{-j}^{(1)}/ > /x_n^{(1)}/ \text{ then } z_{-j}^{(2)} = x_n^{(1)}$$

$$\text{if } /z_{-j}^{(1)}/ \leq /x_n^{(1)}/ \text{ then } z_{-j}^{(2)} = z_{-j}^{(1)}$$

The resulting set of amplitudes is stacked in the second step of the iterative stack to obtain

50

$$x^{(2)} = x_p^{(2)} + x_n^{(2)} \qquad\qquad .. \ (24)$$

where

$$x_p^{(2)} = (1/M) \sum_{i=1}^{m} z_{+i}^{(2)}$$

and

$$x_n^{(2)} = (1/M) \sum_{j=1}^{n} z_{-j}^{(2)} \ .$$

The procedure is generalized so that $(q-1)$ successive changes of amplitudes occur to produce the qth stack. This is achieved through

$$x^{(q)} = x_p^{(q)} + x_n^{(q)} \qquad\qquad .. \ (25)$$

where

$$x_p^{(q)} = (1/M) \sum_{i=1}^{n} z_{+i}^{(q)}$$

and

$$x_n^{(q)} = (1/M) \sum_{j=1}^{m} z_{-j}^{(q)}$$

and the amplitudes are obtained from the following algorithm;

if $z_{+i}{}^{(s)} > x_p{}^{(s)}$ then $z_{+i}{}^{(s+1)} = x_p{}^{(s)}$

if $z_{+i}{}^{(s)} \leqslant x_p{}^{(s)}$ then $z_{+i}{}^{(s+1)} = z_{+i}{}^{(s)}$ .. (26)

if $/z_{-j}{}^{(s)}/ > /x_n{}^{(s)}/$ then $z_{-j}{}^{(s+1)} = x_n{}^{(s)}$

if $/z_{-j}{}^{(s)}/ \leqslant /x_n{}^{(s)}/$ then $z_{-j}{}^{(s+1)} = z_{-j}{}^{(s)}$

where $s = 1,2,3....,q-1$ for the qth stack. After the qth stack, $(q-1)$ successive changes of the original amplitudes have occurred. They all amount to a reduction in absolute amplitude values. The contributions of anomalously high but inconsistent amplitudes are weakened by this procedure. Since primary events are assumed to give the same contributions to the stack, the noise (including multiples) is reduced and the iterative stack represents an increase in the S/N ratio. The amount of reduction of a given amplitude depends on the amplitude distribution at that time level, the normalisation factor M and the number of iterations q (or the level of the stack).

A stepwise summary of the algorithm is as follows;

(1) separate positive and negative amplitudes that are present at the given reflection time level,

(2) calculate the sums of the positive and negative amplitudes separately and normalize them with a factor M,

(3) if any amplitude is larger (in absolute value) than the absolute value of the normalized sum with the same polarity, change the amplitude by setting it equal to the normalized sum.

52

(4) repeat (2) and (3) with the amplitudes obtained in (3). The number of repetitions is optional.

(5) calculate the final amplitude value (iterative stack result) by summing the last positive and negative normalized sums.

The implementation of this technique requires the choice of the normalization factor M and the number of iterations q. The convergence of the algorithm depends on the efficiency with which the effect of an anomalous amplitude is corrected for as q increases, also on the value of M and on the actual distribution of the amplitude values. In the examples shown by Naess, (1979), Naess and Bruland, (1981), and Naess, (1982), values of M that are less than the fold of cover at the given time level produce good results if the number of iterations is sufficiently high. There are no set rules for the choices of q and M. The given data set should be examined in order to have an estimate of the ranges of values of q and M that can be used.

Examples of the application of this technique are given below. The values of the normalization factor for each stack were stated in terms of a fraction f of the fold of cover; for example, if f=0.5, then the normalization factor that was applied in equation (25) is given by f times the fold of cover.

Figures 2.8(a) - (e) show 'sections' that were obtained by stacking the CMP gather of Figure 2.5(c) iteratively. Different values of q and f were used as indicated. Figures 2.8(a), 2.8(b) and 2.8(c) were obtained by stacking with a value of f equal to 0.5 and with q equal to 2, 8, and 12 respectively. In comparison

53
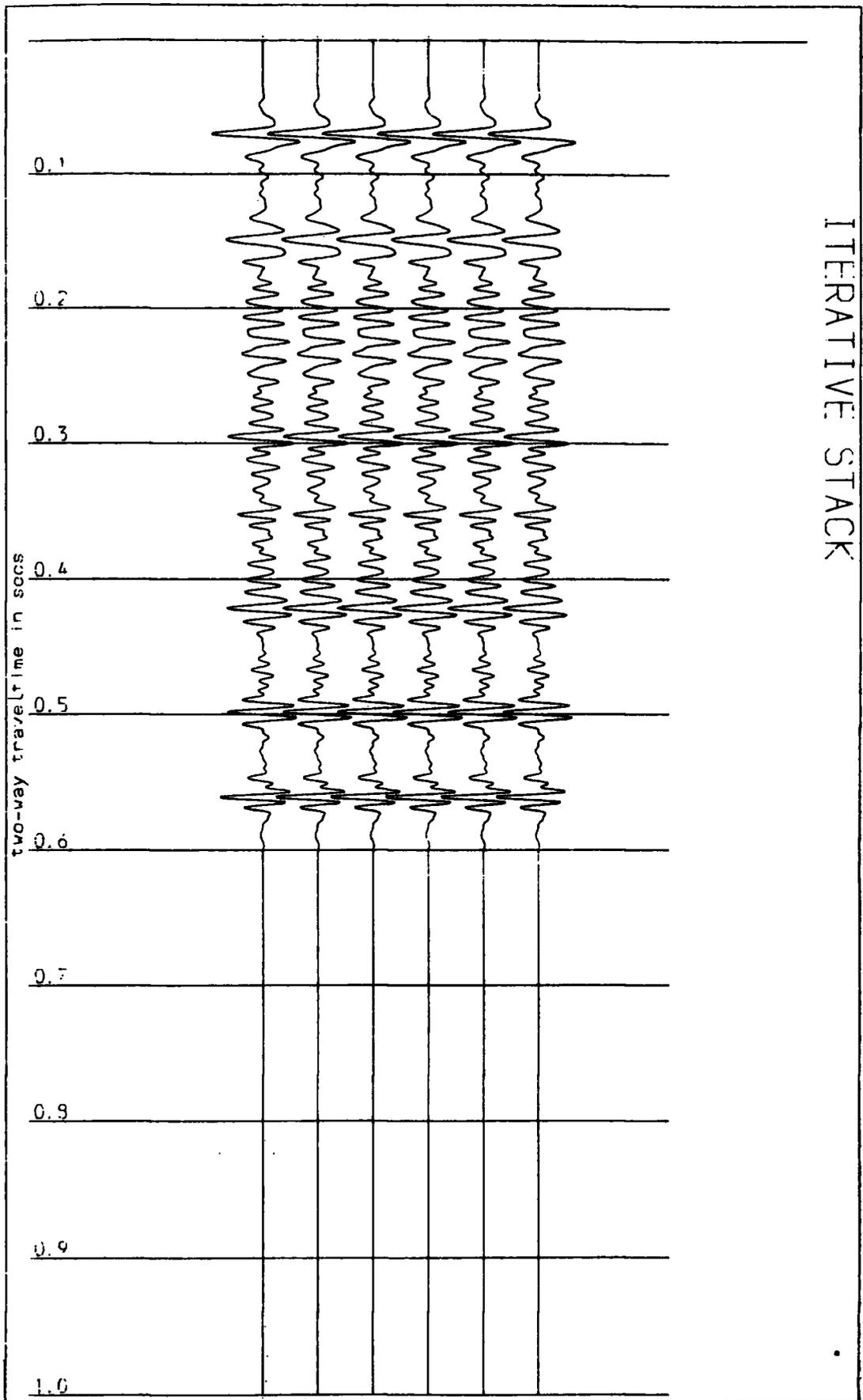
Figure 2.8(a). Iterative Stack (q=2, f=.5) of the CMP gather of Figure 2.5(c) followed by band-pass filtering, AGC (gate of 100 msec) and normalisation to unit amplitude.
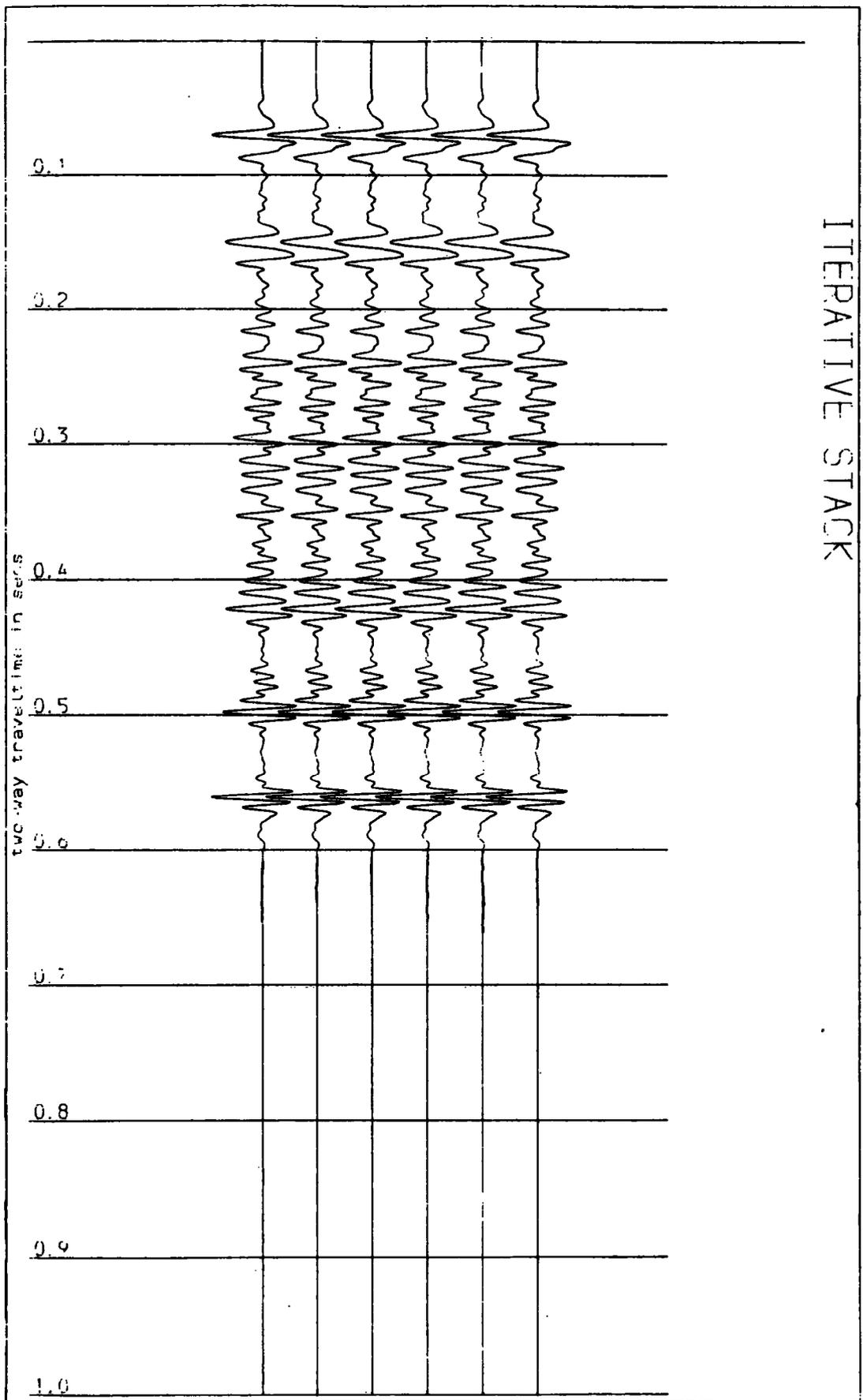
Figure 2.8(b). Iterative Stack (q=8, f=0.5) of the CMP gather of Figure 2.5(c) followed by band-pass filtering, AGC (gate of 100 msec) and normalisation to unit amplitude.
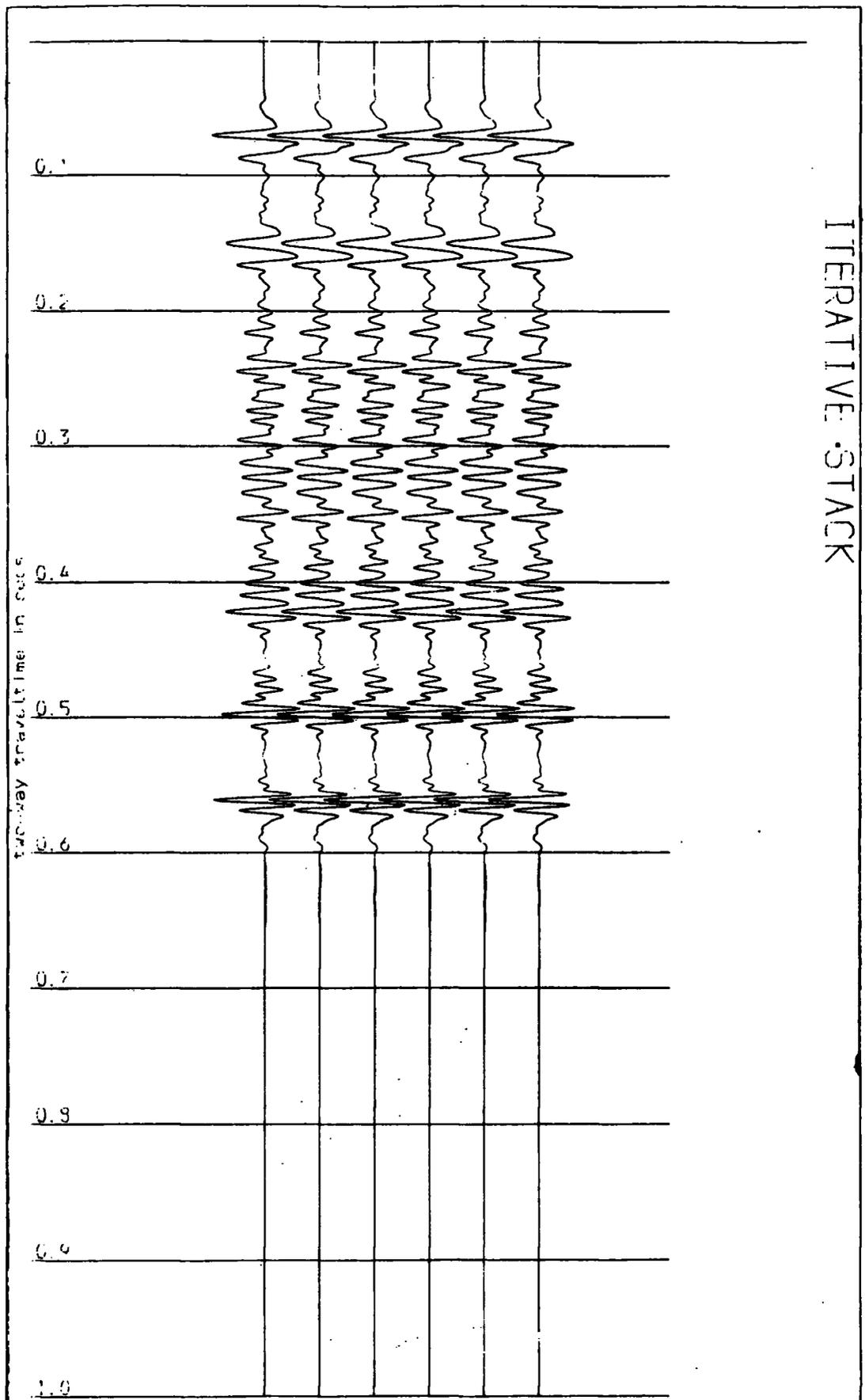
Figure 2.8(c). Iterative Stack (q=12, f=0.5) of the CMP gather of Figure 2.5(c) followed by band-pass filtering, AGC (gate of 100 msec) and normalisation to unit amplitude.

with the horizontal stack, any level of the iterated stack introduced more signal distortion. The second stack (q=2, Figure 2.8(a)) was not much of an improvement relative to the straight stack. The eight stack (q=8, Figure 2.8(b)) produced better resolution. The multiple at 220 msec was eliminated while the primary reflections at 150 and 240 msec have been much enhanced. The character and phase of the former correspond to those of the seabed reflection although its frequency content is lower. Some of the multiples below 350 msec were not properly suppressed as there are no strong primaries in this interval and the AGC tends to range up any residual multiple amplitudes that are present. The twelfth stack (q=12, Figure 2.8(c)) was very similar to Figure 2.8(b) as were the sixteenth and the twenty-fourth stacks (not shown). Further increases in the value of q showed no gain in resolution.

A normalization scheme with f equal to 1.0 was tested for different values of q. The results (Figures 2.8(d) and 2.8(e)) were less satisfactory than those for (q=8, f=0.5) which was optimum for this gather after fixing q and varying f in the range [0.1,1.5].

Finally, all the examples showed that each of the stacking techniques has its merits and demerits in so far as they were tested with the same synthetic gather. The horizontal stack is easily implemented but will not always produce the best attenuation of both categories of noise. The optimum weighted stack would give a trace with the maximum S/N ratio but the statistically complicated structure of geological noise (and
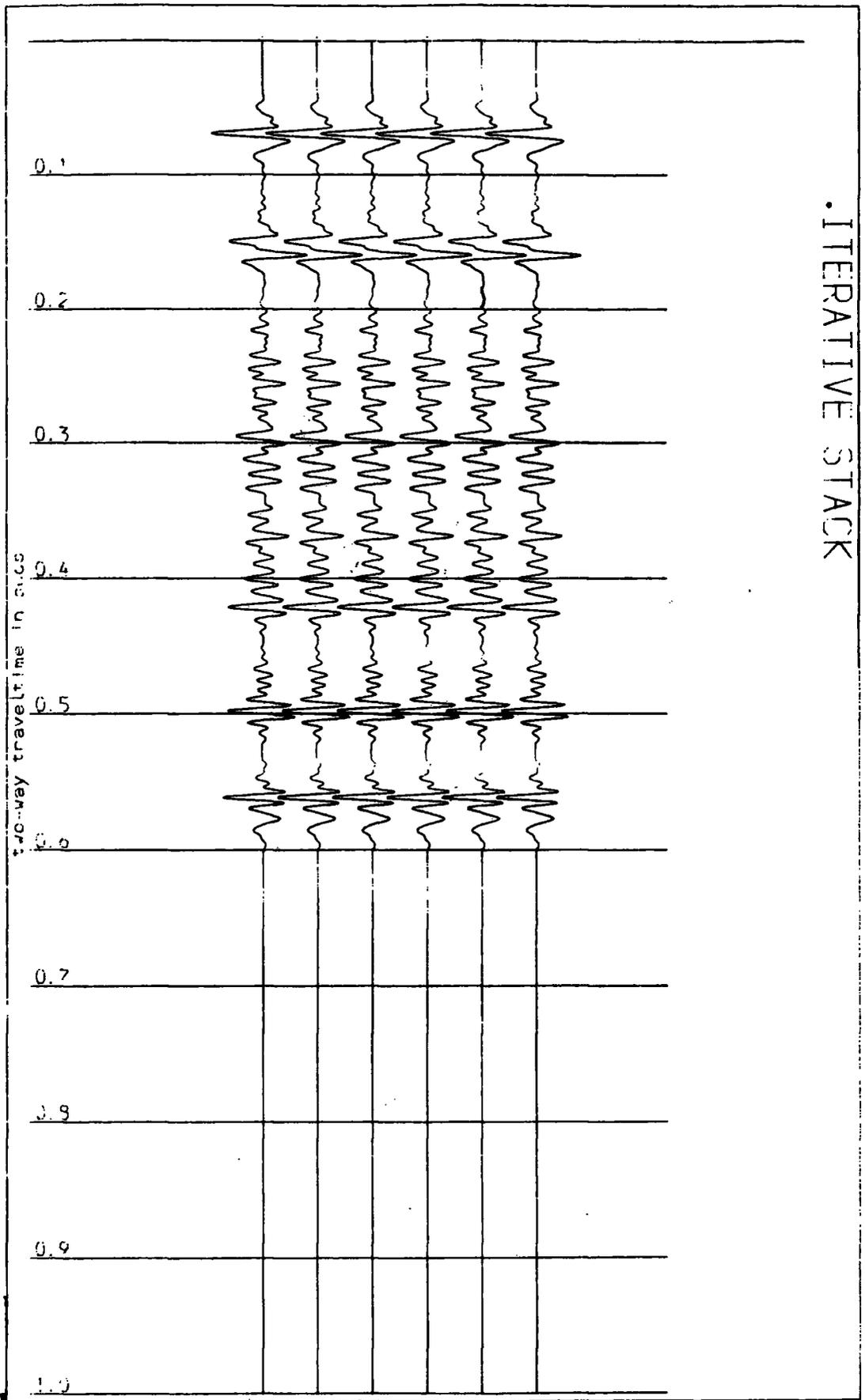
Figure 2.8(d). Iterative Stack (q=8, f=1.0) of the CMP gather of Figure 2.5(c) followed by band-pass filtering, AGC (gate of 100 msec) and normalisation to unit amplitude.
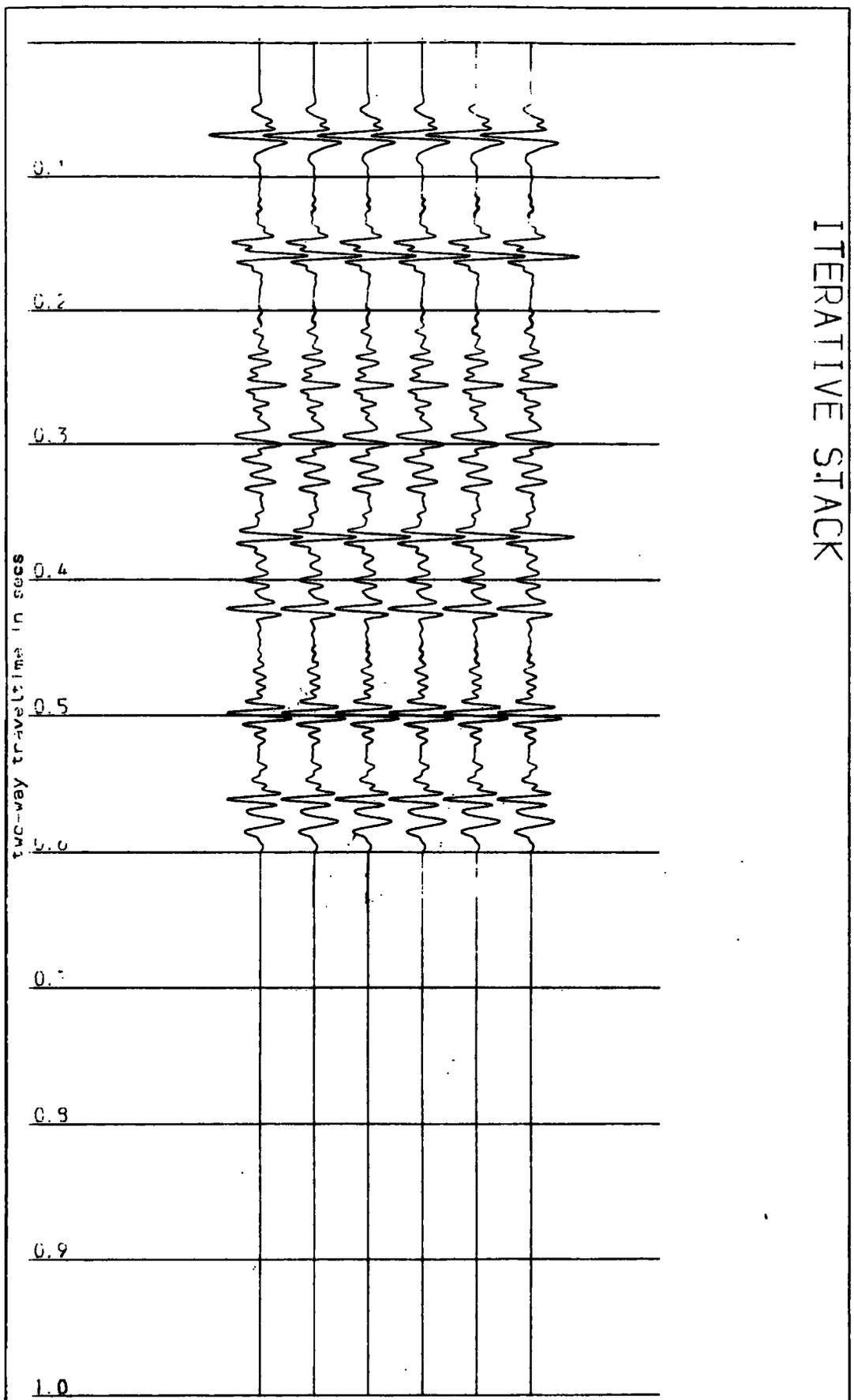
Figure 2.8(e). Iterative Stack (q=12, f=1.0) of the CMP gather of Figure 2.5(c) followed by band-pass filtering, AGC (gate of 100 msec) and normalisation to unit amplitude.

even processing noise in these examples) would make its design critical. The iterative stack, when carefully applied, deals best with random noise and attenuates strong multiples but introduces more signal distortion than any other technique. This should not be particularly harmful if there is a good S/N ratio enhancement.

2.4 Summary.

Standard and non-standard stacking techniques for multiple and random noise attenuation have been presented in outline and those that were used in this study reviewed. The prediction-error deconvolution technique and these stacking algorithms were applied in the processing of seismic reflection data that were acquired off the coast of Durham. The task of estimating the weights for an optimum weighted stack becomes onerous if the S/N ratio of the data is too low. This was the case and the technique could not be applied as discussed in this chapter. A simpler weighting scheme was used. Weighted stacking was carried out only on the 24-fold data and iterative stacking was performed only on the 6-fold data. The reasons for this are summarized at the beginning of chapter 4.

Deterministic Filtering.

3.1   Deterministic and Statistical methods.

The concept that seismic data can be treated in one of two equivalent approaches - namely the deterministic or the statistical approach was put forward by Wadsworth et al., (1957). This work was published at a time when seismic data processing was carried out almost entirely by deterministic criteria and it contributed to the foundations of the robust statistical methods of data analysis that are currently in use.

The deterministic approach to seismic data processing relies on the physical laws that govern the seismic phenomenon. The laws can be expressed in the form of differential equations. The approach is to seek the solutions of these equations when specific boundary conditions are given. Boundary conditions arise from physically feasible situations, e. g., the geometrical condition in seismic wave propagation which requires that the displacements should be continuous across the interface of a physical discontinuity or the dynamical condition that pressure must be continuous at such a boundary. Initial conditions are connected with or arise from observations of propagating wavefields.

The nature of the observations limits the power of this technique. No matter how precisely the observations are made, they are often inaccurate and certainly incomplete. The

assumptions that are made in order to derive the physical laws on which the approach relies are often too simplistic. This lowers the efficiency of its techniques when they are applied in real, general situations.

The statistical approach tends to establish the dynamics of a physical system by using quantities as they are measured. Distributions and statistical functions of these quantities are examined in such combinations as one chooses and there is a freedom to choose any set of statistical parameters for use in such an investigation. A choice of all possible parameters would lead to a very complex problem. It is adequate to select a group of parameters that are connected by rigid dynamical laws with each other and with the desired information. Details of this approach can be obtained from Wadsworth et al. (loc. cit.). The flow chart on Figure 3.1 was adapted from this publication and shows the logical steps into which exploration seismology can be broken down and how the observations may be subjected to either of the two mathematical approaches.

In the next part of this chapter, the deterministic filters that were studied are proposed. These are respectively the 3-point operator (Backus (1959), Neidell (1972)) and the 4-point filter (Kunetz (1964), Koehler (1964) and Neidell (1972)). In section 3.2, the earth model and the assumptions that are made in order to carry out the present study are given. Details of the 3-point filter and the results of its application are outlined in section 3.3 while the same is presented for the 4-point operator in section 3.4. The application of prediction-error deconvolution

PHYSICAL SITUATION	DATA	TREATMENT OF DATA	
		DETERMINISTIC	PROBABILISTIC

INITIAL MATERIAL

| SEISMIC WAVES FROM AN IMPULSIVE SOURCE | SEISMOGRAM TRACES | PHYSICAL THEORIES ON WAVE PROPAGATION | STATISTICAL THEORIES ON TIME SERIES |

DESIRED INFORMATION

| INTERPRETATION OF GEOLOGIC STRUCTURE | REFLECTION AND REFRACTION TIME DETERMINATIONS | SOLUTIONS OF INTEGRAL AND DIFFERENTIAL EQUATIONS | DYNAMIC AND PROBABILISTIC CHARACTERISTICS OF THE TRACES |

The deterministic and probabilistic approaches to seismology.

Figure 3.1 . The logical steps into which the seismic process can be broken down. (after Wadsworth et. al. (1953)).

to the same examples and the comparison of its performance with those of the above methods is given in section 3.5 .

3.1.1   Deterministic Operators.

In section 2.3.1 (b), the problems of the choices of the parameters N, α and λ for the prediction-error deconvolution technique were discussed. Deterministic filters for multiple attenuation (deferred from section 2.3.1(a)) do not present these problems. The value of N in particular, is fixed by the earth model that one chooses to represent the geology and the z-transform (Jury, 1964) of the given filter is analytically evaluated for such a model.

The design of deterministic operators is simpler and involves the calculation of the complete response of the earth's model that is chosen to approximate the geology. Their implementation (for an N-layered model) requires the knowledge of N+1 reflection coefficients and N two-way travel times. The filter has a polynomial z-transform of the form

$$D(z) = \sum_{i=1}^{N} d_i \, z^{t_i} \qquad\qquad .. \ (1)$$

where

$$d_i = d_i(c_0, c_1, \ldots, c_N),$$

$$t_i = t_i(\tau_1, \tau_2, \ldots, \tau_N),$$

$$c_i = \text{reflection coefficient at interface i, and}$$

τ_i = two-way travel time in layer i. In this thesis, 'N-layer' refers to N finite-thickness layers as in Neidel (1972).

One form of the filter occurs for an earth model with N=1 and it is shown that such a filter requires two reflection coefficients and one two-way time and that it has only three non-zero coefficients (Backus, 1959). Its design, implementation and efficiency in suppressing the seabed multiples are presented and illustrated with synthetic and real data examples.

The addition of another layer to the model results in a filter that requires three reflection coefficients (c_0, c_1, c_2) and two two-way times (τ_1, τ_2) (Kunetz,1964 and Koehler, 1964).The design and use of this filter in suppressing a 2-layer reverberatory wavelet are discussed and illustrated in section 3.4 by using synthetic and real data examples.

The assumptions that are made and the earth's model that is used in such studies are given below.

3.2   The Earth's Model

The layered earth approximation which was prompted in chapter 2 (section 2.2.1(b)) and which led to the convolution model (equation 3, chapter 2) is resumed. The assumptions are that

(a) the earth consists of a finite number of horizontal, homogeneous layers which are isotropic to small strains,

(b) seismic wave propagation obeys the one-dimensional wave equation,

(c) seismic waves propagate at normal incidence to these layers. In noiseless situations, they lead to the discretized representation (Robinson, 1957, Habibi-Ashrafi , 1978) of the

output y(k) from the earth due to an input s(k) as

$$y(k) = q(k) * s(k) \qquad \text{.. (2)}$$

where q(k) is the impulse response of the layered earth and *
denotes convolution. In z-transform notation, equation (2)
becomes

$$Y(z) = Q(z) S(z) \qquad \text{.. (3)}$$

If theinput s(k) is an impulse δ(k), at k=0 (theoretically,
spiking deconvolution can always be performed in order to
establish this), then S(z)=1 and

$$Y(z) = Q(z) \qquad \text{.. (4)}$$

The observed seismogram is equivalent to the impulse response of
the earth. This seismogram can be expressed in the convolutional
model (Robinson, 1979) as

$$y(k) = r(k) * m(k) \qquad \text{.. (5)}$$

                        represents   coefficient
where r(k) $\wedge$ the reflection $\wedge$ sequence of the N-layered earth
model and m(k) is the section multiple train which is the result
of the reverberations occurring within the entire N-layered
geological section. In the representation of equation (5), it is
assumed that the reflection coefficients are small so that
their products of the third and higher orders can be neglected.
If this is not so, then the model is **NOT** convolutional.

Robinson (1979) has depicted the convolutional model of an
observed seismogram y(k) as a pure negative feedback system. A

pure feedback system is necessarily a minimum delay system. It can be asserted that the sectional multiple train m(k) is a minimum delay system. In effect, the earth acts as a minimum delay system in producing the train of multiples that appear on the reflection seismogram. As a consequence, M(z) can be expressed as the inverse of a polynomial D(z), that is

$$M(z) = 1 / D(z) \qquad\qquad .. (6)$$

and

$$Y(z) = R(z) / D(z) \qquad\qquad .. (7)$$

The deterministic filtering methods work as follows. Starting with an N-layered earth model, the expression Y(z) can be evaluated by using the assumptions given above, the physics of seismic wave propagation, and analytical methods. This expression is of the form that is given on the right-hand side of equation (7) and r(k) can be obtained by convolving y(k) with d(k).

The problem is that the coefficients d_i depend on the reflection coefficients c_i which are being sought so that efficient multiple suppression is possible only when the reflection coefficient sequence is properly estimated or is totally available. This is the main difficulty in the use of deterministic filters for multiple elimination. It is shown later that the coefficient d_0 is always unity and that for any k not equal to zero, d_k depends only on the autocorrelation coefficients $\emptyset_{rr}(\tau)$ of the reflectivity sequence at lags that are greater than zero.

This indicates that in theory, prevalent multiple reflection

61

problems exist only in cases where the reflectivity sequence is non-white ($\emptyset_{rr}(\tau)$ is not a spike $\delta(\tau)$ at $\tau = 0$). When $r(k)$ is white, random and stationary , the section multiples should generally cancel the effects of each other out such that

$$D(z) = 1$$

and

$$Y(z) = R(z) \qquad \qquad .. \ (8)$$

3.3 The Simplest form of a Deterministic Filter.

The classical approach to the modelling of the water-layer multiple wavetrain associated with a deeper primary event uses the Backus 3-point operator (Backus, 1959) which is the simplest form of a deterministic filter in this context. It is derived below and the results of its application to synthetic and real data are given.

The method proposed by Neidell (1972) was adopted and the result shows that the application of the filter produces a ghost reflection at twice the two-way travel time of the water layer. The z-transform notation is used through out.

With reference to Figure 3.2, c_0, c_1 and c_2 are the reflection coefficients of the free surface, the seabed and a deeper reflecting interface respectively and τ_1 and τ_2 are the two-way travel times within the sea water and the second layer

62
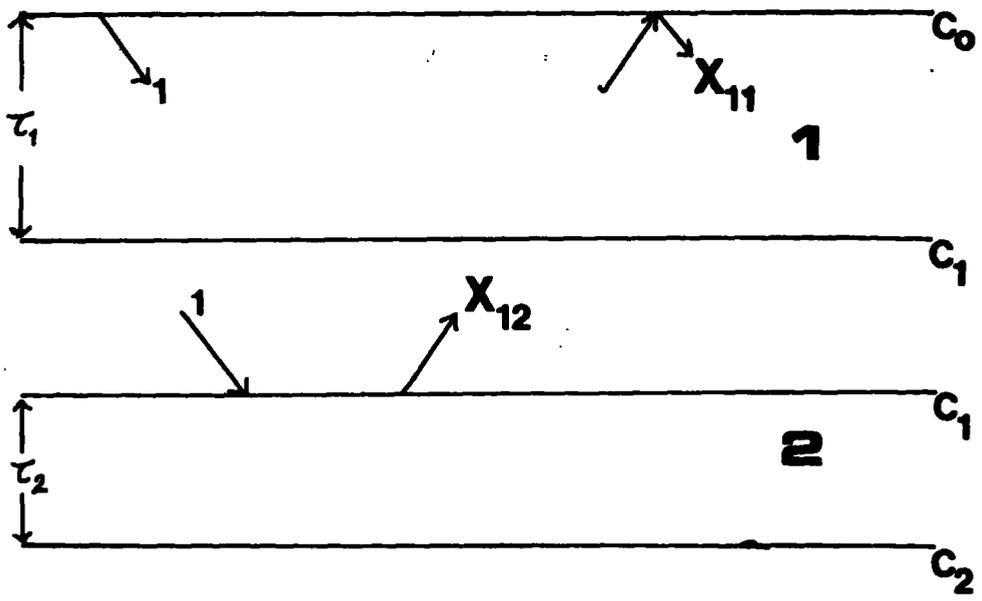
Figure 3.2 . A two-layer system decoupled at the second interface and showing the components of its response to a unit spike input.

respectively. The two layers have been decoupled on Figure 3.2 in order to make the contribution of deeper horizons to the water-trapped reverberation much clearer.

If an impulsive source at time t=0 is generated at the top of the first layer, then the downward travelling wavefield at the top of this layer at a later time has a z-transform

$$X_{11}(z) = 1 - c_0 c_1 z^{\tau_1} + (c_0 c_1)^2 z^2 {}^{\tau_1} - \ldots$$

$$= 1 / (1 + c_0 c_1 z^{\tau_1}) \qquad \ldots (9)$$

This source evokes an upward travelling wavefield with a z-transform of $X_{12}(z)$ at the base of the layer and its expression is

$$X_{12}(z) = t_1 t_1' c_2 z^{\tau_2} - t_1 t_1 c_1 c_2{}^2 z^2 {}^{\tau_2} + \ldots$$

$$= t_1 t_1' c_2 z^{\tau_2} / (1 + c_1 c_2 z^{\tau_2}) \qquad \ldots (10)$$

where t_1, t_1' are the downward and upward transmission coefficients respectively, of the seabed;

$$t_i = 1 + c_i$$

$$t_i' = 1 - c_i$$

The total downward-bound response at the top of the free surface is

$$Y(z) = 1 - [X_{11}(z) / (1 + c_0 X_{12}(z) z^{\tau_2})] \qquad \ldots (11)$$

If only the first two terms of the infinite series in equation

(11) are taken, then

$$Y(z) = 1 - (1 / G) + (c_0 X_{12}(z) z^{\tau_1} / G^2) \qquad \text{.. (12)}$$

where

$$G = 1 + c_0 c_1 z^{\tau_1}.$$

If multiples involving more than one bounce on the deeper reflector are ignored, then the expression of $X_{12}(z)$ can be approximated by its first term so that

$$Y(z) = \frac{c_0 c_1 z^{\tau_1} + (c_0 c_1)^2 z^2 \tau_1 + c_0 t_1 t_1' c_2 z^{\tau_1 + \tau_2}}{1 + 2c_0 c_1 z^{\tau_1} + (c_0 c_1)^2 z^2 \tau_1} \qquad \text{.. (13)}$$

which takes the form of equation (7) and the numerator is equivalent to R(z) and

$$D(z) = 1 + 2c_0 c_1 z^{\tau_1} + (c_0 c_1)^2 z^2 \tau_1 \qquad \text{.. (14)}$$

The deterministic filter has a z-transform D(z) and it has only three non-zero coefficients which depend on the autocorrelation coefficients of the reflectivity sequence at lags other than zero. When it is applied, a ghost event with amplitude $(c_0 c_1)^2$ appears at time $2\tau_1$ (see R(z) or numerator of Y(z)). The z-transform of the result is not exactly equal to that of the reflectivity sequence. This is because the marine case is under

64

consideration and the detecting streamer is assumed to be beneath the free surface. If in addition the effect of the ghost is ignored, the function R(z) will be equal to the z-transform of the reflectivity sequence. The following figures show the performance of this filter in various situations. On Figure 3.3 is the earth's model that was used. Table 3.1 shows the layers' parameters and the 2-way travel times T(i) at which the primary reflections are expected, where

$$T(i) = \sum_{j=1}^{i} \tau_j$$

On Figure 3.4, the source wavelet that was used and its power spectrum (normalized to 1) are shown. The complete normal incidence impulse response of the layering was computed by the layer matrix method (Claerbout, 1976, pp. 150). The seismic trace was obtained by a convolution of the impulse response and the source wavelet. Twelve of such traces are plotted on Figure 3.5(a). The corresponding autocorrelogram is shown on Figure 3.5(b) and it indicates the presence of both long and short-period multiples that are generated by a 2-layer structure. The seabed multiples have a period of 67 msec (τ_1= 67 msec) and the 3-point filter is expected to attenuate them except for a ghost reflection that is expected at 134 msec. The value of c_1 was assumed to be known from the forward procedure (Table 3.1).

The filtered section and its autocorrelogram are shown on Figures 3.6(a) and 3.6(b) respectively. The seabed multiples have
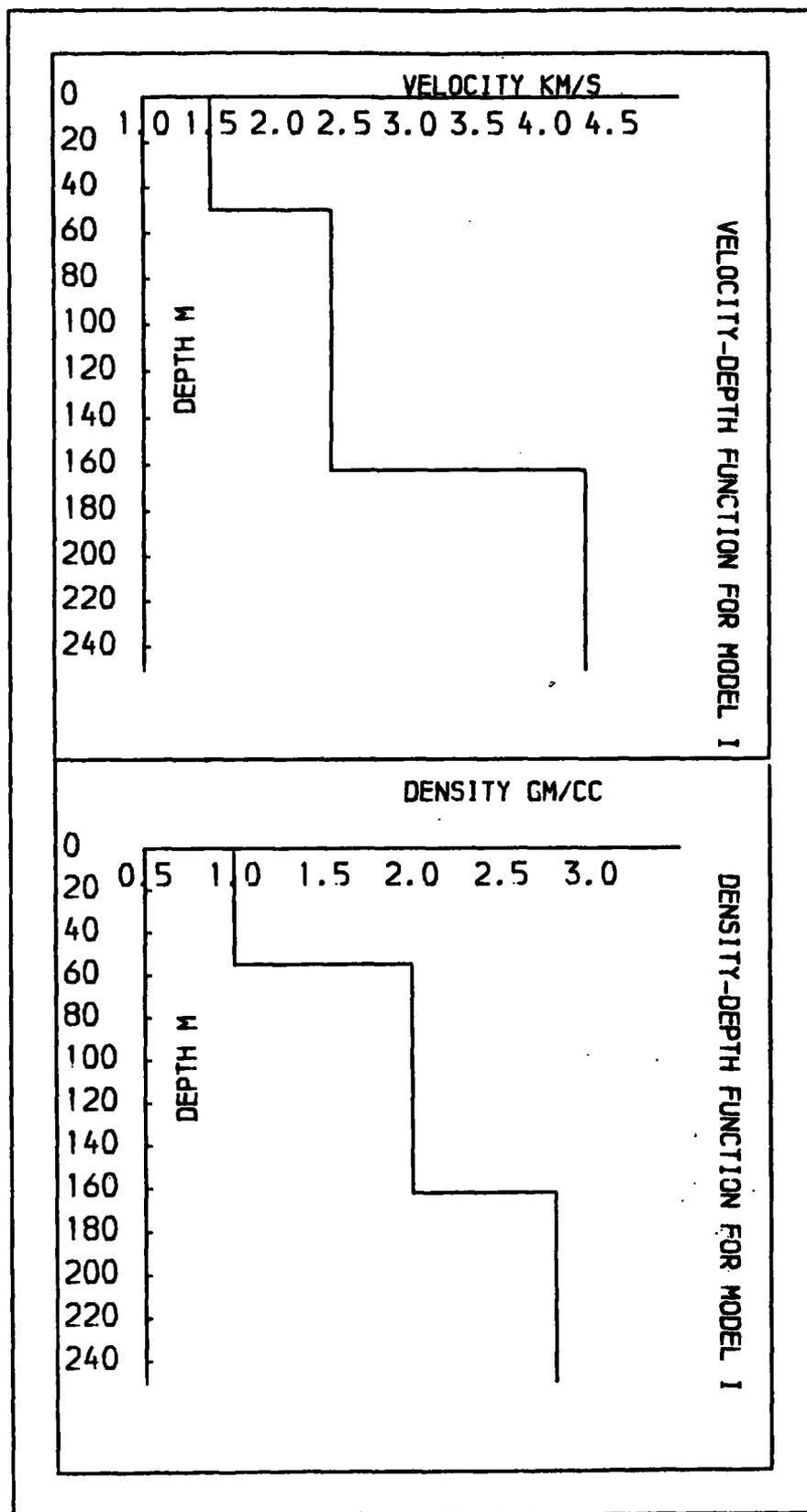
Figure 3.3 . velocity and density models for a two-layer earth.

TABLE 3.1   PARAMETERS FOR 2-LAYER MODEL.
****

LAYER NO. i	V(i)	RHO(i)	C(i)	T(i)
1	1.5	1.	-0.523809	67
2	2.4	2.	-0.429929	161
3	4.3	2.8		

V(i) in Km/sec.
Rho(i) in g/cc.
T(i) in milliseconds.

$$C(i) = \frac{V(i)*Rho(i) - V(i-1)*Rho(i-1)}{V(i)*Rho(i) + V(i-1)*Rho(i-1)} \, .$$

Figure 3.4 . Source wavelet and its power spectrum.

source signal (37hz (3) -158hz (8))

power spectrum
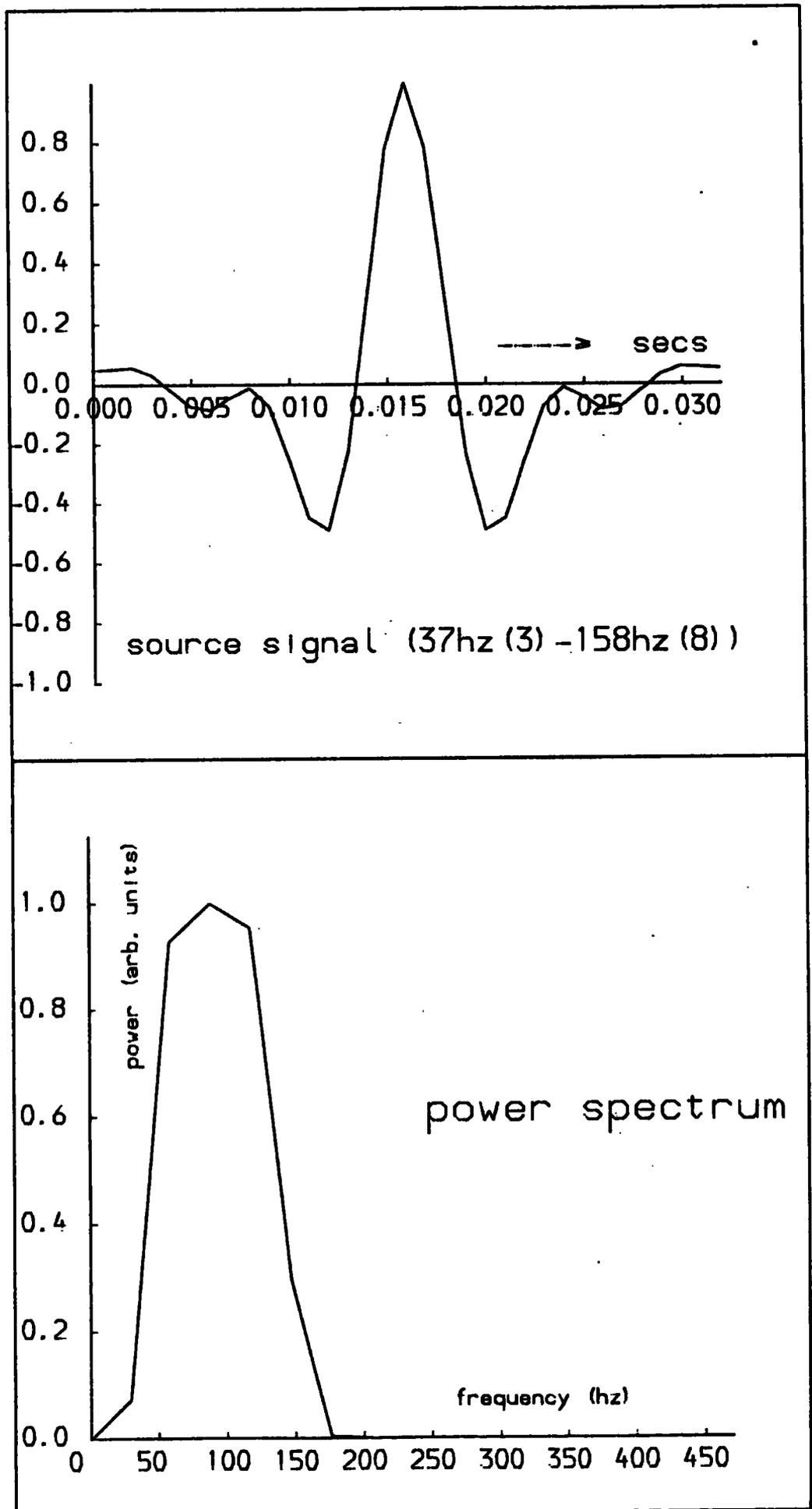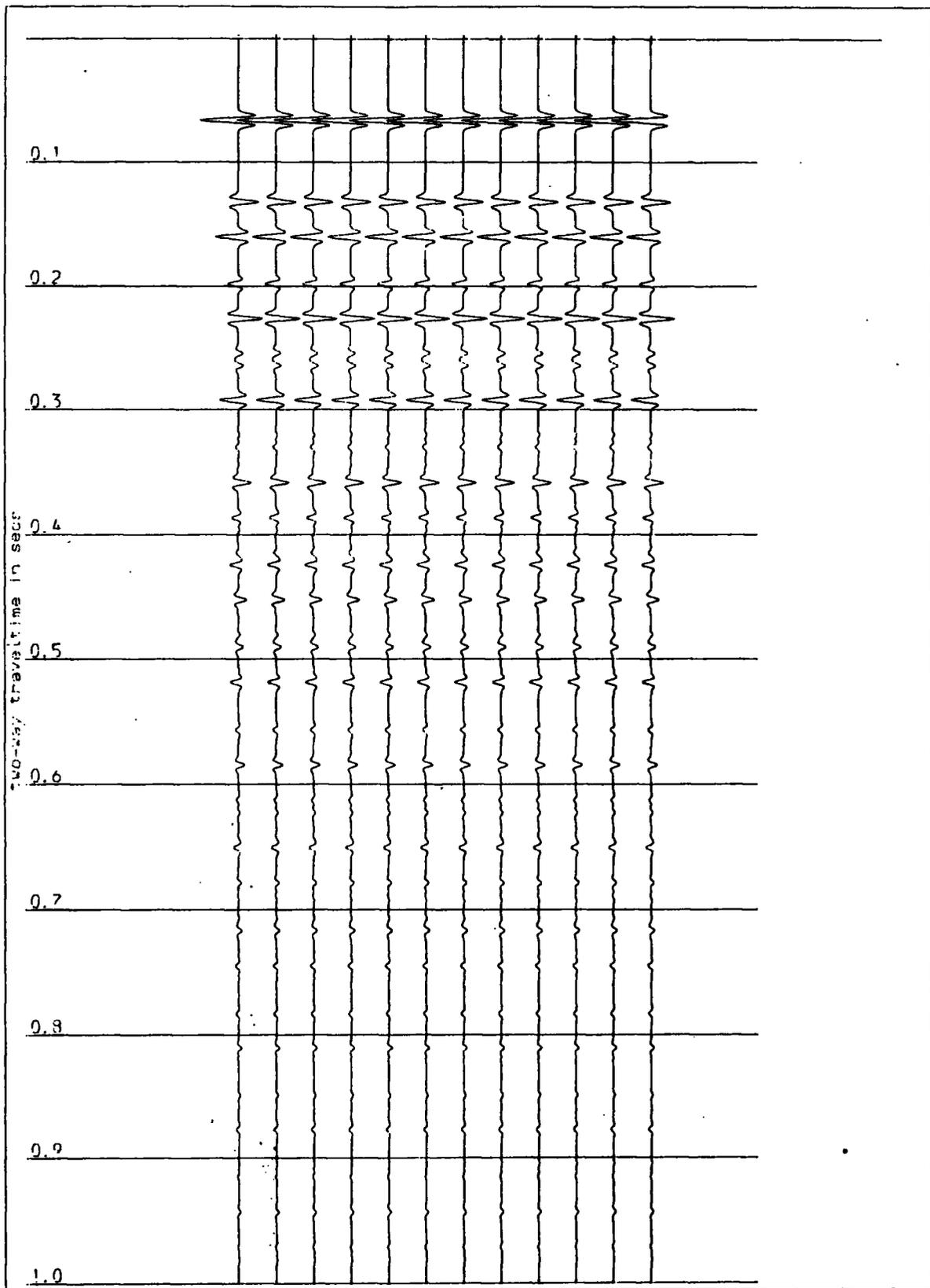
Figure 3.5(a). Synthetic section.
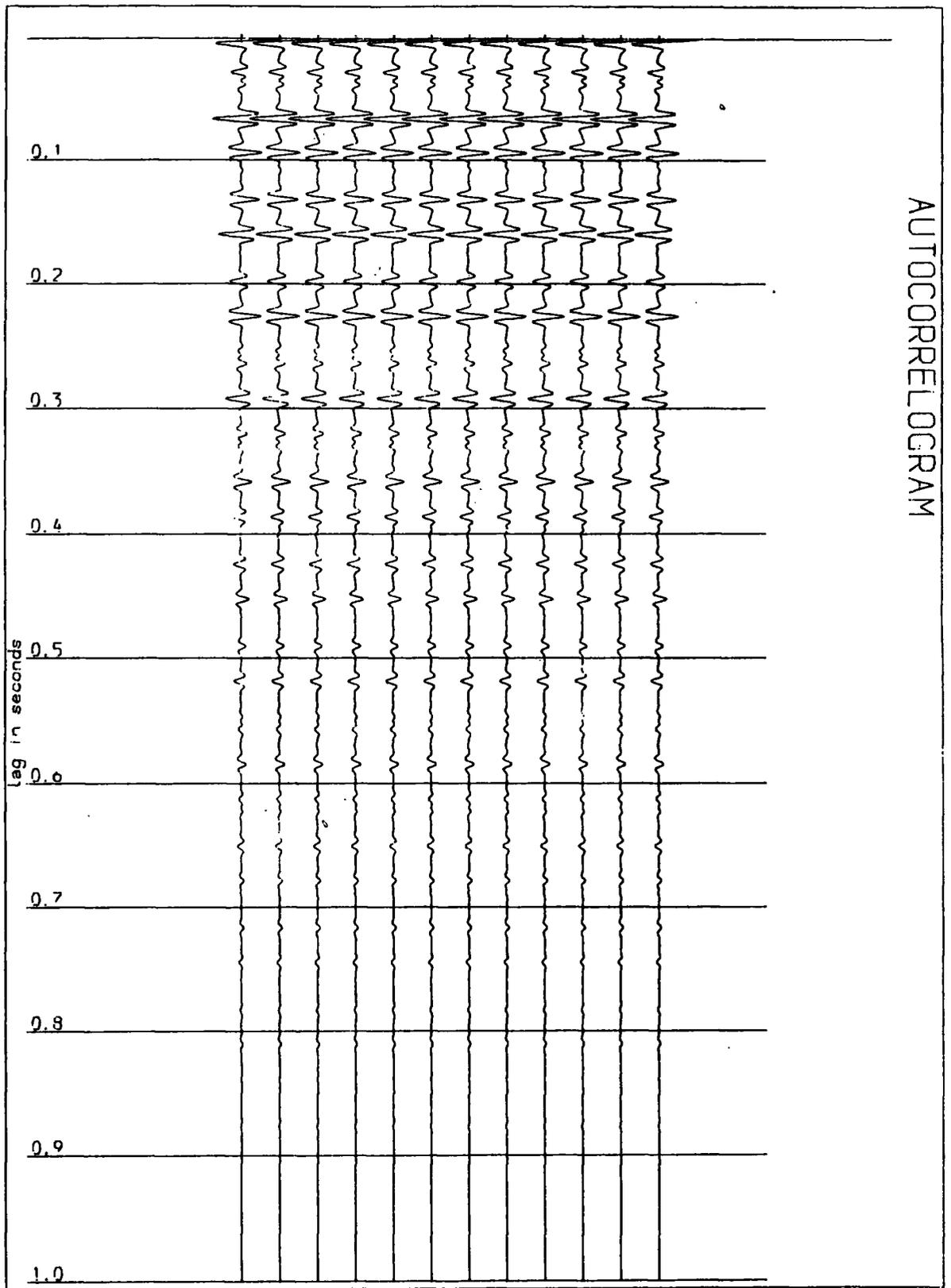
Figure 3.5(b). Autocorrelogram of raw synthetic data.
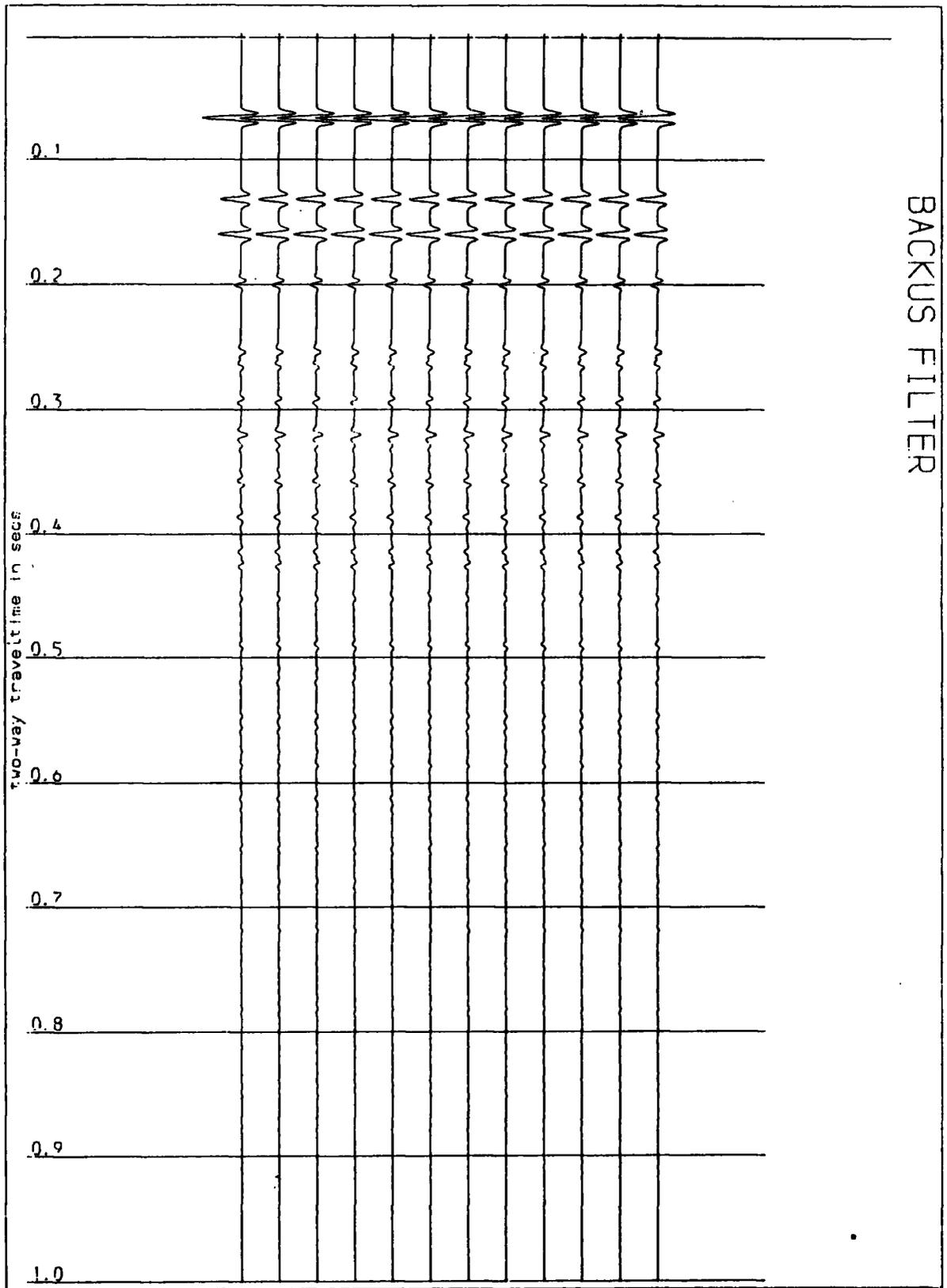
Figure 3.6(a). Section on Figure 3.5(a) after filtering with a three-point filter.
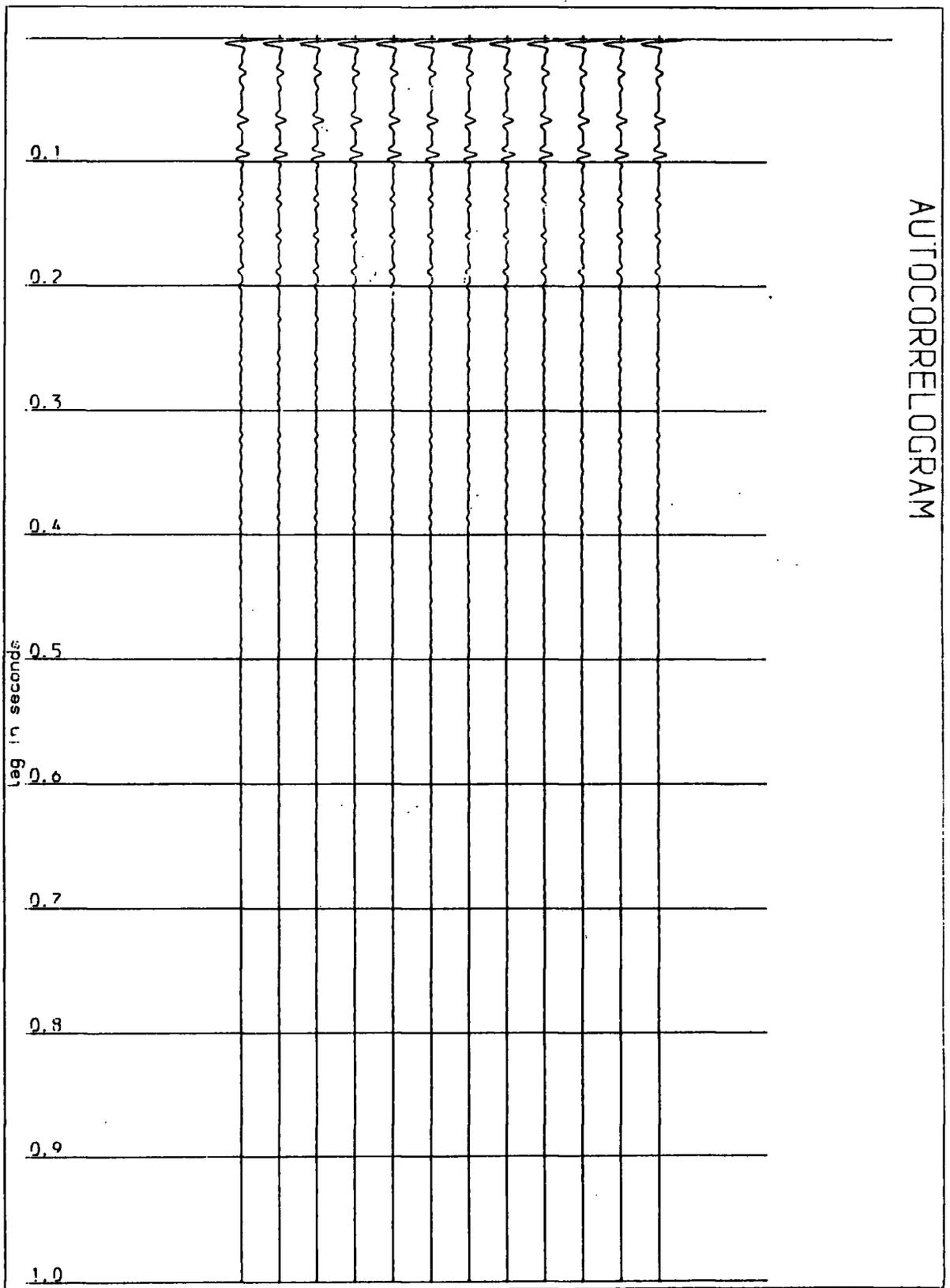
Figure 3.6(b). Autocorrelogram of the section on Figure 3.6(a).

been suppressed. The autocorrelogram of the result has still got peaks which are due to the correlation of residual multiples (peg-legs within the second layer), the ghost reflection and these multiples, and also due to the correlation between the two primaries at a lag of 94 msec.

Real Data Examples

On Figure 3.7(a) are near traces sorted from the 6-fold data (section 1.2). The shot-receiver spacing being 10 m, the moveout is negligible for the range of rock velocities encountered and the records can be approximated to zero-offset traces (the angle of incidence is less than 5° for a water depth of 55 m). An exponential scaling of +5.2 dB/sec (see Appendix B) was applied to compensate approximately for spherical spreading and the other amplitude lowering effects. The direct wave on each trace was muted and it was band-pass filtered. All the sections were plotted with the same gain after the traces were gain ranged (AGC with a gate of 160 msec) and normalized to unit amplitude. All the autocorrelograms were also displayed with the same gain.

The seabed reflection (Figure 3.7(a)) is at about 70 msec and there is a primary reflection at about 110 msec. The first seabed multiple arrives at 145 msec. In the absence of any processing, the S/N ratio is low, the character of events is poor and their continuity is patchy. The records are therefore likely to obtain a noisier appearance after any initial processing and the latter can be assessed by the autocorrelogram alone. The
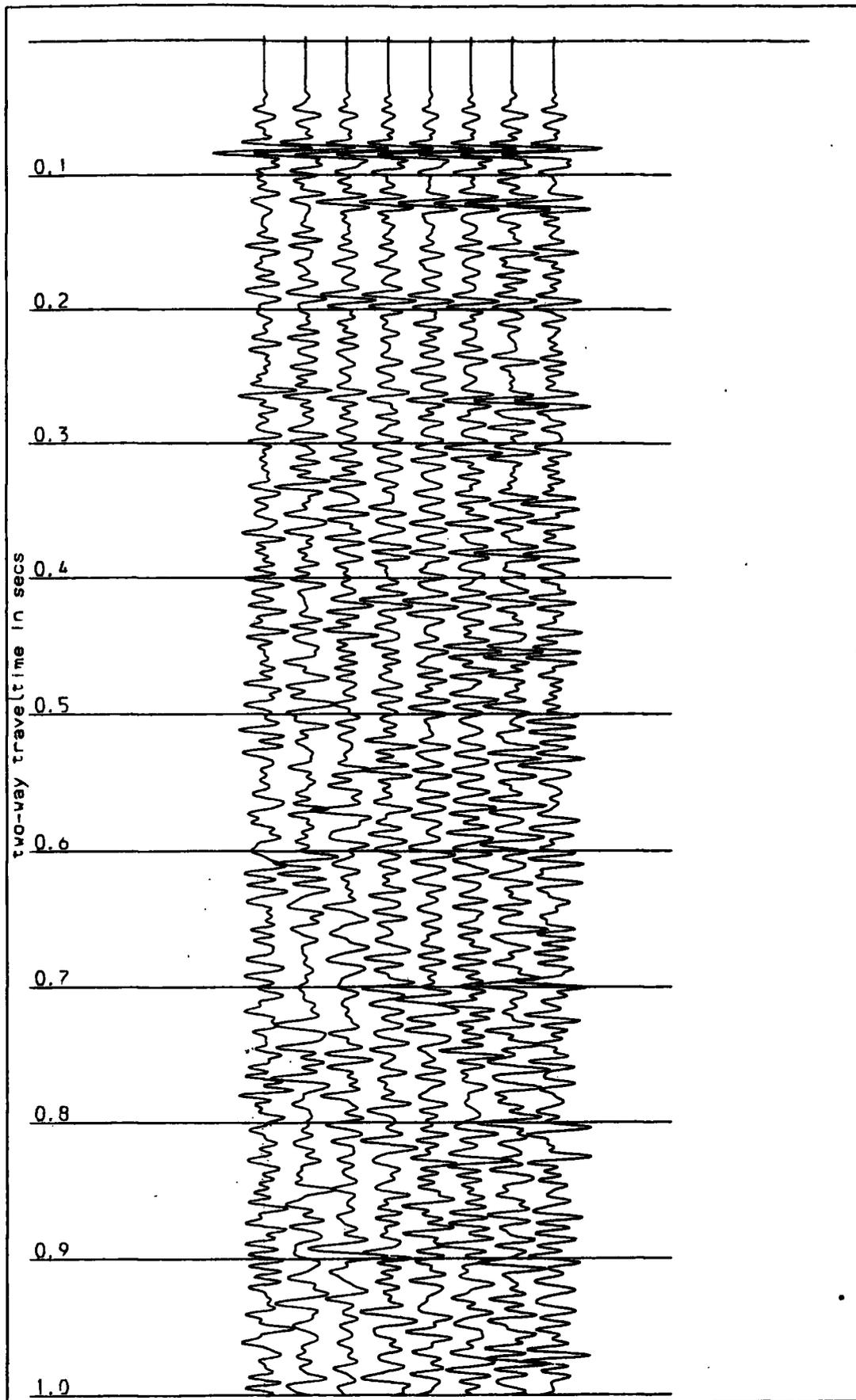
Figure 3.7(a). Near-offset records selected from the 6-fold data (section 1.2) of line 8201A.

autocorrelogram of these records is displayed on Figure 3.7(b). There are both long and short-period multiples present.

The 3-point filter was applied to the data and the results and their autocorrelogram are given on Figures 3.8(a) and 3.8(b) respectively. A reflection coefficient of 0.1556 and a τ_1 of 70 msec were used. The estimation of these parameters is discussed in section 3.4.3.

On Figure 3.8(a), the ghost reflection appears at about 140 msec and it looks **weak** in amplitude than it actually is because of the AGC. The autocorrelogram shows a good but limited performance of the filter and the ghost is more clearly evidenced. Ideally different values of c_1 and τ_1 should be used for each trace but this would be practically inefficient.

Backus (1959) applied this filter to suppress the reverberations present in marine records from the Persian Gulf and Lake Maracaibo (Kanasewich, 1975, pp. 221). Hughes (1980) has applied it in the w-k domain to real seismic data while Morley and Claerbout (1983) used it in a 'split' form for predictive deconvolution in the shot-receiver space. The low S/N ratio of the data and hence an unlikely success of spiking deconvolution before filtering contributes to its inefficiency in this study. The application of prediction-error deconvolution to attenuate the same range of multiples is compared to it later.
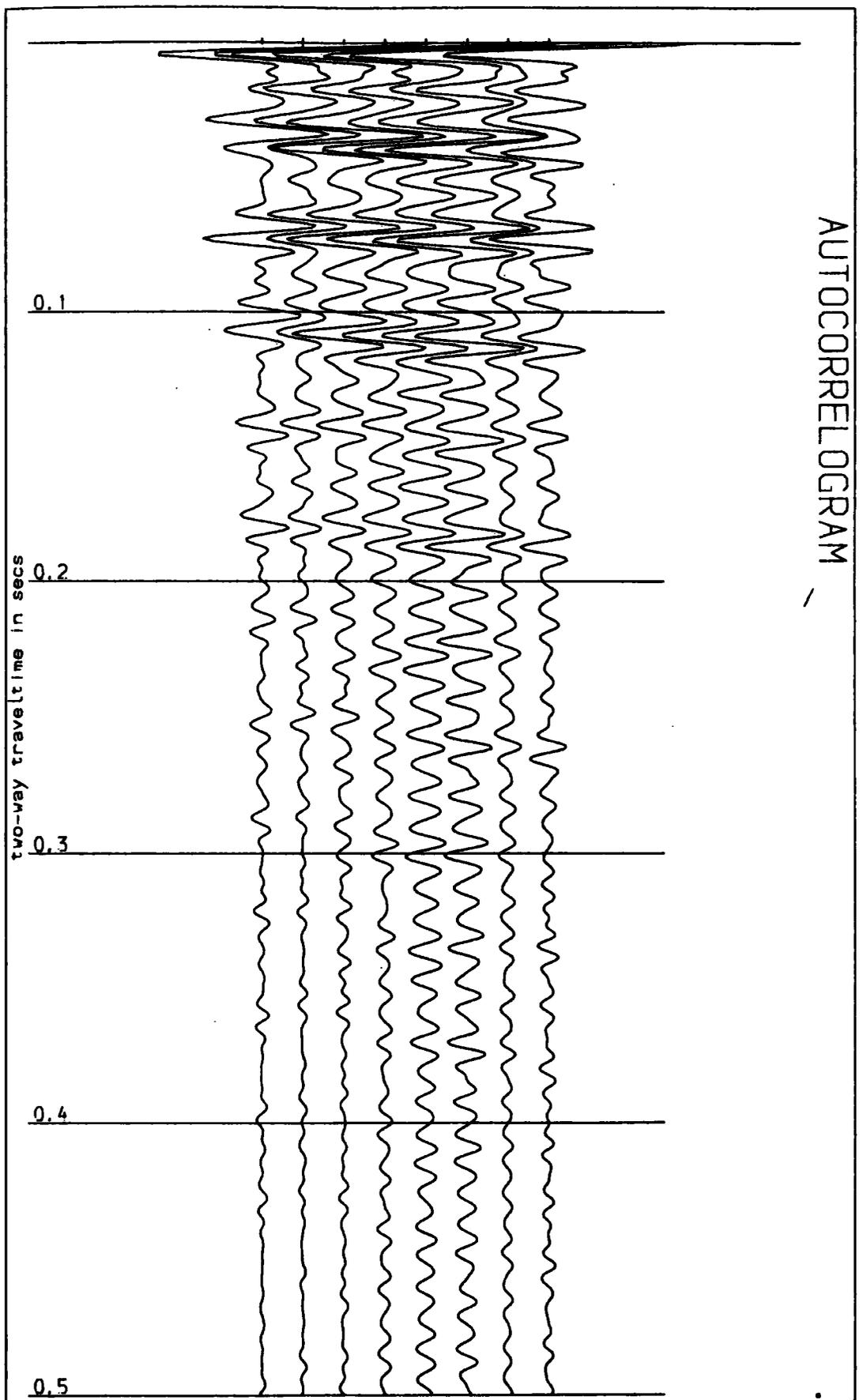
Figure 3.7(b). Autocorrelogram of the real records of Figure 3.7(a).
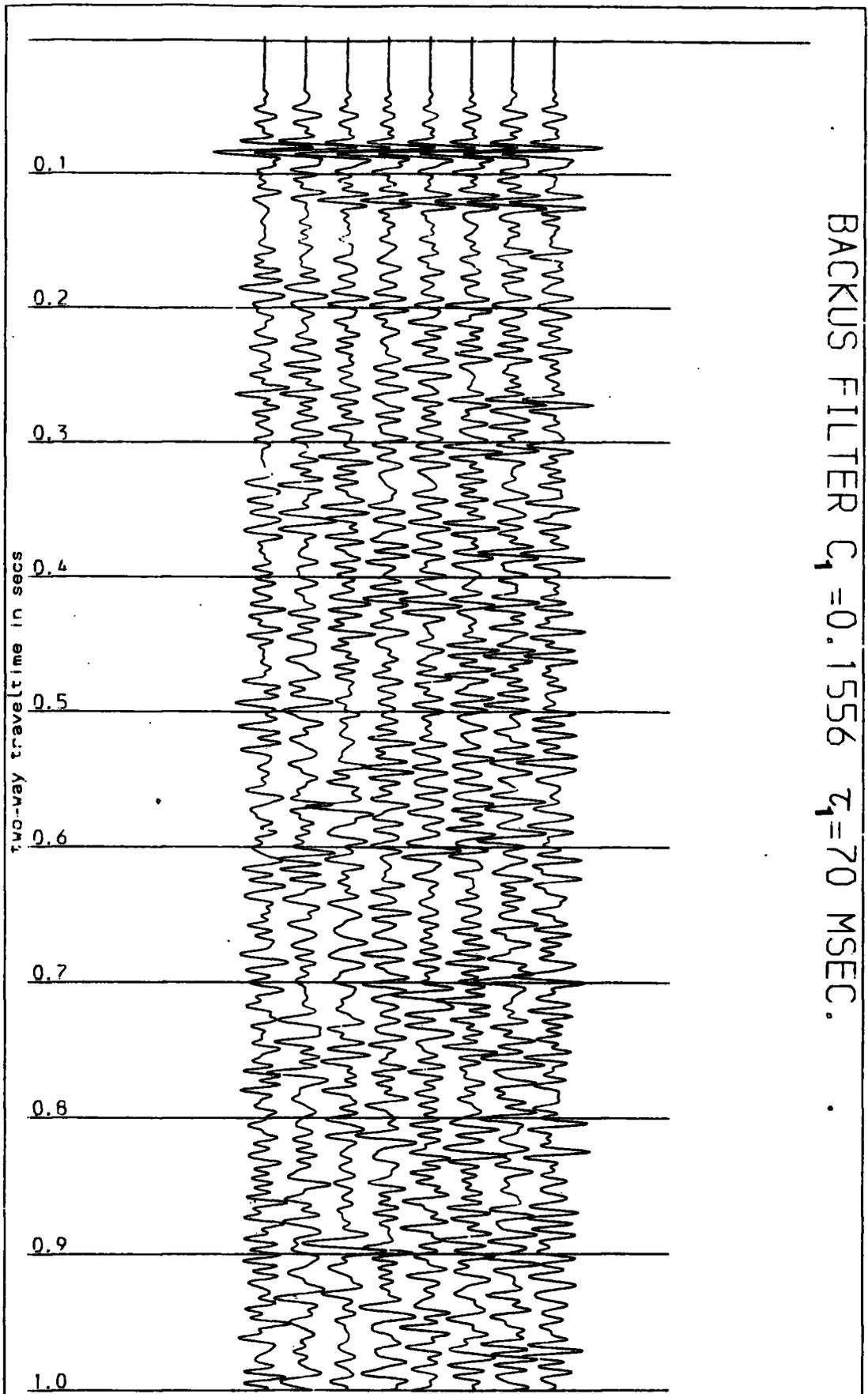
Figure 3.8(a). The section of Figure 3.7(a) after filtering with a three-point operator.
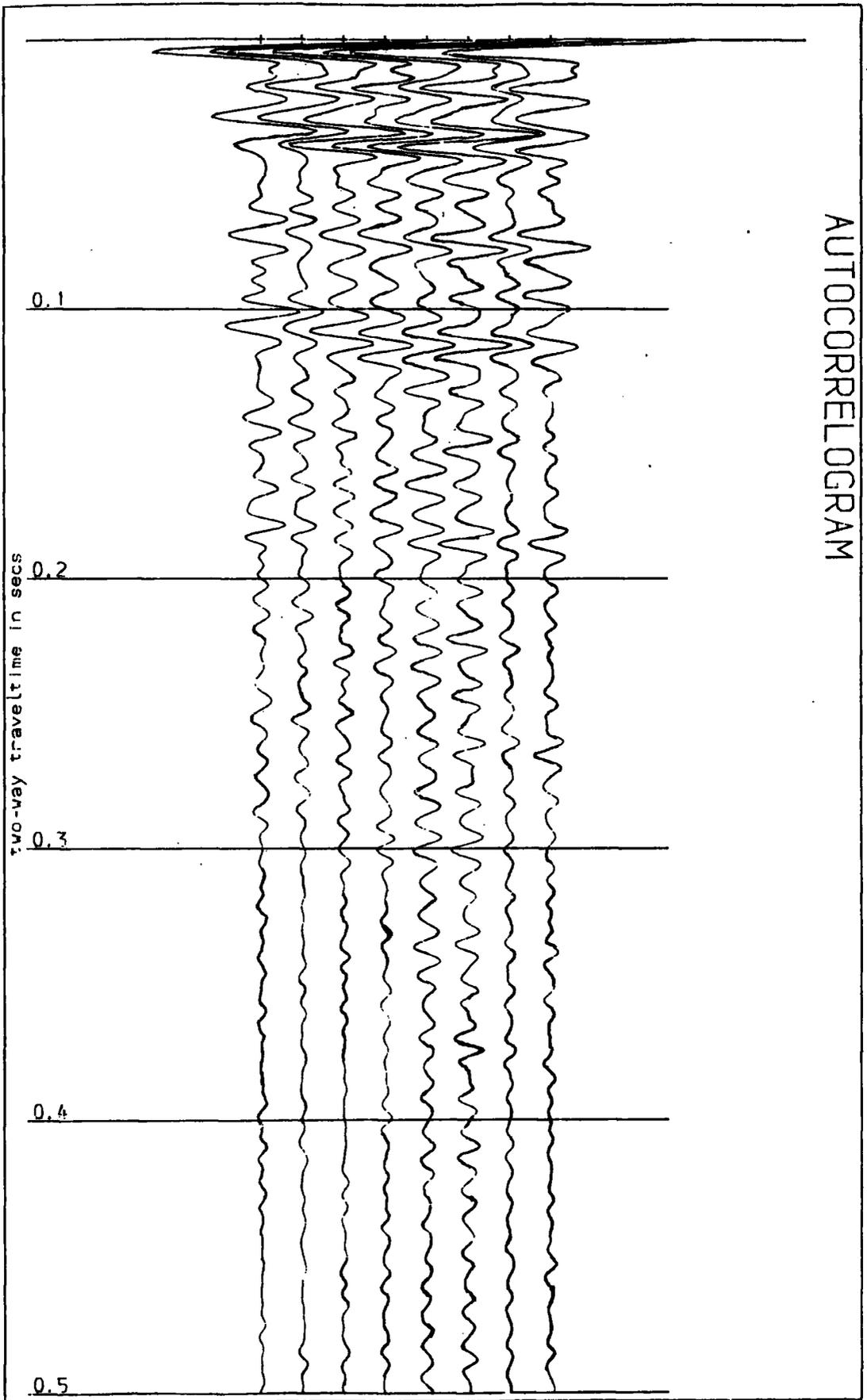
Figure 3.8(b). Autocorrelogram of the section of Figure 3.8(a).

3.4   Extension to a Higher number of Coefficients.

3.4.1   Derivation.

Strong multiple reflections arise when there is a combination of the free surface, a hard seafloor and a strong reflector (for example, the surface of limestone with overlying marl off the coast of Durham) beneath the latter. A theoretical 2-layer (3-interface) situation was used to study the deterministic technique of dereverberating the response of such a system. The complete response of an appropriate 2-layer model is derived and it is shown that a 4-point operator (Koehler, 1964) is adequate to deconvolve the multiple wavetrain.

The layer-matrix method (Claerbout, 1976) was applied in order to generate normal incidence synthetic seismograms. A matrix method (Robinson and Treitel, 1978) is therefore adopted. Referring to Figure 3.9(i) and 3.9(ii), c_j and t_j are the reflection and transmission coefficients of interface j for a plane normally incident downward travelling wave and c'_j and t'_j are their upward-bound counterparts respectively, such that

$$t_j = 1 + c_j$$

$$c'_j = - c_j \qquad\qquad .. (16)$$

$$t'_j = 1 - c_j$$

D_j and U_j respectively represent the z-transforms for the downward and upward wavefields at the top of layer j and D'_j and
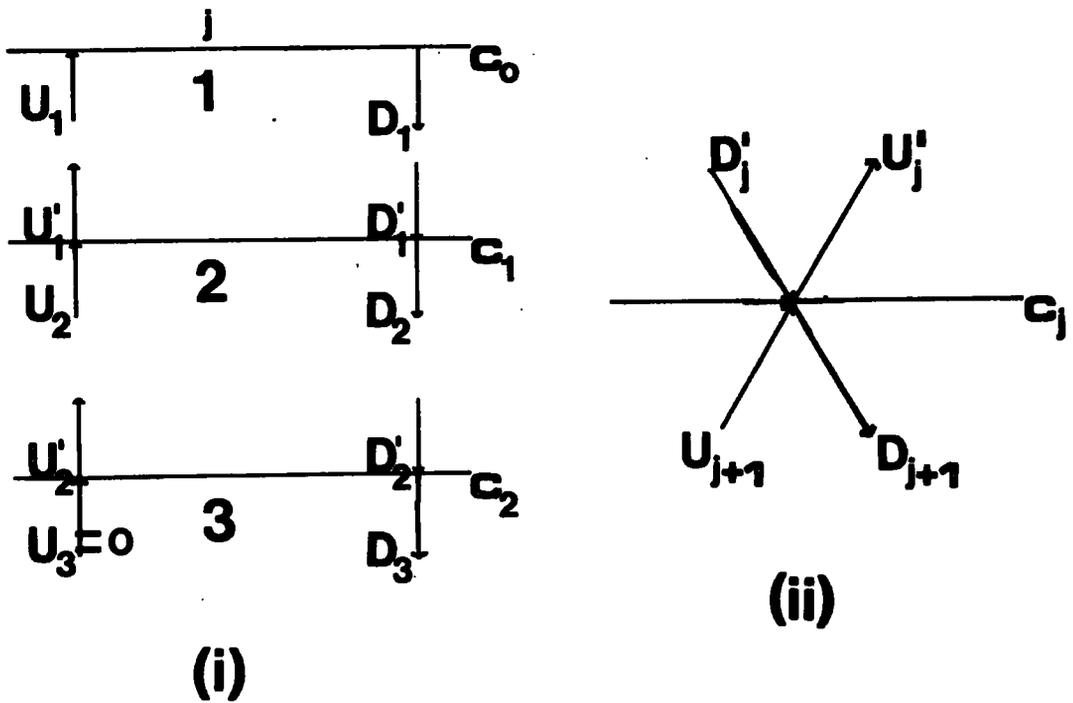
Figure 3.9 . (i) Two-layer earth model showing the upward (U) and
            the downward (D) propagation of the seismic wavefields
    and (ii) the upward and downward reflection of these wavefields
            at any interface j .

U_j' respectively the same quantities at the base of the layer j. The $[D_j, U_j]$ and $[D_j', U_j']$ differ only by a time delay. Absorption effects are not taken into account. Reflection and transmission of the wavefield at interface j (Figure 3.9(ii)) give

$$D_{j+1} = c_j' U_{j+1} + t_j D_j$$

$$U_j' = c_j D_j' + t_j' U_{j+1} \qquad \qquad \text{.. (17)}$$

The vectors

$$\bar{a}_{j+1} = \begin{bmatrix} D_{j+1} \\ \\ U_{j+1} \end{bmatrix} \quad \text{and} \quad \bar{b}_j = \begin{bmatrix} D_j' \\ \\ U_j' \end{bmatrix}$$

can be used to rewrite equation (17) as

$$\bar{a}_{j+1} = \alpha_j \bar{f}_j \bar{b}_j$$

where $\alpha_j = 1 \, / \, t_j'$ and

$$\bar{f}_j = \begin{bmatrix} 1 & -c_j \\ \\ -c_j & 1 \end{bmatrix}$$

Within the layer number j, the matrix $\bar{b}_j$ is obtained from $\bar{a}_j$ by a time-delay linear transformation representable by the matrix

69

$$\bar{e}_j = \begin{bmatrix} z^{\tau_j/2} & 0 \\ 0 & z^{-\tau_j/2} \end{bmatrix}$$

so that

$$\bar{b}_j = \bar{e}_j \, \bar{a}_j \qquad\qquad .. \ (19)$$

and $\quad \bar{a}_{j+1} = \alpha_j \bar{f}_j \bar{e}_j \bar{a}_j$

which can be expressed as

$$\bar{a}_{j+1} = \alpha_j z^{-\tau_j/2} \bar{g}_j \bar{a}_j \qquad\qquad .. \ (20)$$

where

$$\bar{g}_j = \begin{bmatrix} z^{\tau_j} & -c_j \\ -c_j z^{\tau_j} & 1 \end{bmatrix}$$

The matrix $\bar{g}_j$ is called the communication matrix (Robinson, 1966) or the layer matrix (Claerbout, 1976). Equation (20) shows how it can be used to recursively generate any $\bar{a}_{j+1}$ if $\bar{a}_1$ is available. For the 2-layer case, Figure 3.9(i) (j=2),

$$\bar{a}_3 = (\alpha_2 \, \alpha_1 z^{-(\tau_1 + \tau_2)/2}) \bar{g}_2 \bar{g}_1 \bar{a}_1 \qquad\qquad .. \ (21)$$

Figure 3.10 depicts a typical marine case in which an impulsive source is applied at the top of layer 1 and an upward

70
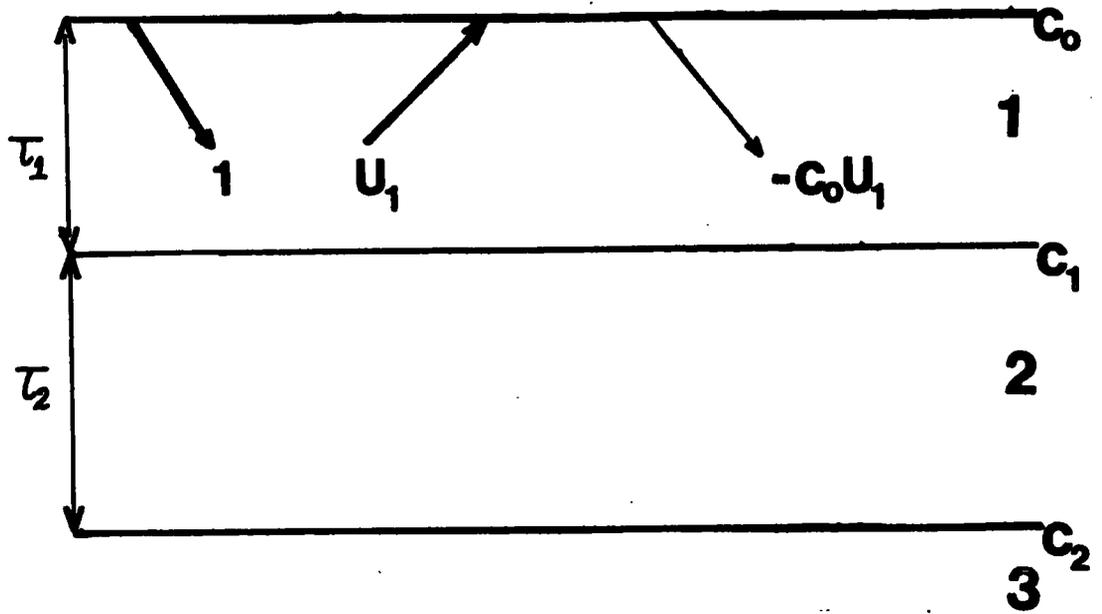
Figure 3.10 : Seismic wavefield near the free surface.

travelling wavefield U_1 undergoes a reflection at the free surface to produce a downward travelling wavefield $-c_0U_1$ so that

$$a_1 = [\ 1-c_0U_1 \quad U_1\ ]'$$

and since $a_3 = [\ D_3 \quad 0\ ]'$

(because there is no upward bound wavefield at the top of layer 3 (the half-space)), an expression of equation (21) yields the seismic response $Y(z)$ $(=U_1(z))$ beneath the free surface as

$$Y(z) = (c_1z^{\tau_1} + c_2z^{\tau_1+\tau_2})/(1 + c_0c_1z^{\tau_1} + c_1c_2z^{\tau_2}+c_0c_2z^{\tau_1+\tau_2}) \ .. \ (22)$$

which is of the form of equation (7) if

$$R(z) = c_1z^{\tau_1} + c_2z^{\tau_1+\tau_2} \qquad\qquad\qquad (a)$$

$$D(z) = 1 + c_0c_1z^{\tau_1} + c_1c_2z^{\tau_2} + c_0c_2z^{\tau_1+\tau_2} \quad (b) \ .. \ (23)$$

Equation 23(b) is the z-transform of the 4-point filter. It has four non-zero coefficients and is completely specified by the knowledge of five parameters. The coefficients depend only the autocorrelation coefficients of the reflectivity sequence at lags other than zero and d_0 is 1.

This procedure can be generalized to any number of layers greater than 2 and it can be shown (Robinson and Treitel, 1978) that the numerator of the right-hand side of equation (22) is equal to the z-transform of the actual reflectivity only when the reflection coefficients are small so that their higher order

products are negligible and that d_0 is always 1.

3.4.2   Application to Synthetic Seismograms.

The earth model of Figure 3.3 was used again and the complete impulse response (IR) was obtained by the layer matrix method. On Figure 3.11(a), the spike sequence (A) represents this response. The two primary events arrive at 67 msec and 161 msec respectively. All the other events are multiples that arise within the 2-layer system. The sequence (B) shows the autocorrelogram of (A) up to the lag of 500 msec and strong peaks can be noticed at lags other than zero showing the periodic events in (A). The sequence (C) shows the result of the application of the 4-point filter to (A). The values of c_1, c_2, and τ_i were those used in the forward approach. The two primary events are clearly resolved and the reverberation has been cancelled as the autocorrelogram (D) of (C) shows. There is a peak at a lag of 94 msec due to the correlation of the primaries. Figure 3.11(b) shows the same response except that an AGC has been applied to (A) and (C) before the plot. The effects of the noise caused by the AGC can be observed on (C) whose counterpart on Figure 3.11(a) appeared entirely dereverberated.

On Figure 3.12(a) the complete seismic trace (A) was plotted. The source wavelet of Figure 3.4 was used. Figure 3.12(b) is the counterpart of 3.12(a) with AGC on (A) and (C).

The effects of random noise were simulated by adding 14 layers to the model on Figure 3.3. The resulting structure is
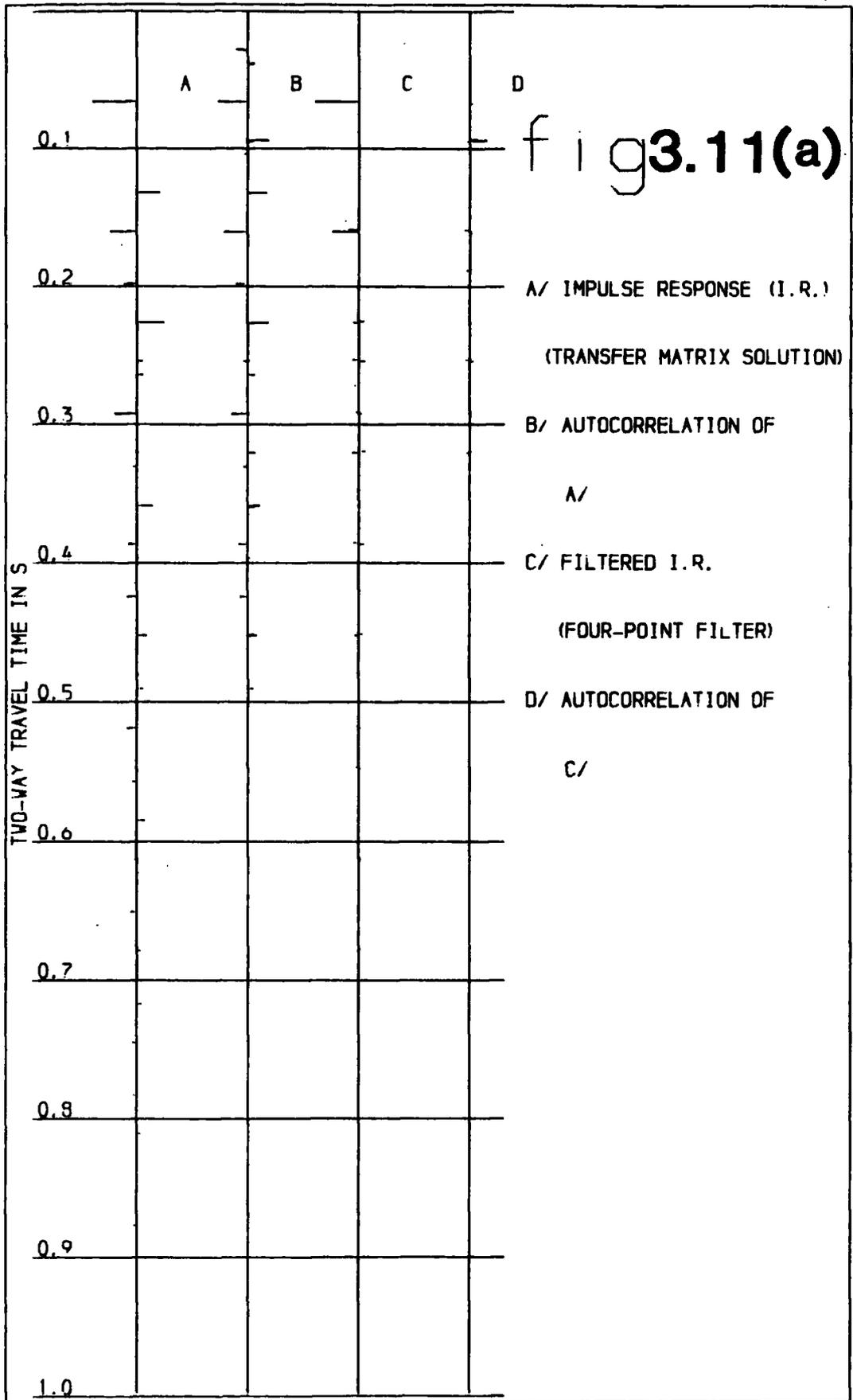
fig **3.11(a)**

A/ IMPULSE RESPONSE (I.R.)

(TRANSFER MATRIX SOLUTION)

B/ AUTOCORRELATION OF

A/

C/ FILTERED I.R.

(FOUR-POINT FILTER)

D/ AUTOCORRELATION OF

C/

fig**3.11(b)**

A/ IMPULSE RESPONSE (I.R.)

(TRANSFER MATRIX SOLUTION)

B/ AUTOCORRELATION OF

A/

C/ FILTERED I.R.

(FOUR-POINT FILTER)

D/ AUTOCORRELATION OF

C/

AGC ON

A/ AND

C/

fig 3.12(a)

A/ SYNTHETIC TRACE

(TRANSFER MATRIX SOLUTION)

B/ AUTOCORRELATION OF

A/

C/ FILTERED TRACE

(FOUR-POINT FILTER)

D/ AUTOCORRELATION OF

C/

fig **3.12(b)**

A/ SYNTHETIC TRACE

(TRANSFER MATRIX SOLUTION)

B/ AUTOCORRELATION OF

A/

C/ FILTERED TRACE

(FOUR-POINT FILTER)

D/ AUTOCORRELATION OF

C/

AGC ON

A/ AND

C/
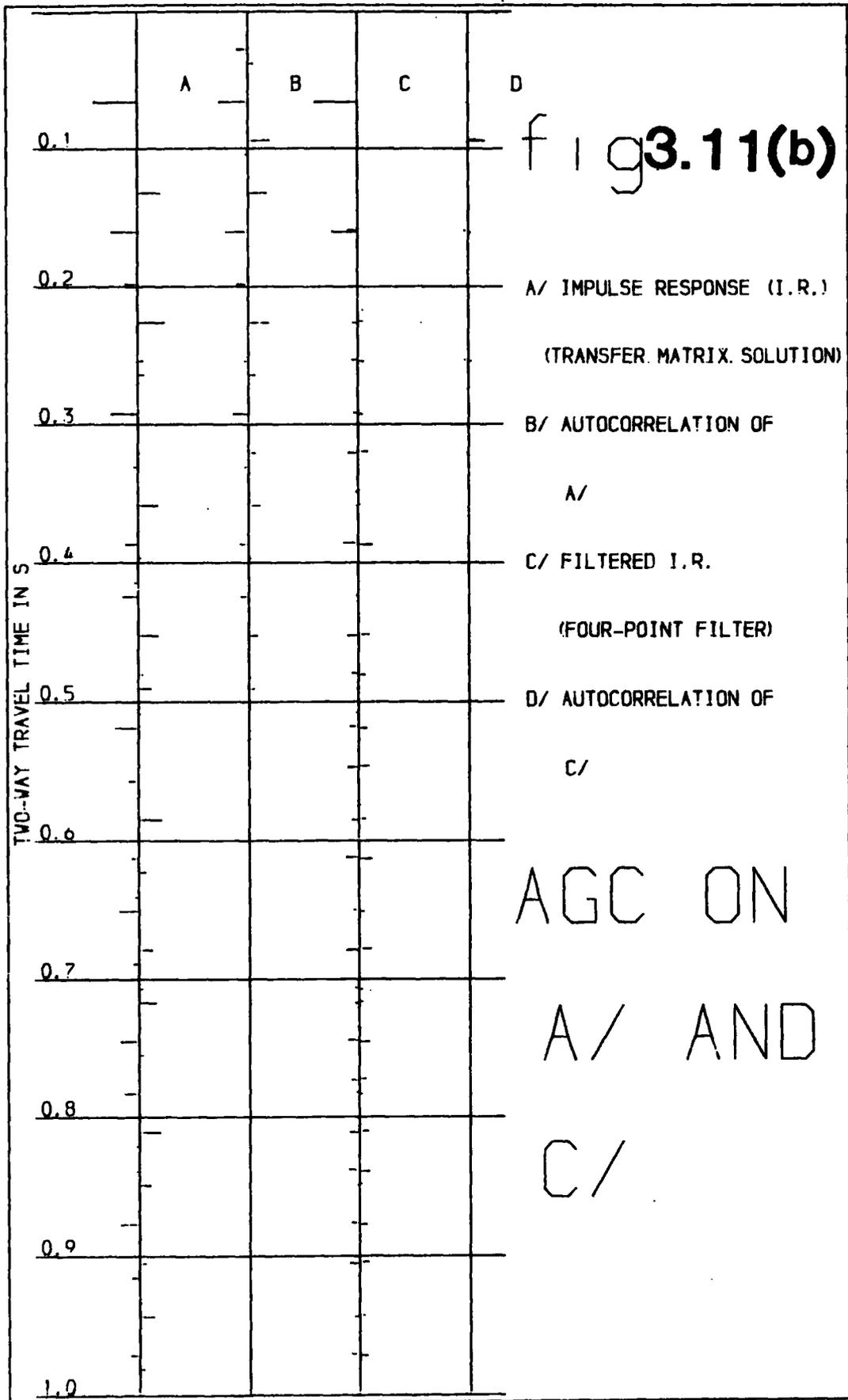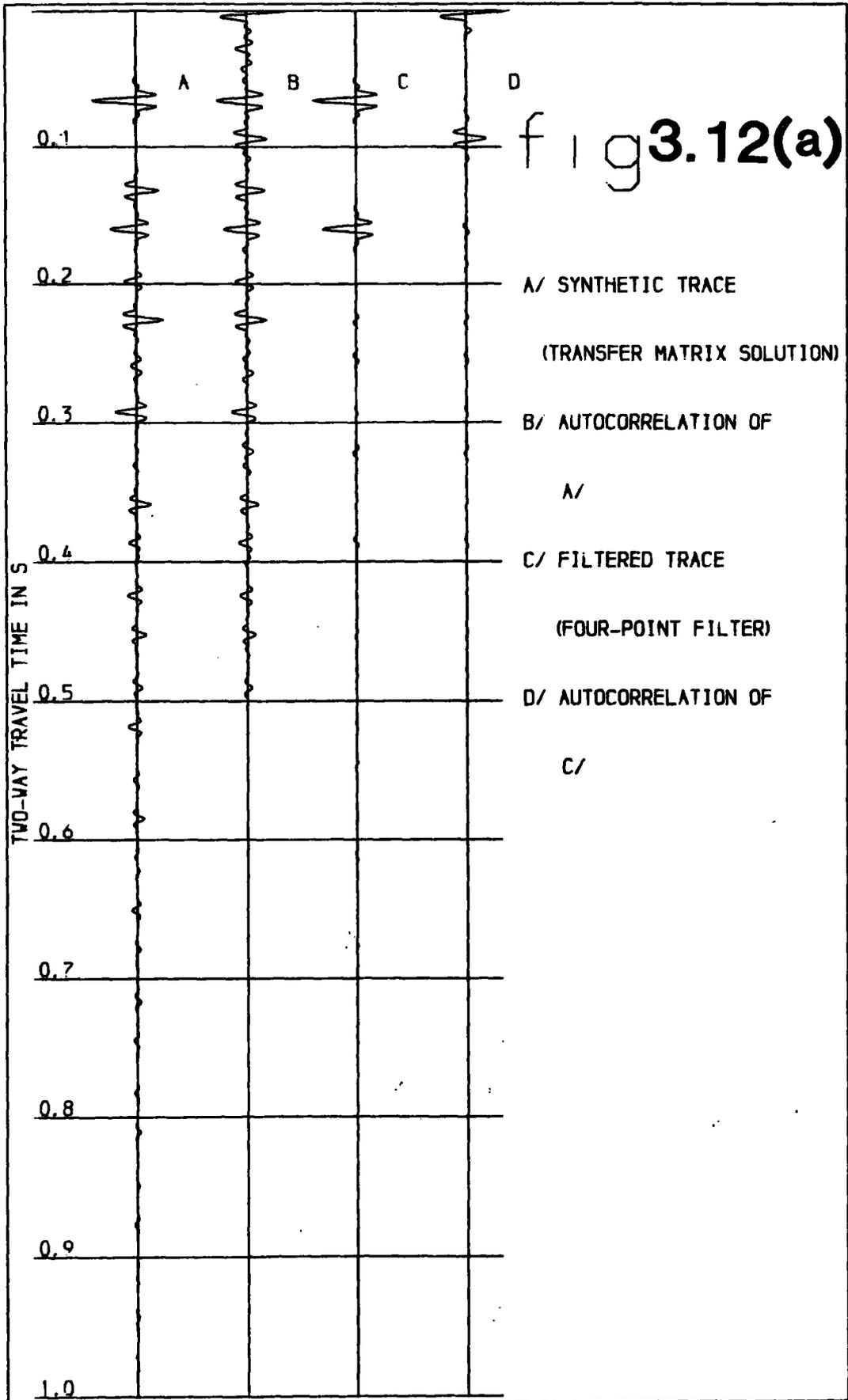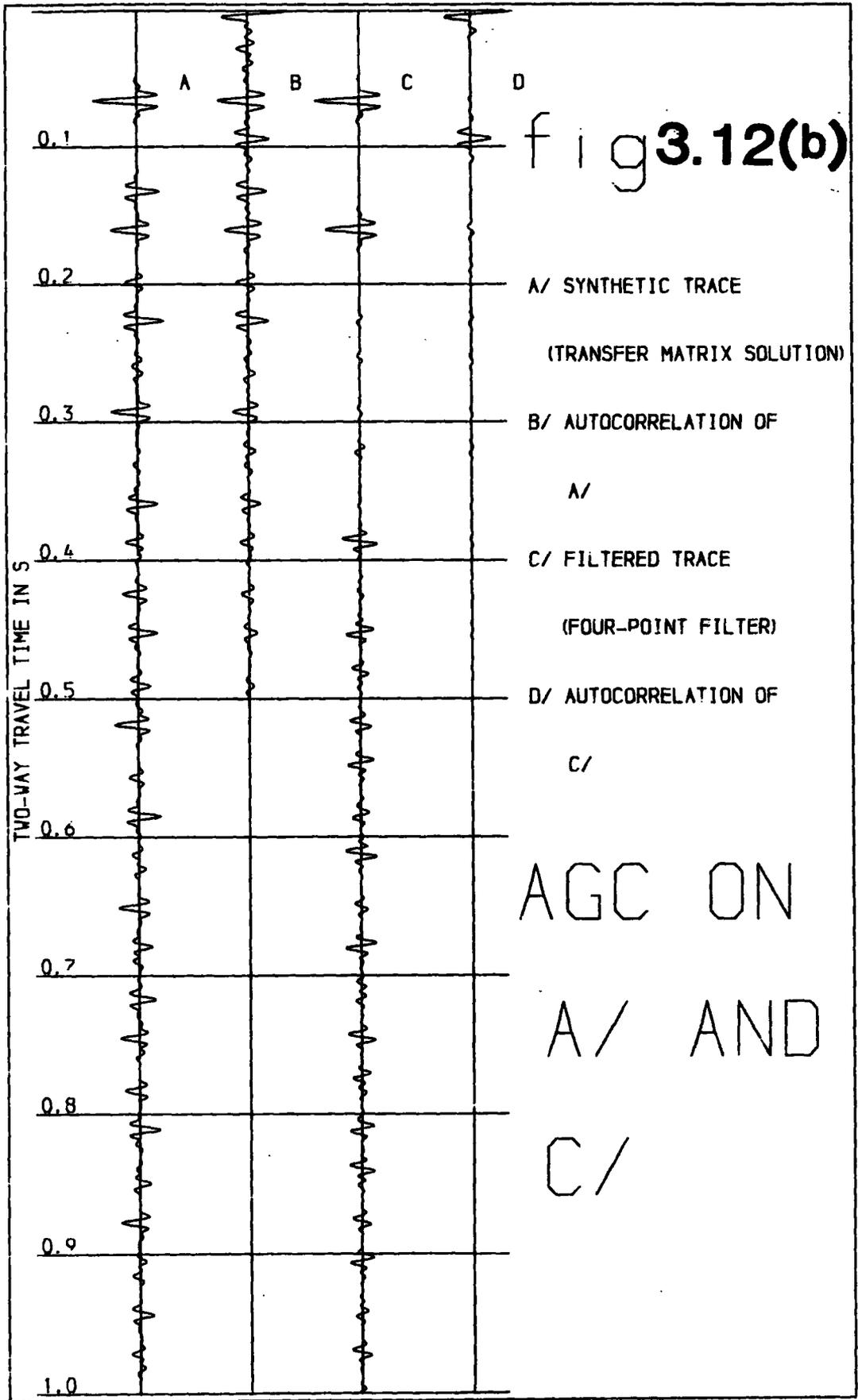
shown on Figure 3.13 and Table 3.2 summarizes the layer parameters and 2-way travel times T(i) at which the primary reflections arrive. The model was chosen by considering the first 16 horizons that can be clearly identified on the lithology of the Wearmouth region (see Figure 1.2). Approximate seismic velocity and density values were ascribed to the layers by using the results of a seismic reference survey (SRS) that was carried out in the borehole for the N.C.B. .

The complete response of this model was computed and the 4-point operator was used to suppress the multiple component due to the configuration of the free surface, the seabed (at 74 msec), and the strong reflector (top of the Magnesian Limestone) at 159 msec. Multiple reflections that were generated by other means were not expected to be removed by this operator.

Figure 3.14 shows the IR (sequence (A)) of the 16-layer model. The filtered sequence (C) and its autocorrelation sequence (D) show that most of the reverberation has been cancelled. The effects are clearer on Figure 3.15 where the seismic traces have been displayed instead. A comparison of the traces (A) and (C) shows that primary reflections are more clearly observed on (C) and at the arrival times that correspond with those of Table 3.2. The autocorrelation functions (B) and (D) show a relatively good suppression of multiples and the peaks on the former are due to the correlation of primary reflections and residual multiples. This filtering has enhanced the Coal Measures reflections at 296, 339 and 359 msec respectively.

73
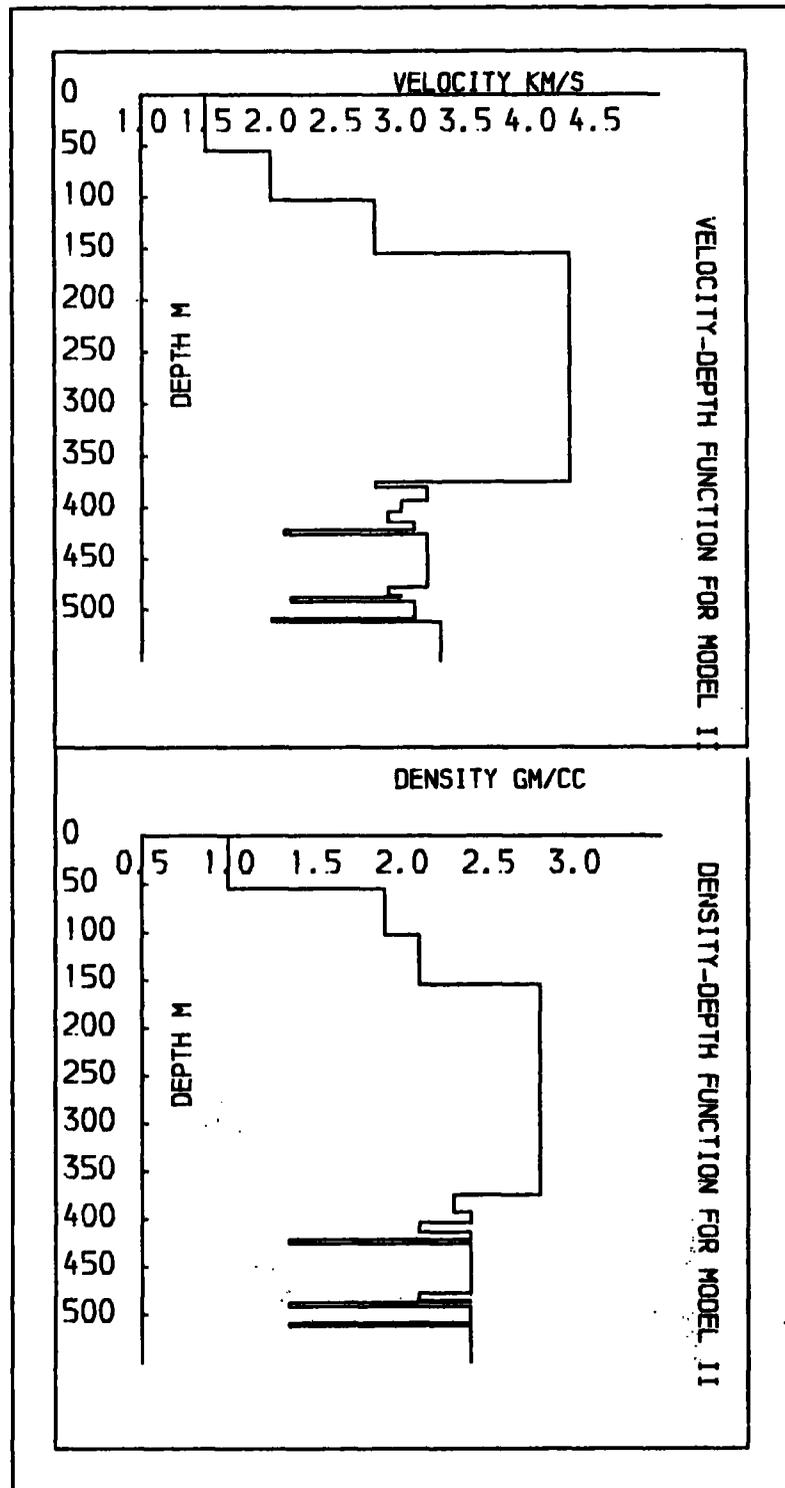
Figure 3.13 .   Interval velocity and density models for a
                 16-layer earth.

TABLE 3.2   PARAMETERS FOR 16-LAYER MODEL.
****

LAYER NO. i	V(i)	RHO(i)	C(i)	T(i)
1	1.5	1.	-0.433962	74
2	2.	1.9	-0.214876	122
3	2.8	2.1	-0.343750	159
4	4.3	2.8	0.303030	261
5	2.8	2.3	-0.066667	265
6	3.2	2.3	0.010989	273
7	3.	2.4	0.083521	280
8	2.9	2.1	-0.099778	287
9	3.1	2.4	0.448175	292
10	2.1	1.35	-0.460770	296
11	3.2	2.4	0.115468	329
12	2.9	2.1	-0.083521	334
13	3.	2.4	0.425389	336
14	2.15	1.35	-0.438723	339
15	3.1	2.4	0.467455	350
16	2.	1.35	-0.491525	353
17	3.3	2.4		

$V(i)$ in Km/sec.
$Rho(i)$ in g/cc.
$T(i)$ in milliseconds.

$$C(i) = \frac{V(i)*Rho(i) - V(i-1)*Rho(i-1)}{V(i)*Rho(i) + V(i-1)*Rho(i-1)}$$

fig 3.14

A/ IMPULSE RESPONSE (I.R.)

   (TRANSFER MATRIX SOLUTION)

B/ AUTOCORRELATION OF

   A/

C/ FILTERED I.R.

   (FOUR-POINT FILTER)

D/ AUTOCORRELATION OF

   C/

fig **3.15**

A/ SYNTHETIC TRACE

(TRANSFER. MATRIX SOLUTION)

B/ AUTOCORRELATION OF

A/

C/ FILTERED TRACE

(FOUR-POINT FILTER)

D/ AUTOCORRELATION OF

C/

AGC ON

A/ AND

C/

3.4.3   Estimation of Parameters.
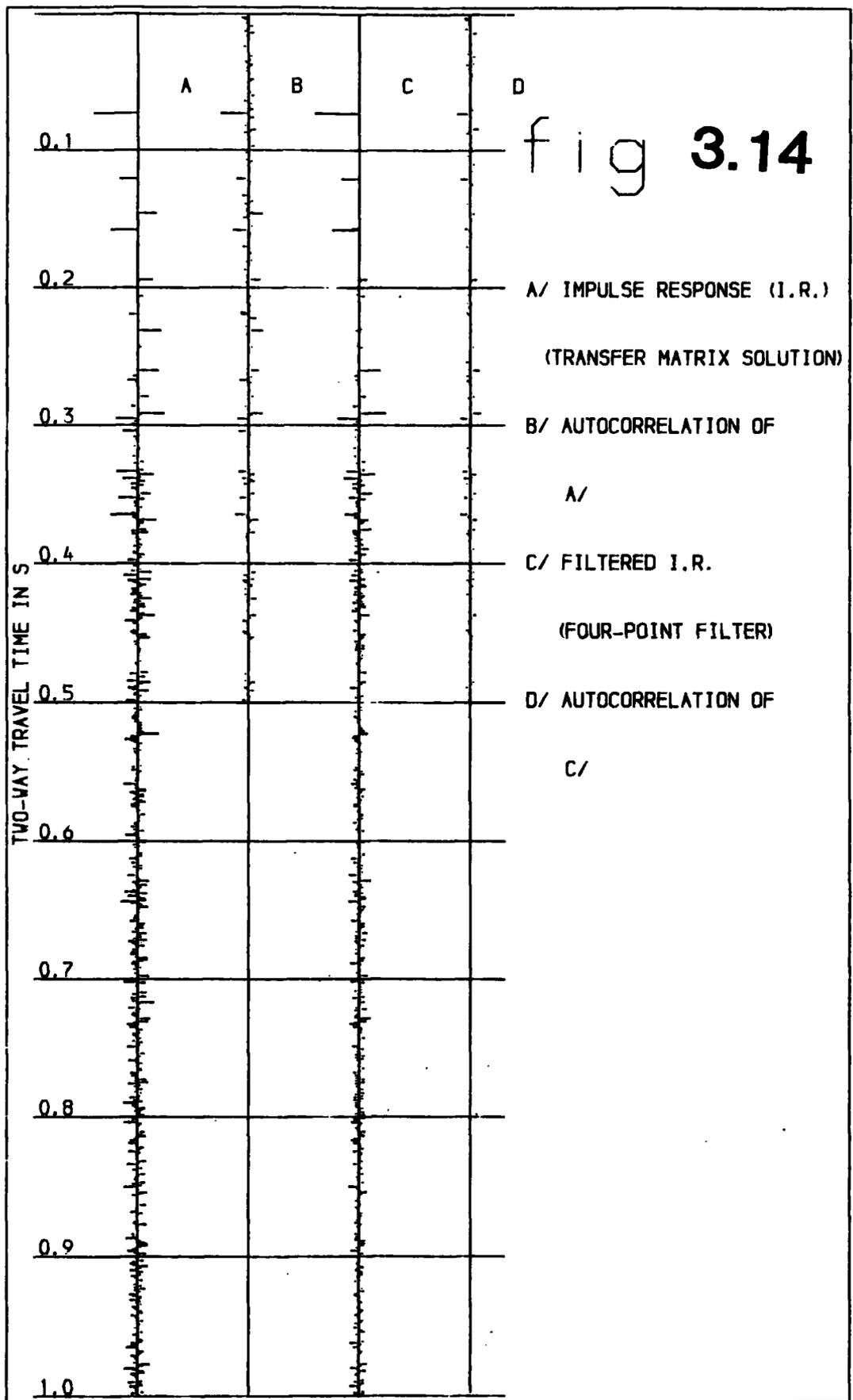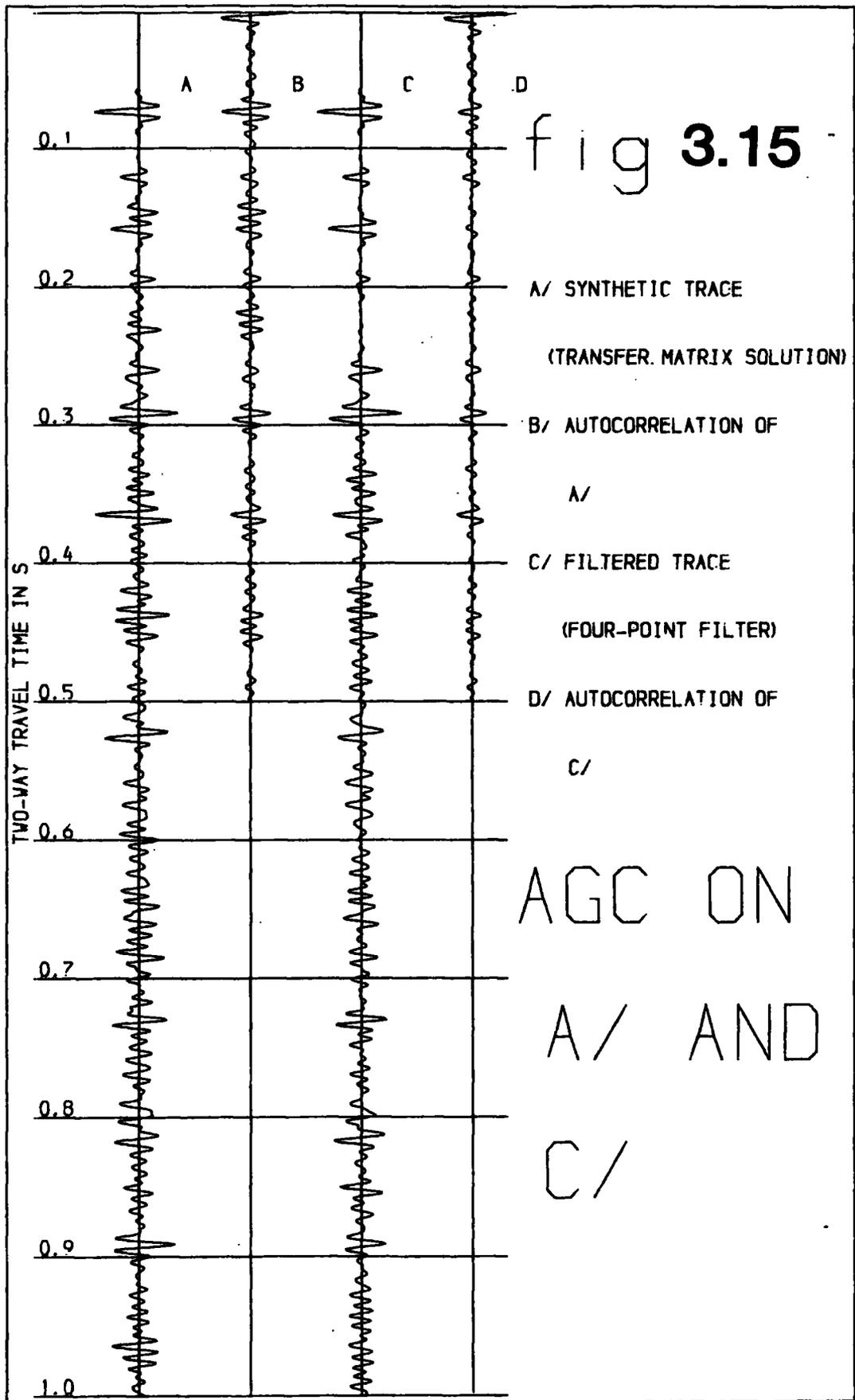
(a) Filter Terms.

The 2-way times τ_1 and τ_2 can be estimated (Morley and Claerbout, 1983) from the autocorrelogram of the data if the reflection coefficients c_1 and c_2 are high enough. These coefficients themselves are more difficult to estimate from the data when their S/N ratio is low. The seabed reflection coefficient can be estimated from peak amplitudes of the autocorrelation functions (Pflueger, 1972) but this is worthwhile for noise-free cases only. When the density and seismic velocity values (ρ_1, v_1), (ρ_2, v_2) and (ρ_3, v_3) are known, the plane wave, normal incidence assumptions can be used to estimate c_1 (Hughes, 1980) and c_2 from the equations

$$c_1 = (\rho_2 v_2 - \rho_1 v_1)/(\rho_2 v_2 + \rho_1 v_1)$$

In this chapter, the values of τ_1 and τ_2 were read from the autocorrelogram. The 24-channel shot records of the 1979 data were used to estimate v_1, v_2 and v_3 from the direct arrivals and the refracted headwaves and they were 1.68 km/s, 2.3 km/s and 3.8 km/s respectively. Approximations of c_1 and c_2 were made from the above formula and the best results of dereverberation were obtained when the density values were ignored.

74

(b) Effects of Errors in the Filter Coefficients.

In order to investigate the effects of errors in the estimates of filter coefficients, an example of a synthetic trace for which the paramaters c_i and τ_i are exactly known and which can be completely dereverberated by the 4-point filter was considered. Relative errors were simultaneously introduced in the reflection coefficients and the 2-way travel times respectively. The errors ranged from -30% to +30% of the true values and increased in steps of 10% from the lowest to the highest value. Each time the trace was deconvolved with the resulting filter and the residual energy of the output was evaluated. This procedure gave rise to an error energy matrix P_{ij} where (i or j=1,2,....7) and each element P_{ij} is the residual energy of a trace after deconvolution with reflection coefficients that are assumed to be determined with a relative error of $10(i-4)\%$ and travel times with a $10(j-4)\%$ relative error.

A contour plot of the results (Figure 3.16) shows the effects of the errors on the parameters c_i and τ_i respectively. Along the X direction, the reflection coefficients undergo a relative variation from -30% to +30% of the true values. Along the Y direction, the same variation occurs for the travel times. The contour heights are given.

These contours show that it is better to have the 2-way times more accurately. If these times are estimated with an absolute relative error of less than 7%, then the relative errors with an absolute value of up to 25% in the c_i will lead to low
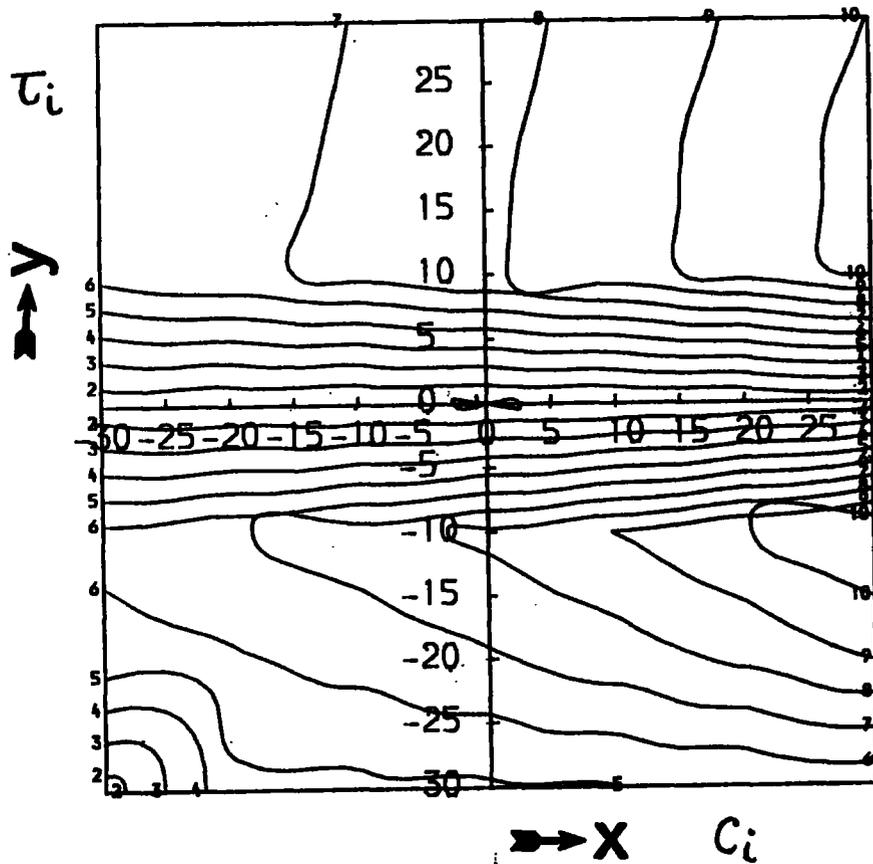
Figure 3.16 . A contour plot of the residual energies after
deconvolution with various inexact operators.

CONTOUR HEIGHTS

HEIGHT	RESIDUAL ENERGY
2	.2
3	.3
4	.4
5	.5
6	.6
7	.7
8	.8
9	.9
10	1.0

residual energies or good dereverberation. If the errors in the τ_i increase any further, the behaviour of the filters becomes unpredictable in this case.

In practice, it is possible to estimate the τ_i with this accuracy and a failure of the filter to produce satisfactory dereverberation can be attributed to the nature of the real trace rather than to the fact that the estimates of the c_i are too crude.

3.4.4   Application of Filter to Real data.

The 4-point filter was tested on the same data as the 3-point filter and Figures 3.17(a) and 3.17(b) show the output. The values of the parameters that were used are shown on Figure 3.17(a). Some multiple suppression occurred but the results were not as good as for the 3-point filter. This may be due to the fact that the reverberation is more complicated than the simple 2-layer case depicts. If the seabed reveberations predominate in the multiple train, then the 3-point filter will suppress it more efficiently.

The autocorrelogram (Figure 3.17(b)) was very similar to that of Figure 3.8(b) and showed a residual seabed multiple reflection relatively stronger than the ghost left on by the 3-point filter. These particular traces could therefore be better treated with a 3-point filter than with a 4-point filter.
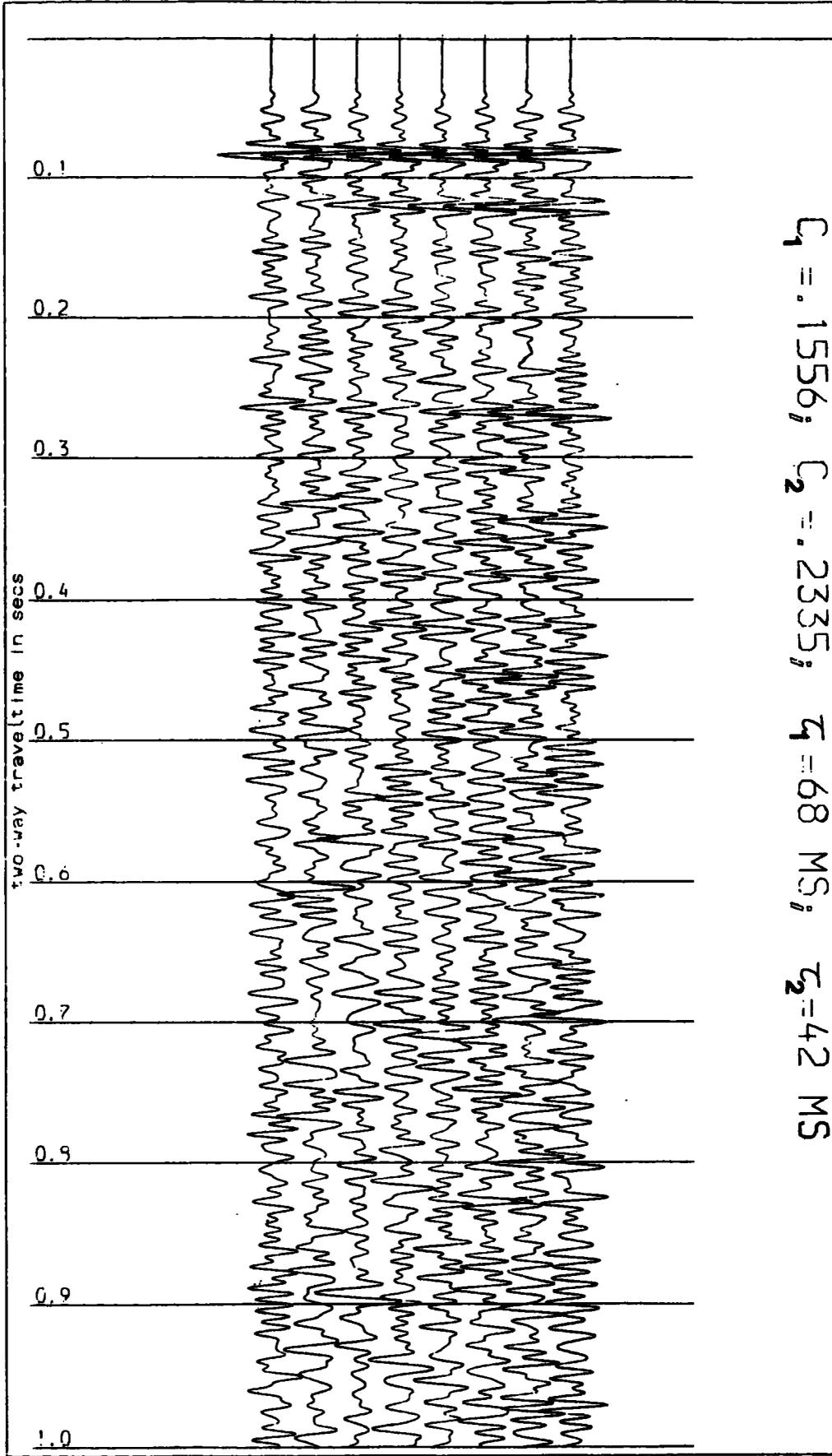
Figure 3.17(a). The section of Figure 3.7(a) after filtering with a four-point filter.
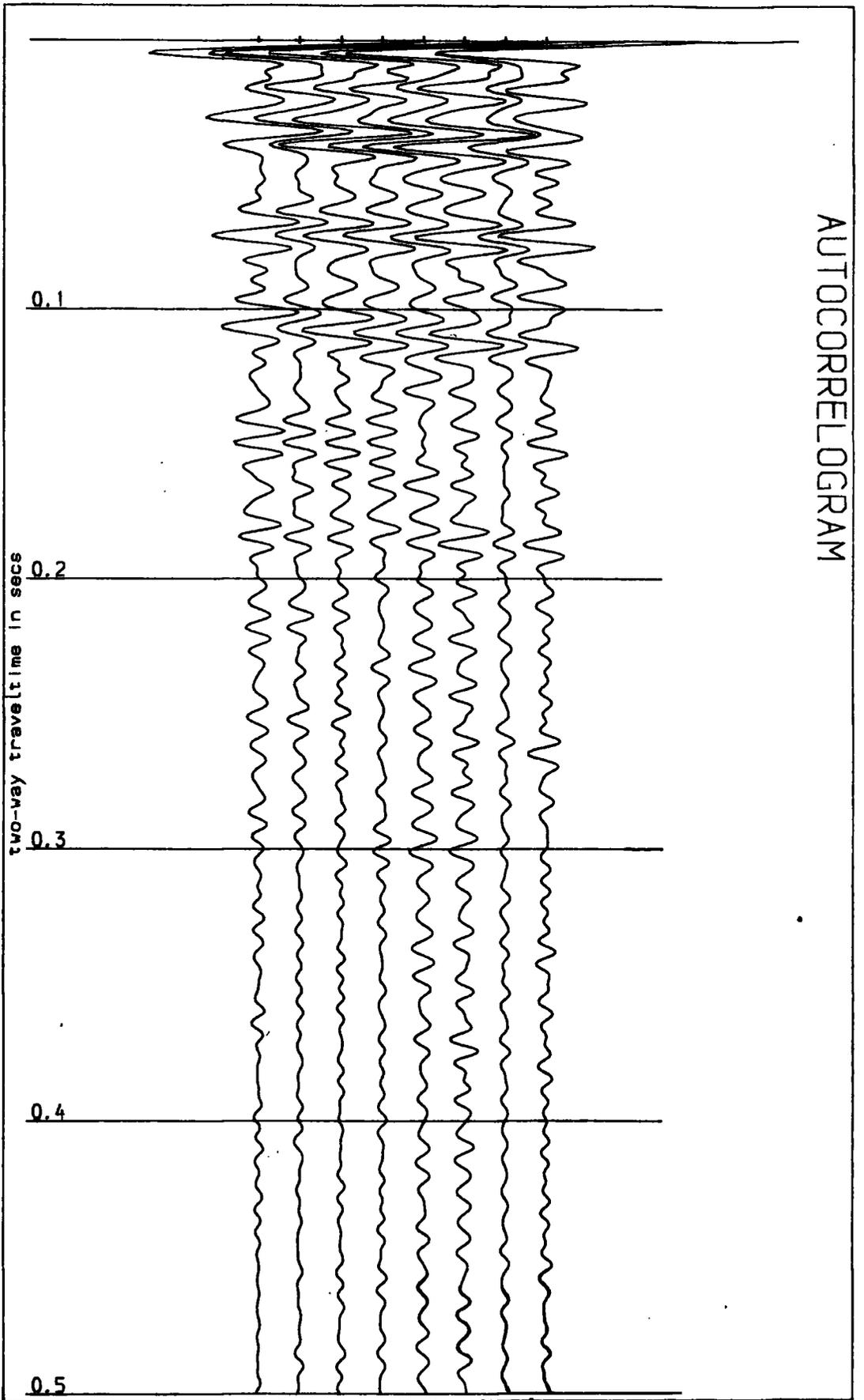
Figure 3.17(b). Autocorrelogram of the section of Figure 3.17(a).

3.5   <u>Prediction-error Deconvolution.</u>

The deterministic filters were compared to corresponding prediction-error filters. The latter were designed to suppress only the range of periodicities that either of the former filters could possibly attenuate.

3.5.1   Prediction-error Filter for Seabed Multiples.

When the seabed multiple period is obvious, a prediction-error filter can be designed to have a short predictive filter and a gap just less than the multiple period. A filter with a length of 30 msec and a gap of 50 msec was designed. A prewhitening parameter of 3% was applied and the time window of 950 msec long was used.

The results of the application of this filter are shown on Figures 3.18(a) and 3.18(b) respectively. If the effect of the ghost is ignored on Figure 3.8(a), this autocorrelogram shows a better improvement of that of Figure 3.7(b). The resulting section is less noisy although it is not more interpretable.

3.5.2 Prediction-error Filter for 2-layer Reverberatory Wavelet.

Following the theoretical background of section 3.4, the 2-layer reverberatory wavelet has periods of up to $\tau_1 + \tau_2$. In designing a prediction-error filter to suppress it, only periodicities of up to $\tau_1 + \tau_2$ are included. The length of the

PREDICTIVE DECONVOLUTION.
length of filter=30 ms; gap=50 ms
design window (50-1000) ; lambda=3%
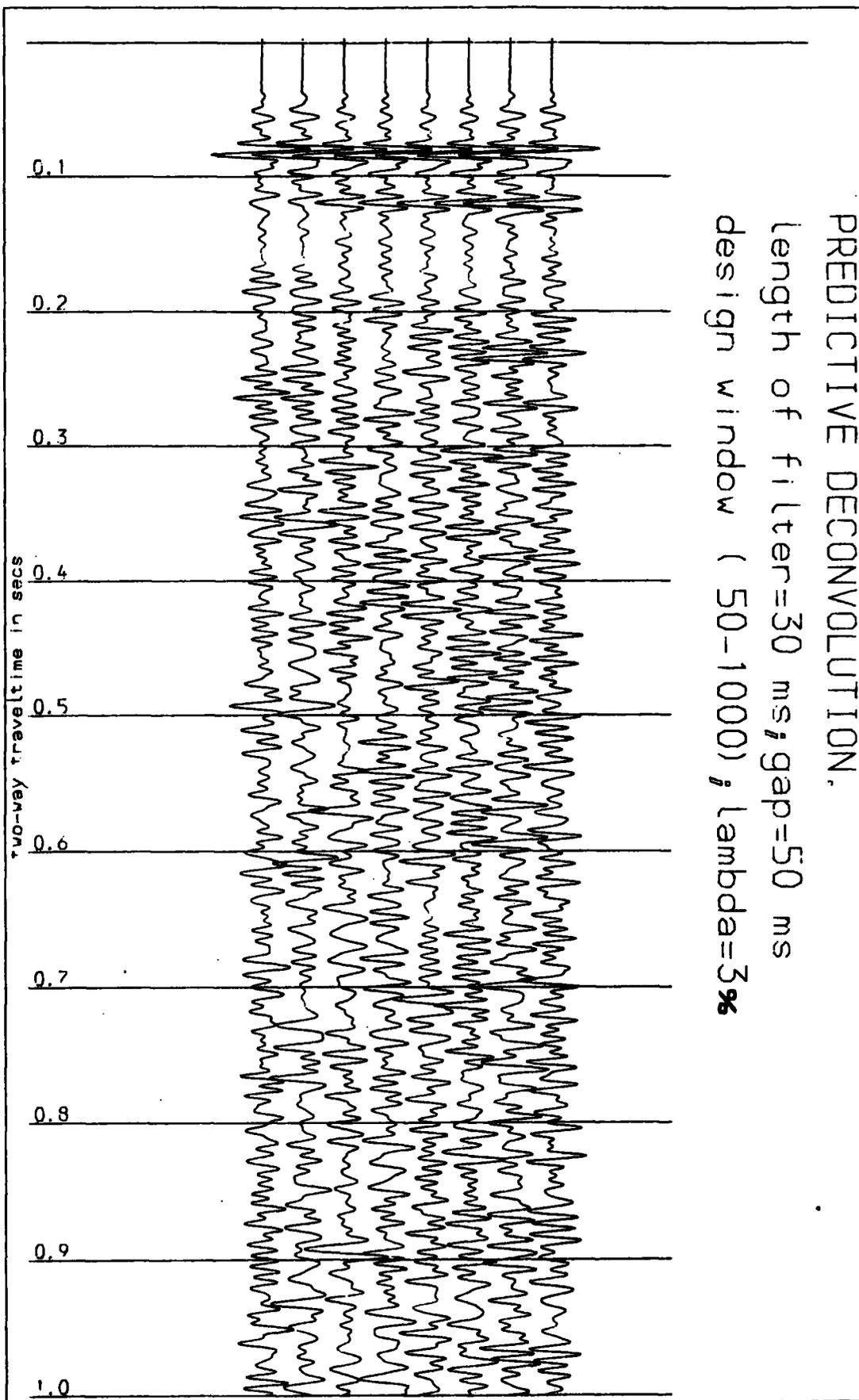
Figure 3.18(a). The section of Figure 3.7(a) after predictive deconvolution.
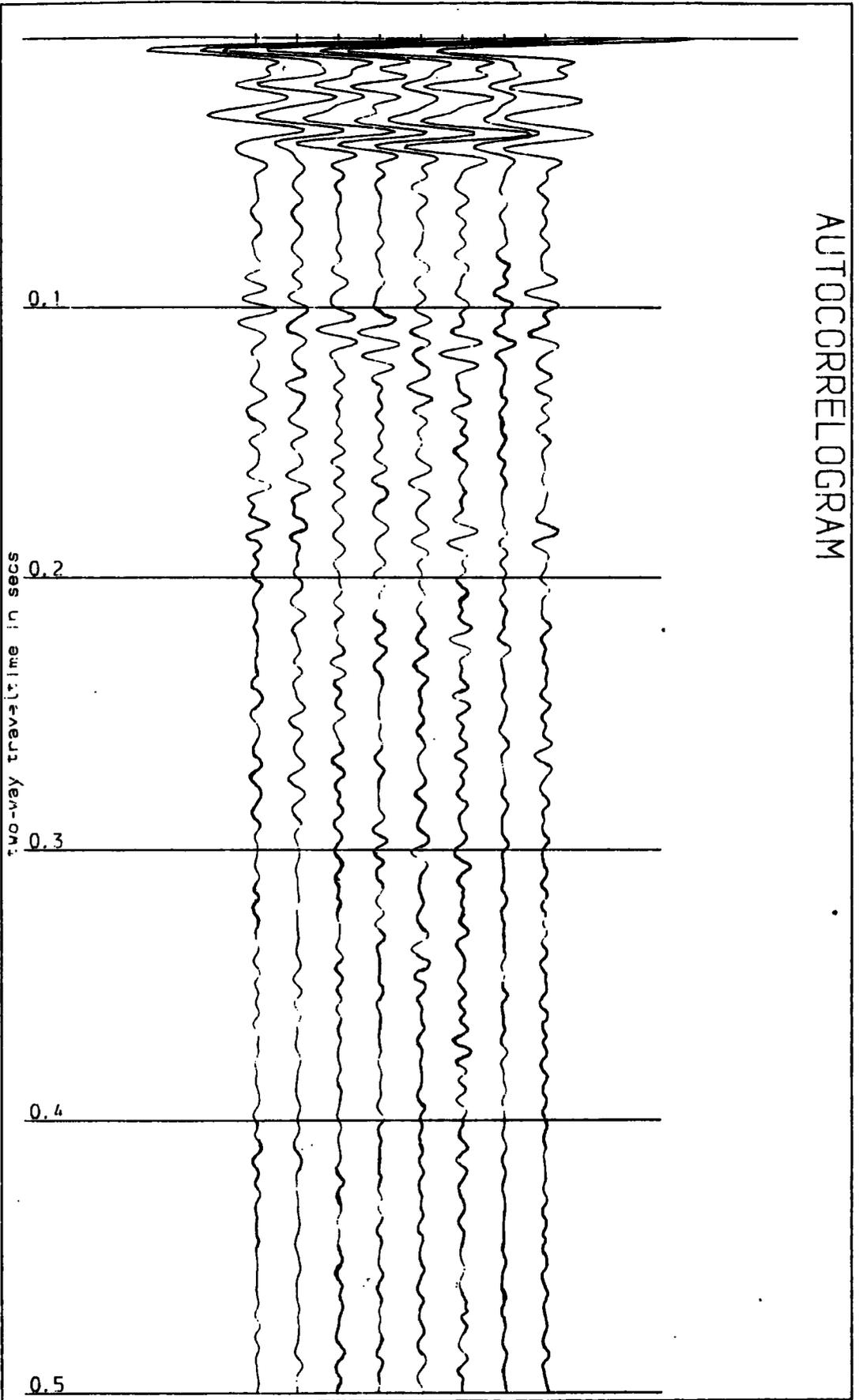
Figure 3.18(b). Autocorrelogram of the section of Figure 3.18(a).

operator was 70 msec and the gap was 30 msec. the prewhitening parameter was 3% and the same design gate was applied as in section 3.5.1 .

The results of its application are shown on Figures 3.19(a) and 3.19(b). Compared with all the previous autocorrelograms, Figure 3.19(b) shows that the filter has attained the best suppression. The section itself (Figure 3.19(a)) has got a higher S/N ratio but the primary reflections are not coherent across it.

Figures 3.20(a) and 3.20(b) show the results ofapplying a longer filter to the traces. Periodicities within the range [30,200] msec were effectively attenuated. On the basis of the autocorrelogram, the data have been effectively 'whitened'.

3.6   Discussion.

Although it was not possible to estimate accurately the parameters of the deterministic filters, the results confirm that statistical methods are more efficient for real data cases. The S/N ratio of real records that were used was poor and the potential of the deterministic filters may have been underestimated. The geometrical spreading effects would not have been exactly compensated for so that true (corrected) amplitudes did not meet the normal incidence , plane wave predictions in the estimation of filter parameters. Instead of applying an exponential trace scaling to correct for spreading, an attempt was made to include the spreading correction in the design of the

PREDICTIVE DECONVOLUTION.
length of filter= 70ms; gap= 30ms
design window (50-1000) ; lambda= 3▽

two-way traveltime in secs

0.1
0.2
0.3
0.4
0.5
0.6
0.7
0.8
0.9
1.0
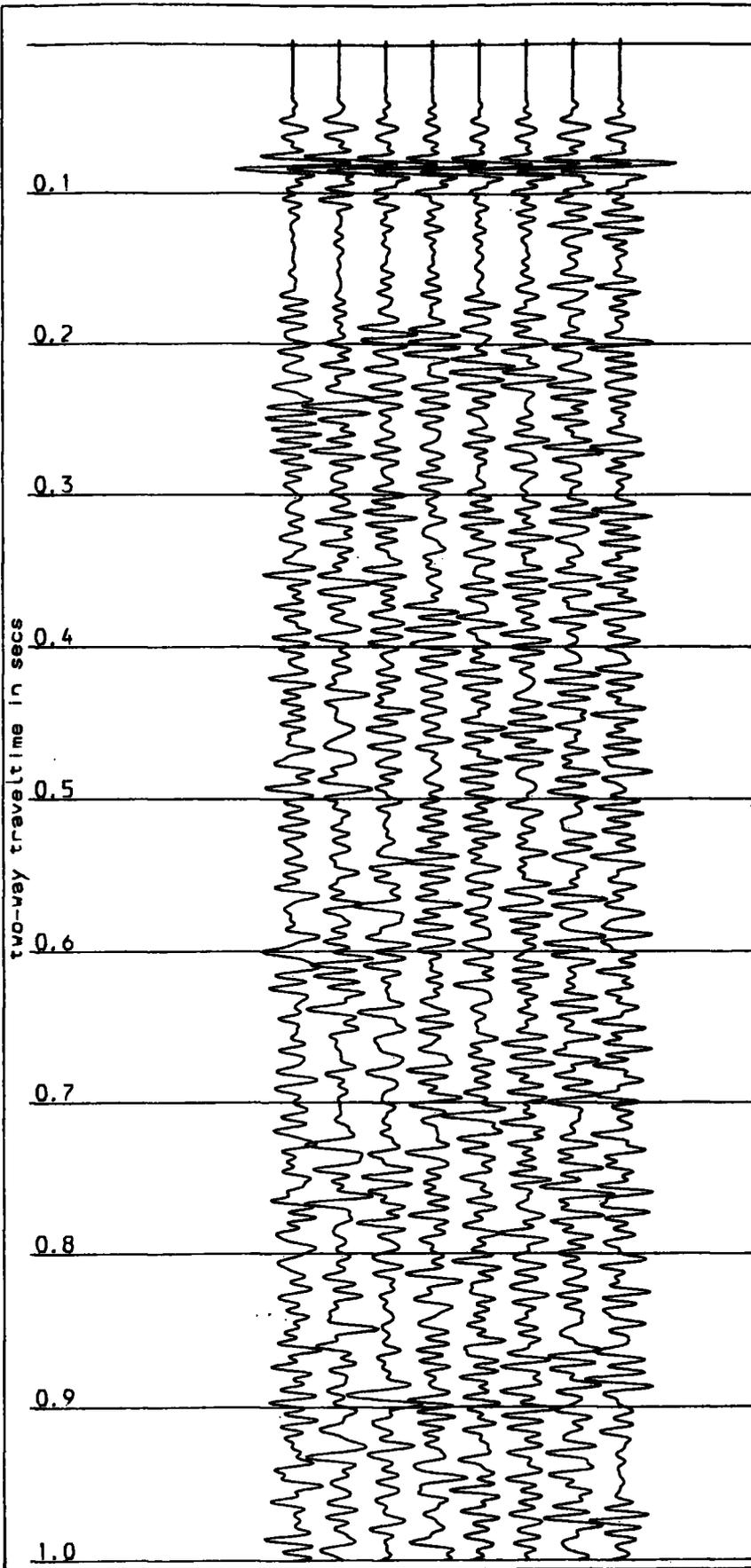
Figure 3.19(a). The section of Figure 3.7(a) after predictive deconvolution.
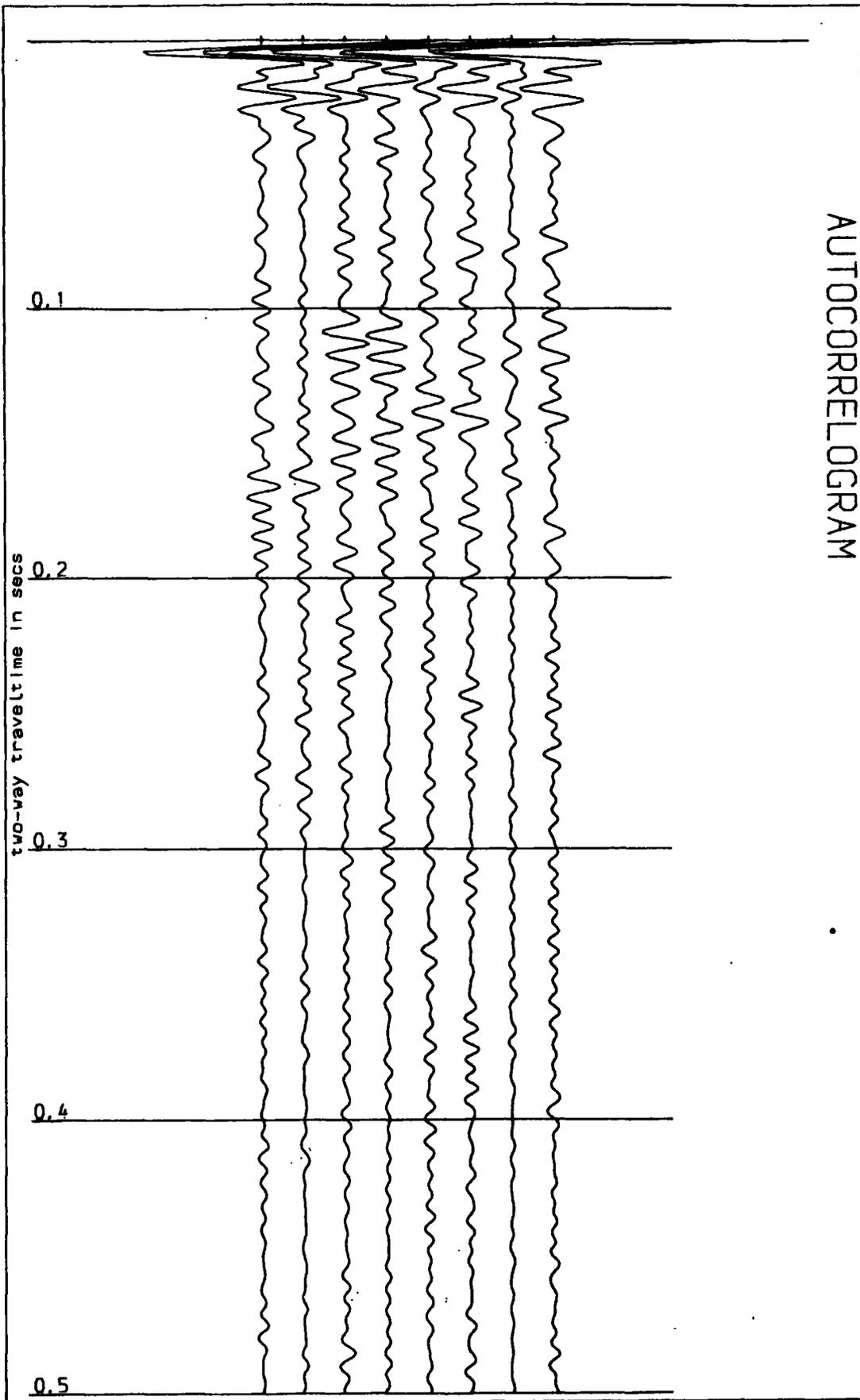
Figure 3.19(b). Autocorrelogram of the section of Figure 3.19(a).

PREDICTIVE DECONVOLUTION.

length of filter=170ms; gap=30 ms

design window (50-1000) ; lambda=3 %

two-way traveltime in secs
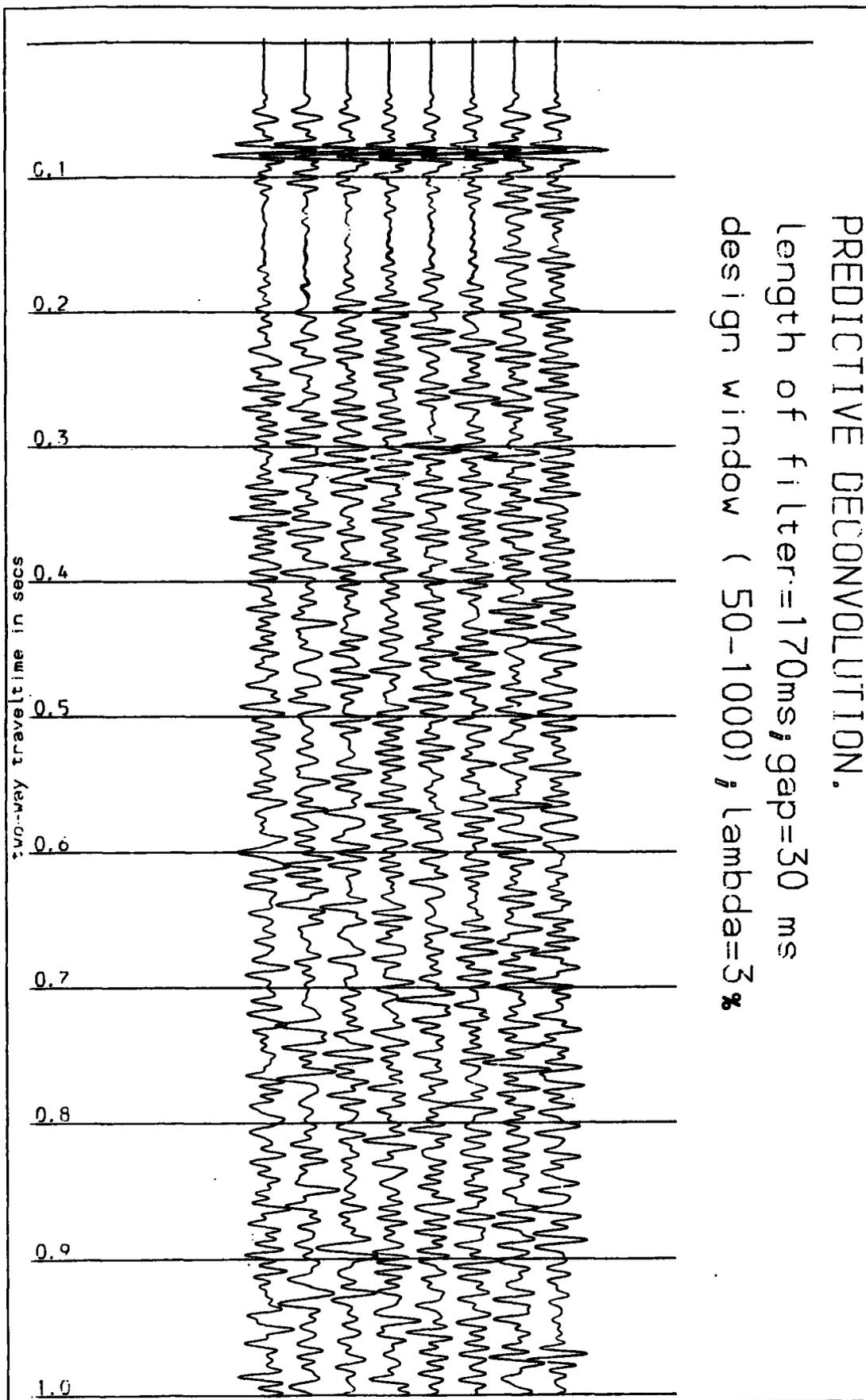
Figure 3.20(a). The section of Figure 3.7(a) after predictive deconvolution.
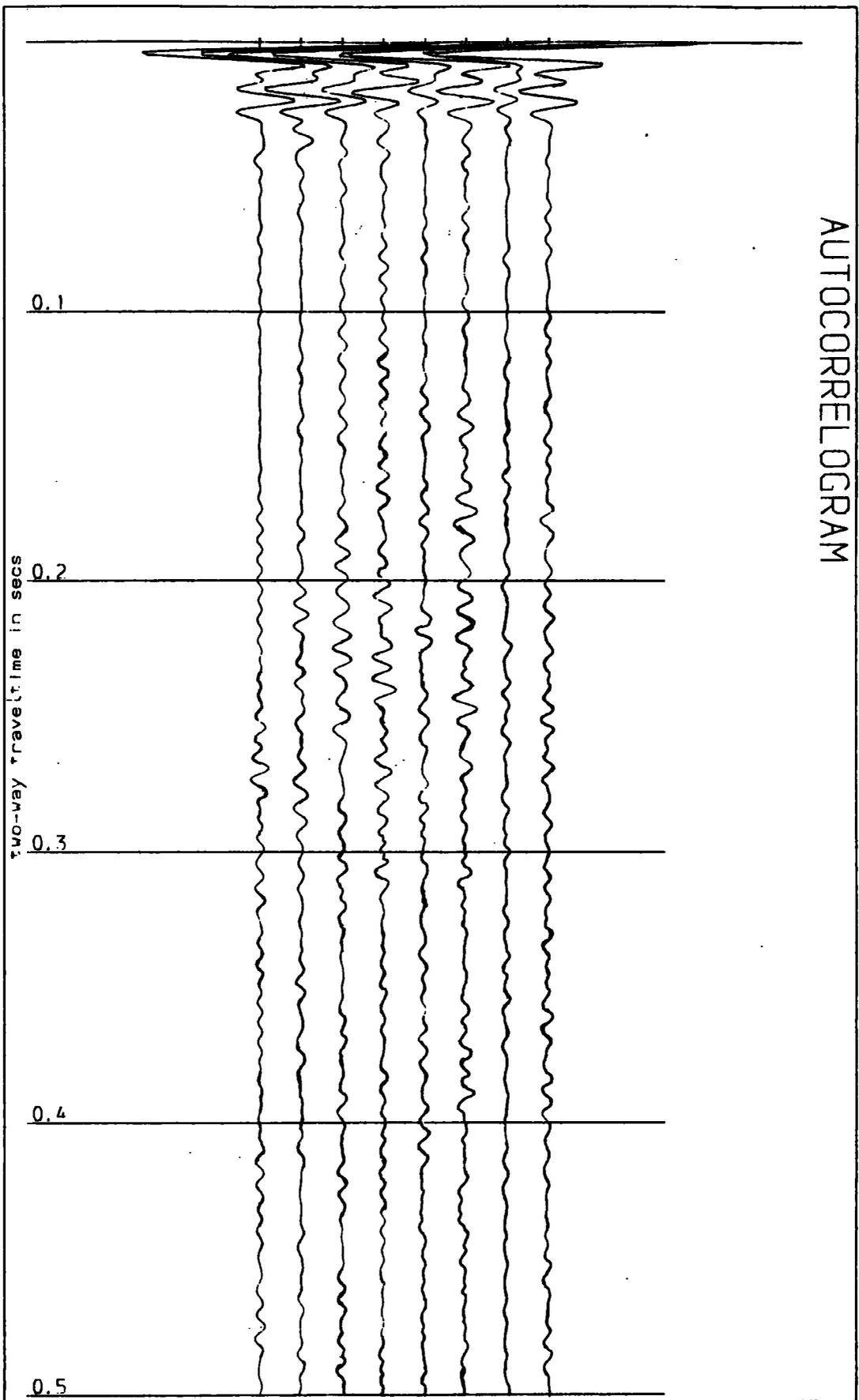
Figure 3.20(b). Autocorrelogram of the section of Figure 3.20(a).

deterministic filter. The resulting operators were time-variant as was pointed out recently by Mendel (1984). Furthermore, the best design would require the incorporation of the $T-V^2$ function (Newman, 1973) which is worthwhile only when accurate velocity information is available.

Statistical deconvolution (in the form of prediction-error deconvolution) has another advantage in that the statistical distribution of the filtered noise can be evened out by the use of the prewhitening parameter. Deterministically filtered sections (Figures 3.8(a) and 3.16(a)) look much noisier than their predictively filtered counterparts (Figures 3.18(a) and 3.19(a)) respectively.

In the presence of accurate parameters for their design, deterministic operators can be useful in dereverberating synthetic seismograms for use in theoretical problems and applicable to situations where synthetic traces are generated from well log information in order to match them with processed sections during interpretation. The need arises because it is inappropriate to compare a processed field record with an unprocessed synthetic trace. There is noise that arises in the well log data and its sampling and is often less severe than field-recorded noise in the original seismic traces. Prediction-error deconvolution can be used for this purpose but if it suppresses primary reflections to any extent, then a mismatch of the result will be inevitable.

C H A P T E R 4

Processing of the Real Data.

4.1   ## Scope.

In section 1.2, the real seismic reflection data sets that have been used in this study were presented. The results of the processing of these data by using various processing sequences are outlined and discussed in this chapter.

Following pre-stack processing, different techniques of CMP stacking were applied to each data set and post-stack processing was carried out when necessary. The extent of multiple suppression of each scheme and the degree of resolution obtained in the final section are discussed.

Pre-stack processing included either prediction-error deconvolution or a velocity filtering technique for multiple suppression. Velocity analysis was performed by the semblance method (Taner and Koehler, 1969) and NMO corrections were then carried out. Three methods of stacking were applied - the straight stack (Mayne, 1962 - section 2.3.2(a) and here considered as standard), the weighted stack (section 2.3.2(b)), and the iterative stack (Naess, 1979 - section 2.3.2(c)). Post-stack processing comprised mainly prediction-error deconvolution and is generally referred to on the seismic sections as DAS (Deconvolution After Stack).

The processing schemes for the 24-fold data (line 7940) are presented in section 4.2. In section 4.2.1, some observations

80

about the field records are outlined and the final seismic sections are presented in section 4.2.2. Both straight and weighted stacks were applied to these data. The interpretation and discussion of the results are deferred to section 4.2.3.

The processing methods that were applied to the 6-fold data (line 8201A) are given in section 4.3. Straight and iterative stacking were performed on these data and the final sections are displayed. All the discussion and the interpretation of these results are given in section 4.3.2. The chapter terminates with a summary in section 4.4.

Both data sets were processed on the PDP11/34 computer of the Seismic Reflection Data Processing Laboratory (SRDPL), Department of Geological Sciences, University of Durham. The computing system has an FPS 120 array processor (AP) which speeds up seismic computations compared to the main computer of the University, an IBM 4341/1 computer, run as part of the NUMAC (Northumbrian Universities Multiple Access Computer) network.

In addition to this advantage of speed, the computer system has more efficient seismic plotting facilities and also, seismic processing software that was not available on NUMAC.

The AP has a memory of 24K (1K = 1024 memory locations), and limits the iterative stacking technique to 6-fold data if each trace has a length less or equal to 2K samples. By using the AP matrix routines, the iterative algorithm (equation (26) - section 2.3.2(c)) was programmed to run as an option of the weighted stacking program DK1:WSTACK. Due to the limitations of the memory available on the AP device, line 7940 could not be iteratively

stacked in an efficient way although any 6-fold window of each
CMP gather could be iteratively processed if required. Weighted
stacking was not applied to line 8201A because the offsets are
small and there is very little differential moveout between
primary and multiple events within the Coal Measures.

4.2   **Processing of Line 7940.**

4.2.1   Field Records.

An examination of the seismic records reveals that there are
spatial intervals of line 7940 in which there are strong
refracted arrivals on CMP gathers between 200 and 270 msec and
others in which they are very weak or absent. When they exist,
seismic refraction analysis produced an average velocity of about
5.0 km/s for the refractor. Approximate calculations (using the
borehole and lithological information of chapter 1) show that the
seismic reflections from the top and base of the Magnesian
Limestones would be expected at 2-way times of about 155 and 260
msec respectively. The refractor must therefore be within the
limestone since it is observed within this time interval. It
probably corresponds to some anhydrite and these data suggest
that it is laterally discontinuous. This is geologically
plausible if it formed more poorly in some areas than in others
or if it diminished by dissolution to a greater extent in such
areas.

Figures 4.1(a) and 4.1(b) are examples of CMP gathers
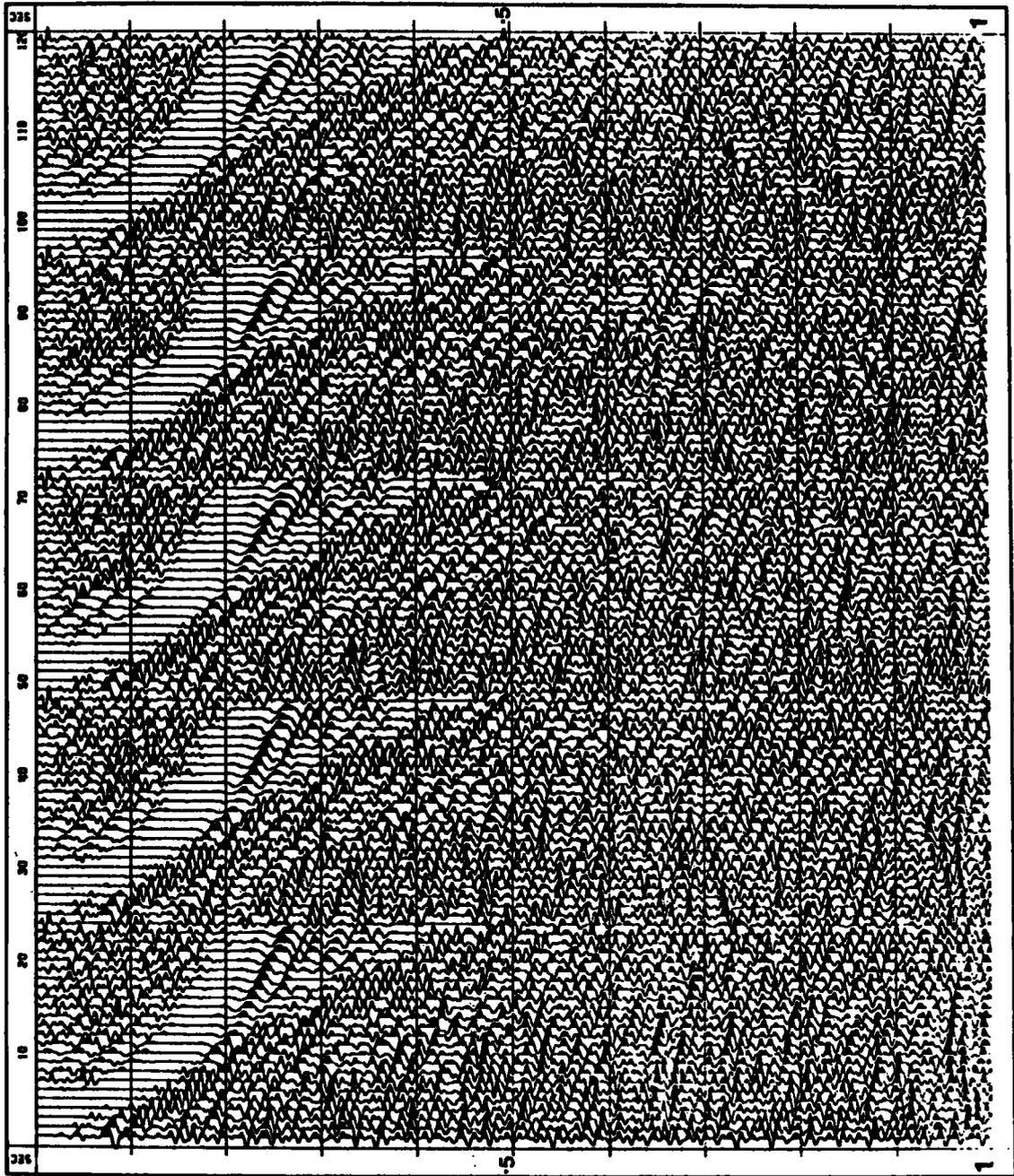
Figure 4.1(a). CMP 100 - CMP 104 of line 7940 showing the
refraction arrival below 200 msec.
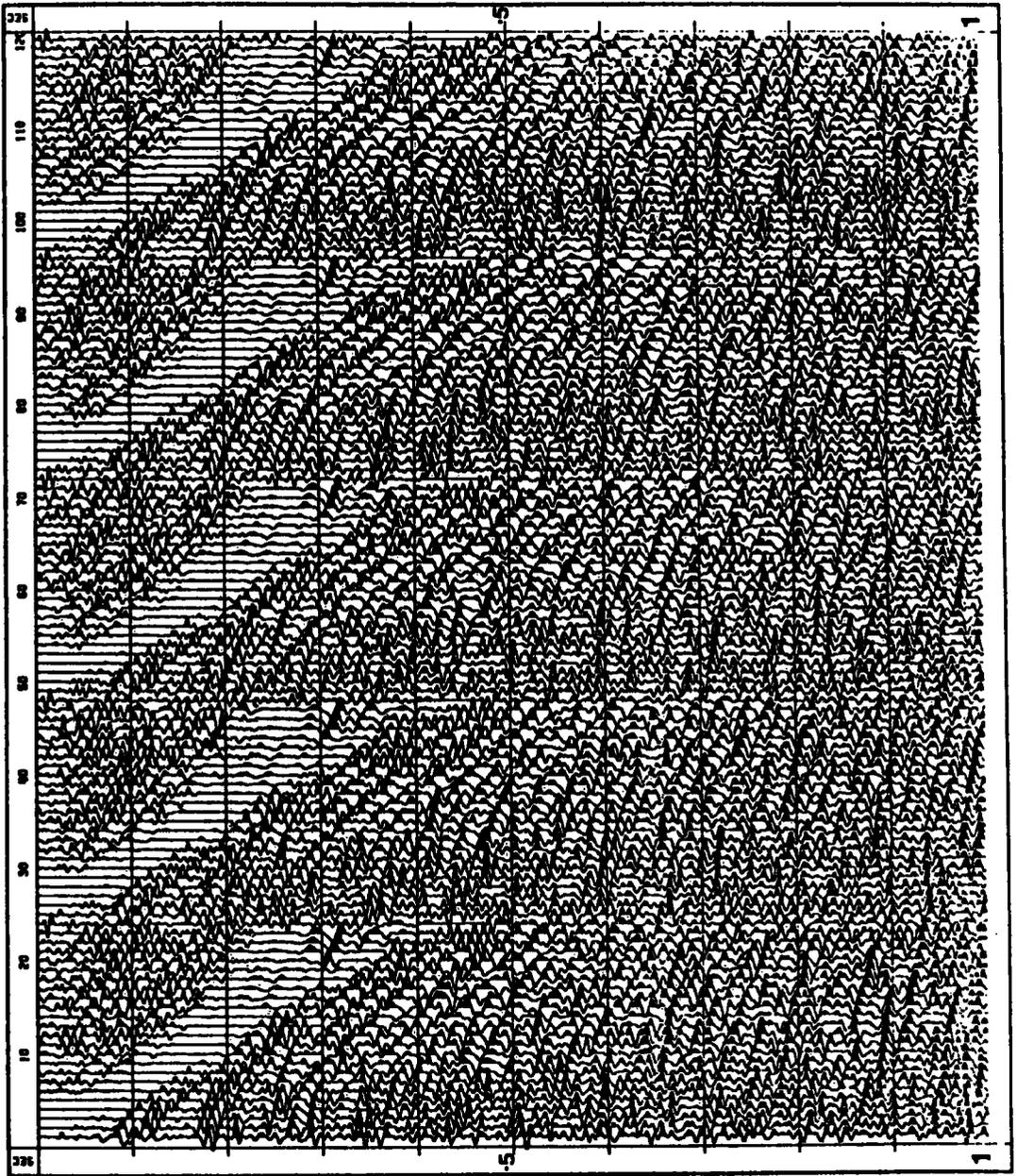
Figure 4.1(b). CMP 400 – CMP 404 of line 7940. The refracted
arrival is weak or absent compared to Figure 4.1(a).

selected from line 7940. The traces were band-pass filtered, gain ranged (AGC gate of 100 msec) and normalized to unit amplitude. Figure 4.1(a) shows CMP 100 to CMP 104 and Figure 4.1(b) shows CMP 400 to CMP 404. On the former, the refracted arrivals are between 200 and 270 msec at offsets greater than about 340m. Between 300 msec and 700 msec at these offsets, there are few discernible reflected arrivals. At shorter offsets, more of them are evident but their continuity is poor. The water wave also has a high amplitude. Figure 4.1(b) shows CMP gathers selected about 3.5 km further on along the line. The water wave is weaker, the refracted event is almost absent and the reflected arrivals can be observed at greater offsets than on Figure 4.1(a).

Twenty-four fold stacks of short segments of the line at the locations of the gathers of Figure 4.1(a) and 4.1(b) are shown on Figure 4.2(a) and 4.2(b) respectively. Approximate stacking velocity functions were obtained from an initial velocity analysis. Only band-pass filtering was carried out after stacking. Coal Measures type dipping events are clear on the latter at about 350 msec but not on the former. Although the event at 450 msec on Figure 4.2(a) has got a slight dip, it is not as clear as that of Figure 4.2(b) at 350 msec. These observations are born/e out by a comparison of the CMP gathers and the final stacked section in which reflections with Coal Measures characteristics are only observed in segments of the line in which the refractor is weak or absent.

This lateral variation of data quality meant that the muting pattern that was chosen for the poor quality data segment (such
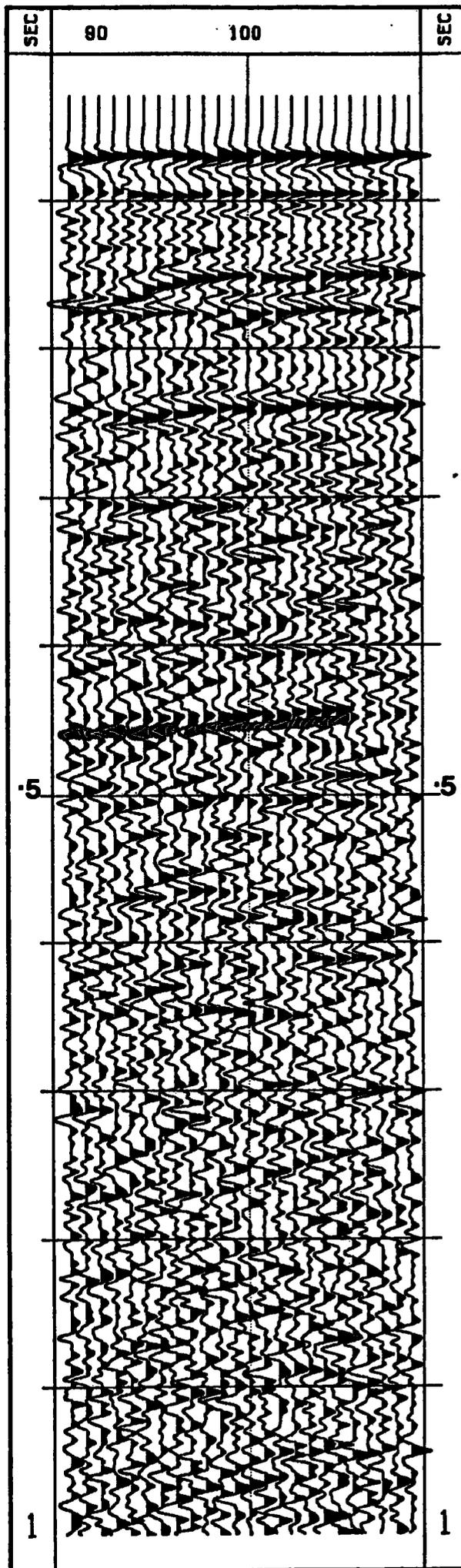
Figure 4.2(a). A 24-fold stack of a short segment of line
7940 (CMP88 -CMP 111).It shows no Coal Measures except
for the event at about 450 msec which has a slight dip
but is very weak.
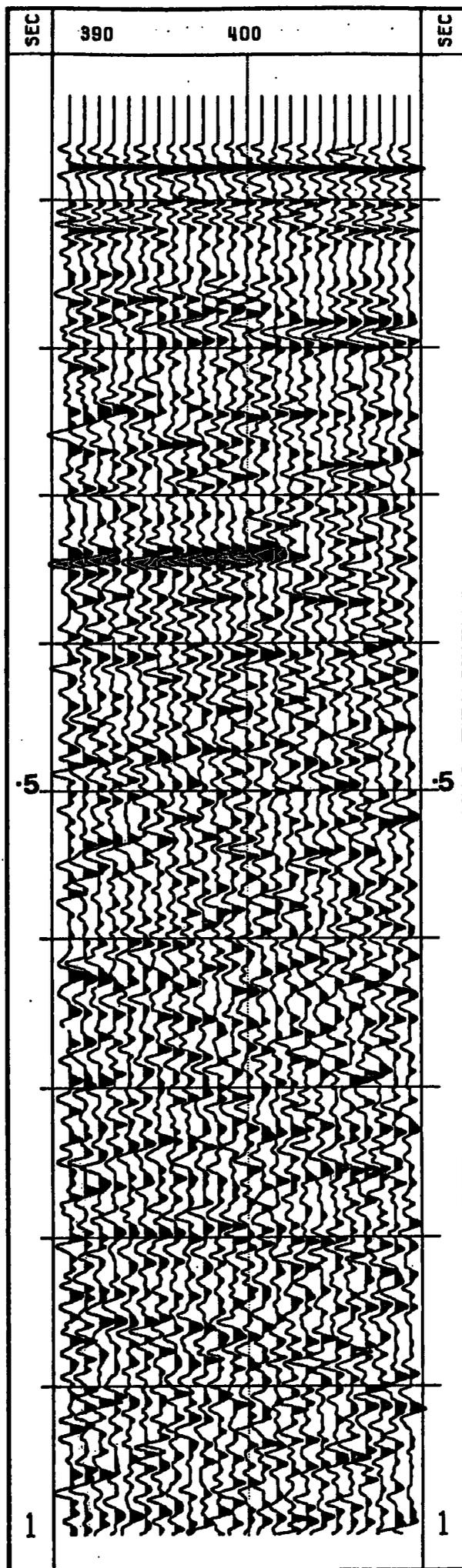
Figure 4.2(b). A 24-fold stack of a short segment of line 7940. It shows Coal Measures type reflections just below 350 msec.

as Figure 4.1(a)) was too severe for the areas with good data. This could only be avoided by choosing different muting patterns for different CMP gathers or for different lateral windows of CMP gathers which would have been an inefficient option. Most of the gathers along line 7940 had the character exibited by CMP 26 on Figure 4.3(a). The best muting pattern to eliminate the direct waves, wide-angle reflections and the refractions was chosen as shown on Figure 4.3(b). It was found to be adequate for CMP gathers with the lowest S/N ratio and it was chosen after a set of alternative functions was tested by stacking selected gathers with approximate velocity functions. It was applied to the whole line.

4.2.2   Processing Sequence.

The processing procedures that were applied to this line are summarized below. The major steps in the scheme are outlined and the results are given.

(a) Data Translation.

The 24-fold data were transmitted to Durham as CMP gathers in standard SEG 'Y' format on magnetic tapes. In order to process them on the PDP11/34 computer, they were translated into an in-house format DSEGY (Durham SEG 'Y'). DSEGY is a DEC (Digital Equipment Corporation) format used in SRDPL and it differs from standard IBM SEG 'Y' in the way that the bytes are arranged on tape and the representation of the floating point numbers.
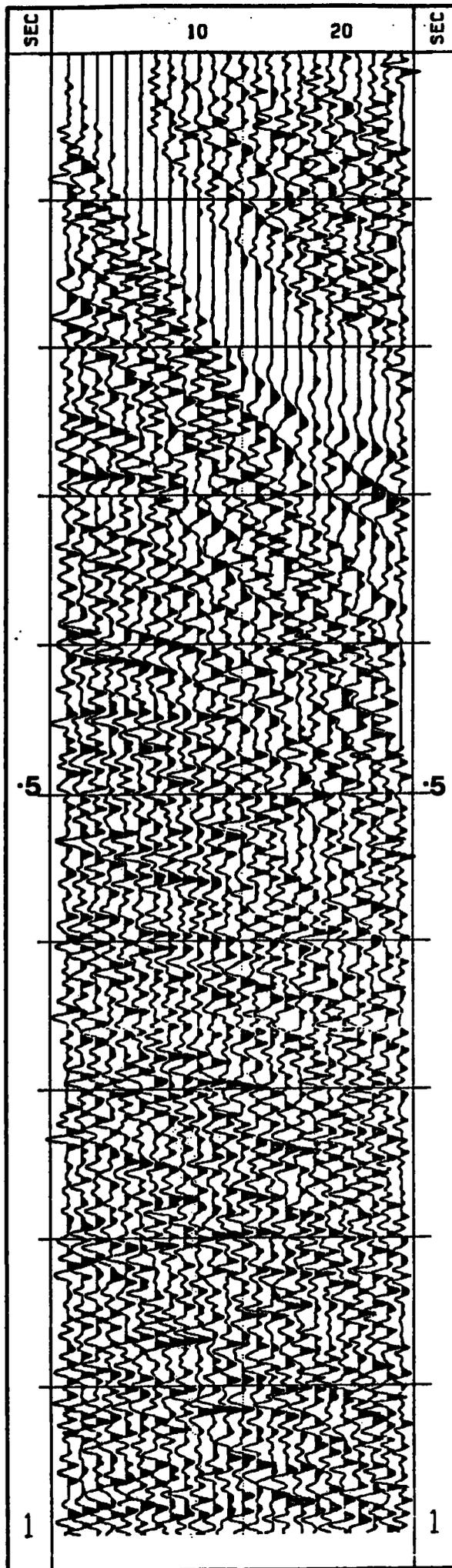
Figure 4.3(a). CMP 26 of line 7940.
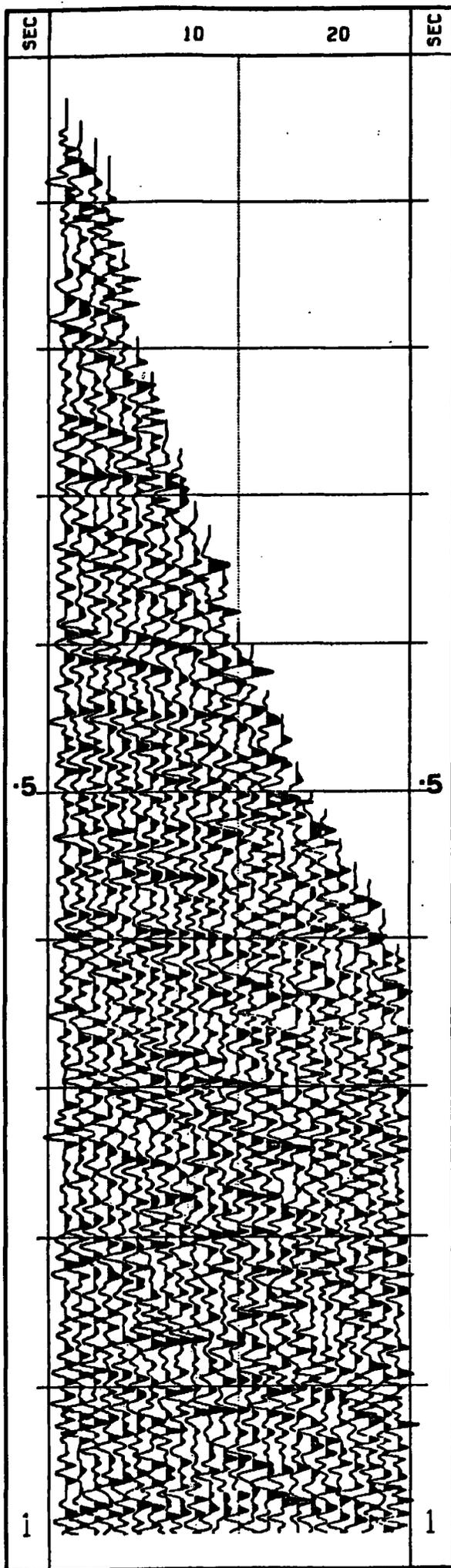
Figure 4.3(b). CMP 26 of line 7940 with the mute function applied. Between 300 msec and 500 msec, the fold of cover ranges from 9 to 17 (offset of 245m-445m).

The translation was carried out by means of the sort program DK1:SORT which is used mainly for sorting data into various gathers of traces. Since the data were already sorted, the program was used for altering its format only. It is also capable of writing out specified velocity files during data sorting and/or translation. Velocity files were therefore selected during translation and written on magnetic tape in preparation for velocity analysis at a later stage.

(b) Pre-stack Processing.

After translating the data into a DEC format, they were muted and then band-pass filtered to 30 Hz low-cut and 150 Hz high-cut frequencies respectively.

(i)   Prediction-error Deconvolution.

The first type of pre-stack processing was the application of prediction-error deconvolution. This was done by means of the program DK1:PROC. Various trials of prediction-error deconvolution were made mainly by varying the predictive gap, the length of the prediction operator, the pre-whitening parameter and the type of pre-deconvolution trace scaling.

The predictive gaps used were 1, 4, 8, 16, 32 and 48 msec respectively. The filter lengths were chosen less than 300 msec and an autocorrelation design gate of about 1300 msec was maintained. The prewhitening parameters were chosen between 1% and 3%. Different forms of scaling were tested in order to

improve the stationarity of the data (by compensating approximately for spreading and other losses). Exponential scaling ranged from +2 to +12 dB/s and the alternative time-ramp functions such as t^2, $te^{\alpha t}$, $t^2 e^{\alpha t}$ were also tested. Exponential scaling of up to +12 dB/s was found to be excessive although it has been applied in some high resolution data processing schemes. Scaling that was less than +6 dB/s was generally found to be adequate. An examination of the monitor section (Figure 4.4(a)) and its autocorrelogram (Figure 4.4(b)) motivated the choice of the ramp and deconvolution parameters respectively.

A set of CMP gathers was pre-stack processed with a chosen filter and then stacked with approximate velocity functions. This procedure generally showed only a slight improvement in the S/N ratio of the output for line 7940. The results were poor for the shorter prediction gaps such as 1, 4, 8 and 16 msec.

From the processing trials, a filter with an active length of 130 msec, a gap of 20 msec and a design window of 1300 msec were chosen. The amplitude scaling before deconvolution was +2 dB/s. For each trace of the CMP gather, the autocorrelation design gate was time offset from the value of the mute function for that channel. A different filter was designed from and applied to each trace. The whole line was processed with the above parameters and the output traces were band-pass filtered after deconvolution in preparation for stacking.

Figure 4.4(a). A section of line 7940 showing the near-traces
after NMO corrections and prediction-error deconvolution.
The S/N ratio is very low.
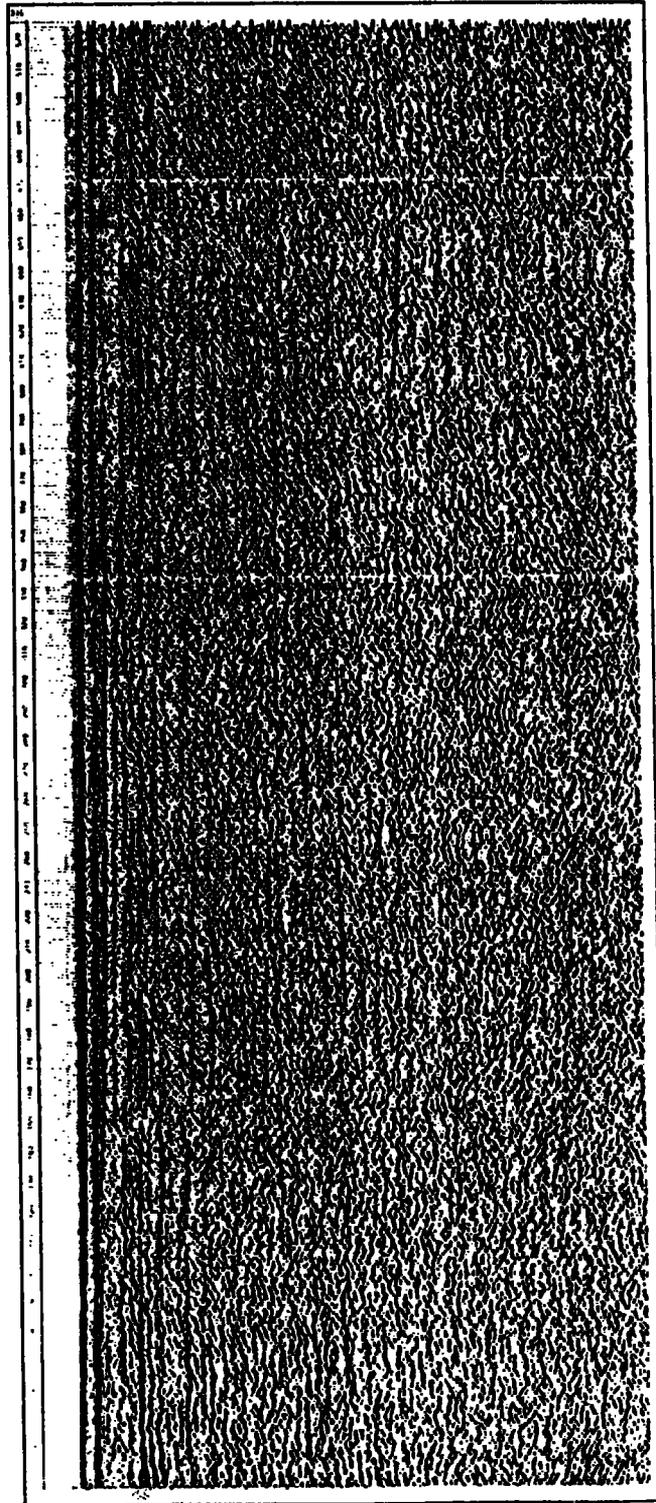
Figure 4.4(b). The autocorrelogram for Figure 4.4(a).
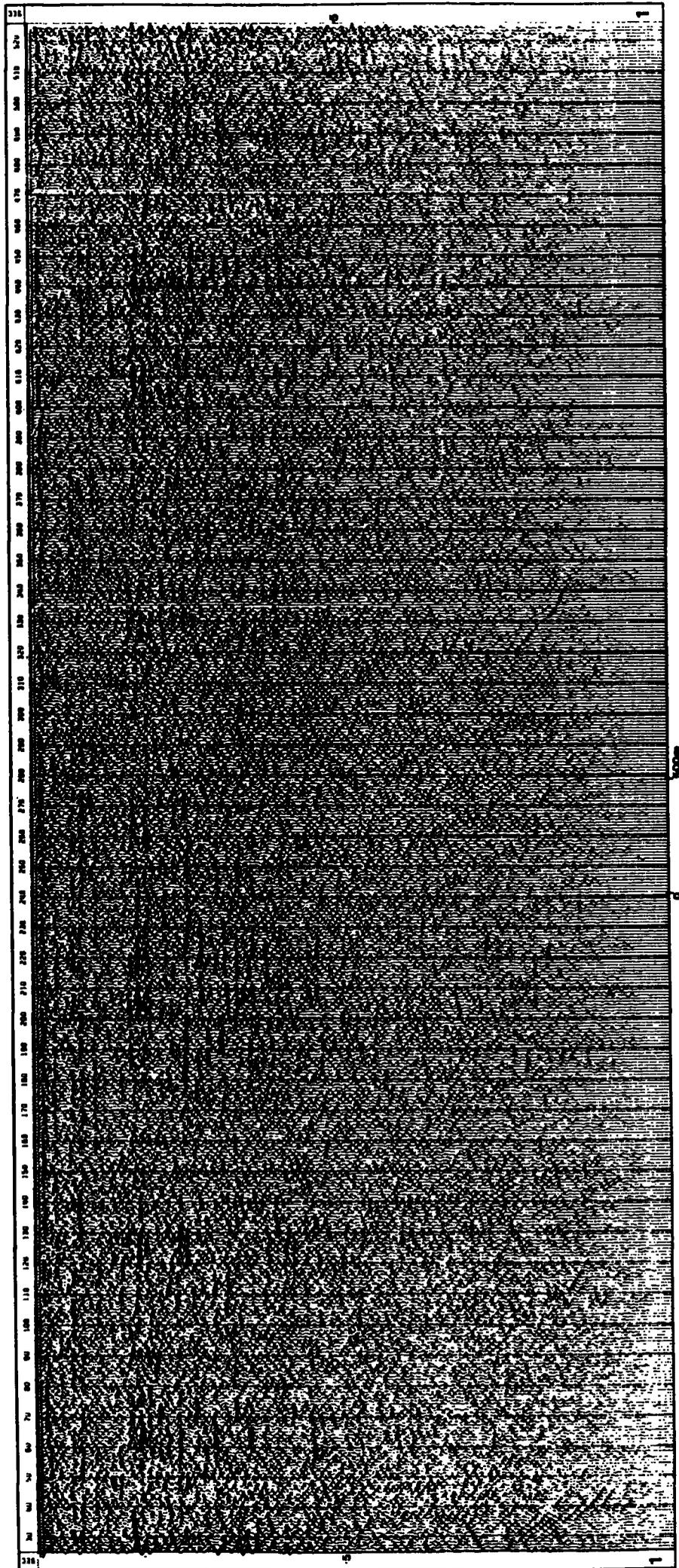
(ii) Velocity Filtering.

The second type of pre-stack processing was the application of velocity filtering. A method of wavefield analysis of seismic reflection records has been presented by Ryu (1982). In cases of multiple domination, a cut-off velocity function is easily chosen between the 'primary stacking velocity function' and that of the multiples. The function is used to correct the gather for NMO so that primary reflections and multiples become overcorrected and undercorrected respectively. The resulting gather is convolved with a time-space (t-x) operator that 'rejects' the undercorrected events and 'passes' the primaries. The filter can be specified as a 2-dimensional band-pass or band-reject Butterworth operator (Hale and Claerbout, 1983) and then inverse-Fourier transformed to the t-x space for the convolution. Each trace of the output gather is a weighted sum of a number of filtered input traces that is at most equal to the dimension of the operator. The fold diminishes towards the right and left edges of the gather where it levels up at half the operator dimension (always odd) plus one-half. The gather is next corrected for residual moveout (as in SOUSTON - chapter 2) and normal processing can be carried out. An w-k approach to the filtering of seismic events with a given apparent velocity has also been given by Christie et al. (1983) for high resolution data of these kind and the problems that may be encountered were discussed (loc. cit.).

87

Line 7940 was velocity filtered by using an 11X11 point operator and the cut-off velocity functions that were used during velocity analysis (part (c) below) were applied after lateral interpolation. The traces were interpolated to a level of 2 (resampled to 0.5 msec) during the forward and the reverse NMO corrections. There was no evidence from the velocity filtering of the velocity files that there was extensive spatial aliasing of these data so the entire line was velocity filtered. The resulting CMP gathers were written out on magnetic tape in preparation for stacking. An example of a velocity filtered gather is shown in part (c). Velocity filtering and prediction-error deconvolution were not applied in the same processing stream. Only one or the other was applied before stack.

(c) Velocity Analysis.

In order to maximize the lateral resolution, velocity analysis was carried out every 1/2 km. At each location, four successive gathers were summed to improve the S/N ratio of the input. This is physically equivalent to a lateral coverage of about 75m of the subsurface per file, and is a good approximation for a laterally continuous subsurface geological structure only.

The technique of Taner and Koehler, (1969) was used and the results were displayed as semblance contour plots (2-way time versus rms velocity) backed up by a display of the variation of the smoothed semblance maxima with 2-way time. The velocity analysis suite, DK1:VELAN, was used and it comprises of eight

separate programs linked together and entered by running the input routine DKl:VELYSM.

The results of the analysis on these composited files were not satisfactory for the picking of the stacking velocity functions. Figure 4.5(a) shows the file for CMP 187. The CMP gather is displayed on the left-hand side of the contour plot. The reflection at 400 msec is easy to pick up on the contour plot. The other maxima cannot be associated with reflected energy as clearly. The CMP gather was plotted without muting although it was muted before velocity analysis.

The results were improved by velocity filtering the composite gather prior to the analysis. This filtering was carried out with a 9X9 point operator after choosing a cut-off velocity function to exclude sea-floor multiples. The operator was not expected to suppress the peg-leg multiples within the Permian Limestones because their moveout would be similar to that of primaries with the same arrival times. Figure 4.5(b) shows the file for CMP 187 after velocity filtering and there are more events evident than on Figure 4.5(a) because of the improved S/N ratio. The cut-off function for this file is shown on the contour plot and the stacking velocity function was easier to choose and is indicated.

The method of velocity scans or constant velocity stacks (Dobrin, 1976, pp. 233) was also applied for velocity analysis but the results were more unreliable and were not applied in this work.

Figure 4.5(a). The velocity file for CMP 187 and the results of velocity analysis on it. The event at 400 msec shows a high semblance correlating with a reflection on the gather. Other maxima are difficult to correlate and interpret .

PROCESSING PARAMETERS

NO. OF CHANNELS = 24
SAMPLES PER CHANNEL = 1024
TRACE DELAY MS = 0
LEVEL OF INTERPOLATION = 4
CHANNEL 1 OFFSET M = 45.0
CHANNEL SPACING M = 25.0
SAMPLING INTERVAL MS = 1
START OF ANALYSIS MS = 0
END OF ANALYSIS MS = 1000
TIME STEP MS = 4
OPERATOR GATEWIDTH MS = 16
START VELOCITY KM/S = 1.00
END VELOCITY KM/S = 4.50
VELOCITY STEP KM/S = 0.05
MIN. CONTOUR VALUE = 0.20
CONTOUR INTERVAL = 0.10

VELOCITY FILTERING APPLIED
OPERATOR DIMENSION = 9

Cut-off Velocity Function

Stacking Velocity Function.
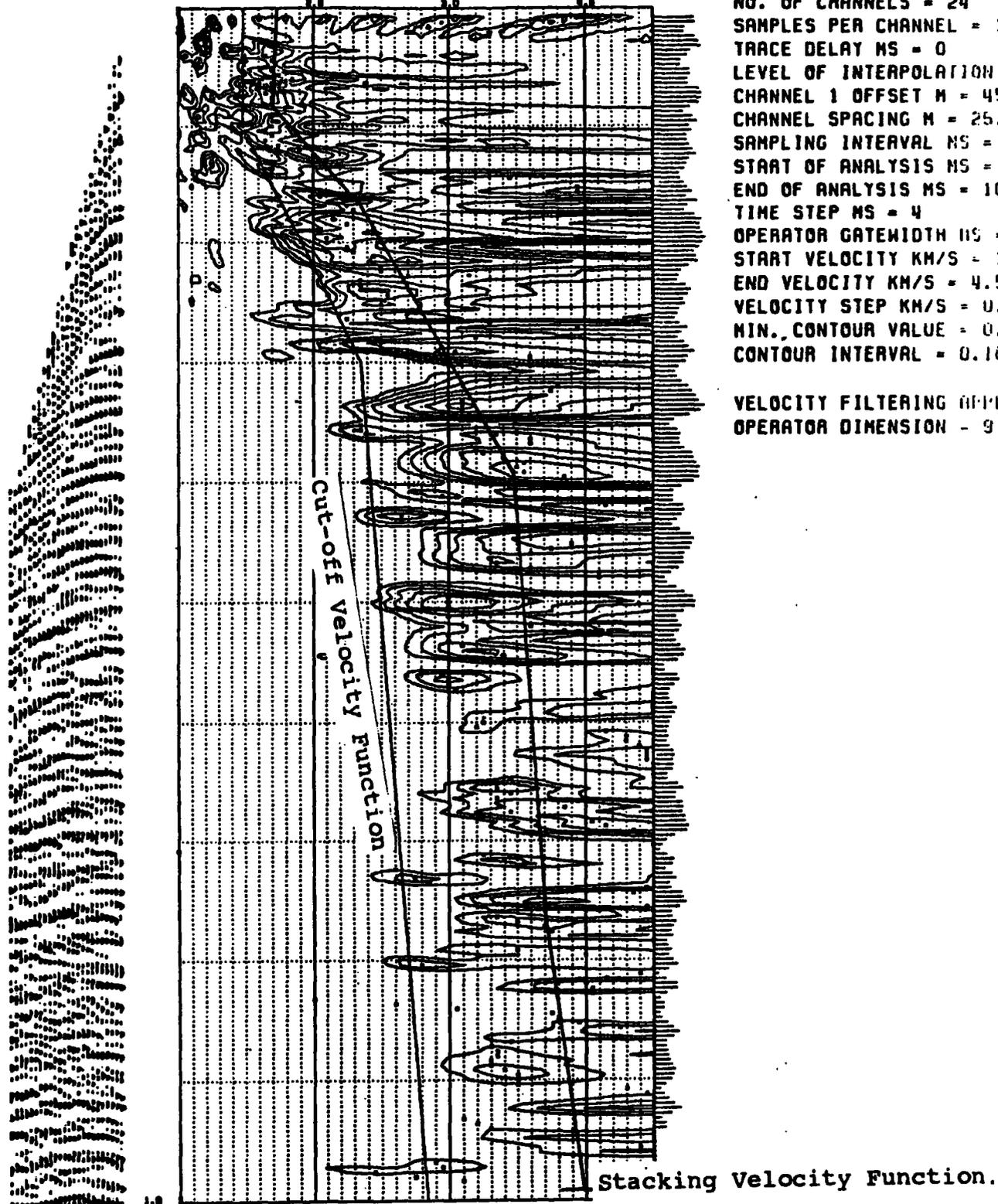
Figure 4.5(b). The velocity file for CMP 187 and the results
of velocity analysis after velocity filtering with a 9X9
point operator. The lower line is the cut-off function
that was chosen from Figure 4.5(a). There is an improvement
of the S/N ratio of the input gather and of the results
of the analysis. The upper line shows the stacking
velocity function that was picked for this file.

(d) Stacking.

Rms velocity functions obtained from the above analysis were spatially interpolated such that every CMP gather along the line had a stacking velocity function. The NMO corrections were carried out followed by stacking with the program DK1:STACK. During NMO orrections, each trace was interpolated (Lu and Gupta, 1978) to a level of 4 (resampled to .25 msec).

(i) Straight Stacking.

A 24-fold straight stack was carried out and the final section and its autocorrelogram are displayed as Figures 4.6(a) and 4.6(b) respectively. The tables of the stacking velocity functions are shown and the entire processing sequence for this section is indicated. Only the first second of the final stack is displayed. The CMP numbers are printed on the top of the section and the stars (*) indicate the positions of the velocity files. Figures 4.7(a) and 4.7(b) show the 24-fold straight stack of the data after velocity filtering and the autocorrelogram. A discussion of the results is given later.

(ii) Weighted Stack.

Tests on NUMAC proved it difficult to have consistent estimates of the optimum stacking weights (as in section 2.3.2(b)) for these data. However, a 15-fold distance weighted
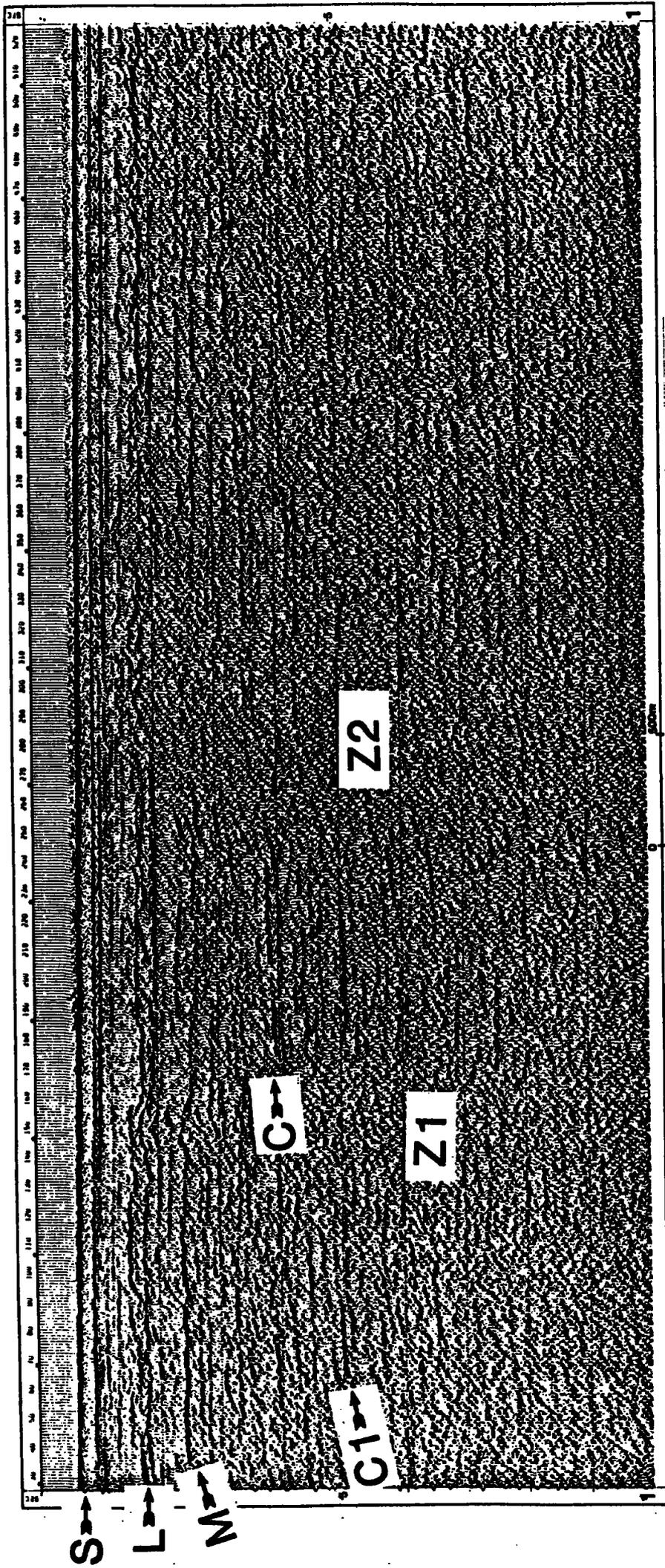
Figure 4.6(a). The 24-fold final stack of line 7940 with deconvolution applied before stack. The entire processing sequence is shown on the adjacent diagram. The stars (*) indicate the positions of the the velocity files.

DURHAM UNIVERSITY
SEISMIC PROCESSING
WEARMOUTH 79   LINE 7940

SYSTEM PARAMETERS

COLLECTED BY HORIZON EXP. LTD.

FIELD DATA
FIELD LAYOUT
NO. OF CHANNELS   24
SHOT INTERVAL   12.5 METRES
GROUP INTERVAL   25 METRES
NEAR TRACE OFFSET   45 METRES
SOURCE TYPE   SODERA HICAT WATER GUNS (8×80 CU.INC.)
RECORDING
SAMPLING INTERVAL   1 MSEC
RECORD LENGTH   1.5 SECONDS
FILTERS   27 LO. 248 HICUT
PROCESSING
DEMULTIPLEX

SORT

DBS
PRE-DECON. AMP. SCALING   +2 DB/S
DECONVOLUTION   DESIGN   1300 MSEC
                     ACTIVE LENGTH   130 MSEC
                     LAG   20 %
                     PRE-WHITENING

POST-DECON. AMP. SCALING   -2 DB/S
BANDPASS FILTER   LOW CUT   30 HZ
                     LOW TAPER   16 HZ
                     HIGH CUT   150 HZ
                     HIGH TAPER   152 HZ

STACK
FOLD   24
TRACE NORMALISATION   EQUAL ENERGY
RE-SAMPLED PRIOR TO NMO   .25 MSEC
MUTE

BANDPASS FILTER   LOW CUT   30 HZ
                     LOW TAPER   16 HZ
                     HIGH CUT   150 HZ
                     HIGH TAPER   152 HZ

AGC
NORMALISATION   100 MSEC
                                           UNIT AMP.

DISPLAY
TRACE SPACING   0.05 INCHES
GAIN   25.0

PROVIDED BY   NCB

Figure 4.6(b). The autocorrelogram section for Figure 4.6(a).
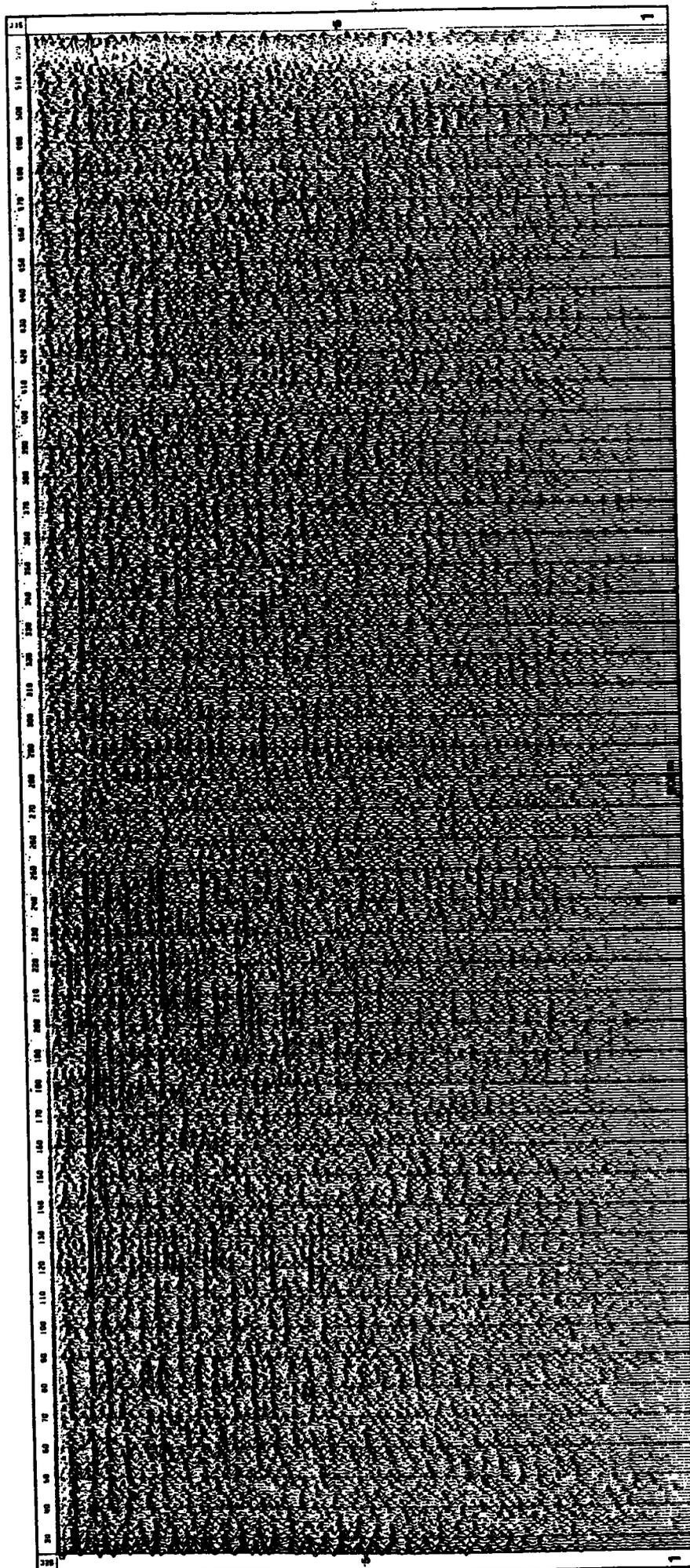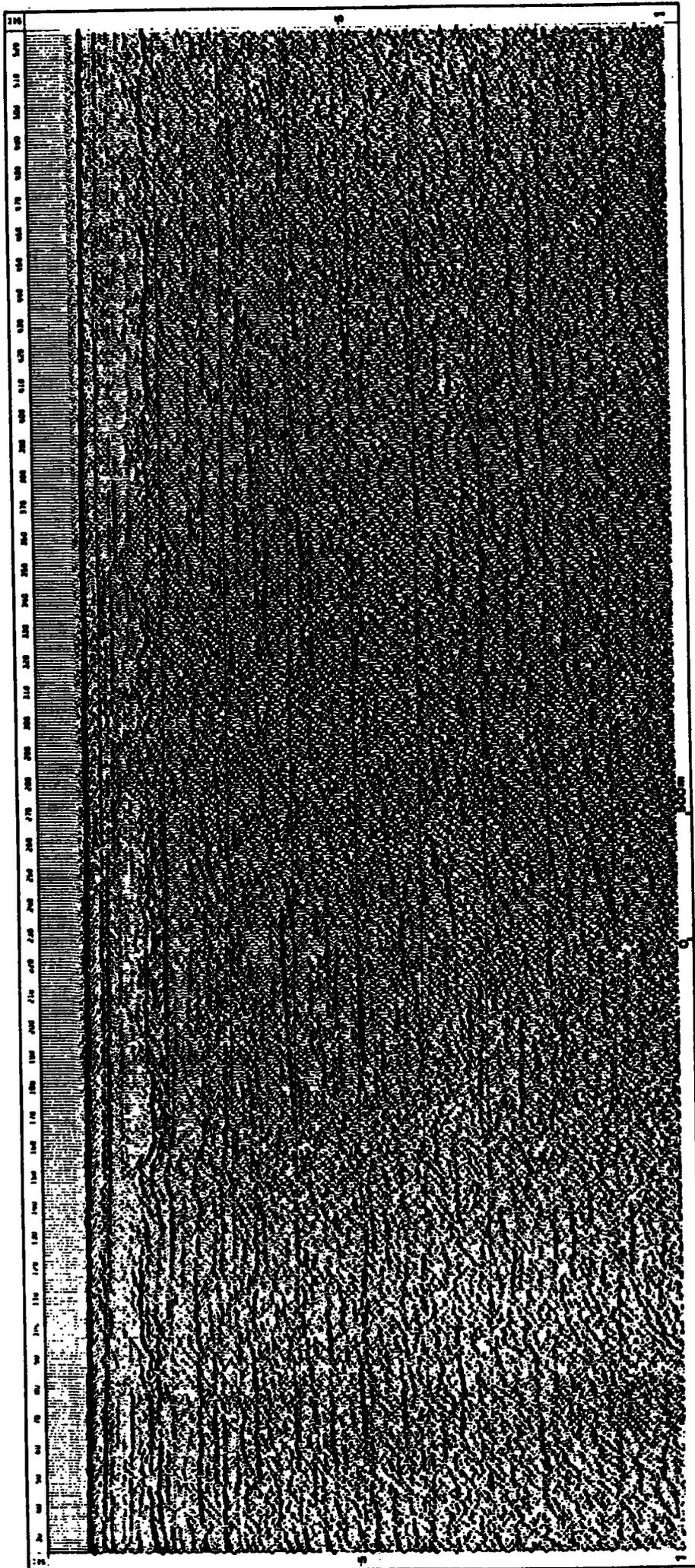
Figure 4.7(a). The 24-fold final stack of line 7940 after velocity filtering with an 11X11 point t-x operator.

DURHAM UNIVERSITY
SEISMIC PROCESSING
WEARMOUTH 79   LINE 7940

SYSTEM PARAMETERS

FIELD DATA   COLLECTED BY HORIZON EXP. LTD.
    FIELD LAYOUT
NO. OF CHANNELS   24
SHOT INTERVAL   12.5 METRES
GROUP INTERVAL   25 METRES
NEAR TRACE OFFSET   45 METRES
SOURCE TYPE   SODERA MICAT WATER GUNS (8×80 CU.INC.)
    RECORDING
SAMPLING INTERVAL   1 MSEC
RECORD LENGTH   1.5 SECONDS
FILTERS   27 LO, 248 HICUT
    PROCESSING
DEMULTIPLEX

SORT

VELOCITY FILTERING

STACK
FOLD   24
TRACE NORMALISATION   EQUAL ENERGY
RE-SAMPLED PRIOR TO NMO   .25 MSEC
MUTE

AGC   100 MSEC
NORMALISATION   UNIT AMP.

DISPLAY

TRACE SPACING   0.05 INCHES
GAIN   20.0

PROVIDED BY   NCB

Figure 4.7(b). The autocorrelogram section for Figure 4.7(a).
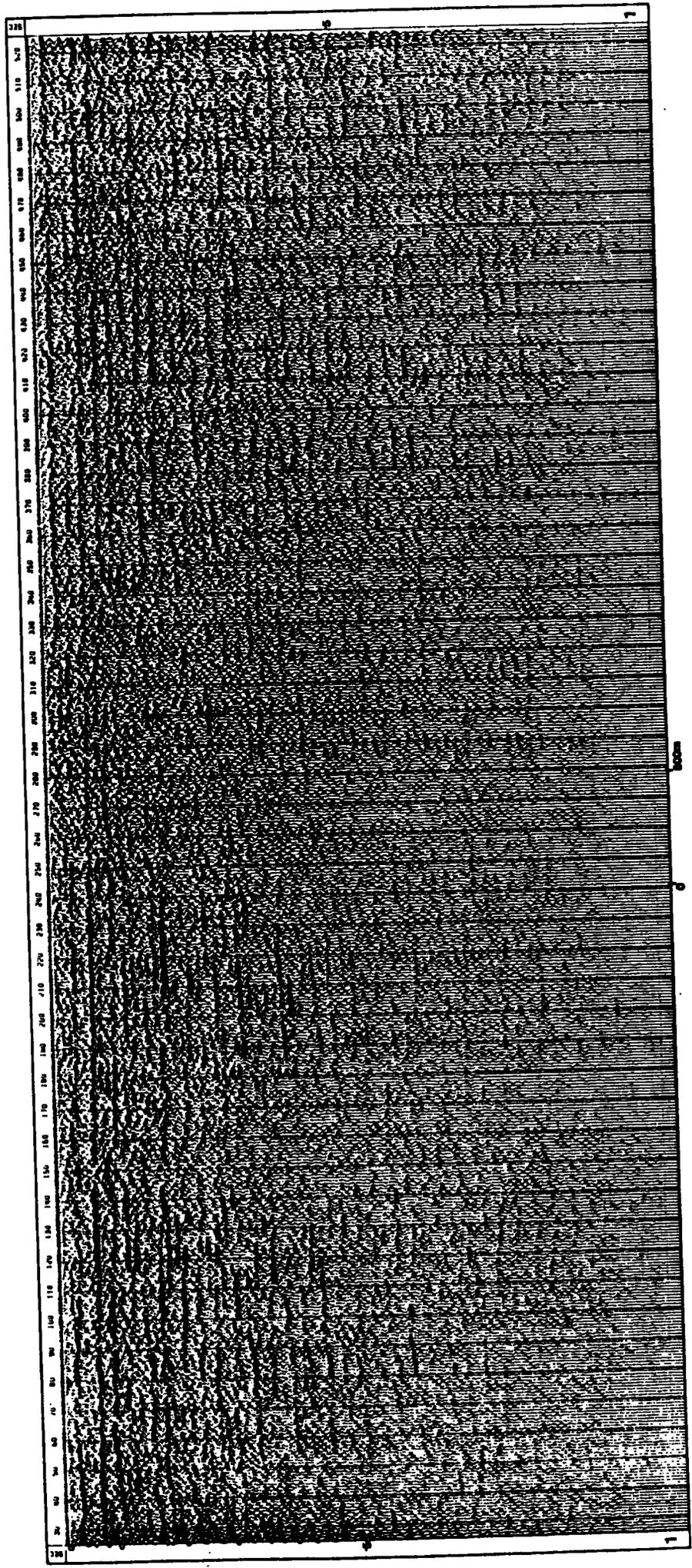
stack was performed. Although this meant that the last trace was relatively enhanced by a factor of about 9, the differences with the straight stack were tempered as the final section and its autocorrelogram on Figure 4.8(a) and 4.8(b) respectively show. Other forms of weighting were tested but the results did not match those of Figures 4.8(a) and 4.8(b).

(e) Post-stack Processing.

The only processing applied after stack was prediction-error deconvolution and band-pass filtering. The section obtained after this treatment of the straight stack is shown on Figure 4.9(a) with the corresponding autocorrelogram displayed on Figure 4.9(b). No significant differences with these plots were obtained by the same filtering of the weighted stack.

The prediction filter length was 218 msec, the predictive gap was 32 msec, an autocorrelation design window of 1300 msec was used and the prewhitening parameter was 2%. The S/N ratio of the result is higher than that of the input and the other significant differences are discussed below.

4.2.3   Discussion.

The seismic sections that have been presented above are examined in this section with regard to their differences and from an interpretative viewpoint.

It is appropriate to consider the straight stack without DAS
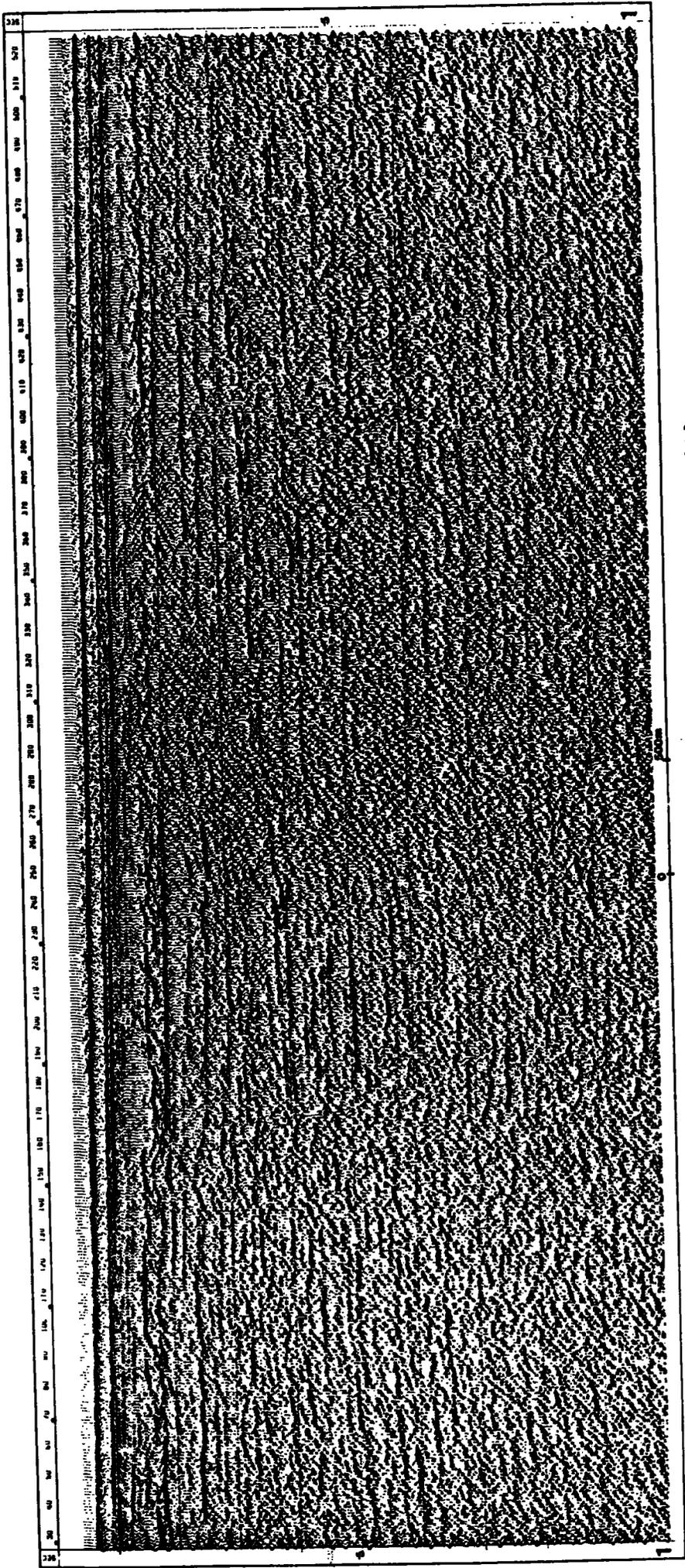
Figure 4.8(a). The 15-fold final stack of line 7940 with
weighting (proportional to offset X) applied to the
NMO corrected traces before stack.

DURHAM UNIVERSITY
SEISMIC PROCESSING
WEARMOUTH 79   LINE 7940

SYSTEM PARAMETERS

FIELD DATA

FIELD LAYOUT	COLLECTED BY HORIZON EXP. LTD.	
NO. OF CHANNELS	24	
SHOT INTERVAL	12.5 METRES	
GROUP INTERVAL	25 METRES	
NEAR TRACE OFFSET	45 METRES	
SOURCE TYPE	SODERA MICAT WATER GUNS (8*80 CU.INC.)	

RECORDING
SAMPLING INTERVAL	1 MSEC
RECORD LENGTH	1.5 SECONDS
FILTERS	27 LO, 248 HICUT

PROCESSING

DEMULTIPLEX

SORT

OBS

PRE-DECON. AMP. SCALING		
DECONVOLUTION	DESIGN	+2 DB/S
	ACTIVE LENGTH	1300 MSEC
	LAG	130 MSEC
	PRE-WHITENING	2 %
POST-DECON. AMP. SCALING		-2 DB/S
BANDPASS FILTER	LOW CUT	30 HZ
	LOW TAPER	16 HZ
	HIGH CUT	150 HZ
	HIGH TAPER	152 HZ

STACK

FOLD	15 (DISTANCE WEIGHTED)	
TRACE NORMALISATION	UNIT RMS ENERGY	
RE-SAMPLED PRIOR TO NMO	.25 MSEC	
MUTE		
BANDPASS FILTER	LOW CUT	30 HZ
	LOW TAPER	16 HZ
	HIGH CUT	150 HZ
	HIGH TAPER	152 HZ
AGC		100 MSEC
NORMALISATION		UNIT AMP.

DISPLAY

TRACE SPACING	0.05 INCHES
GAIN	20.0

PROVIDED BY   NCB

Figure 4.8(b). The autocorrelogram section of the distance
weighted stack of Figure 4.8(a).
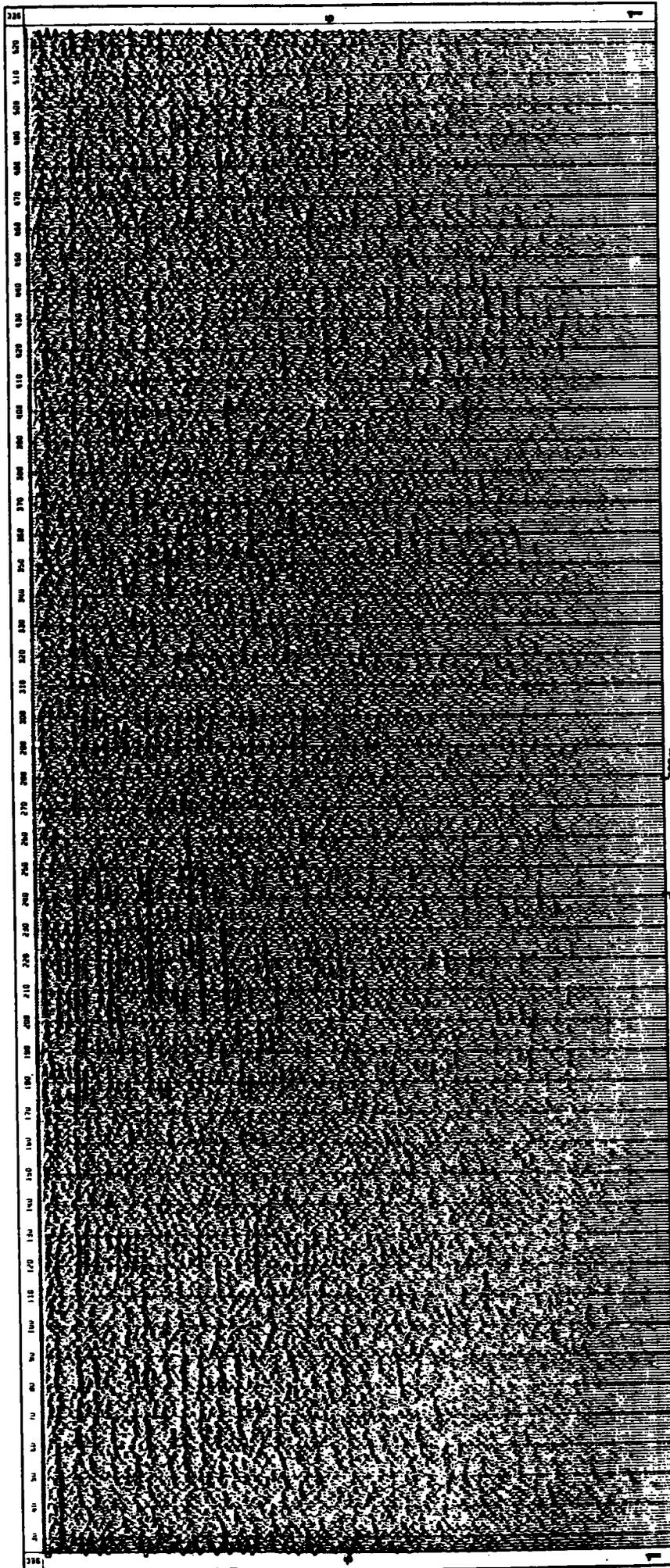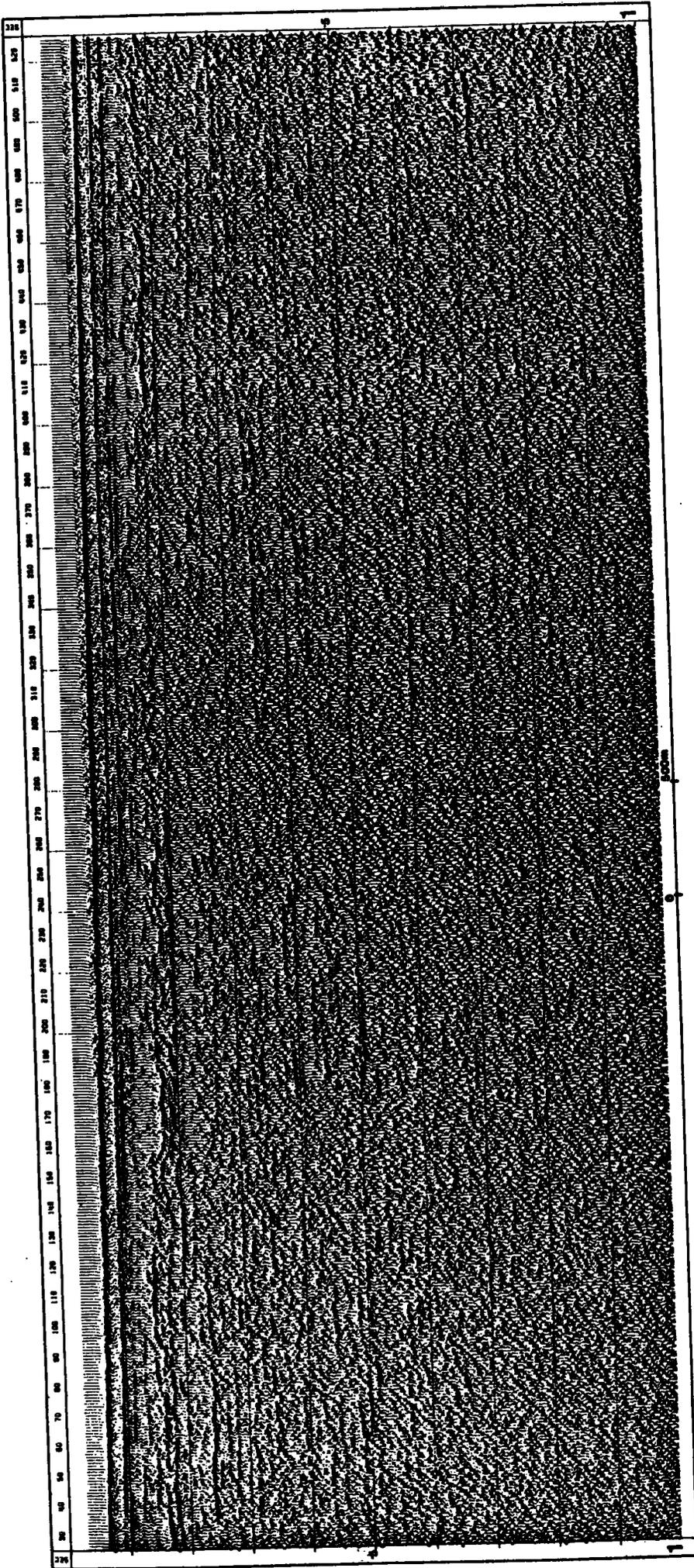
Figure 4.9(a). Straight (24-fold) stack of line 7940 with
prediction-error deconvolution applied after stack.

DURHAM UNIVERSITY
SEISMIC PROCESSING
WEARMOUTH 79   LINE 7940

SYSTEM PARAMETERS

COLLECTED BY HORIZON EXP. LTD.

FIELD DATA

FIELD LAYOUT	
NO. OF CHANNELS	24
SHOT INTERVAL	12.5 METRES
GROUP INTERVAL	25 METRES
NEAR TRACE OFFSET	45 METRES
SOURCE TYPE	500EAA MICAT WATER GUNS (8×80 CU.INC.)
RECORDING	
SAMPLING INTERVAL	1 MSEC
RECORD LENGTH	1.5 SECONDS
FILTERS	27 LO, 248 HICUT
PROCESSING	

DEMULTIPLEX

SORT

OBS

PRE-DECON. AMP. SCALING		
DECONVOLUTION	DESIGN	1300 MSEC
	ACTIVE LENGTH	130 MSEC
	LAG	20 MSEC
	PRE-WHITENING	2 %
POST-DECON. AMP. SCALING		-2 DB/S
BANDPASS FILTER	LOW CUT	30 HZ
	LOW TAPER	16 HZ
	HIGH CUT	150 HZ
	HIGH TAPER	152 HZ

STACK

FOLD		24
TRACE NORMALISATION		EQUAL ENERGY
RE-SAMPLED PRIOR TO NMO		.25 MSEC
MUTE		

DAS

PRE-DECON. AMP. SCALING		+3.5 DB/S
DECONVOLUTION	DESIGN	1300 MSEC
	ACTIVE LENGTH	250 MSEC
	LAG	32 MSEC
	PRE-WHITENING	2 %
POST-DECON. AMP. SCALING		-3.5 DB/S
BANDPASS FILTER	LOW CUT	30 HZ
	LOW TAPER	16 HZ
	HIGH CUT	150 HZ
	HIGH TAPER	152 HZ

AGC   100 MSEC
NORMALISATION   UNIT AMP.

DISPLAY

TRACE SPACING   0.05 INCHES
GAIN   20.0

+2 DB/S

Figure 4.9(b). The autocorrelogram section for Figure 4.9(a).
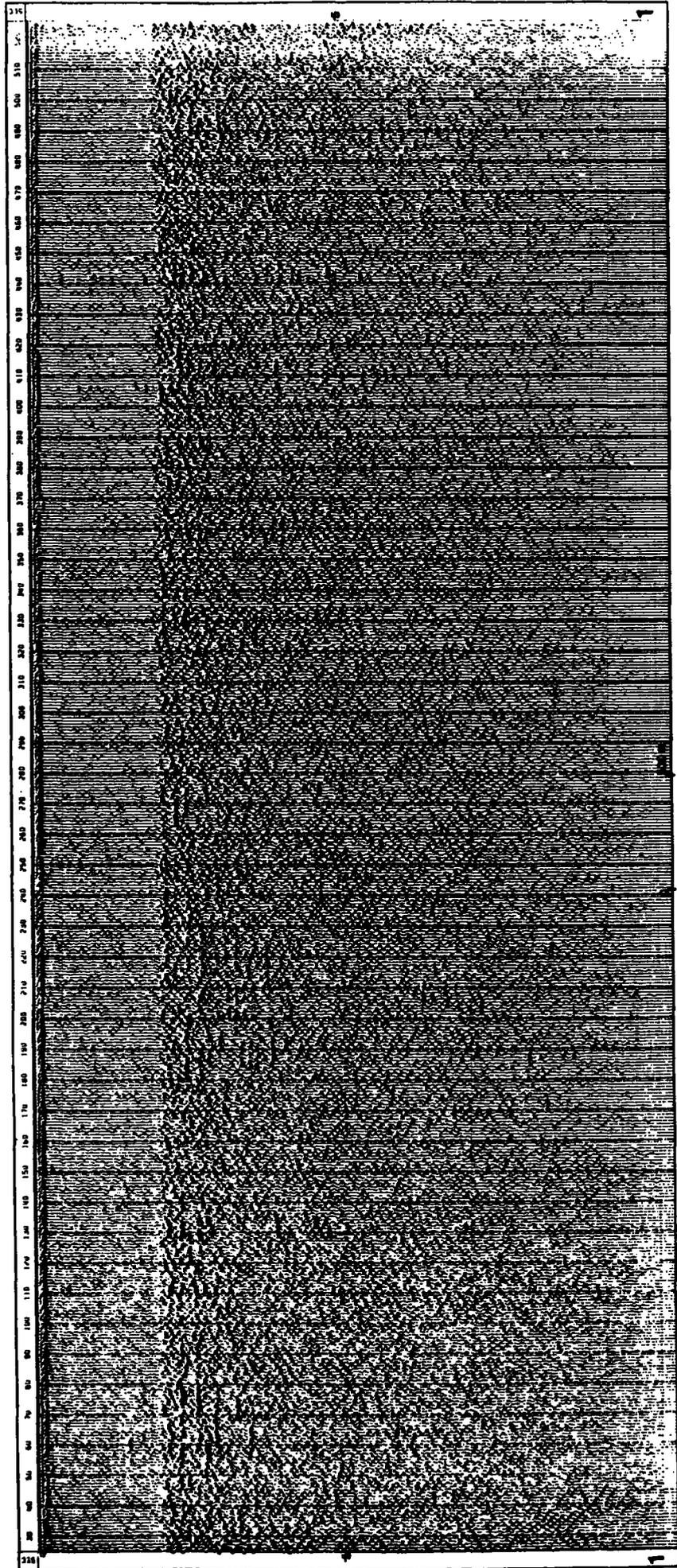
(Figure 4.6(a)) in detail. Within the first 150 msec of the section, the most obvious event (the seabed reflection) dips from about 74 msec on the left of the section to about 84 msec on its right (event S). The only other characteristic evident is the group of events that run across the section just below the seabed with 2-way travel times between 100 and 132 msec. These events can be explained in one of two ways. Firstly, the fact that they are not very prominent on the section processed before (by the N.C.B.) suggests that the present muting function may not have been steep enough at the near offsets. Therefore, some of the earliest refracted phases are not sufficiently edited out and consistently pass through the stack to appear as coherent reflections from seabed muds and sediments. In that case their presence can be considered irrelevant to the interpretation of deeper structure although they might affect post-stack prediction error deconvolution slightly. Secondly, Figure 1.2 showed that the Boulder Clay has a thickness of about 48m and if it is considered that some consolidation of this formation has taken place so that it has a seismic velocity of about 2.2 km/s, then the 2-way time to its base (assuming a sea water velocity of 1.5 km/s) should be about 121 msec. However, the reflection from the base of the Boulder Clay is relatively weak and may not be evident if the S/N ratio is not good. Furthermore, the relatively strong seabed event prevents the AGC from sufficiently ranging up such close and weaker arrivals. The strength of this event between CMP 310 and CMP 350 supports the idea that it is the top of the Upper Permian Marls and in the absence of further evidence

to the contrary, the entire arrival (at 121 msec) can be considered as the Upper Permian Marls.

The first prominent event (event L) runs across the section from about 170 msec on the left to about 190 msec on the right. It is not as smooth a reflection as the seabed reflection. It probably corresponds to the top of the Magnesian Limestones though the primary reflection from this interface would normally be expected to have the same waveform and polarity as the seabed reflection. Although the difference in picking a trough or a peak as the event only amounts to a time delay and should not affect the interpretation of the deeper events, explanations for this difference in waveform are possible. If the seismic wavelet has undergone appreciable dispersion during propagation, then such a change of waveform is expected and if there is more than one interface close to the top of the limestone formation , then the composite reflection cannot have the same form as the original signal.

The continuity of the reflection (L) is interrupted by the two zones between CMP 130 and CMP 180 (Z1) and between CMP 270 and CMP 390 (Z2) respectively. The responses within these segments suggest that fault development may probably be taking place within them. Although clear evidence of this is only around Z1, the break in the continuity of the deeper reflections within both Z1 and Z2 supports the idea as well. A displacement of the horizon can be noted around CMP 155 (at about 180 msec) which corresponds to a normal fault with a throw down to the right-hand side. The opposite effect is noticeable around CMP 280 (Z2) but

93

the events at 350 msec show this more clearly. The break in the continuity in this (Z2) segment may be due more to the effects of the erosion and the roughness of the top of the Magnesian Limestone than to the faulting. The scattering of the energy by this surface gives a more 'harsh' look to this segment of the final section. Magnitudes of possible throws of the proposed faulting cannot be estimated at the present stage of the phenomenon along the line.

The next event is the reflection at about 245 msec (event M) which can be followed (except for the segments Z1 and Z2) across the section. It is weaker in amplitude on the right-hand side of the section and also has a slight waveform change. The timing of the event, its phase (relative to the event L) and the fact that it undergoes significant eradication during DAS (Figure 4.9(a)), suggest that it is a seabed multiple of the primary reflection from the top of the Magnesian Limestones. Just below this reflection (at about 280 msec) is a weaker arrival which does not undergo much suppression during DAS. This is probably the primary reflection from the base of the Limestones. It is not continuous on either of the sections (Figure 4.6(a) and 4.9(a)). The Marl Slate horizon and the unconformity cannot be picked on either section .

The only prominent events below 300 msec are the Coal Measures type reflections (event C). As far as this section (Figure 4.6(a)) shows, they are evident from the end of the segment Z1 at about 400 msec (CMP 160 to CMP 170) and dip upwards to the right of the section at about 300 msec. Besides the clear

interruption at Z2, this reflection is not continuous from trace to trace throughout the entire section.

One inference that could be drawn from the arguments in section 4.2.1 is that Coal Measures reflections are not observed in those segments of the line in which there is evaporite (the 5.0 km/sec refractor). One would therefore expect to find primary reflections from the evaporite in segments from which the Coal Measures reflections are absent. These primaries are not clearly evident on this seismic section. However, if a thin layer of evaporite is just below the top surface of the Magnesian Limestones (Magraw, 1978), then the reflections from the two will be composited to form what has already been interpreted as the event L.

The last prominent event (C1) on the section also has Coal Measures characteristics and it dips from about 500 msec at CMP 70 to about 400 msec at CMP 480. The timing of C1 relative to C is just sufficient for the former to appear like a seabed multiple of the latter but the fact that it is not significantly affected during DAS suggests that it is a primary. However it is difficult (Van Riel, 1965) to label such events on a Coal Measures seismic section. The event C1 is laterally more discontinuous than C. The transparent overlay shows a possible interpretation of some of the horizons on this section. The segmentary characters of C and C1 are clearer.

Alternative processing has not resulted in more interpretable sections. Two points can be noted with regard to the weighted stack (Figure 4.8(a)). Firstly, the primaries within

the Coal Measures stand out more prominently in amplitude although their continuity just matches that of the straight stack. Secondly, the events just below the seabed appear stronger through this weighting and this supports the criticism that they are due to a low gradient of the muting function at small offsets. Velocity filtering before stack (Figure 4.7(a)) did provide a slight improvement in the continuity of the Coal Measures primary reflections, notably around CMP 190. It also produced a greater suppression of the event at 240 msec than did the prediction-error deconvolution applied before the stack on Figure 4.6(a).

Detailed standard processing of these data showed Coal Measures but the resulting sections are not satisfactory for conclusive interpretation. The general rule of thumb (Ziolkowski, 1979) that the streamer length (600m in this case) should be of the same order of magnitude as the target depth (about 300 to 800m for this survey) was observed. Straight (standard) stacking and prediction-error deconvolution appear to be adequate for its treatment and the latter does not eliminate the primaries to an intolerable extent despite the fact that the reflectivity sequence for this geology is unlikely to be white and stationary. The Coal Measures are actually observed which means that there is some 'penetration' (defined in terms of the seismic energy that is able to pass through the Permian Limestones into the Carboniferous and back to the surface to be recorded with the prevailing seismic noise) but it is not satisfactory and adequate. The S/N amplitude ratio at about 300 m offsets was

found (on the field records) to be approximately 390 at 2-way times of 400 msec. This 'signal' consists mainly of shot-generated arrivals at the lower frequency end of the bandwidth used.

Finally, Figure 4.10 shows the geometrical considerations inherent in the choices of the parameters for the surveys carried out for the N.C.B. in 1979 and 1982 respectively. BB' and AA' are 24-channel streamers with group spacings of 6.25m and 25m respectively and with near-group offsets of 10m and 45m respectively. If the interval velocity versus depth profile above the Magnesian Limestones is assumed to be as shown on this figure, then the approximate travel time equation (refraction) for the fastest layer is

$$T = 133 + X / 4.0 \qquad msec$$
$$X \quad in \quad meters.$$

The critical distance X_c from the source S is about 203m. The p-wave penetration window is shown through which the point source S radiates a coal seam (C) at depth (about 400m). This window depends on the depth of the fastest layer and on the seismic velocity of this layer. In this situation, the depth is small (about 155m) and the velocity is high (about 4.0 km/s) compared to the sea water velocity (1.5 km/s). The penetration window is therefore narrow and the wide-angle reflections and refractions merge to form high amplitude noise. If anhydrite bands are present below the top of the 4.0 km/s layer, then the uppermost band will form the fastest layer and the critical distance will
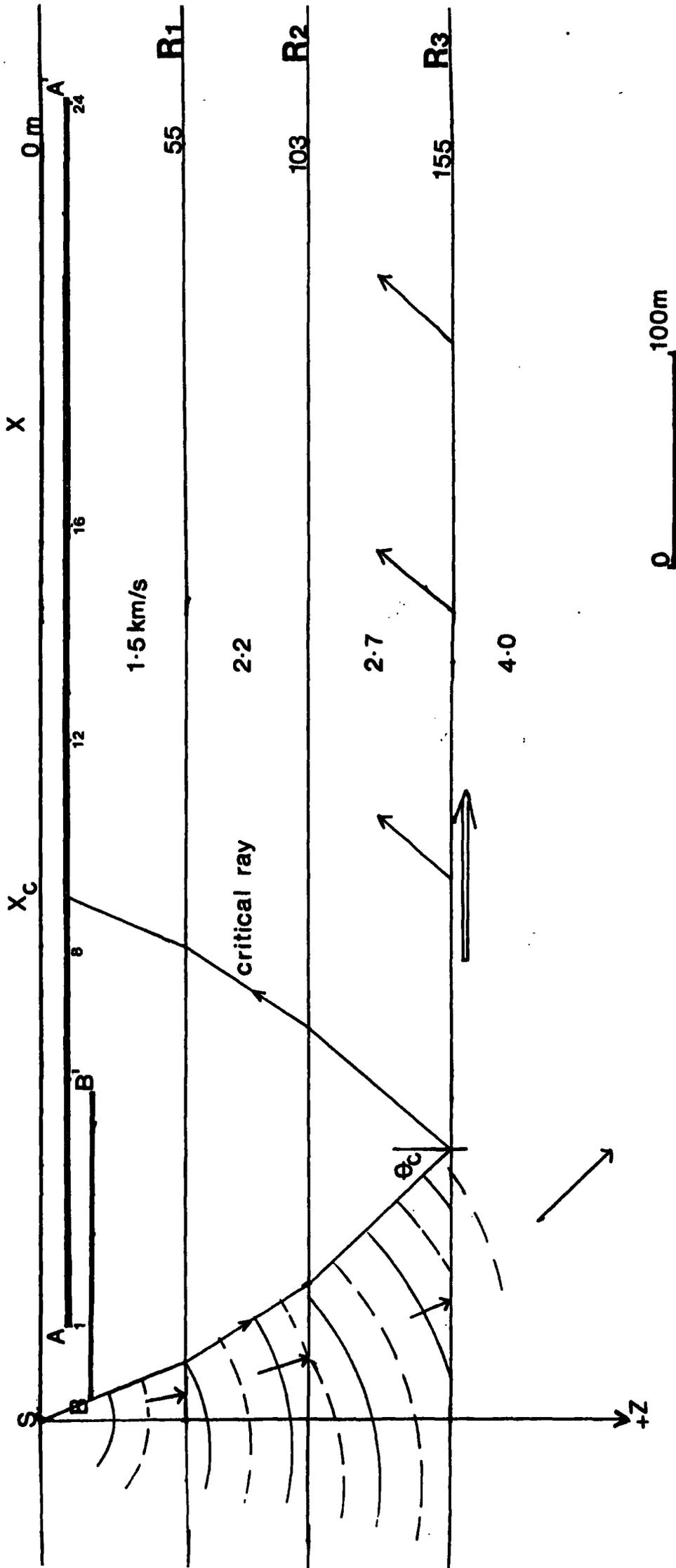
p-wave penetration window
(assuming a point source S)

Figure 4.10. Shows the pressure-wave penetration window for a structure with the velocity-depth profile up to the top of the Magnesian Limestones indicated. Reflections from deeper dipping Coal Measures are recorded with the strong refractions on the longer streamer (AA') but the shorter one (BB') receives a much smaller percentage of the energy returned.

(C)

be less than X_c and the situation is worsened.

The primary reflections from the Coal Measures interfere at far offsets (greater than 200m - 8th channel) with the high amplitude noise and are muted during processing of the 1979 data. A consideration of these effects on the 1979 survey influenced the choice of the acquisition parameters for the 1982 survey. The streamer BB' was used and the high amplitude noise was avoided. In the 1979 survey, a distance weighted water gun source was used but a sleeve exploder source was applied in 1982. Although there is not much difference in the spectral bandwidths of the two sources, the intention would have been to inject more energy at higher frequencies in the later survey and to try to achieve better penetration. A set of data that were acquired along a segment of line 7940 (from about CMP 103 to CMP 370) with the streamer BB' and using this source was processed and the results are outlined next.

4.3   Processing of Line 8201A.

The 6-fold data (section 1.2(b)) show the same characteristics as the records of line 7940. Although many reflected events can be observed on these records, most of them are multiples. Figure 4.11(a) shows a section of the records in which the multiple reflections are not prevalent. Very few primary events can be observed below 400 msec. Figure 4.11(b) shows a section with significant high amplitude reverberation. The records were gain ranged and normalized to unit amplitude
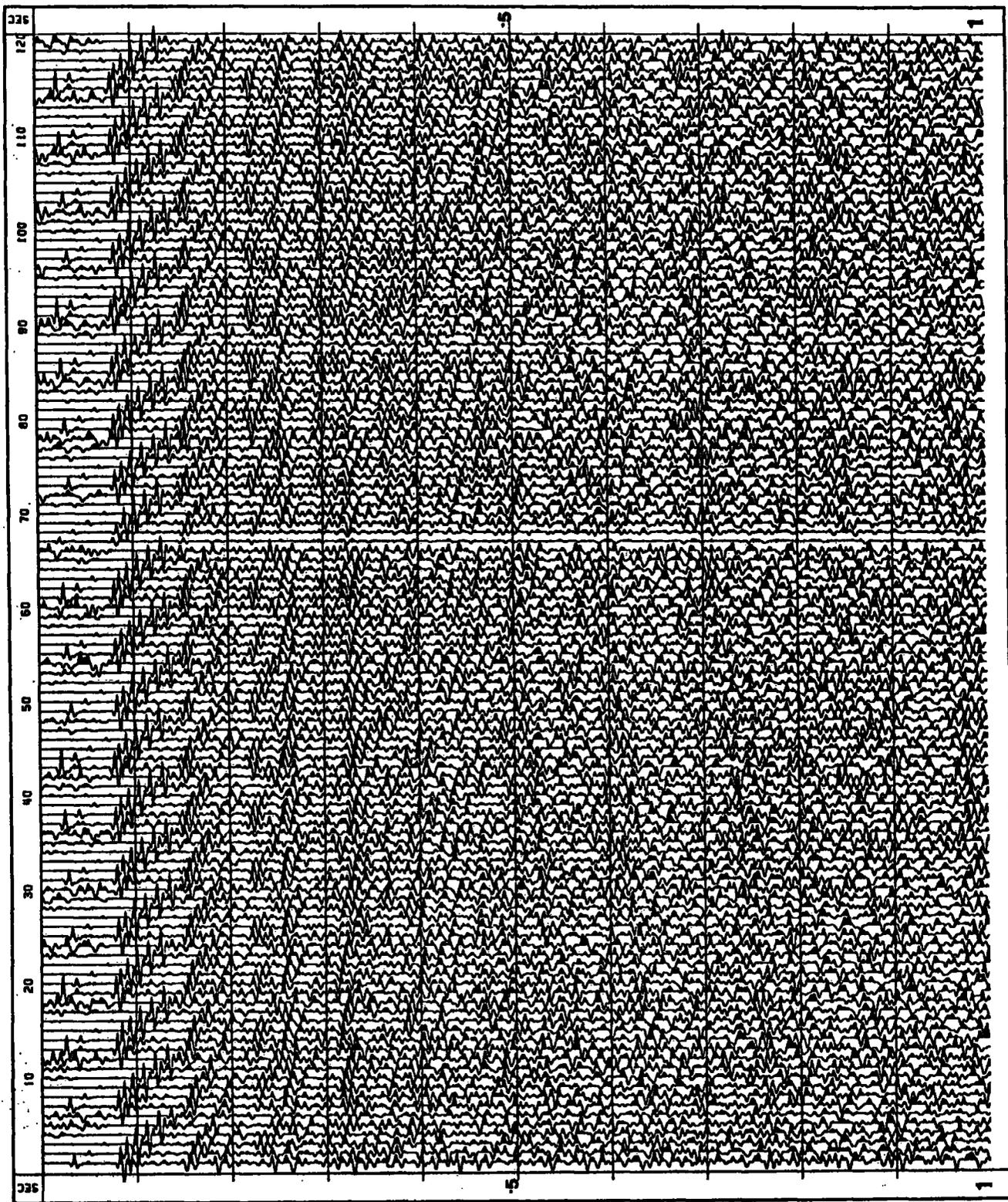
Figure 4.11(a) Field records from the 1982 data showing few
        reflections below 400 msec.
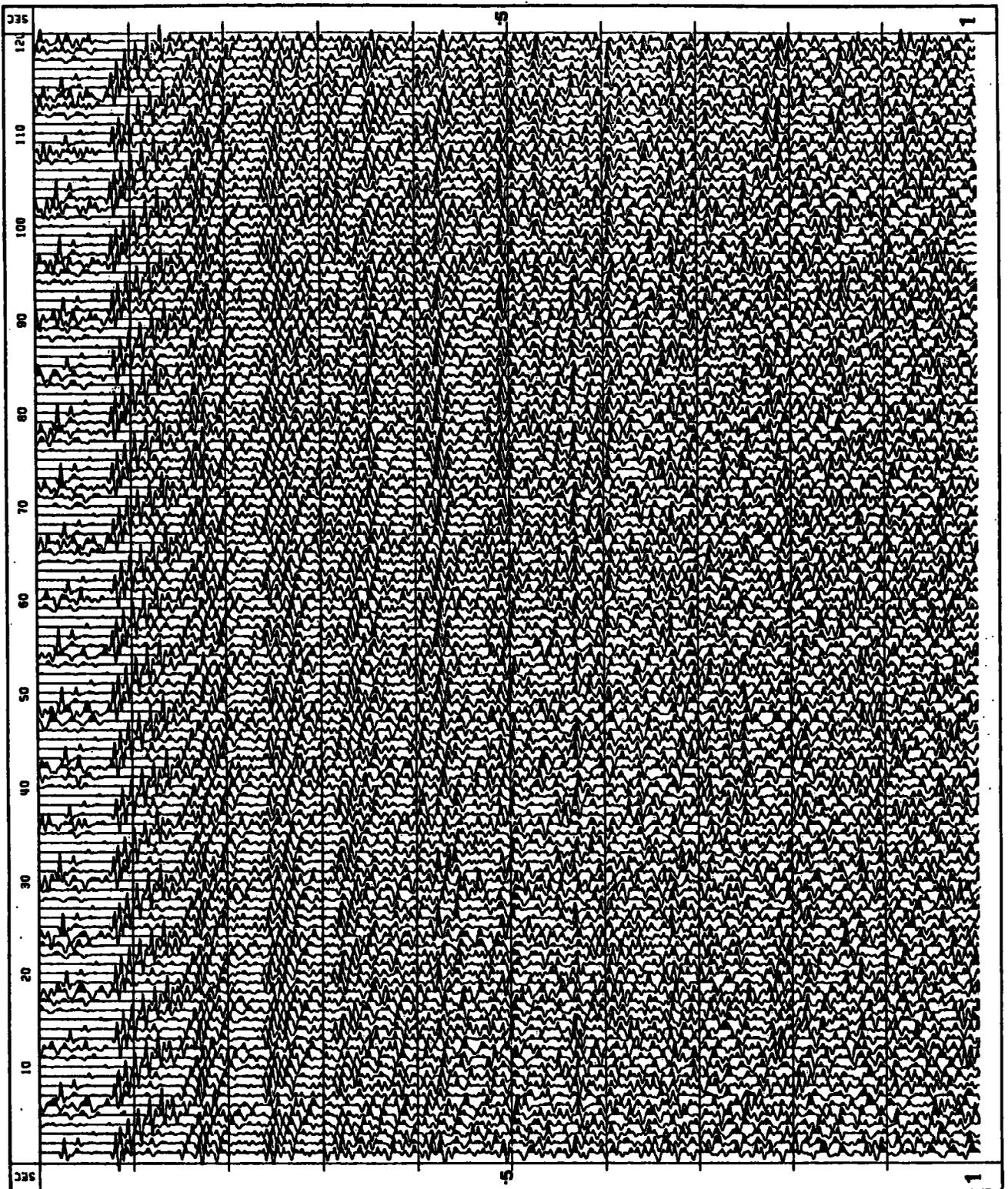
Figure 4.11(b). Field records from the 1982 data showing more
   reflected arrivals below 400 msec. Most of them are seabed
   multiples.

before the plot. Since the streamer length was about 150 m, the muting pattern was simple and aimed at the direct arrivals only.

Figure 4.12 shows a stacked section of line 8201A. The section extends from CMP 46 to CMP 852. Lithological information (Figure 1.2) suggests that the primary reflection from the top of the limestones would be expected between 145 and 175 msec. Although the first seabed multiple generally hampers the resolution within this interval, it can be observed that many diffraction hyperbolae emanate from the top of this formation as well as from shallower horizons. The former indicates that the top of the limestones is not smooth and may have been eroded prior to the deposition of the overlying strata.

The processing steps that were applied to this line are outlined below and the results are discussed.

The rest of the seismic sections of line 8201A displayed in this chapter were reduced in scale by a factor of four by summing up every four adjacent traces. This was done so that they should have the same horizontal scale as those for line 7940. As a consequence, the numbers (1 to 200) that are displayed at the top of these sections are not CMP numbers but trace sequence numbers in the output tape. Approximate CMP numbers can be easily calculated. On some of the sections, approximate positions of the velocity files are marked with a star (*).
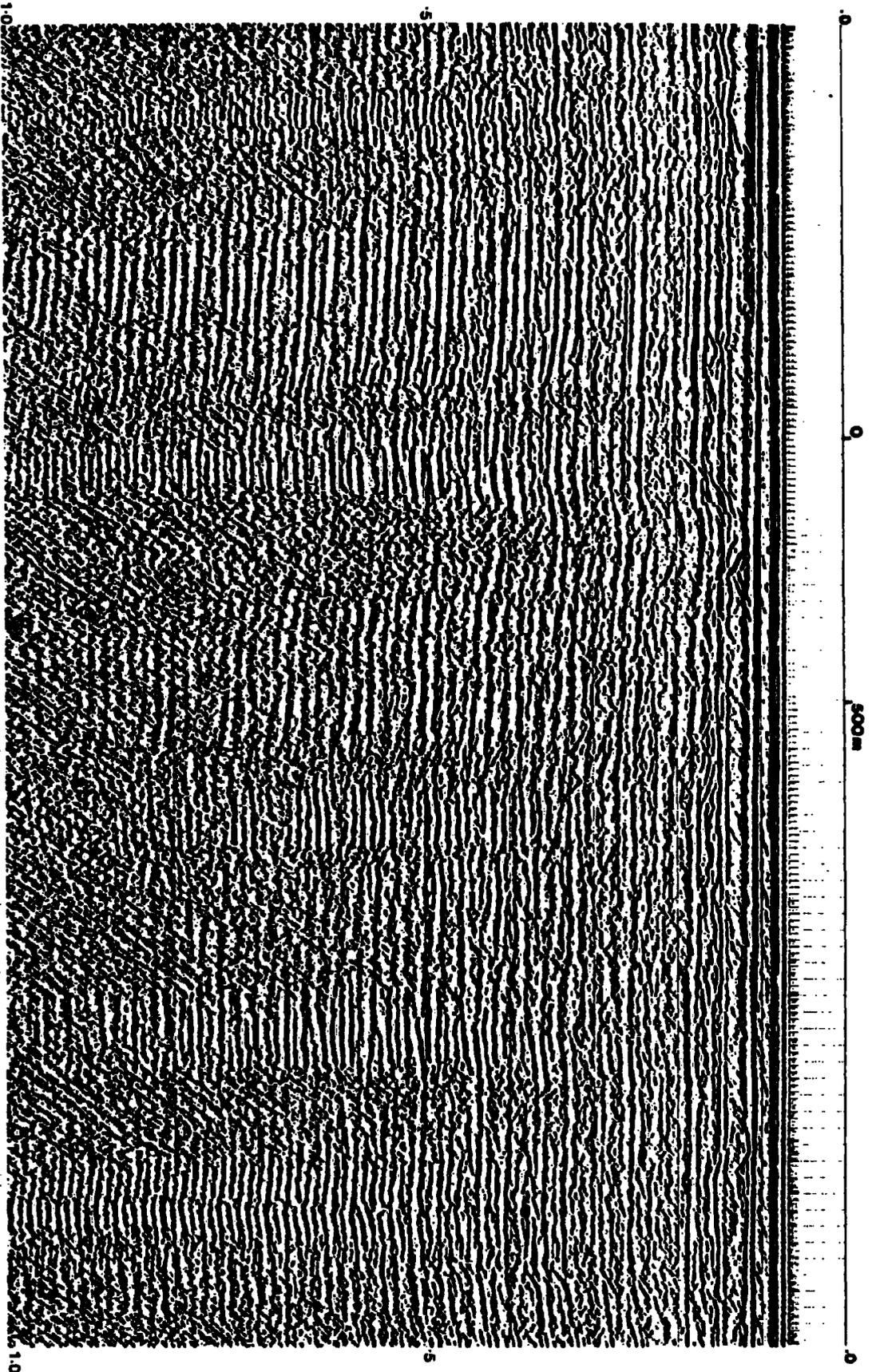
Figure 4.12. A stacked section of line 8201A showing diffractions off the surface of the Limestones and some shallower horizons.

4.3.1   Processing Sequence.

The data were translated to DSEGY as in section 4.2.2(a) and then muted and band-pass filtered.

(a) Pre-stack Processing.

Better results were obtained from pre-stack prediction-error deconvolution of this line than line 7940. A number of tests showed that filters with an active length of up to 200 msec produced results with good S/N ratios before stack although short gaps (1, 2, and 4 msec) gave poorer results as would be expected. There was a significant reduction in seabed multiples as the final sections will show. The prediction gap was 32 msec, the prediction filter length was 168 msec, the design gate was 1800 msec long and a prewhitening parameter of 2% was applied. Pre-deconvolution and post-deconvolution amplitude scaling were ±5.2 dB/s respectively. The filters were designed and applied as in section 4.2.2(b).

Figures 4.13(a) and 4.13(b) show a near-trace section and its autocorrelogram. The section was obtained after one of the pre-stack processing trials.
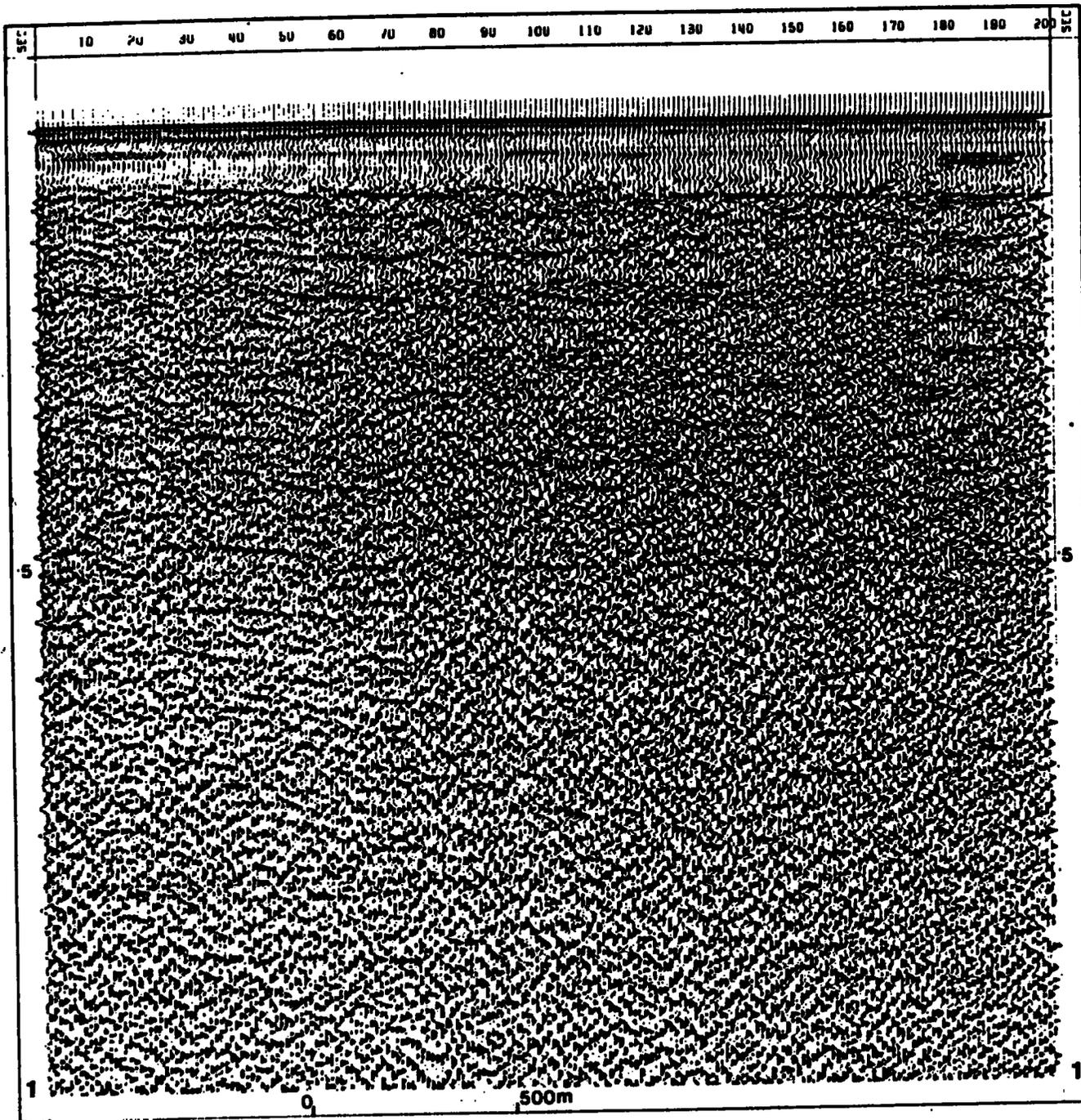
Figure 4.13(a). The near-trace section of line 8201A obtained after one of the deconvolution trials.

DURHAM UNIVERSITY
SEISMIC PROCESSING
WEARMOUTH 82　　LINE 8201A

SYSTEM PARAMETERS

FIELD DATA	COLLECTED BY FAIRFIELD AQUATRONICS LTD.
FIELD LAYOUT	
NO. OF CHANNELS	**1**
SHOT INTERVAL	6.25 METRES
GROUP INTERVAL	6.25 METRES
NEAR TRACE OFFSET	10 METRES
SOURCE TYPE	FAIRFLEX SLEEVE
RECORDING	
SAMPLING INTERVAL	1 MSEC
RECORD LENGTH	2.0 SECONDS
FILTERS	27 LO, 248 HICUT
PROCESSING	
DEMULTIPLEX	

SORT

DBS		
STATIC SHIFT		-8 MSEC
PRE-DECON. AMP. SCALING		+5.2 DB/SEC
DECONVOLUTION	DESIGN	1600 MSEC
	ACTIVE LENGTH	118 MSEC
	LAG	32 MSEC
	PRE-WHITENING	2 %
POST-DECON. AMP. SCALING		-5.2 DB/SEC
BANDPASS FILTER	LOW CUT	40 HZ
	LOW TAPER	21 HZ
	HIGH CUT	160 HZ
	HIGH TAPER	162 HZ

STACK		
FOLD	1 (MONITOR)	
RE-SAMPLED PRIOR TO NMO	.25 MSEC	
MUTE		
BANDPASS FILTER	LOW CUT	40 HZ
	LOW TAPER	21 HZ
	HIGH CUT	160 HZ
	HIGH TAPER	162 HZ
AGC		50 MSEC

DISPLAY	
TRACE SPACING	0.05 INCHES
GAIN	7.0
PROVIDED BY	NCB

Figure 4.13(b). The autocorrelogram section for Figure 4.13(a).

(b) Velocity Analysis.

Velocity analysis was performed every 1/2 km by the semblance method. It was not possible to carry out a 4-gather sum of the files before the analysis because of the variation of the near-trace offsets. Velocity filtering could not be efficiently applied since the fold of cover is too low. Only prediction-error deconvolution was applied before the analysis. The stacking velocity functions that were obtained were likely to be less accurate than those for line 7940 because of the short length of the streamer.

(c) Stacking.

NMO corrections were carried out with or without concurrent stacking depending on the stacking method being applied. Two methods were applied, namely the straight stack and the iterative stack.

(i) Straight Stack.

The straight stack of the data without any deconvolution is shown on Figure 4.14(a) and the corresponding autocorrelogram on Figure 4.14(b). The stack with prediction-error deconvolution before stack and its autocorrelogram are shown on Figures 4.15(a) and (b). Figure 4.14(b) shows strong seabed multiples at a lag of
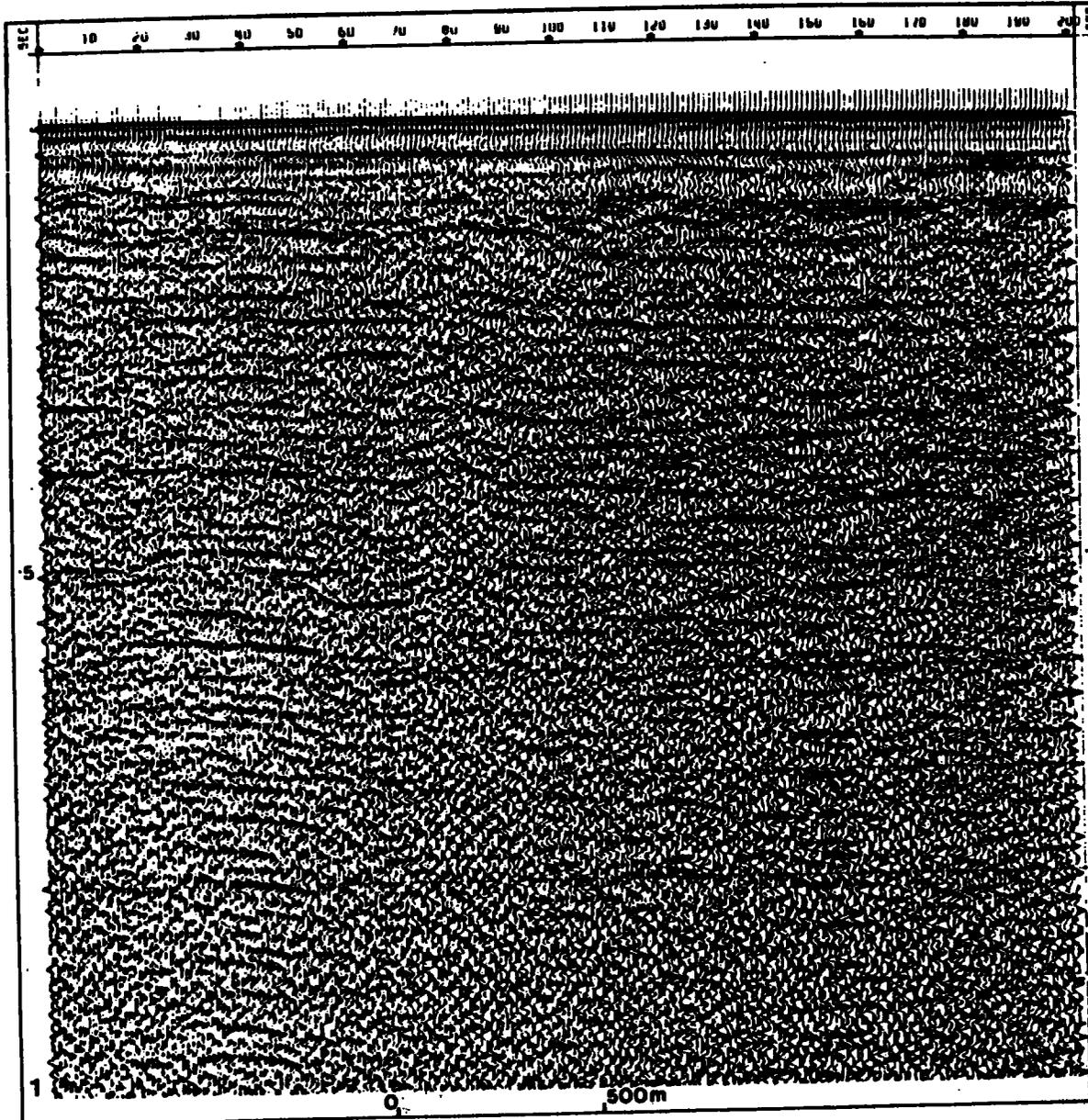
Figure 4.14(a). Straight stack of line 8201A. Prediction-error deconvolution was not applied before stack.

DURHAM UNIVERSITY
SEISMIC PROCESSING
WEARMOUTH 82   LINE 8201A

SYSTEM PARAMETERS

FIELD DATA	COLLECTED BY FAIRFIELD AQUATRONICS LTD.
FIELD LAYOUT	
NO. OF CHANNELS	24
SHOT INTERVAL	6.25 METRES
GROUP INTERVAL	6.25 METRES
NEAR TRACE OFFSET	10 METRES
SOURCE TYPE	FAIRFLEX SLEEVE
RECORDING	
SAMPLING INTERVAL	1 MSEC
RECORD LENGTH	2.0 SECONDS
FILTERS	27 LO, 248 HICUT
PROCESSING	
DEMULTIPLEX	

SORT

STATIC SHIFT		-8 MSEC
BANDPASS FILTER	LOW CUT	40 HZ
	LOW TAPER	21 HZ
	HIGH CUT	160 HZ
	HIGH TAPER	162 HZ

STACK	
FOLD	6 (STRAIGHT STACK)
RE-SAMPLED PRIOR TO NMO	.25 MSEC
MUTE	

BANDPASS FILTER	LOW CUT	40 HZ
	LOW TAPER	21 HZ
	HIGH CUT	160 HZ
	HIGH TAPER	162 HZ
AGC		50 MSEC

DISPLAY

TRACE SPACING	0.05 INCHES
GAIN	7.0

PROVIDED BY	NCB

Figure 4.14(b). The autocorrelogram for Figure 4.14(a).
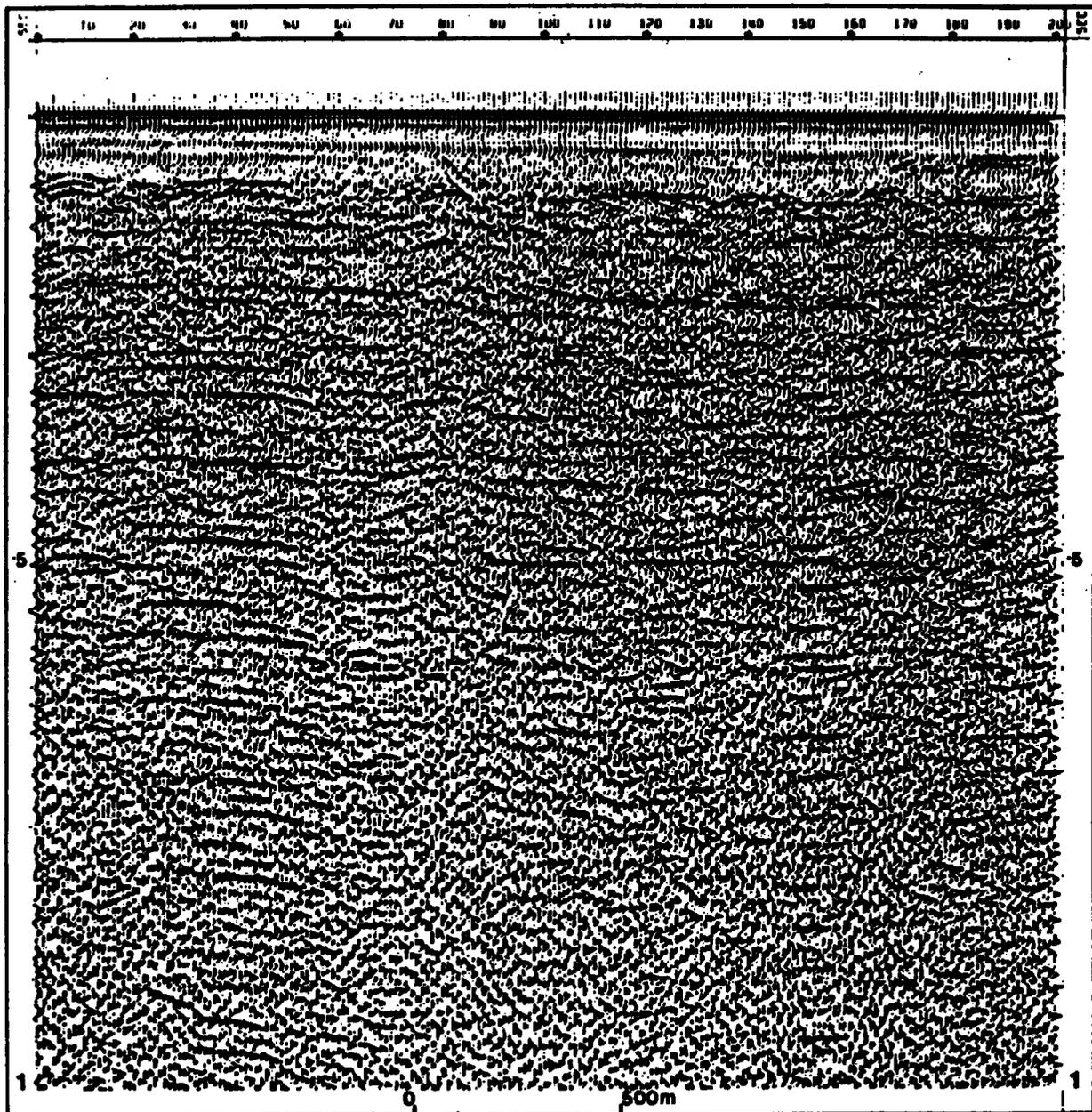
Figure 4.15(a). Straight stack of line 8201A. Prediction-error
deconvolution applied before stack.

DURHAM UNIVERSITY
SEISMIC PROCESSING
WEARMOUTH 82   LINE 8201A

SYSTEM PARAMETERS

```
***FIELD DATA***          COLLECTED BY FAIRFIELD AQUATRONICS LTD.
   FIELD LAYOUT
NO. OF CHANNELS           24
SHOT INTERVAL             6.25 METRES
GROUP INTERVAL            6.25 METRES
NEAR TRACE OFFSET         10 METRES
SOURCE TYPE               FAIRFLEX SLEEVE
   RECORDING
SAMPLING INTERVAL         1 MSEC
RECORD LENGTH             2.0 SECONDS
FILTERS                   27 LO, 248 HICUT
   PROCESSING
***DEMULTIPLEX***

***SORT***

***DBS***
STATIC SHIFT                                      -8 MSEC
PRE-DECON. AMP. SCALING                          +5.2 DB/SEC
DECONVOLUTION             DESIGN                1800 MSEC
                          ACTIVE LENGTH          168 MSEC
                          LAG                     32 MSEC
                          PRE-WHITENING            2 %
POST-DECON. AMP. SCALING                         -5.2 DB/SEC
BANDPASS FILTER           LOW CUT                 40 HZ
                          LOW TAPER               21 HZ
                          HIGH CUT               160 HZ
                          HIGH TAPER             162 HZ

***STACK***
FOLD                      6 (STRAIGHT STACK)
RE-SAMPLED PRIOR TO NMO   .25 MSEC
MUTE

BANDPASS FILTER           LOW CUT                 40 HZ
                          LOW TAPER               21 HZ
                          HIGH CUT               160 HZ
                          HIGH TAPER             162 HZ
AGC                                               50 MSEC

***DISPLAY***

TRACE SPACING             0.05 INCHES
GAIN                      7.0

PROVIDED BY               NCB
```

Figure 4.15(b). The autocorrelogram section for Figure 4.15(a).

about 80 msec which are comparatively weakened on Figure 4.15(b).

(ii) Iterative Stack.

In order to apply a 6-fold iterative stack, the parameters q (number of iterations) and f (type of normalization) had to be determined (section 2.3.2(c)). A set of tests was performed to choose the value of q. The factor f was maintained as 1.0 because of the low fold (M) of cover of line 8201A. The results of these trials are displayed as Figures 4.16(a) and 4.16(b) respectively. Figure 4.16(a) shows 6 panels each of 24 iteratively stacked traces. With the value of f=1.0, the number q was varied from 1 to 24 and the panels correspond to q=1, 2, 4, 8, 16, and 24 respectively. The traces were not summed in fours after stack. As the value of q is increased, more signal distortion is suffered and for $q \geqslant 8$, the prominent events suffer some suppression and the stacks become 'over-saturated'. The data were progressively 'whitened' as the corresponding autocorrelograms on Figure 4.16(b) show. More random noise is eliminated as q increases. The panel q=1 corresponds to the straight stack. The values (q=4, f=1.0) were chosen for these data because a comparison of the panels for q=1 and q=4 show good suppression of random events and multiples for q=4 with a tolerable signal distortion.

Hill (1983) extensively tested this technique on seismic reflection records with high levels of random noise and in such cases as streamer noise and wave noise. He partly concluded that in some situations, the design of prediction-error operators can
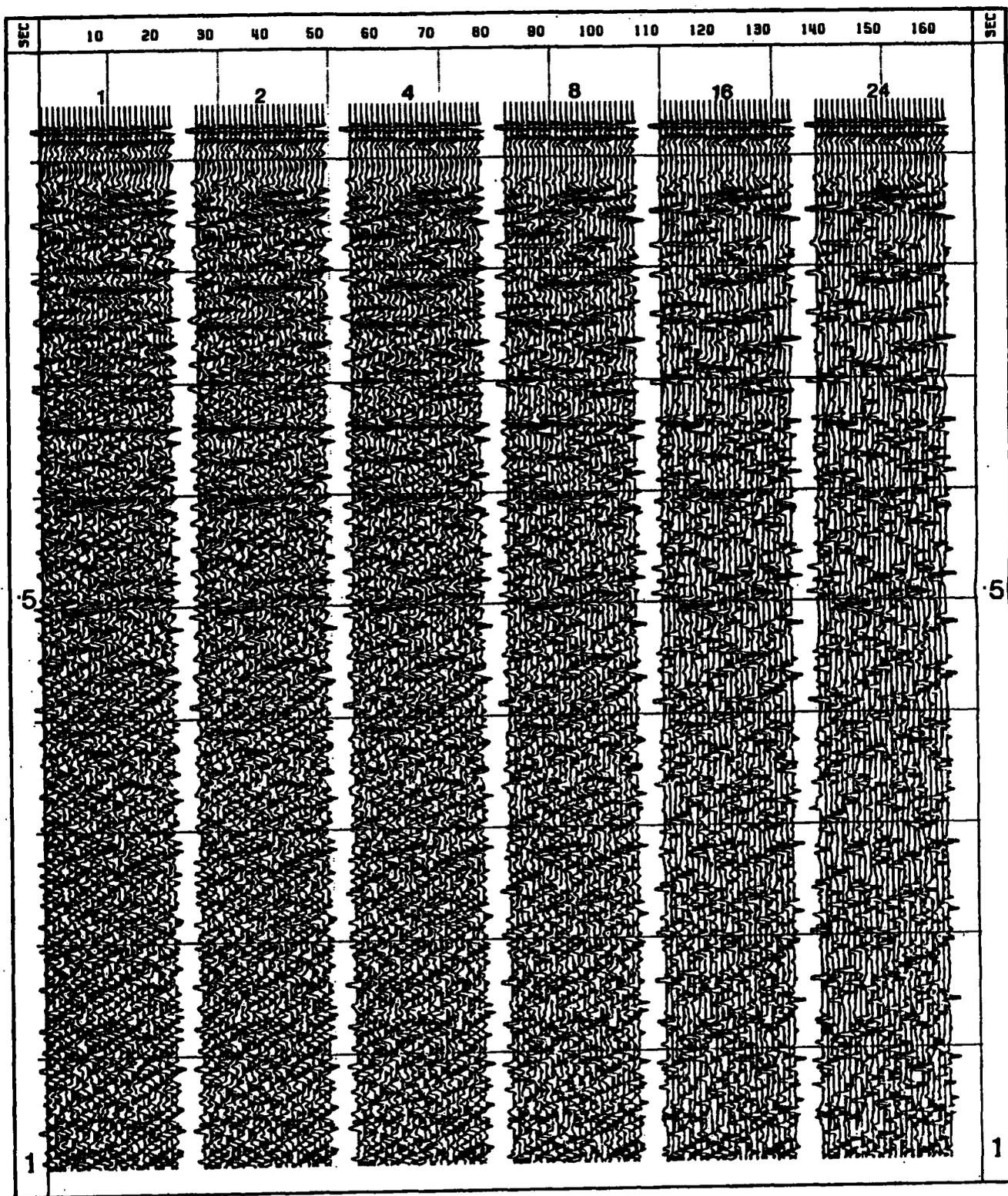
Figure 4.16(a). Test trials for the choice of the parameter q
used for the iterative stack of line 8201A. The value q=4
was chosen.
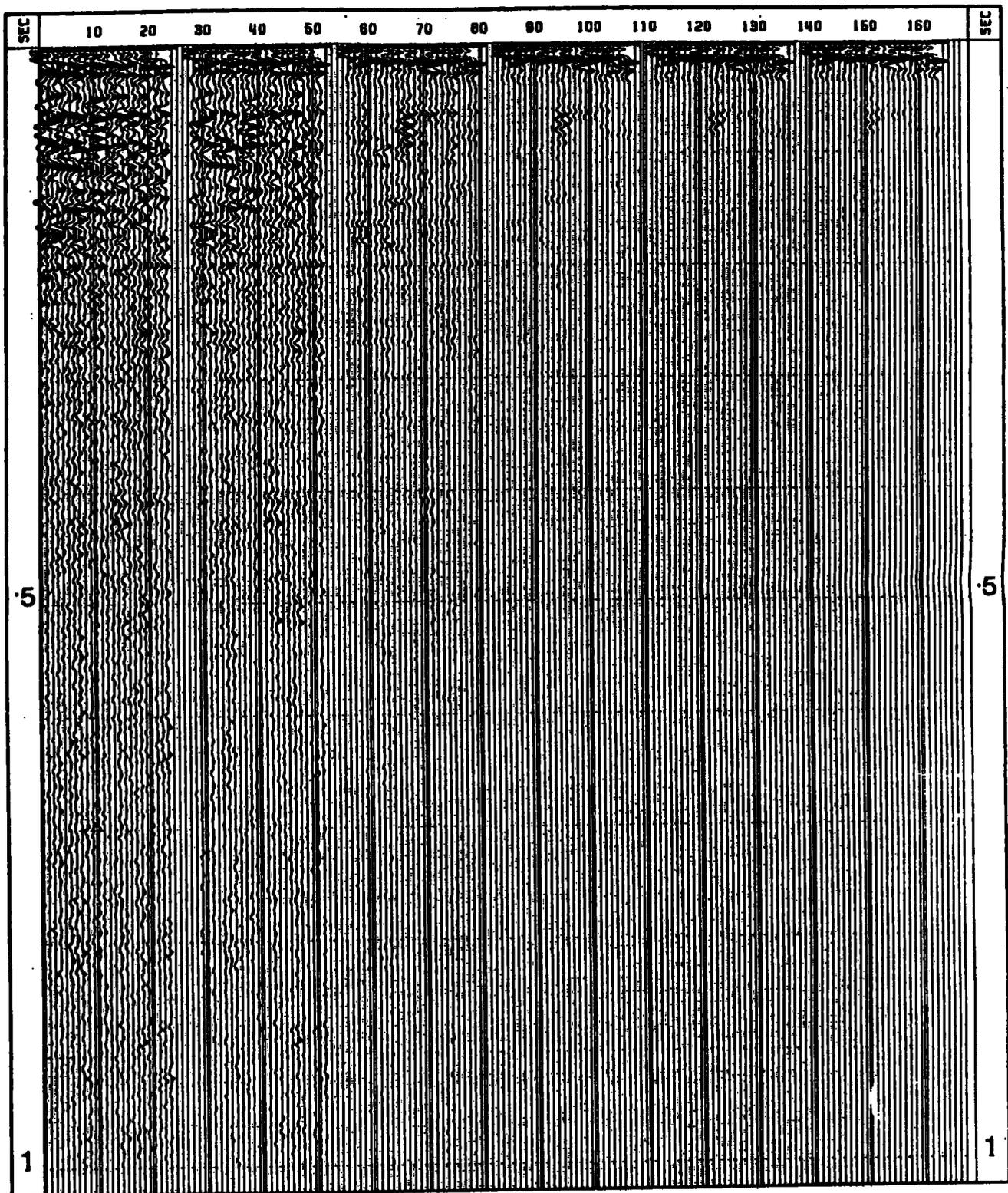
Figure 4.16(b). The autocorrelogram sections for the equivalent panels on Figure 4.16(a).

become easier or even superfluous after an iterative stack . It also produced a greater eradication of seabed multiples than the straight stack.

Figures 4.17(a) and 4.17(b) show the results of the iterative stack of the data with DBS.   The autocorrelogram shows a significant reduction of the seabed multiples.

(d) Post-stack Processing.

This included prediction-error deconvolution and band-pass filtering. Figure 4.18(a) and 4.18(b) show the results of prediction-error deconvolution of the straight stack with DBS (Figures 4.15 (a) and (b)). A long   prediction filter (active length of 168 msec) was used before stack. A shorter operator (active length of 118 msec) was applied after stack and was chosen after an examination of the autocorrelogram of Figure 4.15(b).

4.3.2   Discussion.

The seismic sections that were obtained for line 8201A show no similarities to those of line 7940 as far as Coal Measures are concerned. The stack section with no DBS showed strong reverberation which is progressively reduced during processing to obtain the final section on Figure 4.18(a). The reflections at the top of the limestones and just below it show similar characteristics to those of line 7940. Iterative stacking
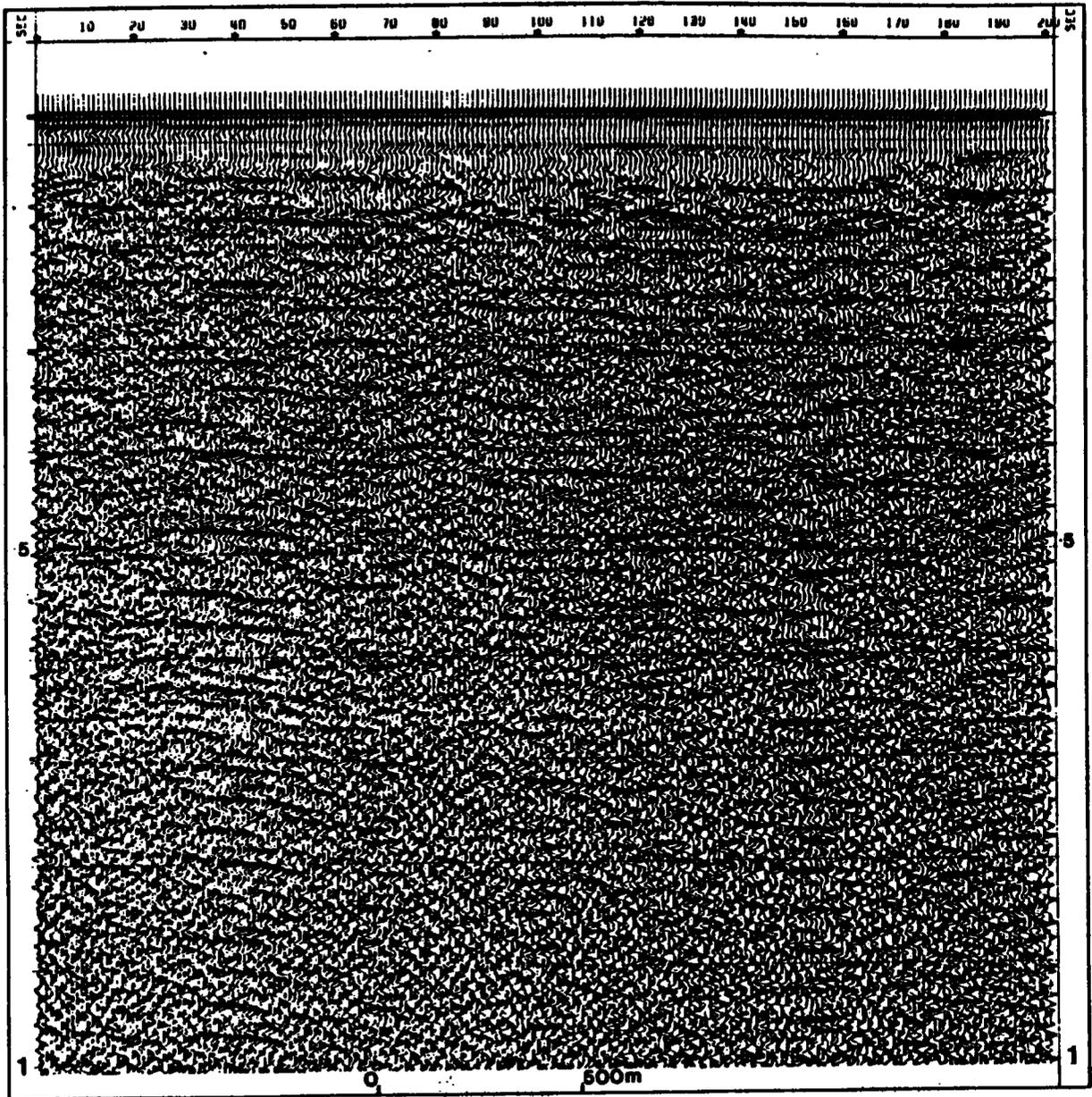
Figure 4.17(a). Iterative stack of line 8201A. Prediction-error deconvolution applied before stack.

DURHAM UNIVERSITY
SEISMIC PROCESSING
WEARMOUTH 82   LINE 8201A

SYSTEM PARAMETERS

FIELD DATA	COLLECTED BY FAIRFIELD AQUATRONICS LTD.
FIELD LAYOUT	
NO. OF CHANNELS	24
SHOT INTERVAL	6.25 METRES
GROUP INTERVAL	6.25 METRES
NEAR TRACE OFFSET	10 METRES
SOURCE TYPE	FAIRFLEX SLEEVE
RECORDING	
SAMPLING INTERVAL	1 MSEC
RECORD LENGTH	2.0 SECONDS
FILTERS	27 LO, 248 HICUT
PROCESSING	
DEMULTIPLEX	

SORT

DBS		
STATIC SHIFT		-8 MSEC
PRE-DECON. AMP. SCALING		+5.2 DB/SEC
DECONVOLUTION	DESIGN	1800 MSEC
	ACTIVE LENGTH	168 MSEC
	LAG	32 MSEC
	PRE-WHITENING	2 %
POST-DECON. AMP. SCALING		-5.2 DB/SEC
BANDPASS FILTER	LOW CUT	40 HZ
	LOW TAPER	21 HZ
	HIGH CUT	160 HZ
	HIGH TAPER	162 HZ

STACK		
FOLD	6 (ITERATIVE STACK: =4)	
RE-SAMPLED PRIOR TO NMO	.25 MSEC	
TRACE NORMALISATION	UNIT RMS ENERGY	
MUTE		

BANDPASS FILTER	LOW CUT	40 HZ
	LOW TAPER	21 HZ
	HIGH CUT	160 HZ
	HIGH TAPER	162 HZ
AGC		50 MSEC

DISPLAY

TRACE SPACING	0.05 INCHES
GAIN	7.0

PROVIDED BY	NCB

Figure 4.17(b). Autocorrelogram section of the iteratively
stacked section on Figure 4.17(a).
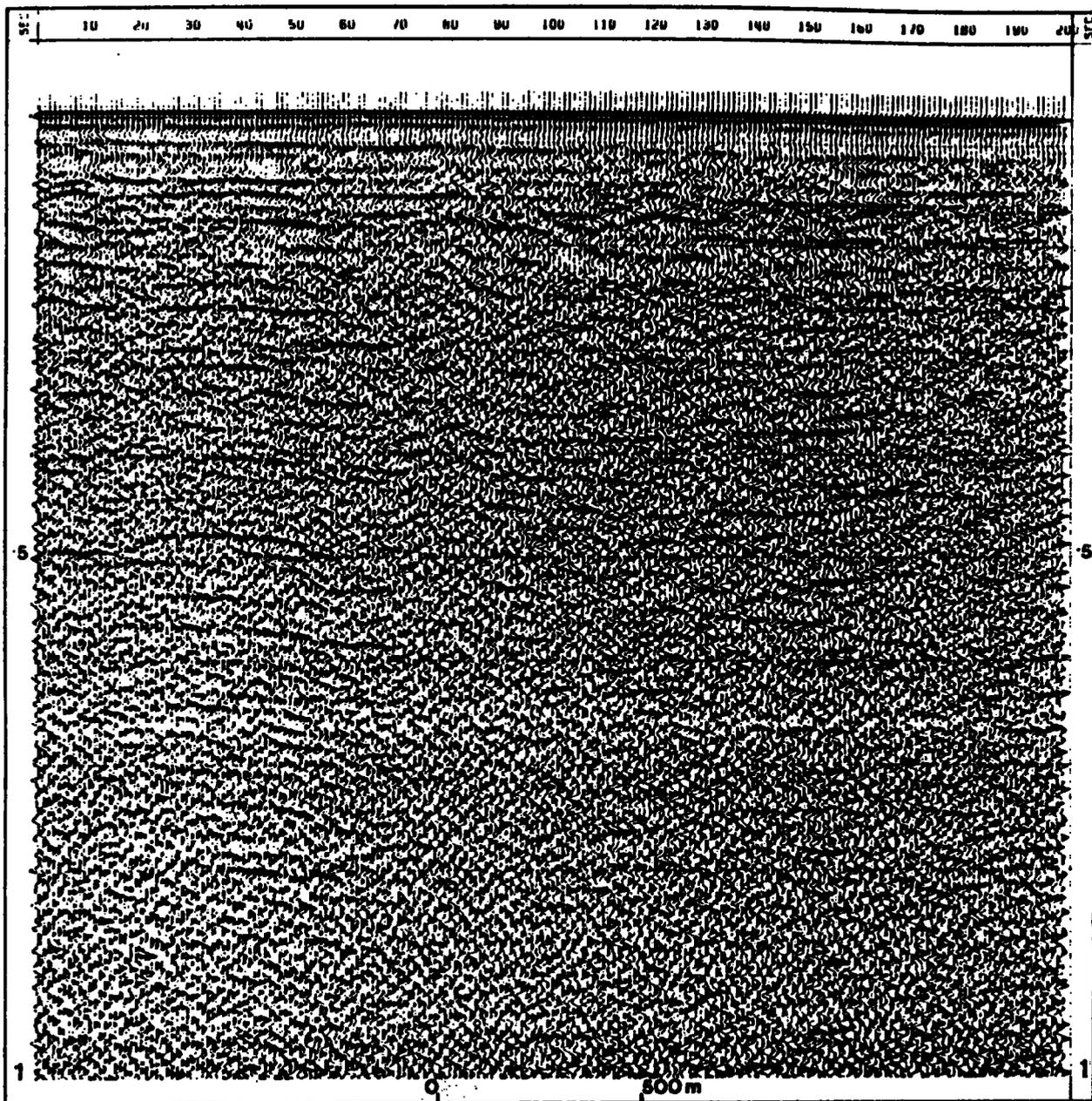
Figure 4.18(a). The Straight stack of line 8201A with both DBS
     and DAS. The deconvolution parameters are shown on the
     annotation box.

DURHAM UNIVERSITY
SEISMIC PROCESSING
WEARMOUTH 82   LINE 8201A

SYSTEM PARAMETERS

```
***FIELD DATA***        COLLECTED BY FAIRFIELD AQUATRONICS LTD.
   FIELD LAYOUT
NO. OF CHANNELS         24
SHOT INTERVAL           6.25 METRES
GROUP INTERVAL          6.25 METRES
NEAR TRACE OFFSET       10 METRES
SOURCE TYPE             FAIRFLEX SLEEVE
   RECORDING
SAMPLING INTERVAL       1  MSEC
RECORD LENGTH           2.0 SECONDS
FILTERS                 27 LO, 248 HICUT
   PROCESSING
***DEMULTIPLEX***
***SORT***
***DBS***
STATIC SHIFT                                     -8 MSEC
PRE-DECON. AMP. SCALING                        +5.2 DB/S
DECONVOLUTION           DESIGN                 1800 MSEC
                        ACTIVE LENGTH           168 MSEC
                        GAP                      32 MSEC
                        PREWHITENING              2 %
POST-DECON. AMP. SCALING                       -5.2 DB/S
BANDPASS FILTER         LOW CUT                  40 HZ
                        LOW TAPER                21 HZ
                        HIGH CUT                160 HZ
                        HIGH TAPER              162 HZ


***STACK***
FOLD                    6 (STRAIGHT STACK)
RE-SAMPLED PRIOR TO NMO .25 MSEC
MUTE


***DBS***
PRE-DECON. AMP. SCALING                        +5.2 DB/S
DECONVOLUTION           DESIGN                 1600 MSEC
                        ACTIVE LENGTH           118 MSEC
                        GAP                      32 MSEC
                        PREWHITENING              2 %
POST-DECON. AMP. SCALING                       -5.2 DB/S
BANDPASS FILTER         LOW CUT                  40 HZ
                        LOW TAPER                21 HZ
                        HIGH CUT                160 HZ
                        HIGH TAPER              162 HZ
AGC                                              50  MSEC
***DISPLAY***
TRACE SPACING           0.05 INCHES
GAIN                    7.0

PROVIDED BY             NCB
```

Figure 4.18(b). The autocorrelogram of the section on Figure
4.18(a).

suppressed the seabed multiples more than straight stacking as the autocorrelograms (Figures 4.17(b) and 4.15(b)) show. The Coal Measures primary reflections are not evident on the final section.

In the 1982 survey, the streamer length was shorter so as to avoid the interference effects observed in 1979 but it may not have been long enough to record significant primary energy from the Coal measures in the prevailing noise conditions. The low angles of incidence involved (Figure 4.10) meant that most of the energy that was received came within the pressure-wave penetration window. The source type (sleeve exploder) generates a high energy pulse and is generally considered to provide sufficient total energy for deep penetration (McQuillin et al., 1979) when used in multiple arrays.

The results that were obtained above by processing this sample of the 1982 data confirm the suspicion from the 1979 data that the penetration of the seismic energy is low in this region. Since the sleeve exploder is a relatively (to the water guns of 1979) high frequency source, an even poorer result would have been achieved because of frictional absorption and scattering both of which affect the higher frequency components more.

The data that were acquired by using the sleeve exploder and a 150 m long streamer therefore failed to resolve any Coal Measures.

4.4 **Summary.**

In conclusion, the processing of samples of real seismic reflection data from the Wearmouth region by using standard and non-standard techniques has not dramatically improved on the results previously obtained by the N.C.B. . The results of each data set have been presented and discussed.

In these discussions, two criticisms of the acquisition procedures with respect to the specific geological conditions of this area arose. These include the source type in each survey in relation to the degree of penetration that it achieves in this geology and the length of the streamer used in each survey in relation to the amount of useful reflection data that it receives. The water gun sources used for the 1979 survey achieved some penetration but the 600m streamer used (with a hydrophone group spacing of 25m) resulted in a very poor S/N ratio at larger offsets so that most of the data had to be muted during processing. The combination showed Coal Measures but the resolution is poor. The sleeve exploder source used in 1982 and the streamer of 150m both failed to show Coal Measures. The combination of the sleeve exploder (sharper high frequency source) and the short streamer (implying smaller differential moveouts between primary and multiple energy) led to very low S/N of the stacked sections. The (hydrophone) groups also act as a filter of the higher frequencies (Ziolkowski and Lerwill, 1979; although this effect is not very severe) which also suffer greater attenuation in the ground and get less depth penetration (Lucas , 1974).

It may well be necessary to use a seismic source with more energy at low frequencies (along with the higher frequencies) together with a streamer of an intermediate length (hydrophone groups greater than 6.25m long) in this survey. The water gun source of 1979 or a well-tuned airgun source (Brandsaeter et al., 1979) can be applied. Another alternative is the more recent ''Starjet''[*] source (a seismic tuned array of steam bubbles, Le Boulch, 1983) which produces high energy for deeper penetration and has a broad bandwidth for good resolution. A 400 m long streamer towed at a depth of about 5 m to avoid the notches caused by the free surface may well be adequate for use with the preferred source in any future survey in the region. The extra costs of specifying and carrying out the data acquisition can be compensated for by reaping the benefits of cheaper conventional processing. The arguments are buttressed by the statement of Ziolkowski and Lerwill, (1979) that ''To extract detail out of (the) data is a processing problem; but to ensure that the detail is there to be extracted is a field problem''. The work that was carried out in the present chapter was in part to ''extract detail'' out of the data as they were obtained but the conclusions and the field procedures could not be divorced.

It is appropriate to investigate the advantages of using the streamer with an intermediate length (400 m) and possibly with alternative hydrophone group intervals given that a satisfactory source has been chosen. These geometrical considerations and other connected problems are included in chapter 5.

* CGG Trademark 106

C H A P T E R 5

MODELLING EXAMPLES.

5.1   Introduction.

In chapter 3, deterministic filters for multiple suppression were studied and the forward modelling approach was used in order to obtain synthetic seismograms which were used for testing these filters. Only the interference of the 2-layer reverberatory wavelet with the Coal Measures primary reflections was treated. In this chapter, some of the effects that cause signal attenuation during the propagation of seismic waves through the Permian horizons and during data processing, as well as the stacked responses for different lengths of the acquisition streamer were also studied by using the forward modelling approach. The computer programs AIMS, YIBEA3, and SYNSEI (See APPENDIX C) were applied depending on the objective and on the limitations of each program.

In section 5.2, the effects of transmission losses, spreading losses, and frictional attenuation losses are considered for a simplified geological section of the region of study. The AIMS program was used to generate appropriate normal incidence synthetic seismograms. The problem of banded anhydrite and of the attenuation of high frequencies due to a simple attenuation profile were included.

In section 5.3, the top surface of the magnesian limestone is modelled as a non-horizontal surface in addition to the effects covered in section 5.2. Only the effects of reflector curvature (focusing and defocusing) on the amplitudes of primary reflections from the Coal Measures are considered. The roughness of the surface gives rise to seismic wave scattering as discussed by Sheriff (1975). This scattering affects the amplitude of the incident wave in a frequency-dependent manner (Kennett, 1983). The effect of reflector rugosity could not be properly modelled with AIMS and is difficult to tackle in general. The seismic responses that were obtained including focusing effects, spreading losses and absorption losses are displayed and discussed.

In section 5.4, a complete vertical incidence synthetic section is shown, which was obtained by using the layer-matrix method and the computer program YIBEA3 written during this study. The reflectivity sequence for the earth model was non-white and non-stationary and the prediction-error deconvolution technique was used to attenuate the multiple components of the seismograms so that the extent of the undesirable suppression of the primary events could be assessed and the results are outlined.

In section 5.5, the geometrical aspects of the acquisition parameters for seismic reflection data in this region are considered. Different streamer lengths were simulated and the processed, stacked responses are displayed and discussed.

The earth model that was applied in this chapter is shown on Figures 5.1 . Figure 5.1 (a) indicates a few strongly reflecting
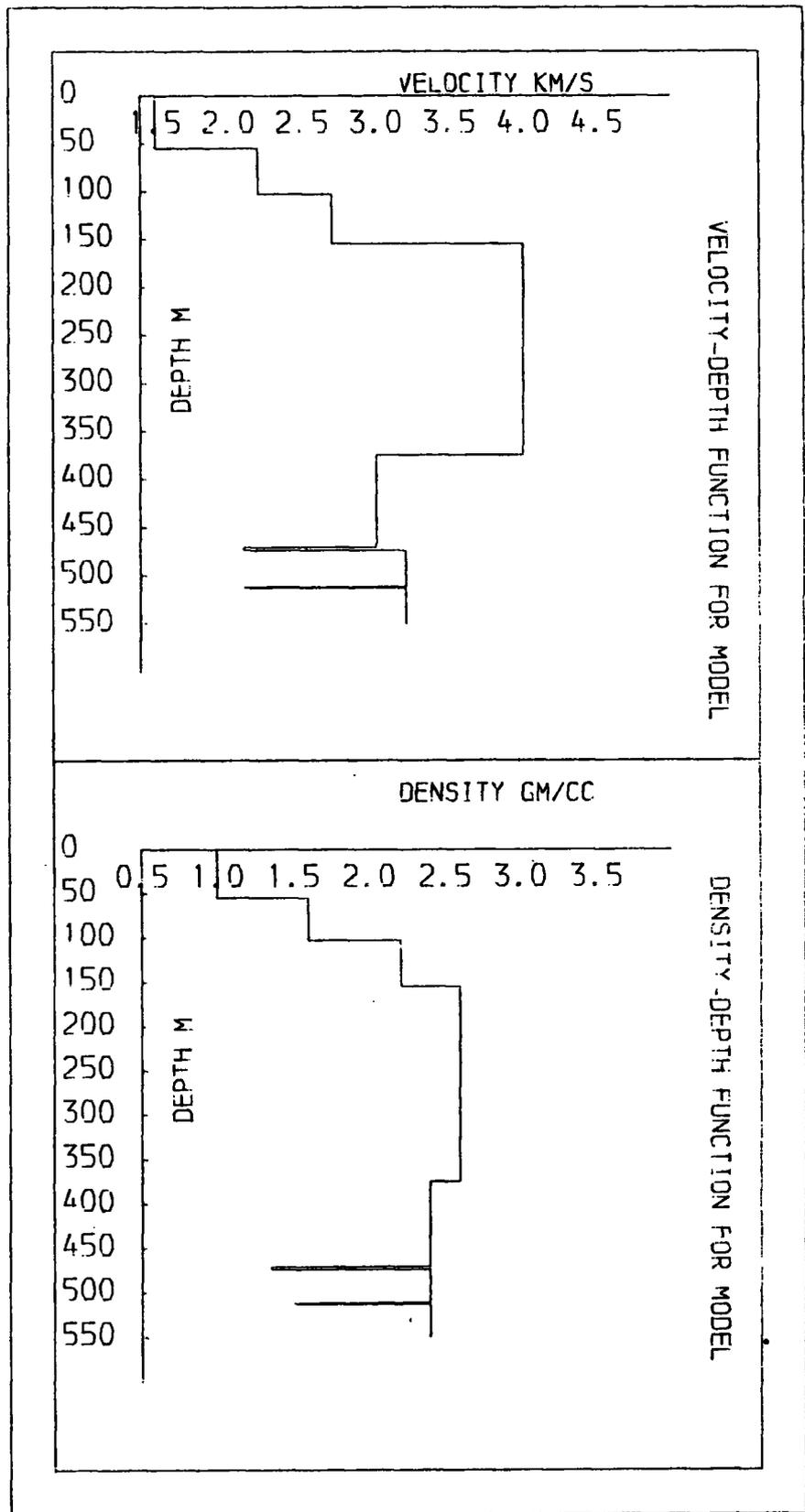
Figure 5.1 (a). Velocity and density versus depth profiles used for modelling in this chapter. They show the main geological interfaces.

interfaces corresponding to the seabed, the top of the marl, the top and base of the limestone and two coal seams respectively. These were chosen with the aid of the borehole data and approximate seismic velocities for these layers were obtained from the results of a seismic reference survey that was carried out in the well for the N.C.B. The density values are approximate values for each formation in question obtained from published values of 'typical density' for the appropriate rock type.

Several small but random reflection coefficients were inserted (Figure 5.1 (b)) in order to simulate both random noise and the real situation and this led to a system with 32 interfaces. Table 5.1 shows the layer parameters and Figure 5.2 displays the unsmoothed power spectrum of the reflectivity sequence $r(i)$. It is clearly not white, and $r(i)$ is certainly not stationary. The mean value and the standard deviation of the reflection coefficients are shown.

The source wavelet that was used in this chapter is displayed in Figure 5.3. It is a 33-point symmetrical wavelet that corresponds to a broadband Butterworth band-pass filter with low and high-frequency cut-offs of 36 and 96 dB/octave respectively. The power is almost evenly distributed between 40 and 240 Hz and the wavelet was obtained by using the AIMS program.
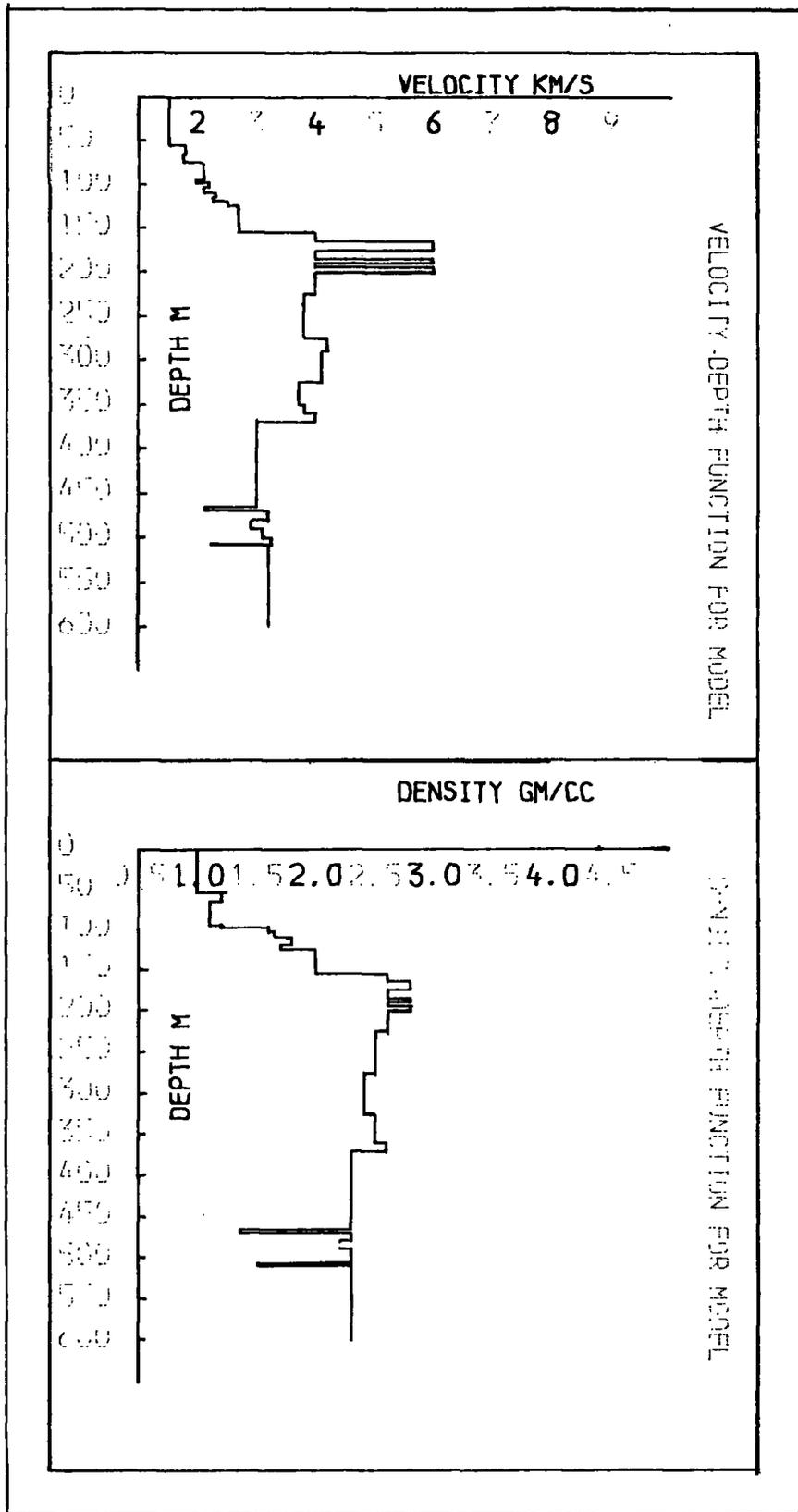
Figure 5.1 (b). Velocity and density versus depth profiles including
a number of small, random reflection coefficients to
the model of Figure 5.1 (a).

TABLE 5.1 . Layer Parameters of a typical earth model
**********   used for modelling in this chapter.

LAYER NO. i	V(i)	RHO(i)	C(i)	T(i)
1	1.5	1.0	-0.1803277	74
2	1.8	1.2	0.0575273	96
3	1.75	1.1	-0.0909091	107
4	2.1	1.1	-0.0064513	127
5	1.95	1.2	-0.2013654	130
6	2.2	1.6	0.0078743	134
7	2.1	1.65	-0.0887575	141
8	2.3	1.8	0.0109890	145
9	2.25	1.8	-0.0240959	150
10	2.5	1.7	-0.1191714	154
11	2.7	2.0	-0.3164557	176
12	4.0	2.6	-0.2352941	181
13	6.0	2.8	0.2352941	184
14	4.0	2.6	-0.2352941	189
15	6.0	2.8	0.2352941	191
16	4.0	2.6	-0.2352941	193
17	6.0	2.8	0.2352941	195
18	4.0	2.6	0.0452261	208
19	3.8	2.5	-0.0296219	234
20	4.2	2.4	0.0120482	241
21	4.1	2.4	0.0309060	258
22	3.7	2.5	-0.0133333	272
23	3.8	2.5	-0.0452261	277
24	4.0	2.6	0.2023121	282
25	3.0	2.3	0.4175654	346
26	2.1	1.35	-0.4438446	349
27	3.2	2.3	0.0713249	355
28	2.9	2.2	-0.0555147	362
29	3.1	2.3	-0.0236220	368
30	3.25	2.3	0.3874710	373
31	2.2	1.5	-0.3808630	374
32	3.2	2.3	-0.0054051	432

V(i) in Km/sec.
Rho(i) in g/cc.
T(i) in milliseconds.

$$C(i) = \frac{V(i)*Rho(i) - V(i+1)*Rho(i+1)}{V(i)*Rho(i) + V(i+1)*Rho(i+1)} .$$

N.B. The C(i) are displacement reflection coefficients.
The pressure coefficients are obtained by
a polarity reversal.

The mean of C(i) is -0.024428
The variance of C(i) is 0.033851
The standard deviation from the mean is 0.197107
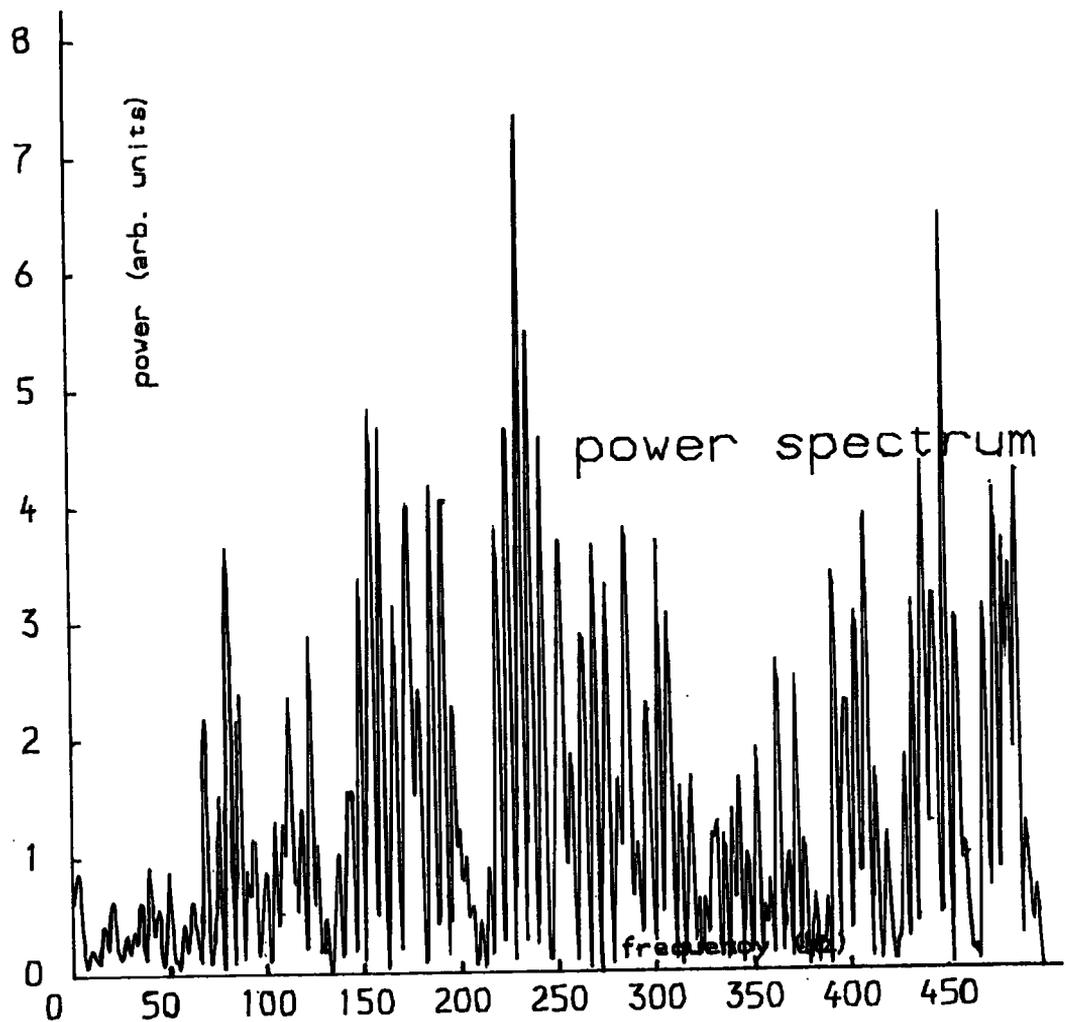
Figure 5.2   The power spectrum of the reflectivity sequence r(t)
obtained from the reflection coefficients c(i);

$$r(t) = 0 \qquad t \neq T(i)$$
$$\qquad c(i) \qquad t = T(i) \qquad \text{for all i.}$$

T(i) = two-way zero-offset time to base of layer i.
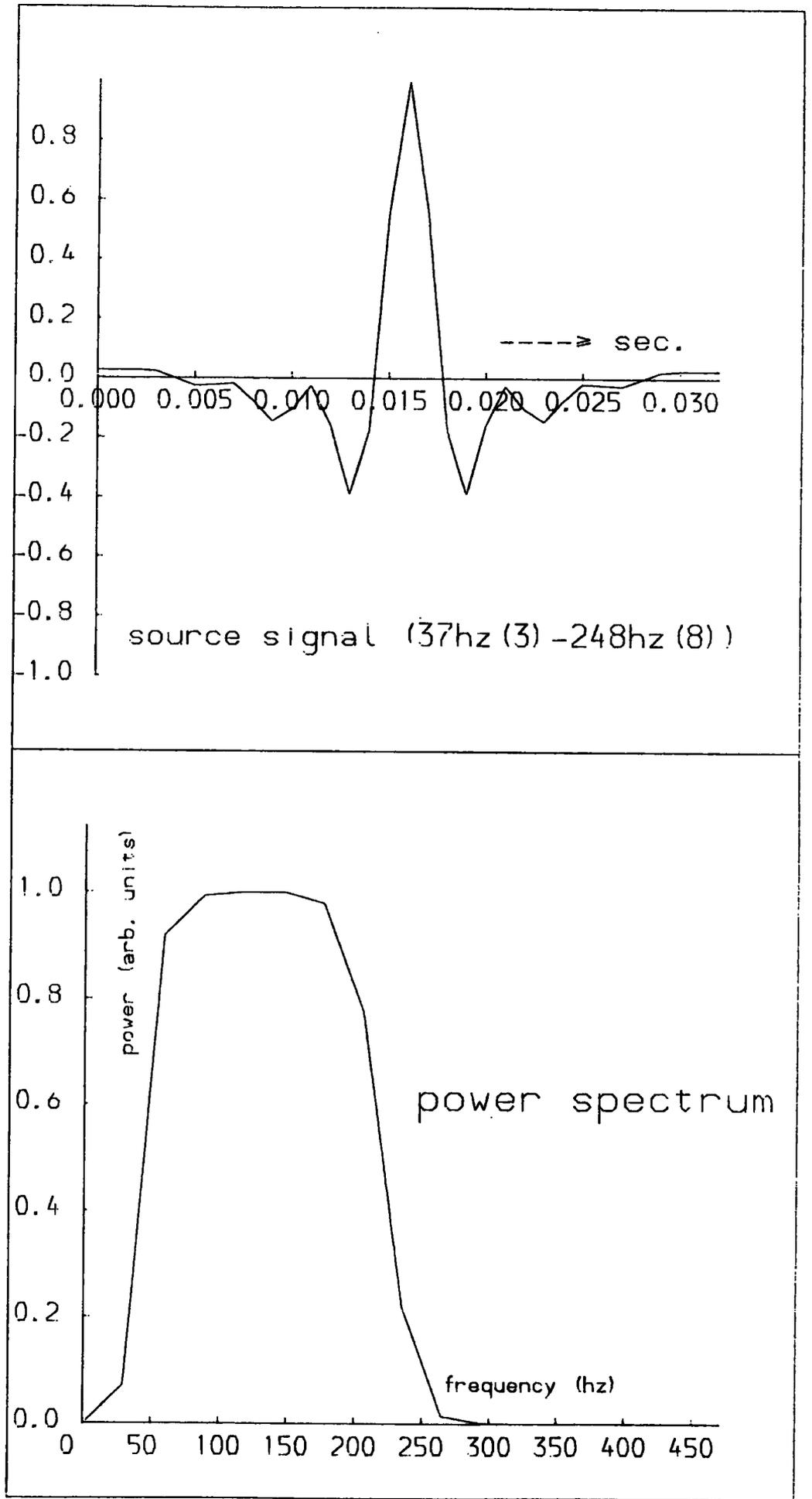
Figure 5.3   The source wavelet and its power spectrum.

5.2 <u>Transmission, Spreading, and Frictional</u>
<u>Attenuation Losses</u>

Besides transmission losses, amplitude decay during seismic wave propagation is mainly due to spherical spreading losses and frictional energy dissipation, which together are of the form $(1/r)\exp(-\alpha r)$ where r is the distance from the source. The exponential term represents the frictional absorption and is frequency-dependent (Waters, 1978, pp. 25) with the absorption coefficient

$$\alpha = \pi f / (Q\ c)$$

where f is the frequency of a plane wave (monochromatic component) with a velocity c and 1/Q is the specific dissipation constant. Sedimentary rocks are generally more absorptive (low Q) than other rock types (Dobrin, 1976, pp.48).

The AIMS modelling program was used to calculate seismograms that have suffered some or all of the above effects. The spherical divergence effect is included in all the responses that were calculated using AIMS and presented in this chapter and multiple reflections were not included. The earth model on Figure 5.1 (b) was used with and without the anhydrite bands. The amplitude and phase spectra of the seismic reflection responses from the two coal seams were computed. Q values with an average of 100 were used for these sedimentary rocks. According to Waters (1978), sedimentary rocks possess such an average value over the range of useful seismic frequencies.

Figures 5.4 show the seismic reflection

NI SECTION — WITHOUT ANHYDRITE BANDS
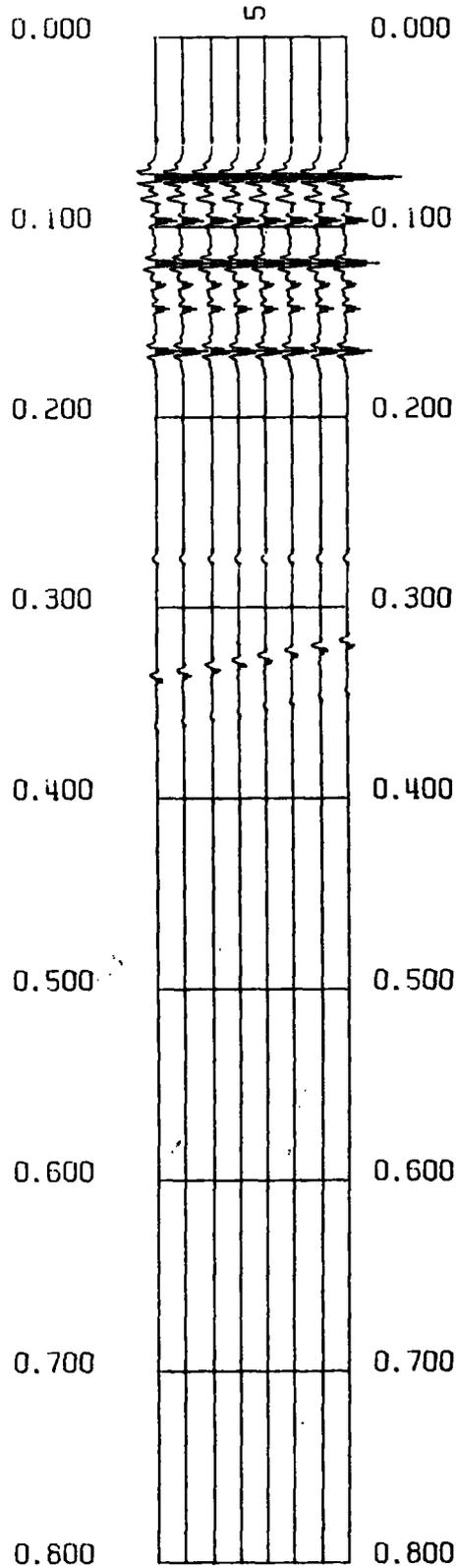
Figure 5.4 (a). Normal incidence seismograms for earth's model
without anhydrite bands. No attenuation is
included.
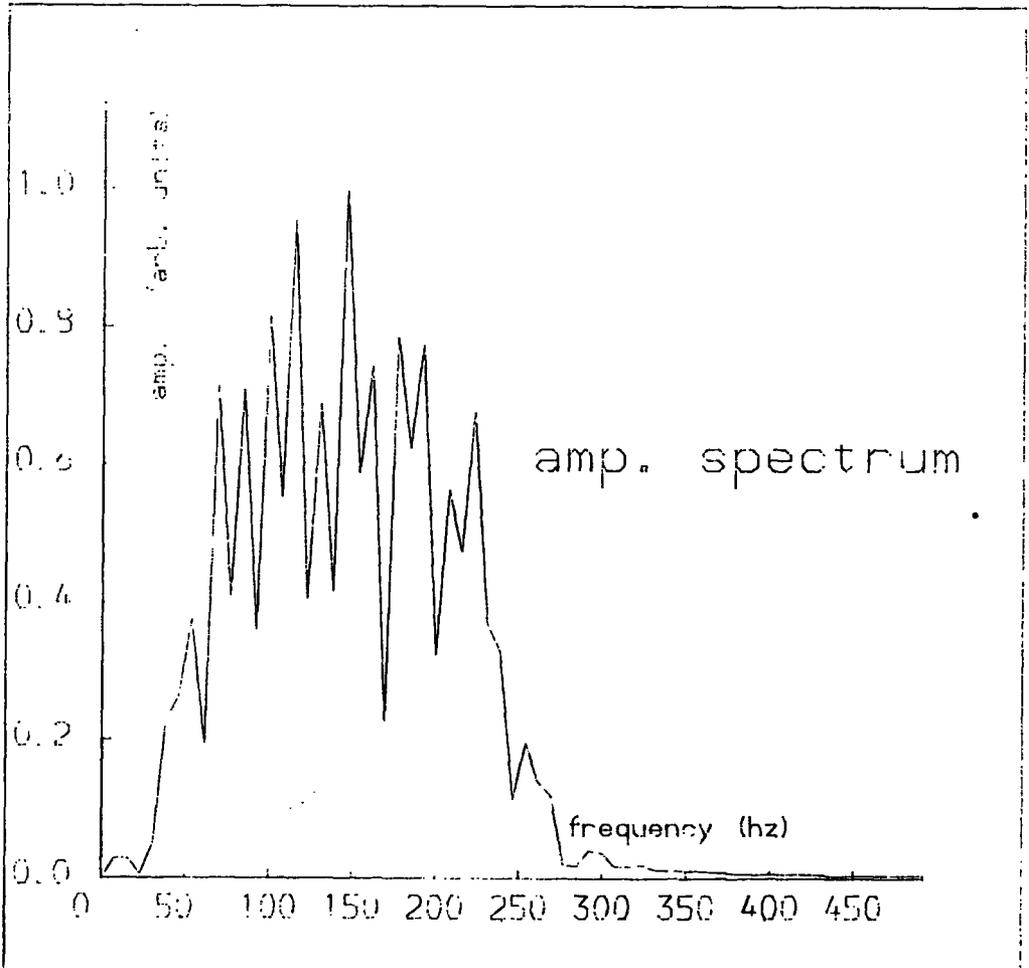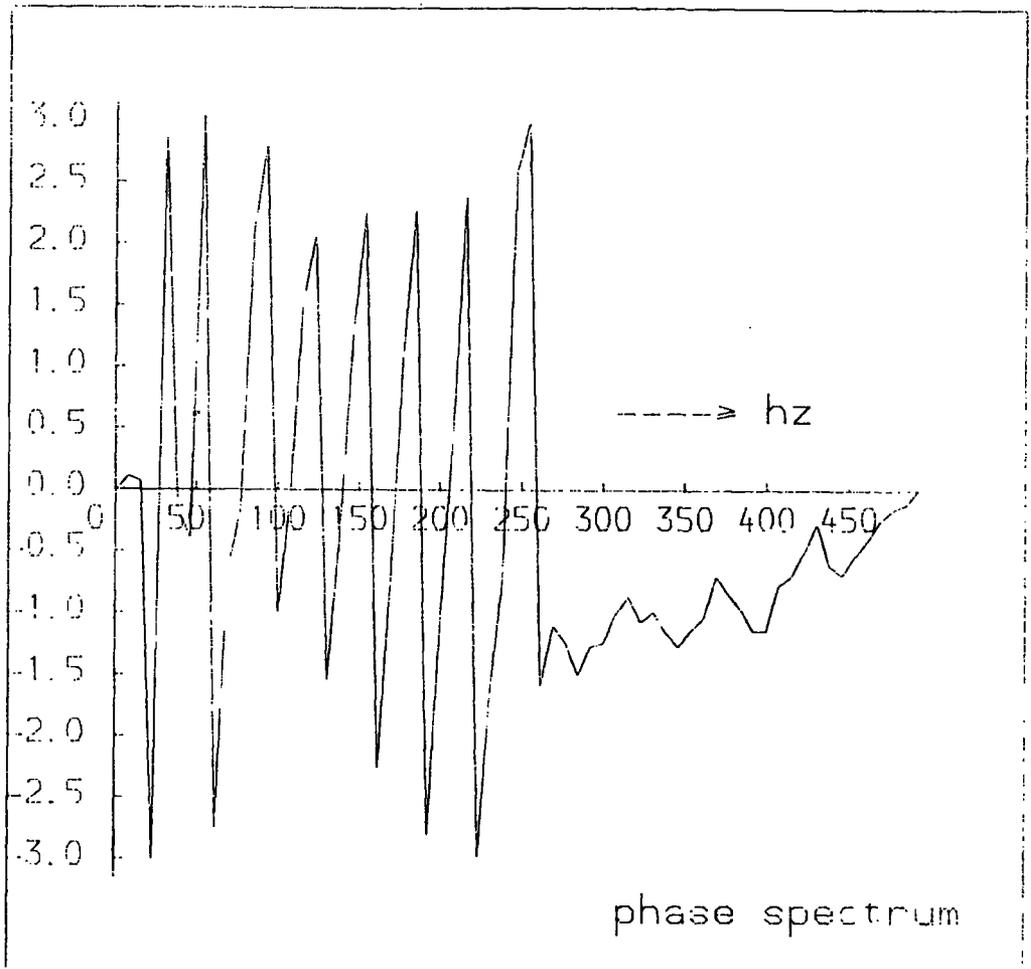
Figure 5.4 (b). Spectra of the Coal Measures reflections. (gate
300 - 428 msec).

NI SECTION – WITH ANHYDRITE BANDS
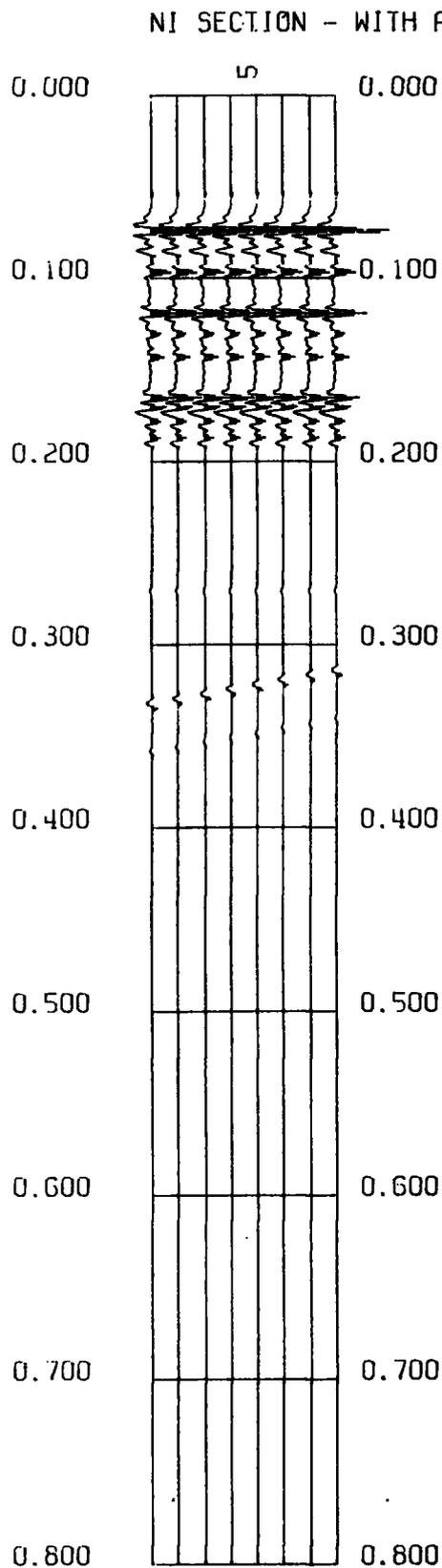
Figure 5.4 (c). Normal incidence seismograms for earth model with anhydrite bands. No attenuation is included.
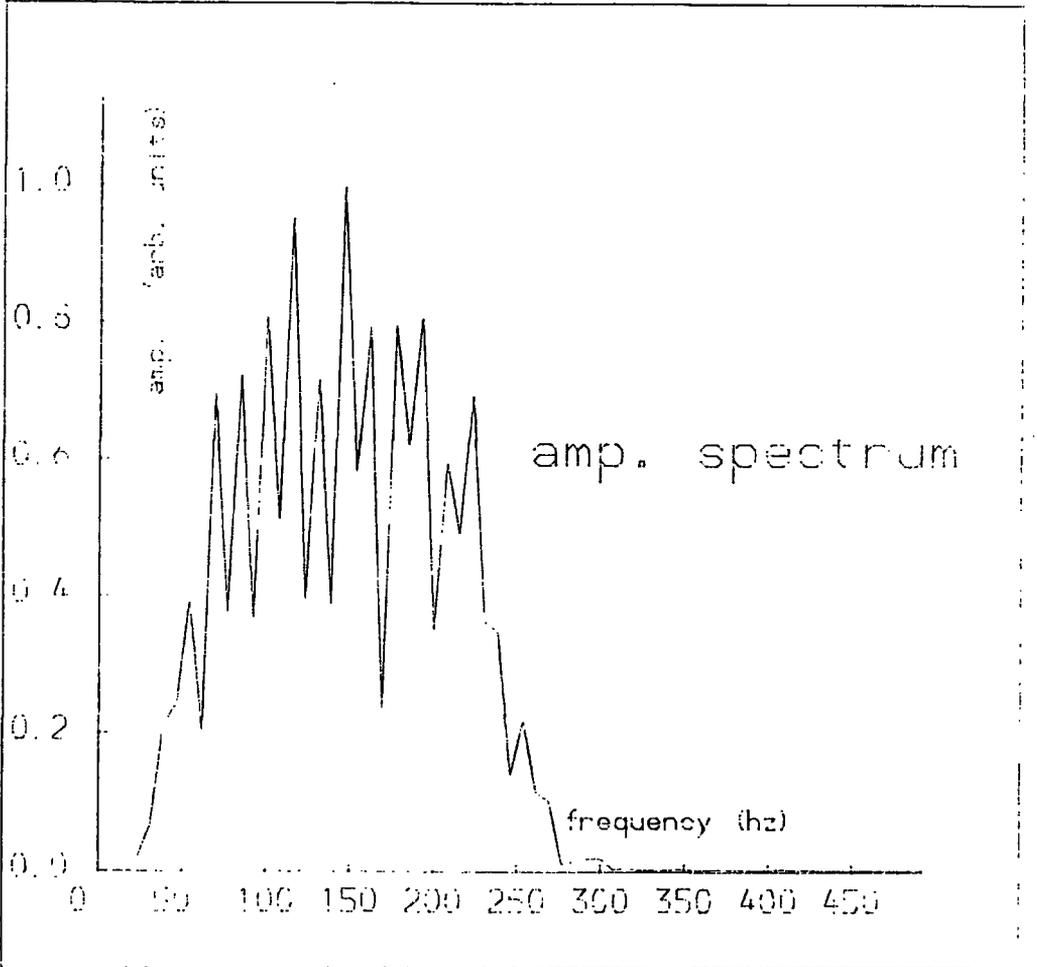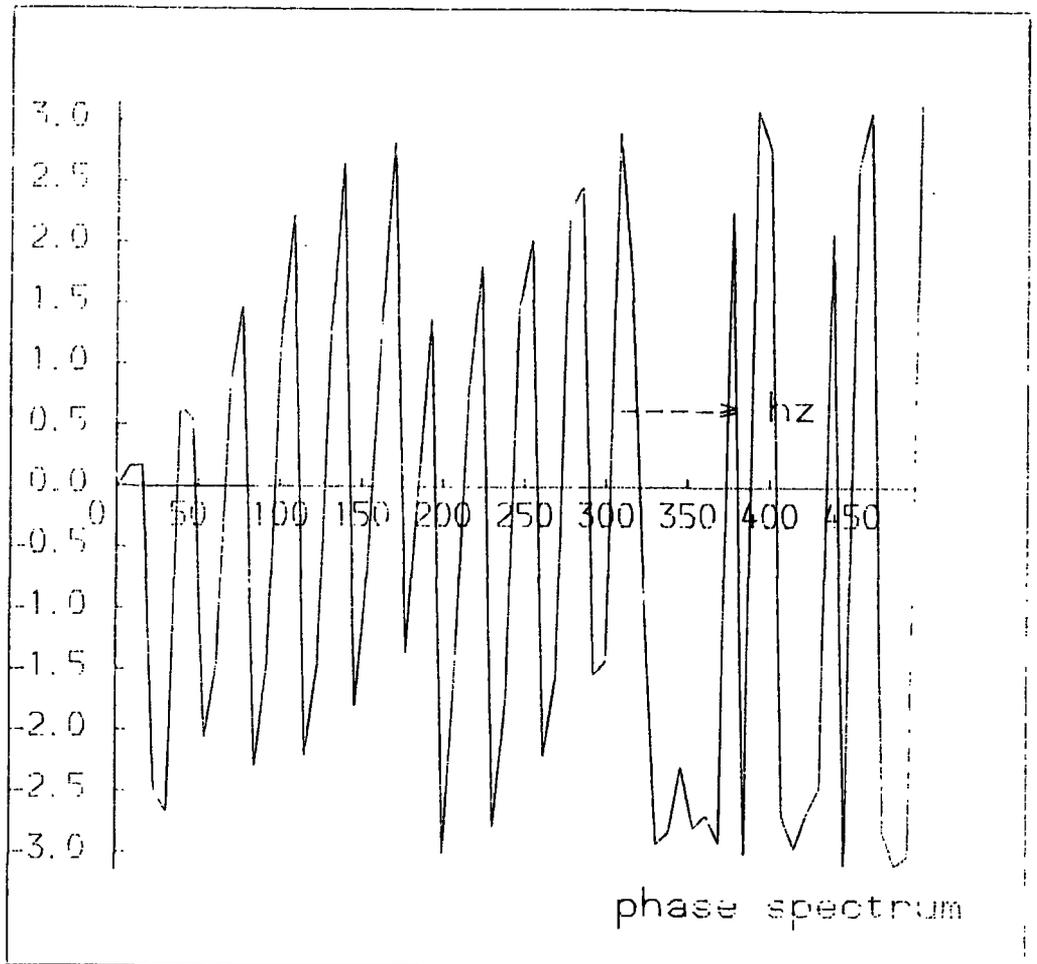
Figure 5.4 (d). Spectra of the Coal Measures response only.

responses (primaries only) and the spectra when no frequency-dependent attenuation $(Q \rightarrow \infty)$ is included. Only transmission and spreading losses account for the final amplitudes within the coal seams. The traces were plotted without an artificial enhancement (ramp or AGC) of the later arrivals. The section for the model with the anhydrite bands shows a lower amplitude for the coal seams as expected and the spectra rightly indicate that there is no change in bandwidth but that there are prominent spectral nulls that repeat at a frequency interval of about 37 Hz which corresponds to the time delay (about 27 msec) between the two Coal seams.

However, Figures 5.5 show the primary reflection responses with the effects of frictional attenuation included. Both responses show that there is a significant loss of power above 150 Hz. If the Q values assigned to the rocks are higher than they would be in the real case, then more high-frequency absorption is expected than these examples depict. The high frequency cut-off of 150 Hz, used in processing the real data will therefore ensure that all the useful bandwidth with adequate S/N ratio has been retained. The spectral nulls introduced by the banded structure (anhydrite or coal seams) affect the power distribution at various frequencies but not the overall bandwidth.

Multiple reflections were not included in the above considerations. If they are added, then the power spectra of the reflection responses within the coal seams will suffer further perturbation because of the short-lag internal multiples within

111

NI SECTION - WITHOUT ANHYDRITE BANDS
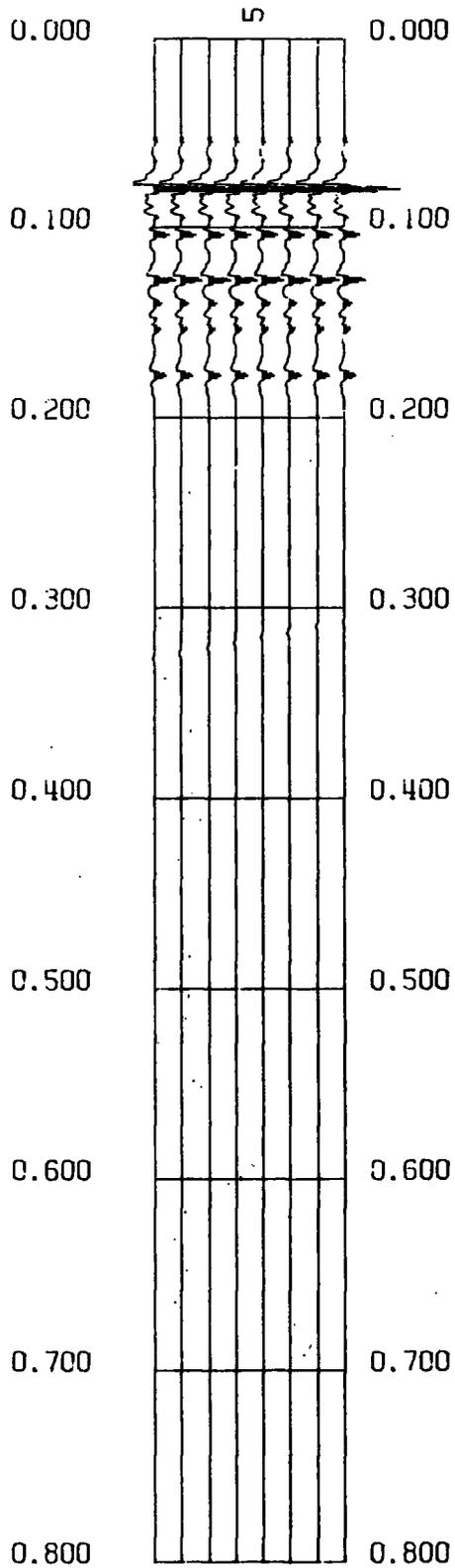
Figure 5.5 (a). Normal incidence seismograms for earth's model
without anhydrite bands. Attenuation is included.
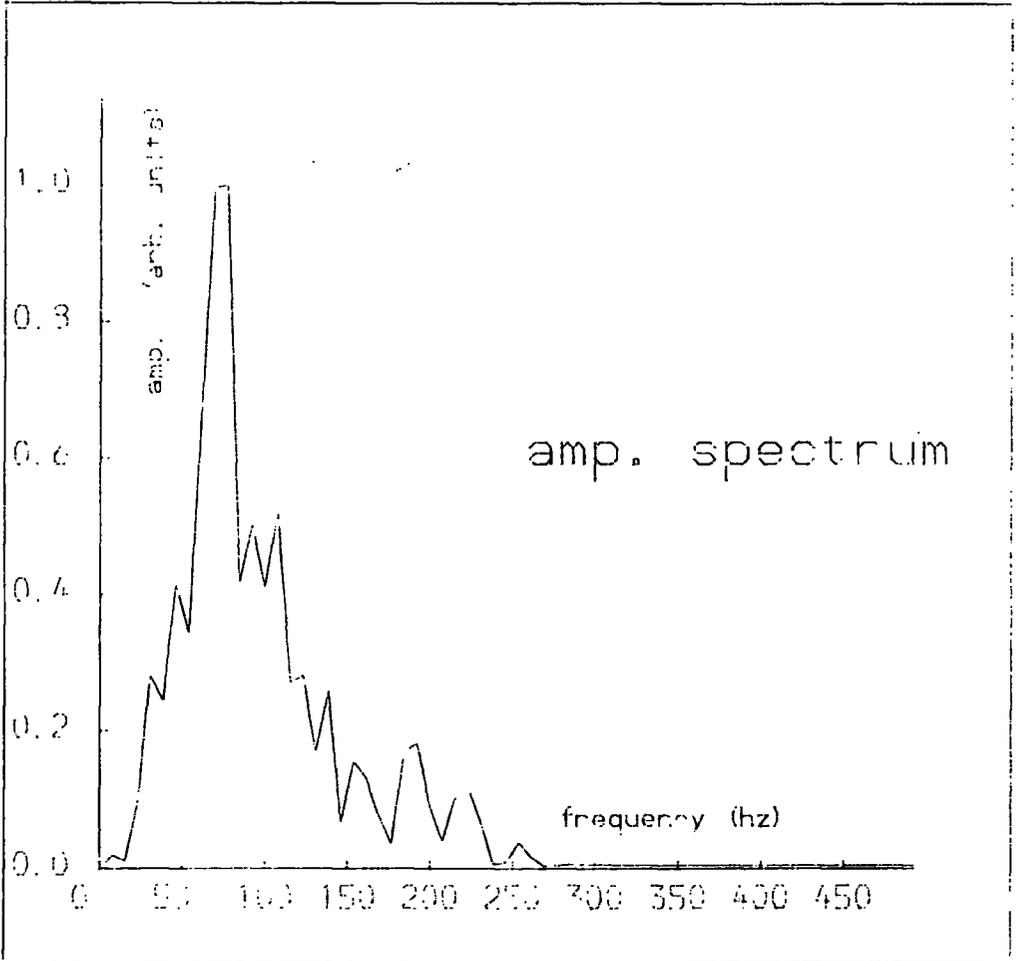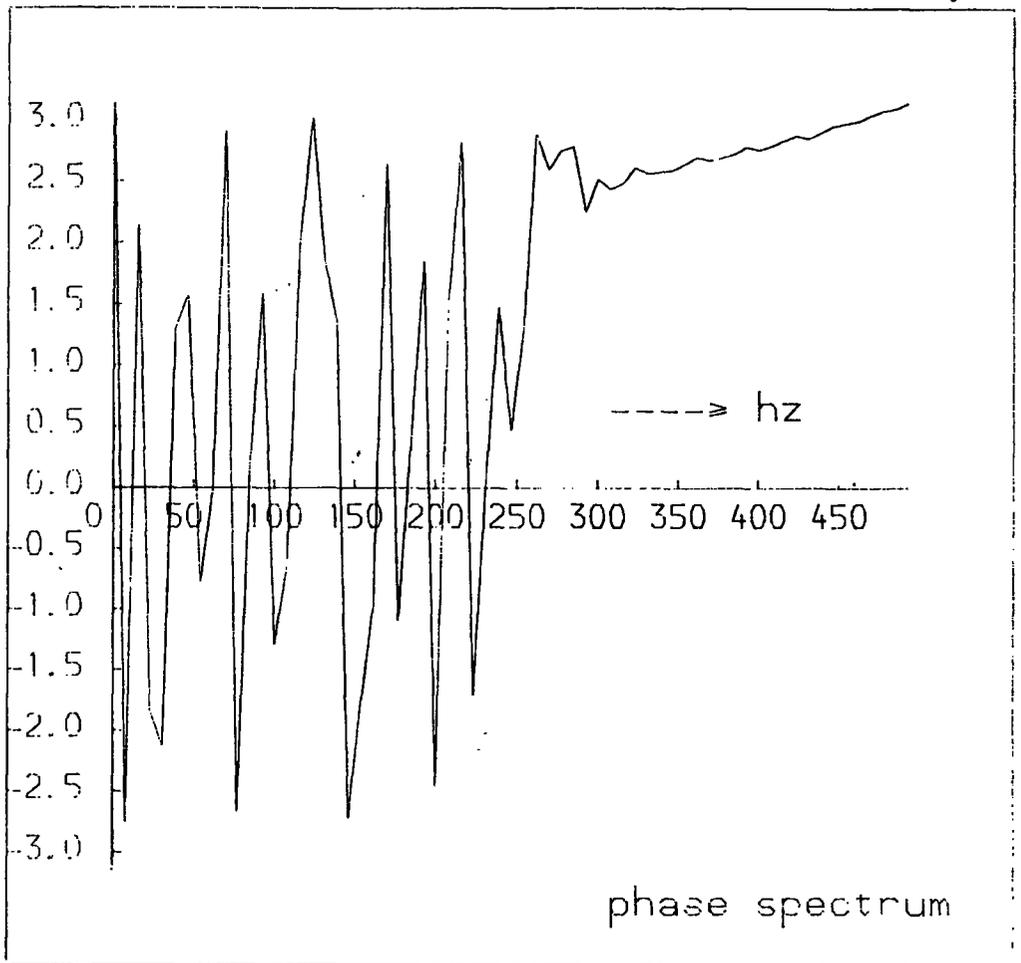
Figure 5.5 (b). Spectra of the Coal Seams's reflection response.
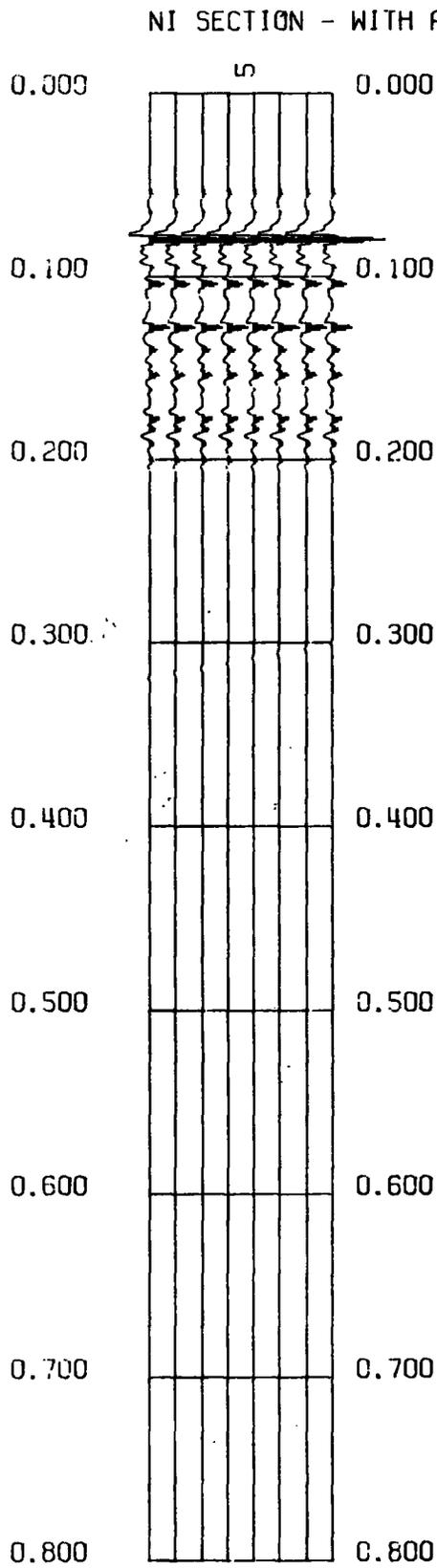
Figure 5.5 (c). Normal incidence seismograms for earth's model with anhydrite bands. Attenuation is included.
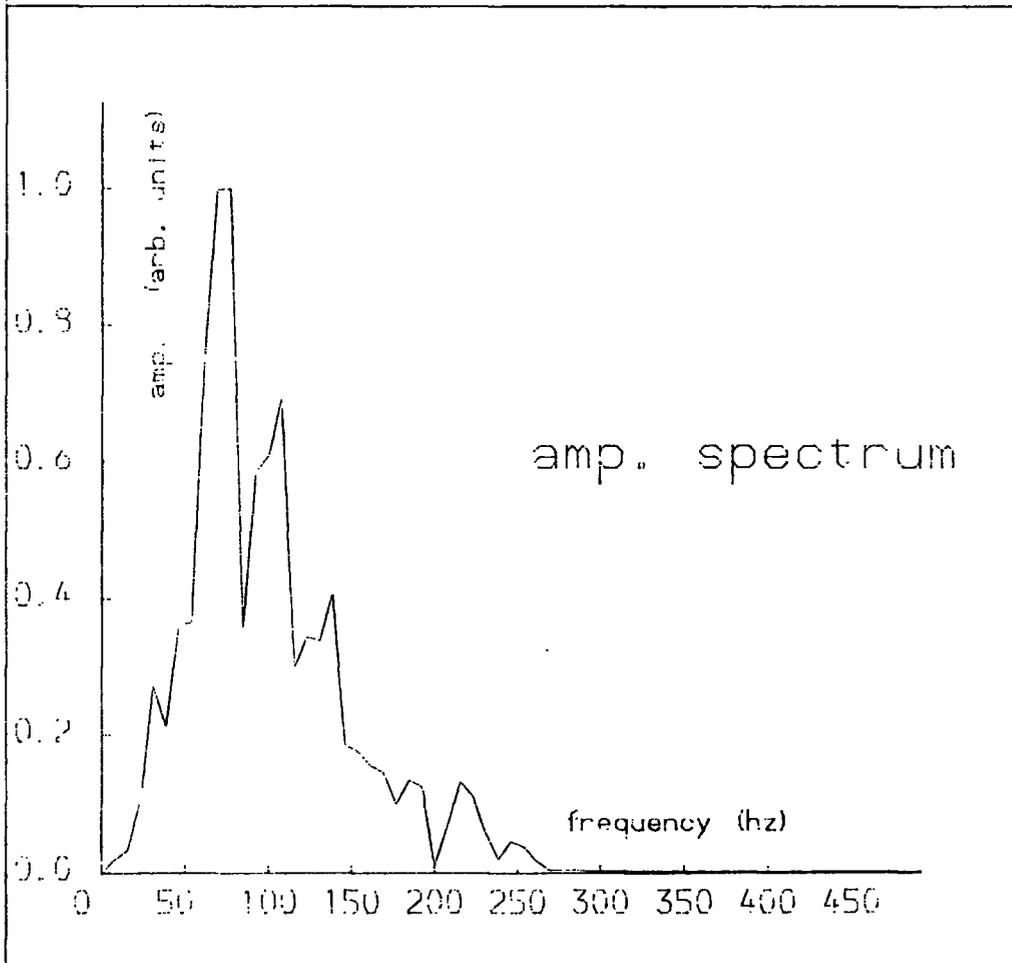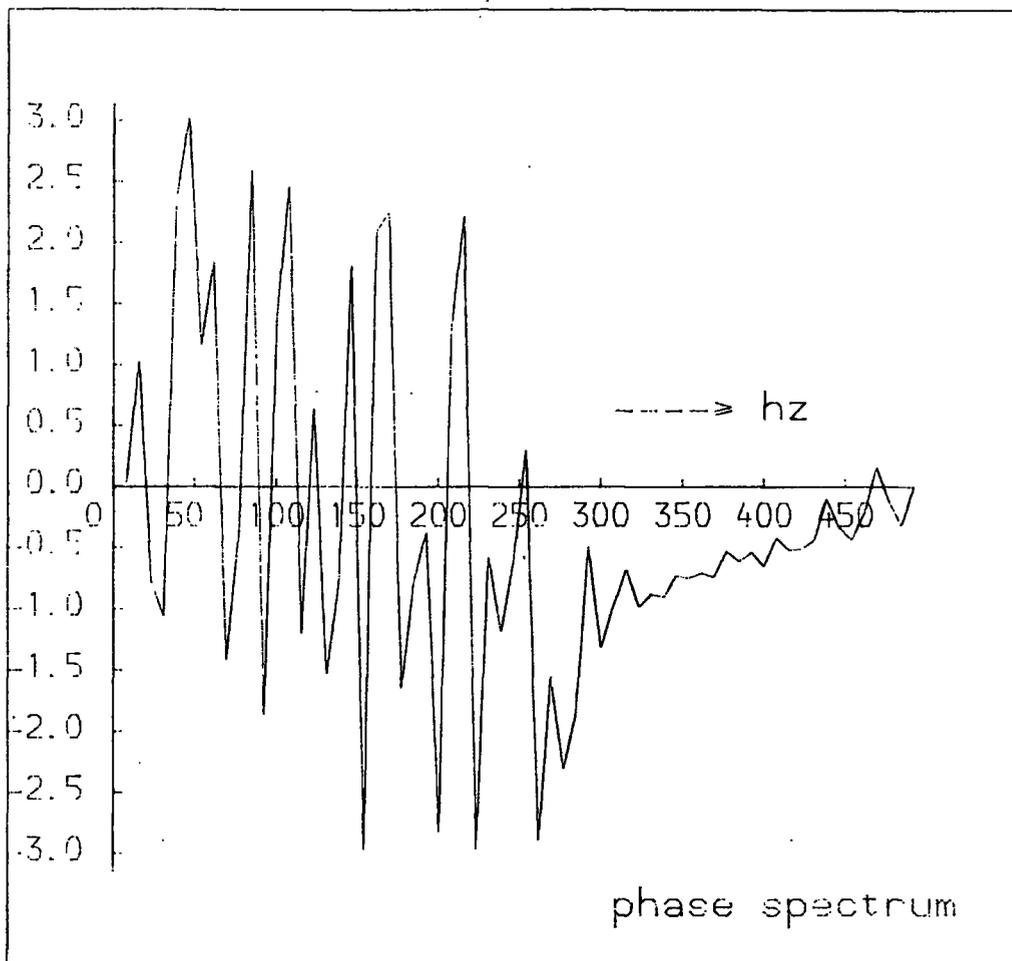
Figure 5.5 (d). Spectra of the Coal Measures reflection response.

them.

5.3   Addition of Focusing effects.

In addition to the transmission, spreading and absorption effects of section 5.2, the top of the limestone was modelled as a non-horizontal interface. The effect of the curvature of the limestone's surface on the Coal Measures primary reflection response was obtained by using the AIMS program. Normal incidence seismograms were computed and displayed with the subsurface geometry in each case and multiple reflections were not included.

Figure 5.6 (a) shows the subsurface geometry when the surface of the limestone is considered to be a smooth horizontal boundary. The 60-trace section displayed in Figure 5.6 (b) shows the Coal Measures primary reflections. A time-ramp function of the form $t\ e^{at}$ (with a = 1.382) was applied to each of the traces in order to enhance the amplitudes of the later arrivals. The traces were computed every 10 m.

Figure 5.7 (a) shows the geometry when the top of the limestone was treated as a non-horizontal surface. The undulations on this surface have an average wavelength of about 200 m. The corresponding section (Figure 5.7 (b)) shows that the lateral resolution of the Coal Measures' events gets poorer than when the surface is planar. The response indicates low amplitudes within various lateral segments of the coal seam's reflections. This is essentially due to a focusing effect at the top of the limestone. Segments of the limestone's surface that

112

Figure 5.6 (a). The subsurface geometry when the Magnesian Limestones' surface (horizon 12) is smooth and horizontal.
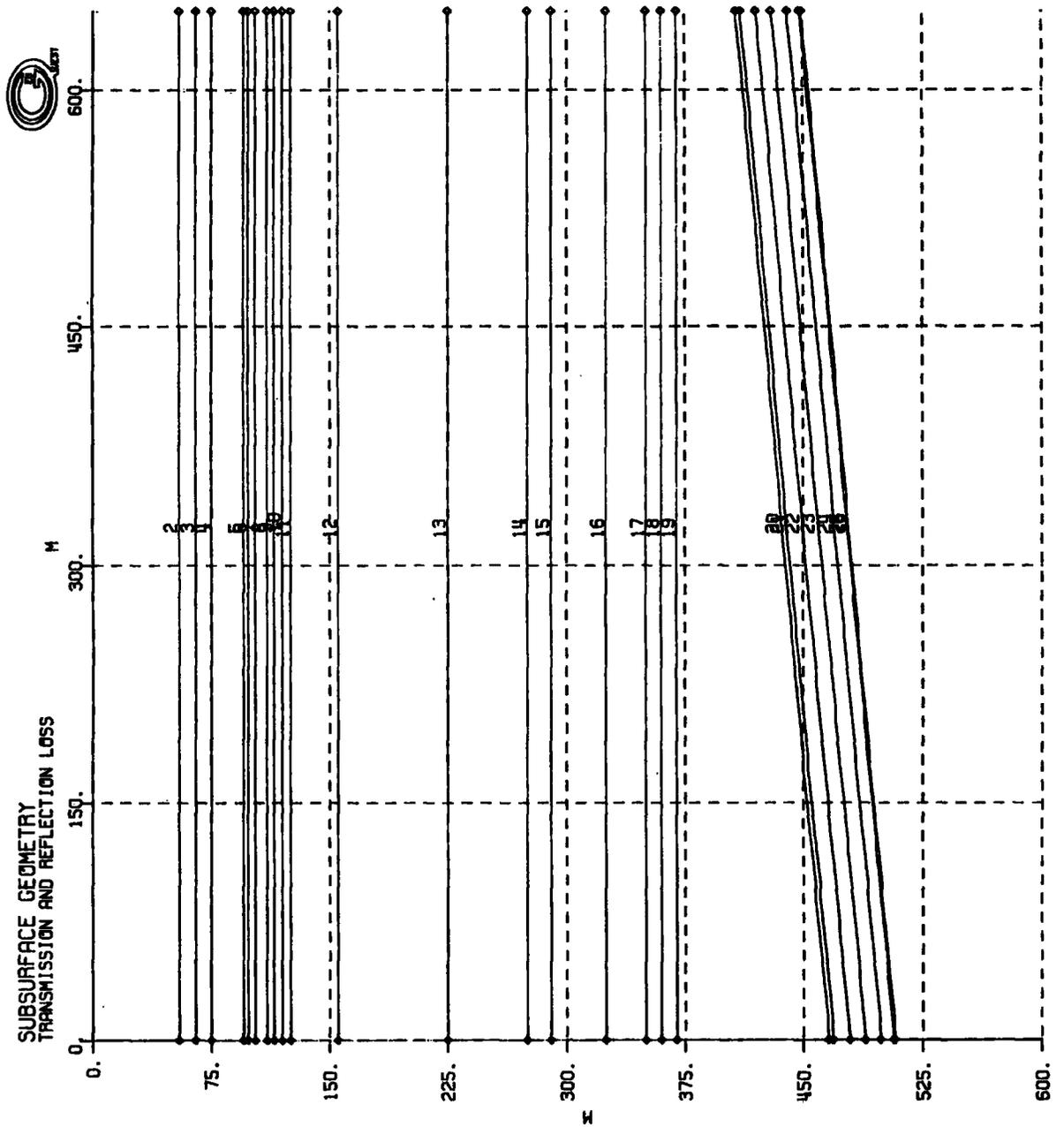
Figure 5.6 (b). Seismic reflection response for the geometry on Figure 5.6 (a). The traces were computed at 10 m intervals and have a time-ramp function applied to them.
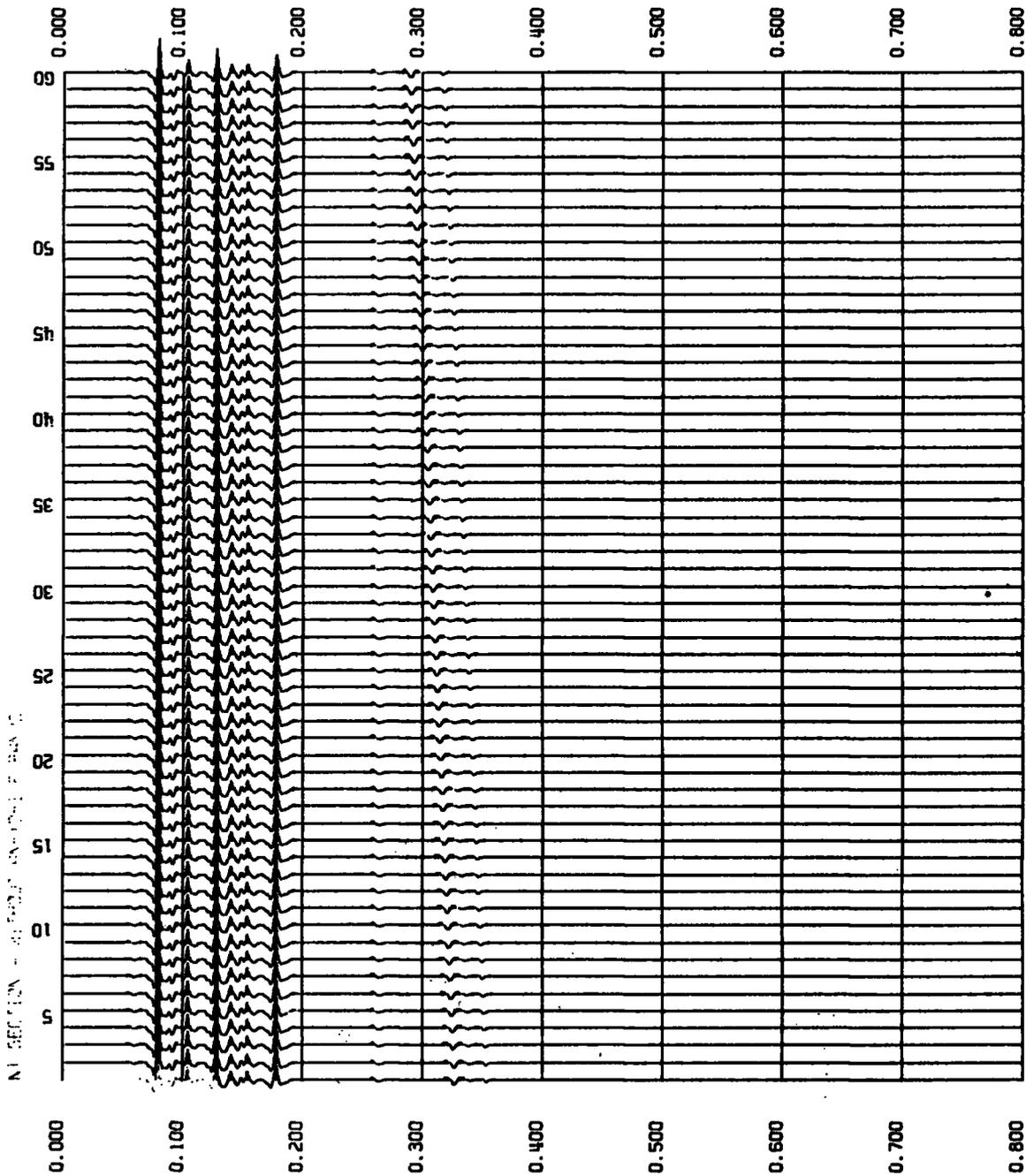
Figure 5.7 (a). Subsurface geometry when the Limestones' surface is
modelled as a non-horizontal interface. No diffraction
points were specified.
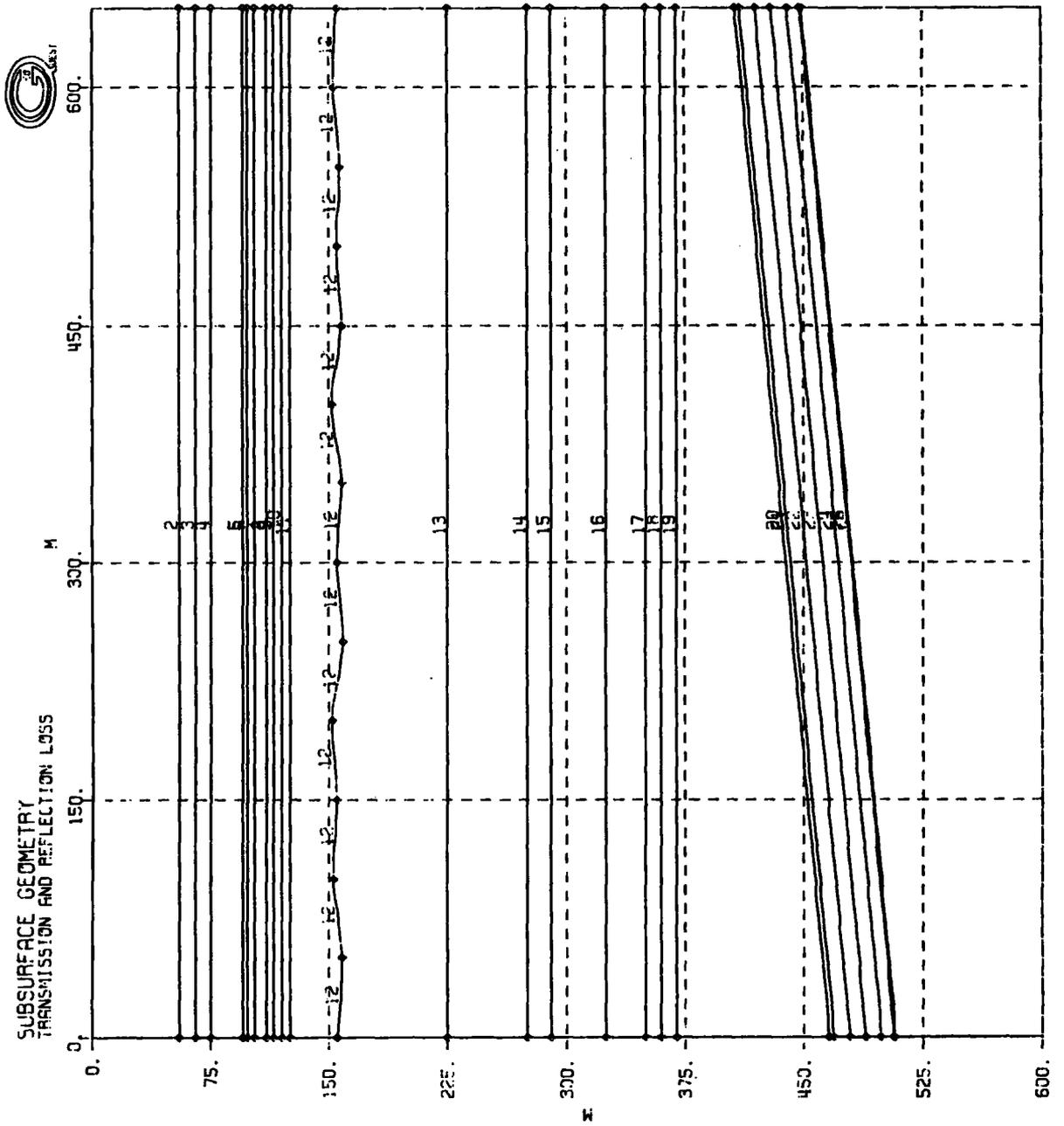
Figure 5.7 (b). Seismic reflection response for the geometry on
Figure 5.7 (a).
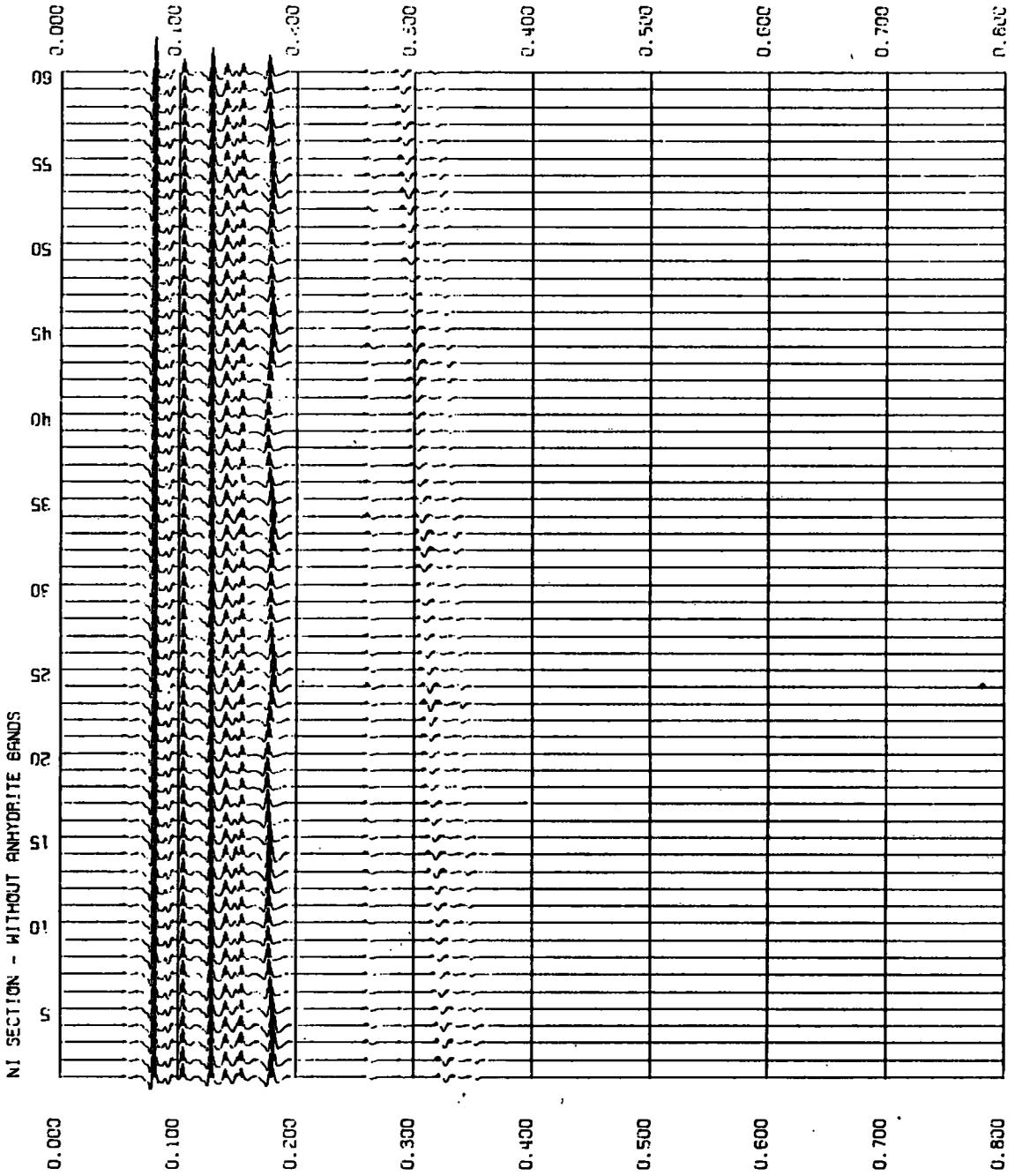
have concave upwards curvature produce an amplitude increase (focusing) and those with a convex upwards curvature result in a decrease in amplitude (defocusing). The effect on the amplitudes of the Coal Measures' reflections follows this pattern on the limestone horizon. If the surface becomes structurally more complicated as depicted on Figure 5.8 (more focusing and defocusing), the coal seam reflections are not properly resolved any more as Figure 5.9 shows.

The focusing or defocusing of seismic energy at the top of the limestone leads to a lateral variation of the amplitudes of the coal seams reflections and hence poor lateral continuity.

The rugosity of this reflector and the presence of fissures within the limestone was not modelled during this study. Such 'erosion' of the formation leads to a scattering of the incident seismic energy through diffraction. Kennett (1983) has pointed out that scattering redistributes the seismic energy and diminishes the apparent amplitude of the seismic waves in a way that is cumulative along the propagation path. It results in a pulse shape which is broadened and diminished in amplitude relative to that in a medium which propagates the seismic wave without scattering it. As the wavelength diminishes, the effect of local irregularities becomes more pronounced and so the scattering loss factor tends to increase. Thus higher frequencies are affected more by the process of scattering. This process and its frequency dependence causes a loss in amplitude by a factor of $(1/\lambda)^2$ where λ is the wavelength of the incident plane wave component if the scatterers have dimensions much smaller than

Figure 5.8   . Subsurface geometry with a more complicated topography
              on horizon 12.
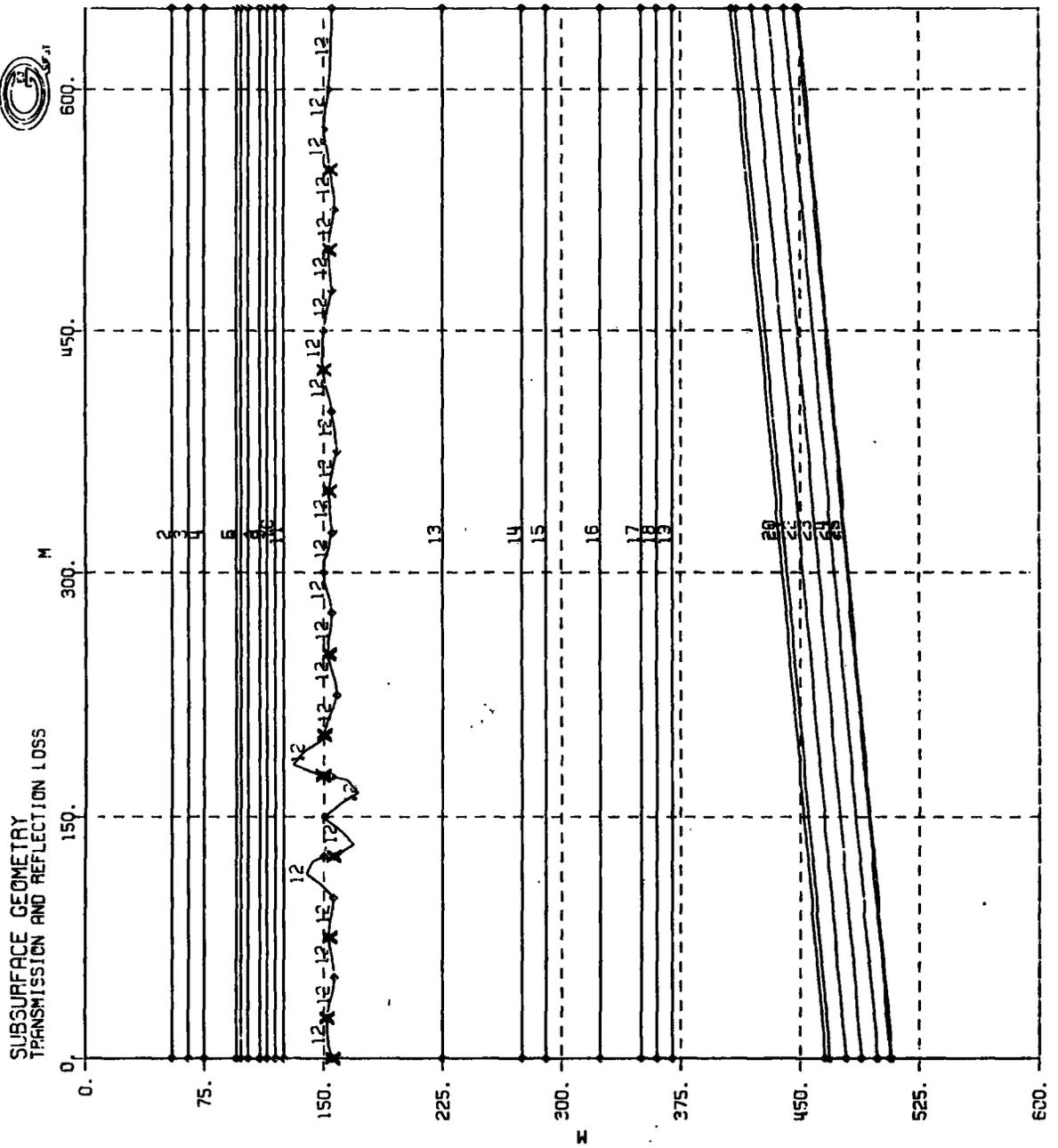
Figure 5.9 . Seismic reflection response for the geometry
on Figure 5.8 .
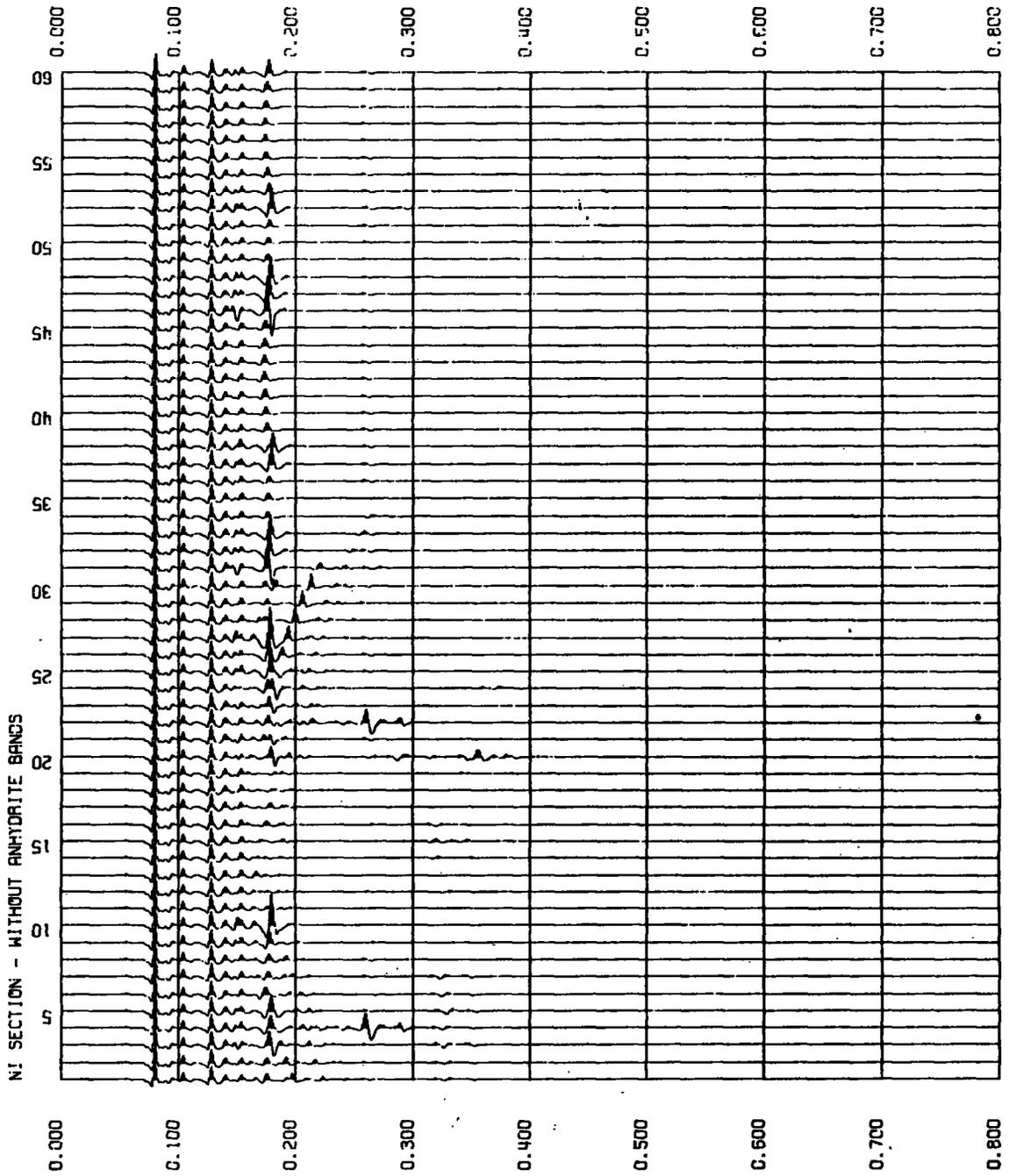
this wavelength (Longhurst, 1968). At high frequencies, there is more scattering and interference as well as more absorption. Consequently, to improve the continuity of Coal Measures reflections one must sacrifice the hoped-for resolution of using high frequencies, and use a source which generates energy below 50 Hz (say 20 Hz to about 100 Hz).

In the above examples, migration of the sections can recover some of the amplitude at the top of the limestone but lateral velocity variations both at the top of the limestone and within it will make it difficult to use the same method to recover the amplitudes of the coal seams' reflections and the consequent horizontal resolution.

5.4   Prediction-error Deconvolution for the
               Non-white Reflectivity Sequence.

Figures 5.10 (a) and (b) show the complete vertical incidence synthetic seismograms for the model of Figure 5.1 (b). The anhydrite bands were not included and spreading losses are not taken into account. The traces were computed by the layer-matrix method to obtain the complete impulse response followed by convolution with the wavelet of Figure 5.3. The computer program YIBEA3 was applied and the method requires the geological model to consist of homogeneous horizontal layers, so the dip of the coal seams was simulated by reducing the overburden thickness by 12 m/trace.
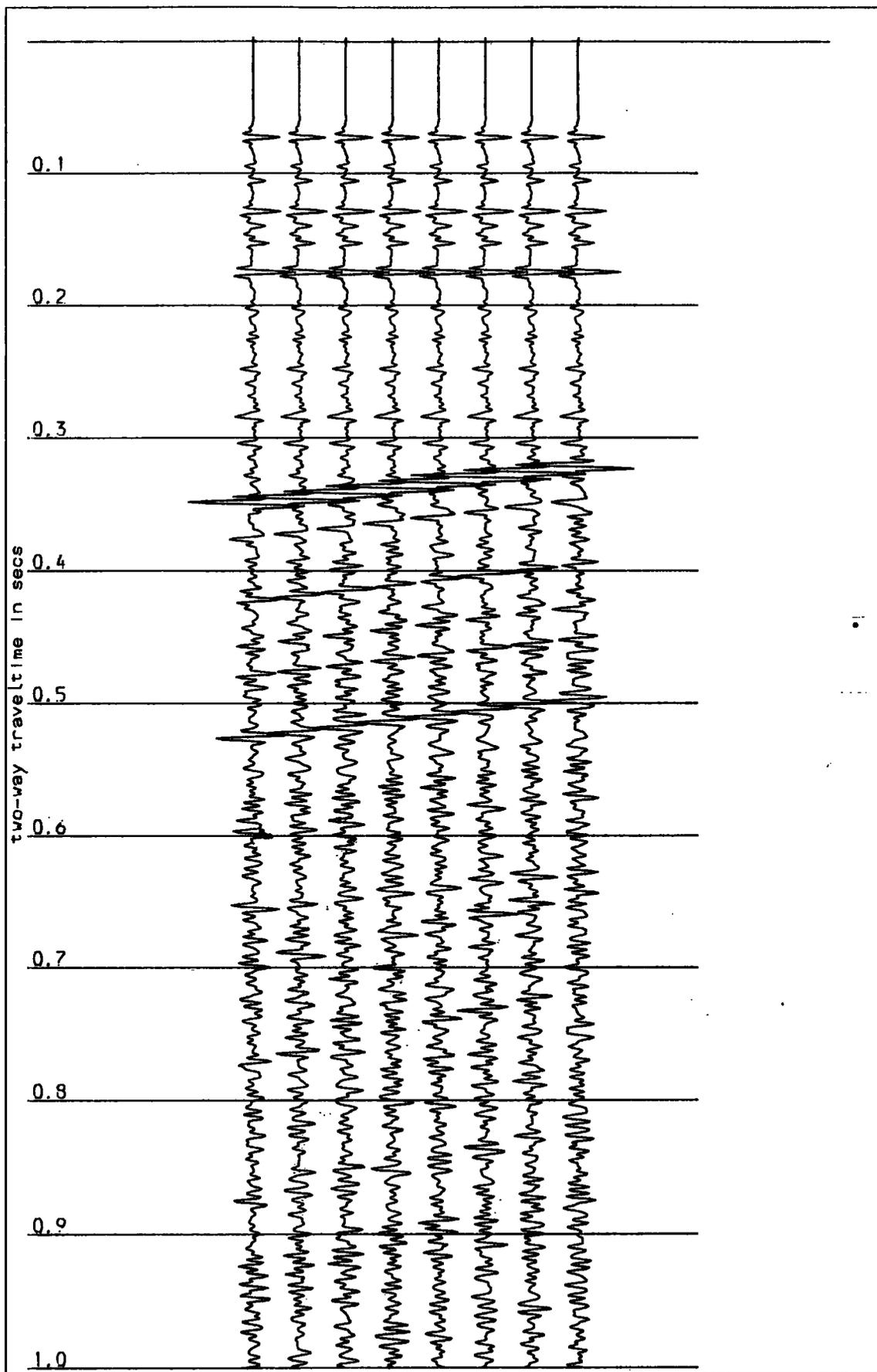
Figure 5.10 (a). Vertical incidence synthetic seismograms for the model on Figure 5.1 (b). The layer-matrix method was used for their computation. The Anhydrite bands were not included.
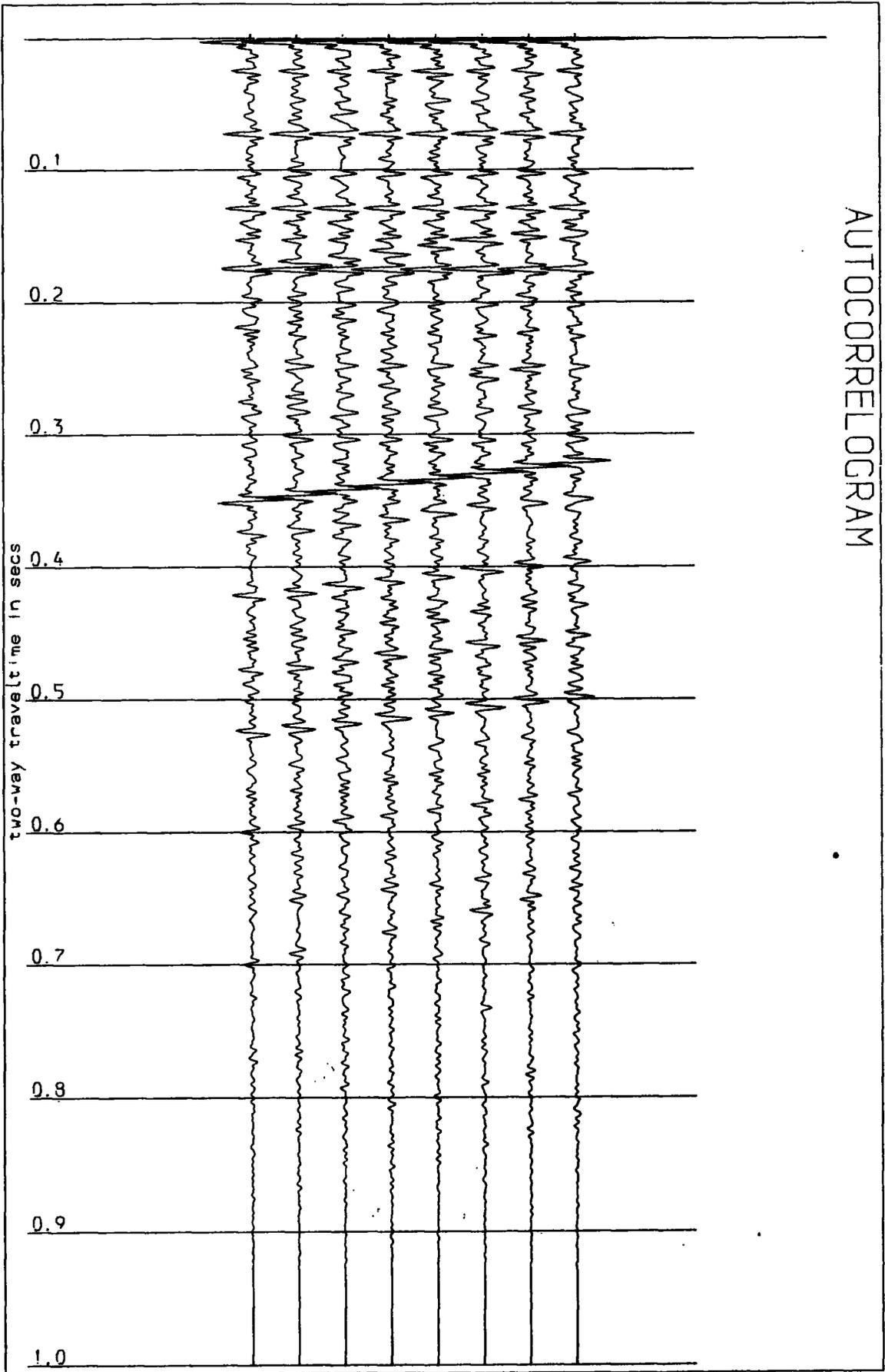
Figure 5.10 (b). The autocorrelogram of the section on Figure 5.10 (a).

Figures 5.11 (a) and (b) show the results of the application of prediction-error deconvolution to the traces. A filter with a gap of 32 msec and an active length of 318 msec was used. The prediction filter length and the prediction distance were deliberately chosen to be long enough to interfere with the primary reflections from the coal seams. The design gate for the autocorrelation function was 1 sec long and a prewhitening parameter of 2 % was applied. The main horizons of the original model can be observed on Figure 5.11 (a). These are the seabed at 74 msec, the top of the marl at 130 msec, the top and the base of the limestone at 176 and 282 msec and the coal seams at 346 and 373 msec respectively. The other primary reflections with smaller amplitudes have either been suppressed or are too weak to be resolved in the noise that arises from the application of the operator. This indicates that if the statistical requirements of the input trace are not met, then the resolution of the events which originally have relatively low amplitudes will deteriorate more after prediction-error deconvolution. The stronger events including the Coal Measures primaries are still well-resolved against the background processing noise after deconvolution.

Figures 5.12 show the results of applying the same filter to the seismograms that were calculated for a model with a few anhydrite bands (a less stationary reflectivity sequence r(i)). The results show that the main interfaces are again resolved after deconvolution although the second coal seam has a weaker amplitude. This can be attributed more to the amplitude losses through reflection and transmission within the

115
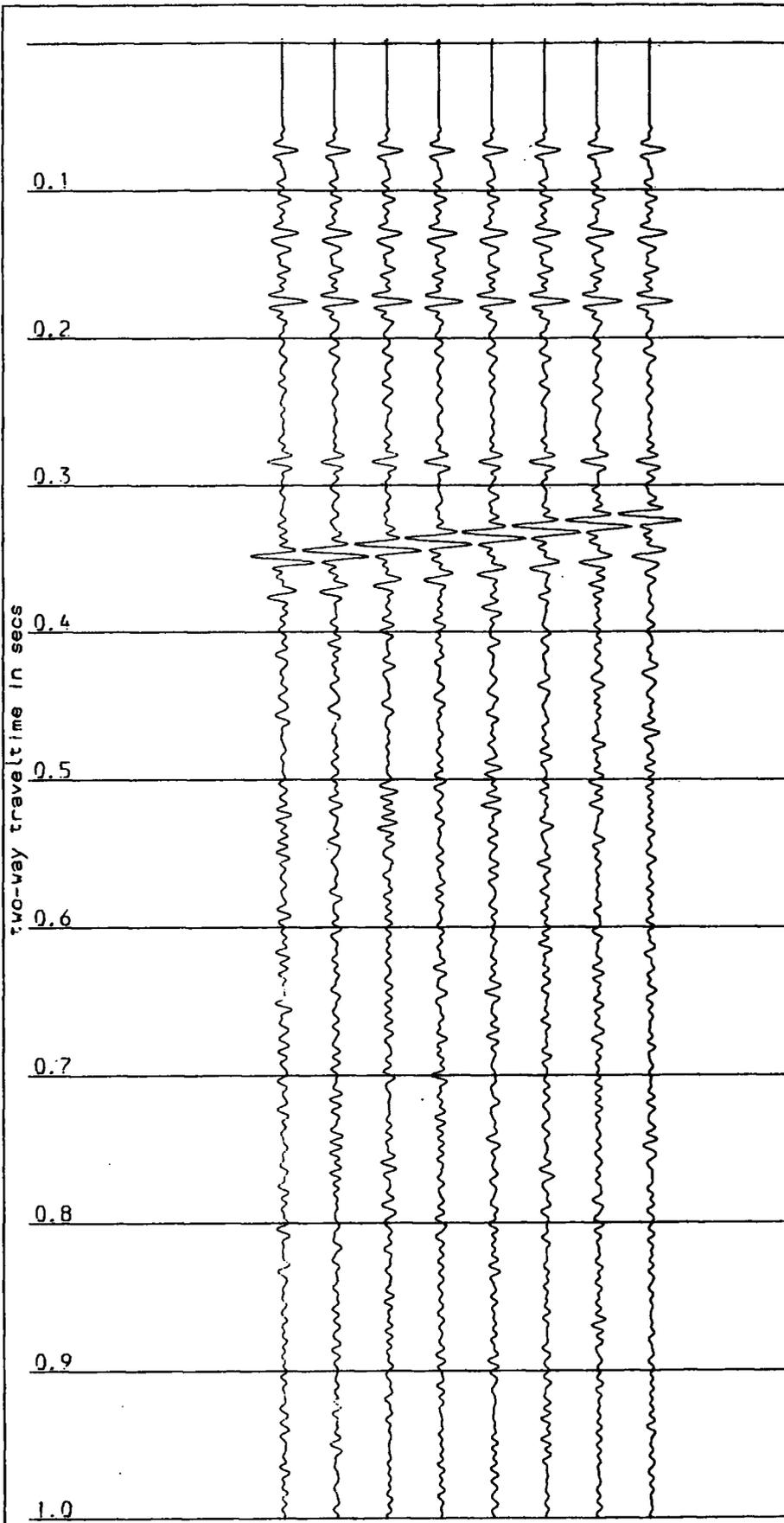
Figure 5.11 (a). The section on Figure 5.10 (a) with prediction-error deconvolution applied.
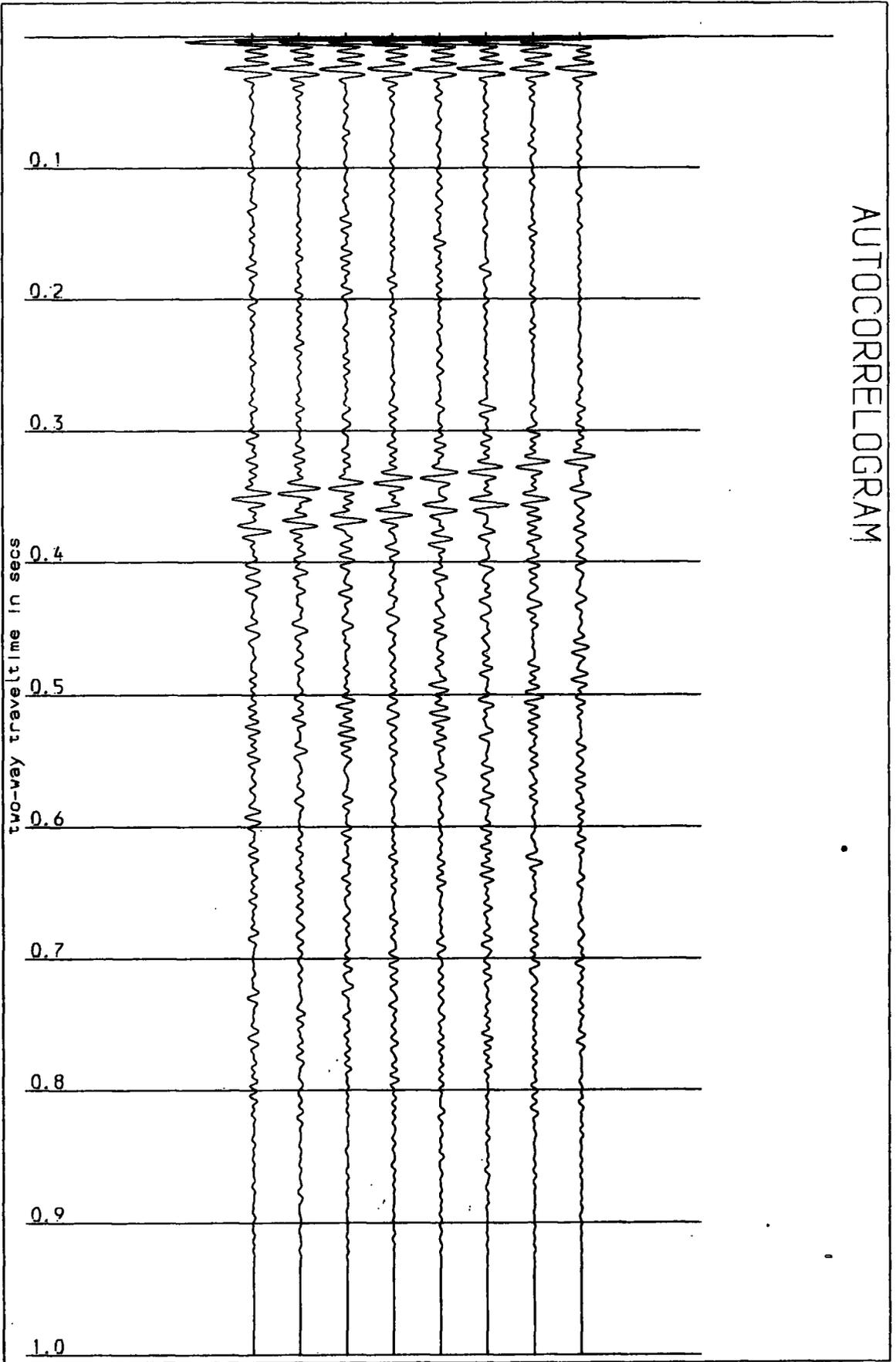
Figure 5.11 (b). The autocorrelogram of the section on Figure 5.11 (a).
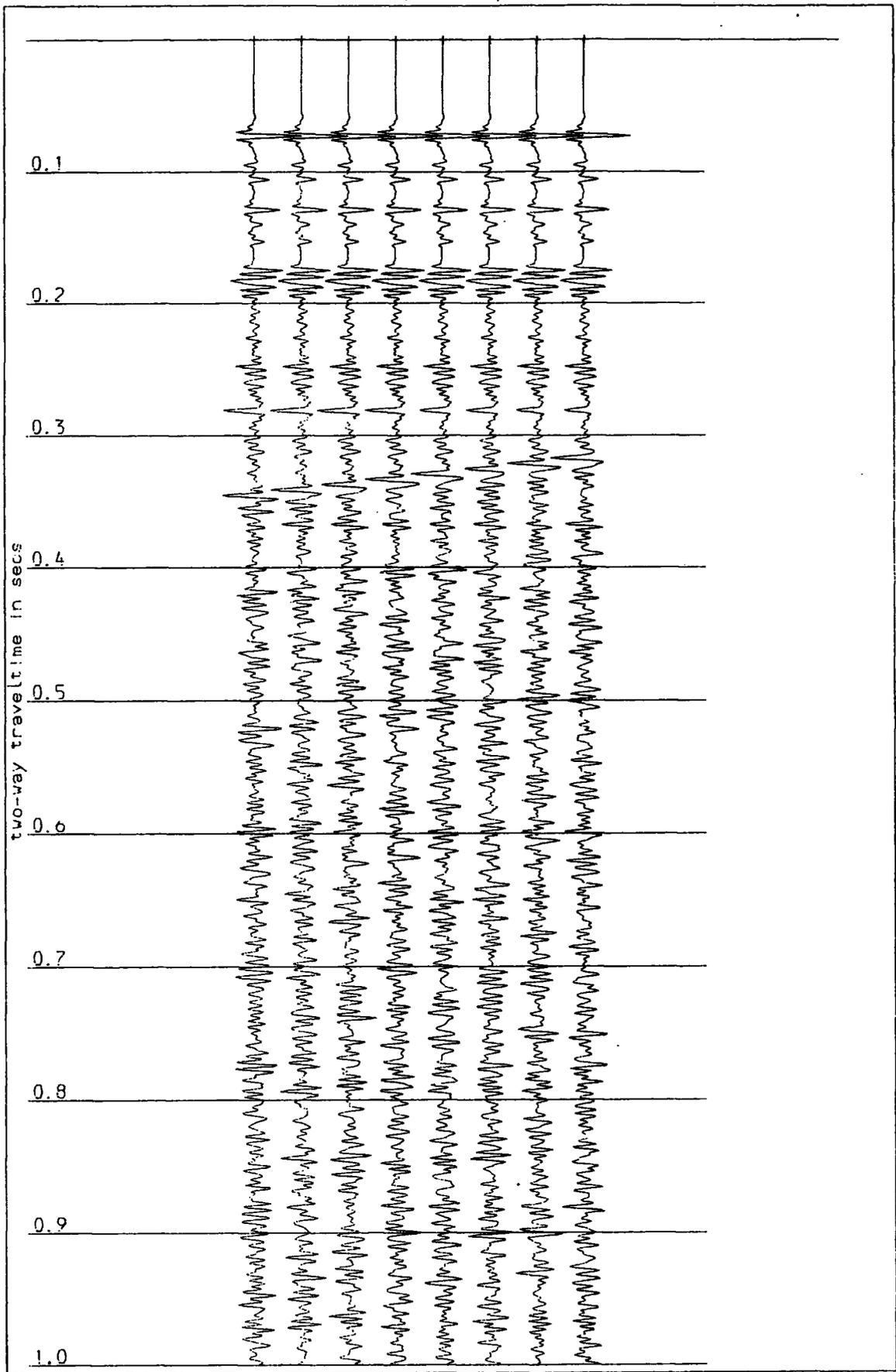
Figure 5.12 (a). Vertical incidence synthetic seismograms for the model of Figure 5.1 (b) with Anhydrite bands included.
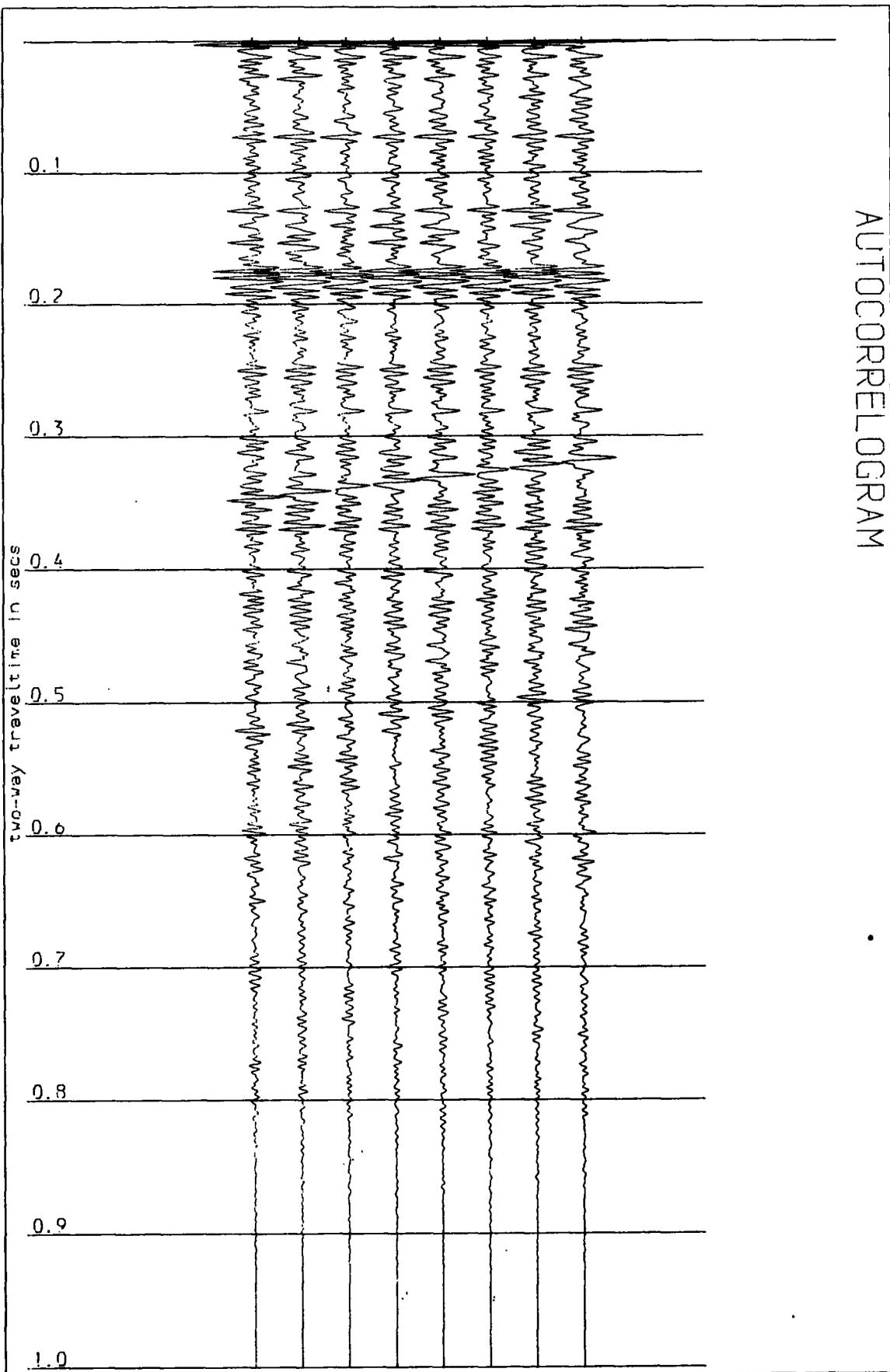
Figure 5.12 (b). The autocorrelogram of the section on Figure 5.12 (a).
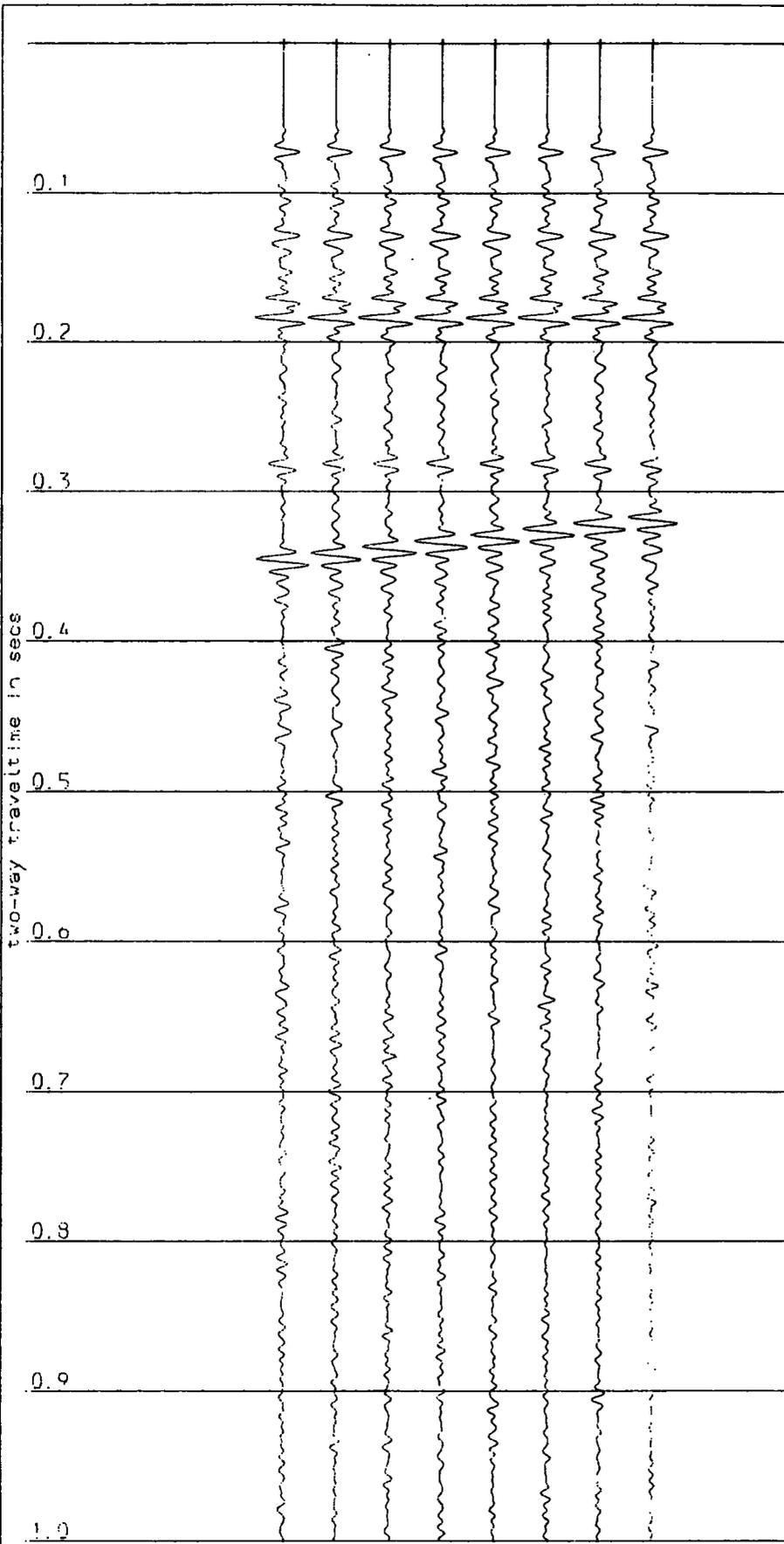
Figure 5.12 (c). The section on Figure 5.12 (a) with prediction-error deconvolution applied.
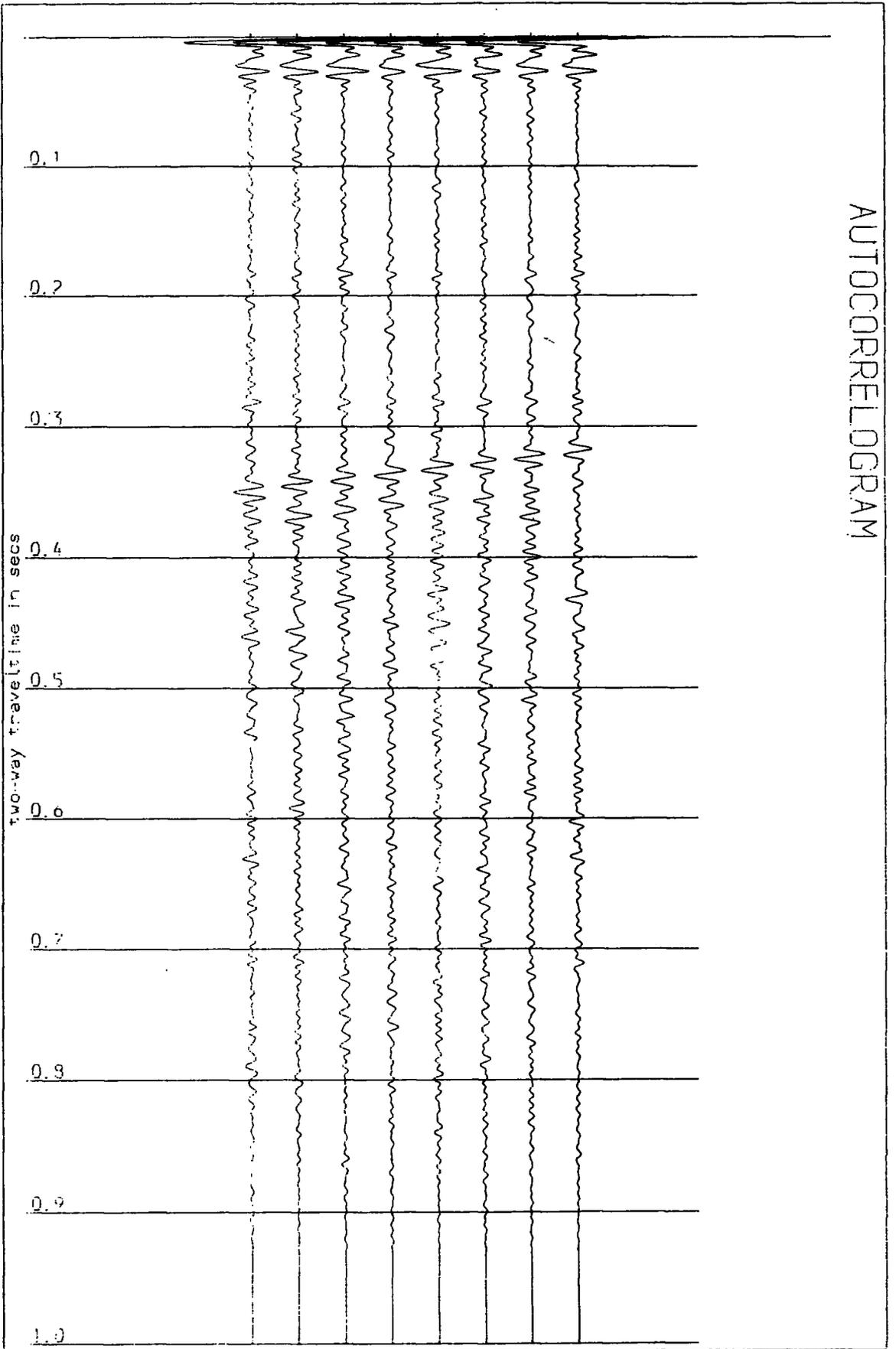
Figure 5.12 (d). The autocorrelogram section for Figure 5.12 (c).

extra interfaces than to the fact that they have suffered more suppression during deconvolution. It can also be noted that the waveform of the reflection off the top of the limestone (at about 176 msec) is not the same as that of the reflection from the seabed (at 74 msec). This is because of the presence of the thin band of anhydrite near the top surface of the limestone as was pointed out in chapter 4 (section 4.2.3).

In conditions of high S/N amplitude or power ratio (small amounts of random noise, no degradation of signal due to NMO corrections and stack, and no spreading losses) prediction-error deconvolution as a standard technique for attenuating multiples is adequate for this geological section with high and alternating reflection coefficients as was asserted in chapter 4.

5.5   Stacked Responses for Different Streamer Lengths.

In order to assess the optimum streamer length, synthetic seismograms with different source-receiver offsets were computed for a model simpler than that of Figure 5.1 (b) by the reflectivity method (Fuchs, 1968, Fuchs, 1970, Fuchs and Muller, 1971). In this method, the numerical integration of the reflectivity (or plane-wave reflection coefficient) of a layered medium is carried out in the horizontal wavenumber or angle of incidence domain. Multiplication with the source spectrum and inverse Fourier transformation yield the seismograms.

The reflectivity method as described by Fuchs (1968) was extended (Fuchs and Muller,1971) to include the transmission

116

losses and time shifts in a stack of layers on top of the reflecting medium and the computer program SYNSEI was written for use in computing the seismograms. This program was applied in this section but since there are no layers between the free surface and the top of the reflecting medium, it was modified to include the effect of the free surface on the computed response. This was done by expanding the reflectivities $R_{pp}(w, \gamma)$ (for the frequency components w and angles of incidence γ) of the medium as $R_{pp}/(1 - R_{pp} \exp(2iwq_\alpha(\gamma)h))^2$ (Kennett, 1984) where w is the frequency, $q_\alpha(\gamma)$ is the vertical slowness for the plane wave velocity of α , γ is the angle of incidence at the top of the layered-medium and h is the depth to the top of the medium. The horizontal wavenumber k and the angle of incidence are related by

$$k = (w/\alpha_o) \sin (\gamma)$$

where α_o = p-wave velocity in the first layer. The final seismograms are obtained by performing a Fourier transform over w and a Hankel transform over k on the w-k response. Velocity windowing was introduced in order to reduce computing time.

The above expansion attaches a double reverberation to all the primary reflections including the seabed primary reflection. However there should only be a single reverberation associated with the seabed primary. To correct for this, the response of the sea-water layer alone is computed with a double reverberation wavetrain by the expansion of all the reflectivities $r_{pp}(w, \gamma)$ as

$$r_{pp} / (1 - r_{pp} \exp(2iwq_\alpha(\gamma)h)^2 \qquad (1)$$

for every frequency w and angle of incidence γ. The response of

the same layer is also computed with a single reverberation attached to the primary by the expansion

$$r_{pp} / (1 - r_{pp} \exp(2iwq_\alpha(\gamma)h) \qquad (2).$$

For each synthetic gather computed the seismograms obtained from expression (1) are subtracted from it and those derived by expression (2) are added to it so that the seabed primary reflection has a single reverberation wavetrain attached.

Table 5.2 shows the layer parameters of the earth's model that was used and the figure below it shows the depth profiles and corresponding lithological units. Twenty-four gathers were generated and dips on the coal seams were simulated by reducing the overburden thickness by 20 m/gather. The two coal seams were 3 and 4 m thick respectively. The above model was used instead of that on Figure 5.1 (b) so as to reduce the computational time required per gather. Velocity windowing (inherent in the method) was also applied for this purpose. The source wavelet displayed on Figure 5.3 was applied in all the computations.

The near-trace spacing was 45 m and 24 channels spaced at 25 m intervals were simulated at a depth of about 5 m below the sea surface, these being the geometrical parameters used in the 1979 survey. The source was assumed to be at the surface and interconversions were neglected, i. e., the acoustic approximation was carried out. Random noise was not added to the computed gathers .

Figure 5.13 (a) shows a computed gather and Figure 5.13 (b) shows a real gather from the 1979 data for comparison. Both gathers have an AGC applied. The effects of wrap-round can be

Table 5.2   Layer parameters used for SYNSEI. The figure
********   below it shows the depth profiles of the seismic
             parameters.

i	th (m)	vi (m/s)	t (msec)	T (msec)	vs (m/s)
1	55.000000	1.500000	73.333328	73.333328	1.500000
2	48.000000	1.800000	53.333313	126.666641	1.633046
3	12.000000	2.400000	10.000001	136.666641	1.700932
4	15.000000	2.500000	12.000000	148.666641	1.778798
5	25.000000	2.700000	18.518509	167.185150	1.902927
6	220.000000	4.000000	110.000000	277.185059	2.921241
7	101.000000	3.300000	61.212112	338.396973	2.993307
8	3.000000	2.100000	2.857141	341.253906	2.986938
9	48.000000	3.200000	30.000000	371.253906	3.004716
10	4.000000	2.100000	3.809523	375.063232	2.996901

i = layer number.
th = thickness of layer i.
vi = interval velocity for layer i.
t = 2-way delay in layer i.
T = 2-way normal incidence travel time to base of layer i.
vs = stacking velocity for event i (Dix' Formula).
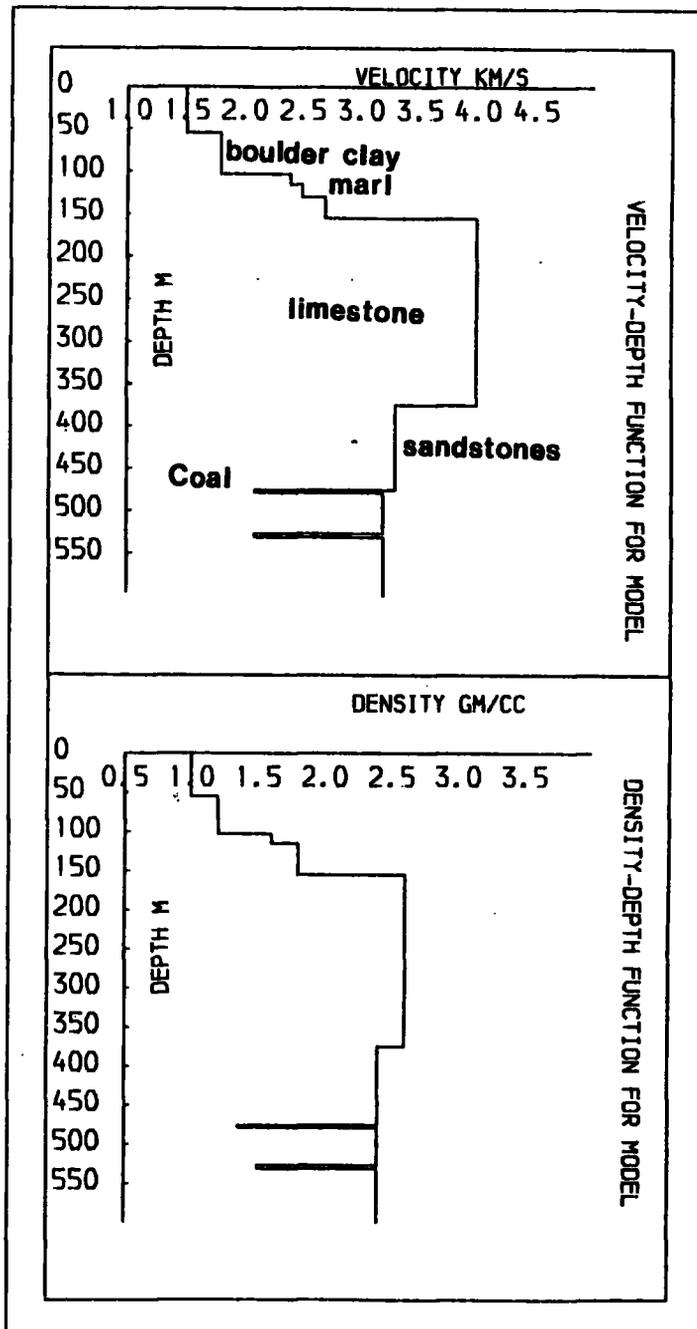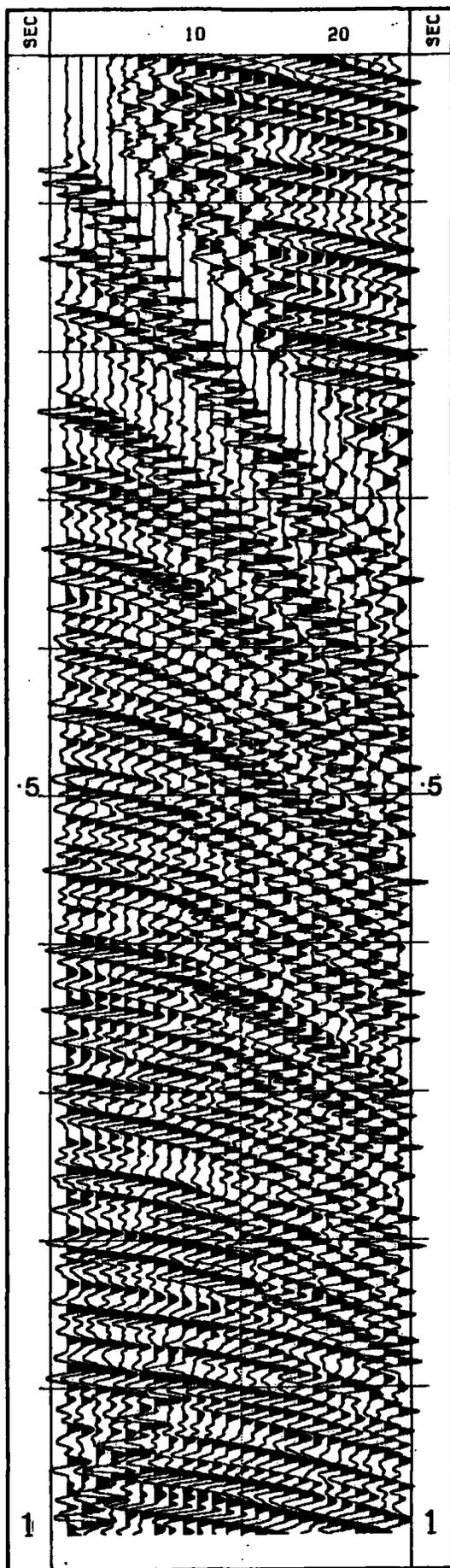
Figure 5.13 (a). Synthetic seismic gather computed for the model w
parameters on Table 5.2 by the reflectivity metho
AGC is applied. Gain of plot is 14.0 .
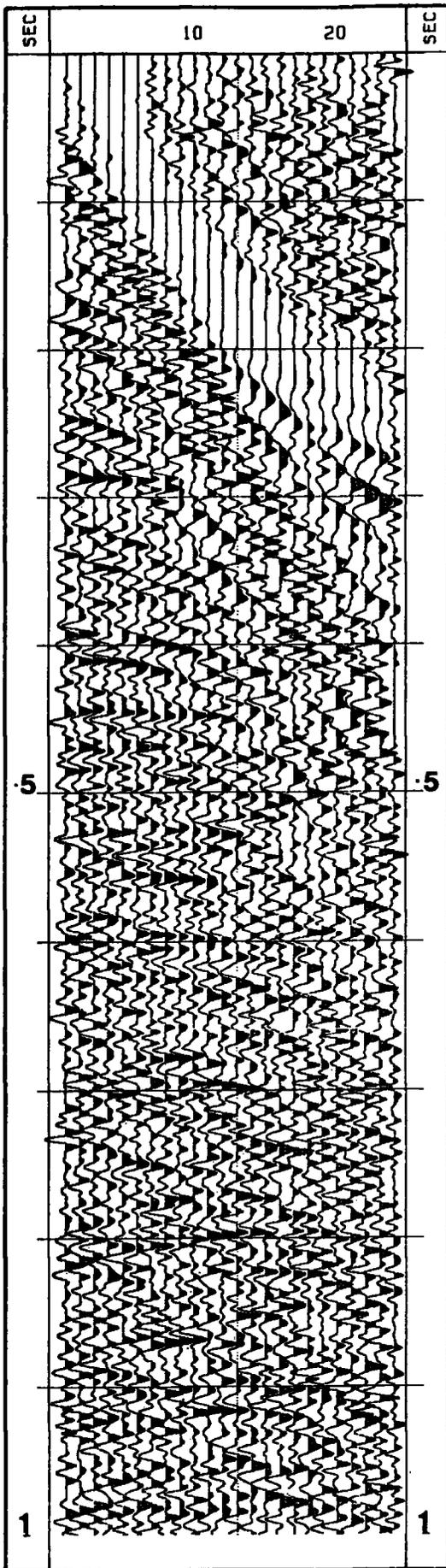
Figure 5.13 (b). Real seismic gather that was acquired in 1979 using the
same geometry as for the synthetic on Figure 5.13 (a).
Gain of plot is 7.0 .

observed as the patch of energy on the top right-hand corner of Figure 5.13 (a). Another numerical arrival crosses this gather from about 1000 msec on the first trace to about 700 msec on the 24th trace. The latest primary event should have a 2-way zero-offset time of about 375 msec.

The gathers were processed in order to simulate different folds of stack corresponding to different streamer lengths. The muting pattern that was applied to the 1979 data was used in the processing. Three processing sequences were applied to the synthetic data. Firstly, the gathers were stacked without any DBS and the sections were displayed. Secondly, DBS was applied (gap of 20 msec and an active filter length of 130 msec) and the stacks are shown. Finally, velocity filtering with an 11×11 point operator was applied before stacking. The results for each processing sequence are displayed along with their corresponding autocorrelograms as seven panels of 24 stacked traces. The panels correspond to 1, 6, 8, 12, 16, 20, and 24-fold stacks respectively. These are theoretically equivalent to streamer lengths of 0, 125, 175, 275, 375, 475, and 575 m respectively with a near-channel spacing of 45 m; thus giving maximum source-receiver offsets of between 45 and 620 m.

Figures 5.14 (a) and (b) show the results of the stacks without any pre-stack processing applied. The resolution of the coal seams' reflections improved as the level of stack increased. For the given muting pattern, this resolution changes very little beyond the 16-fold stack (corresponding to a streamer of about 375 m). There is high frequency ringing in the 12, 16, 20 and 24-

119

Figure 5.14 (a). Stacked sections of the synthetic data set. Pre-stack
processing was not applied. High-cut frequency is 150
Hz.
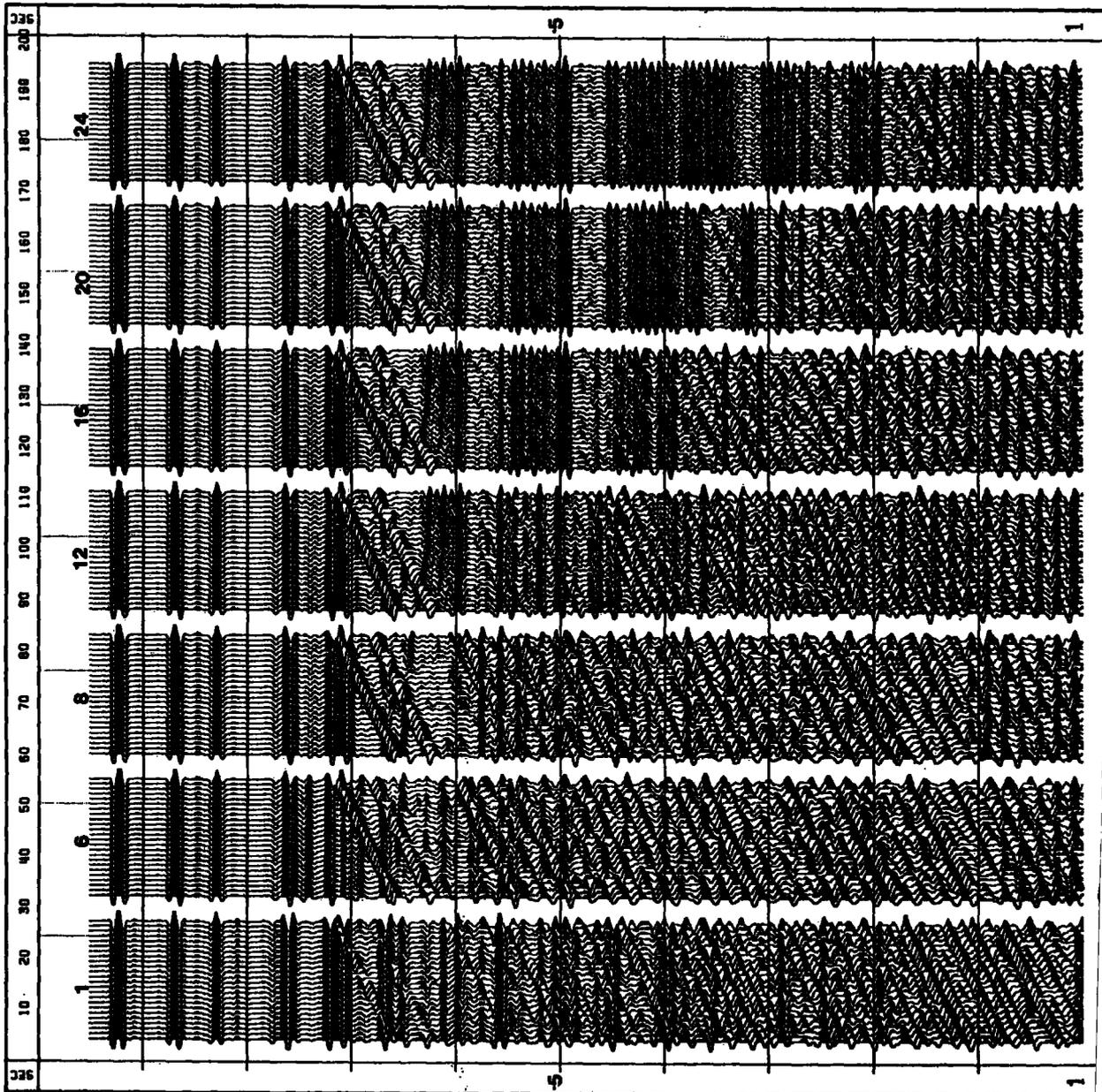
Figure 5.14 (b). Panels of autocorrelograms for corresponding sections on Figure 5.14 (a).
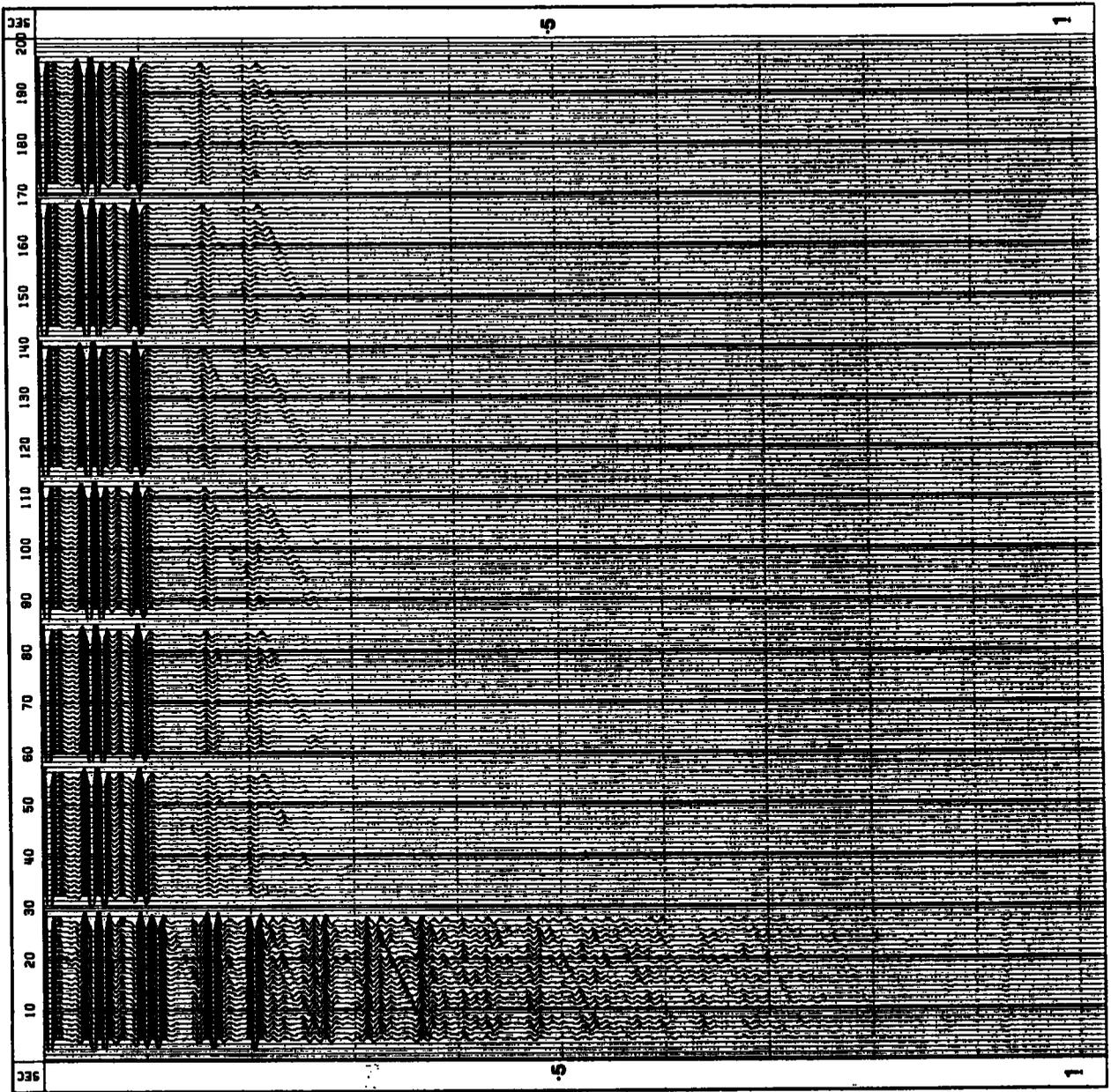
fold stacks. This arises from the use of the reflectivity method in the computation of the original gathers. The results were all filtered to a maximum high cut-off frequency of 70 Hz in order to eliminate this ringing. Figures 5.15 (a) and (b) show the results after this filtering.

Figures 5.16 (a) and (b) display the results obtained when DBS was applied. The deconvolution parameters that were used are the same as those that were applied to line 7940. The predictive gap was 20 msec and the filter length was 130 msec. The multiple reflection at about 240 msec was efficiently suppressed but that which interferes with the coal seams was not effectively cancelled even by stacking. The resulting stacked sections do not change much after 16-fold stacking.

Figures 5.17 (a) and (b) show the sections that were obtained by velocity filtering before stack. The resolution of the coal seams' reflections is excellentfrom 8 - 24 fold stacking. The suppression of seabed multiples is efficient but the peg-leg multiples within the limestone are not expected to be eliminated by this technique as was explained in section 4.2.2 (c). Since the ordinary seabed multiples are so efficiently suppressed by this filtering, the residual peg-leg energy after stacking is much enhanced by the AGC applied to the result. The multiple at 240 msec is suppressed although not as effectively as on Figure 5.16 (a). For the mute pattern applied, the 16-fold and higher stacks are not significantly different for targets between 300 and about 700 msec 2-way travel time.

A streamer of about 375 m was therefore considered to be

Figure 5.15 (a). Stacked sections of the synthetic data set. Pre-stack processing was not applied. High-cut frequency is 70 Hz.
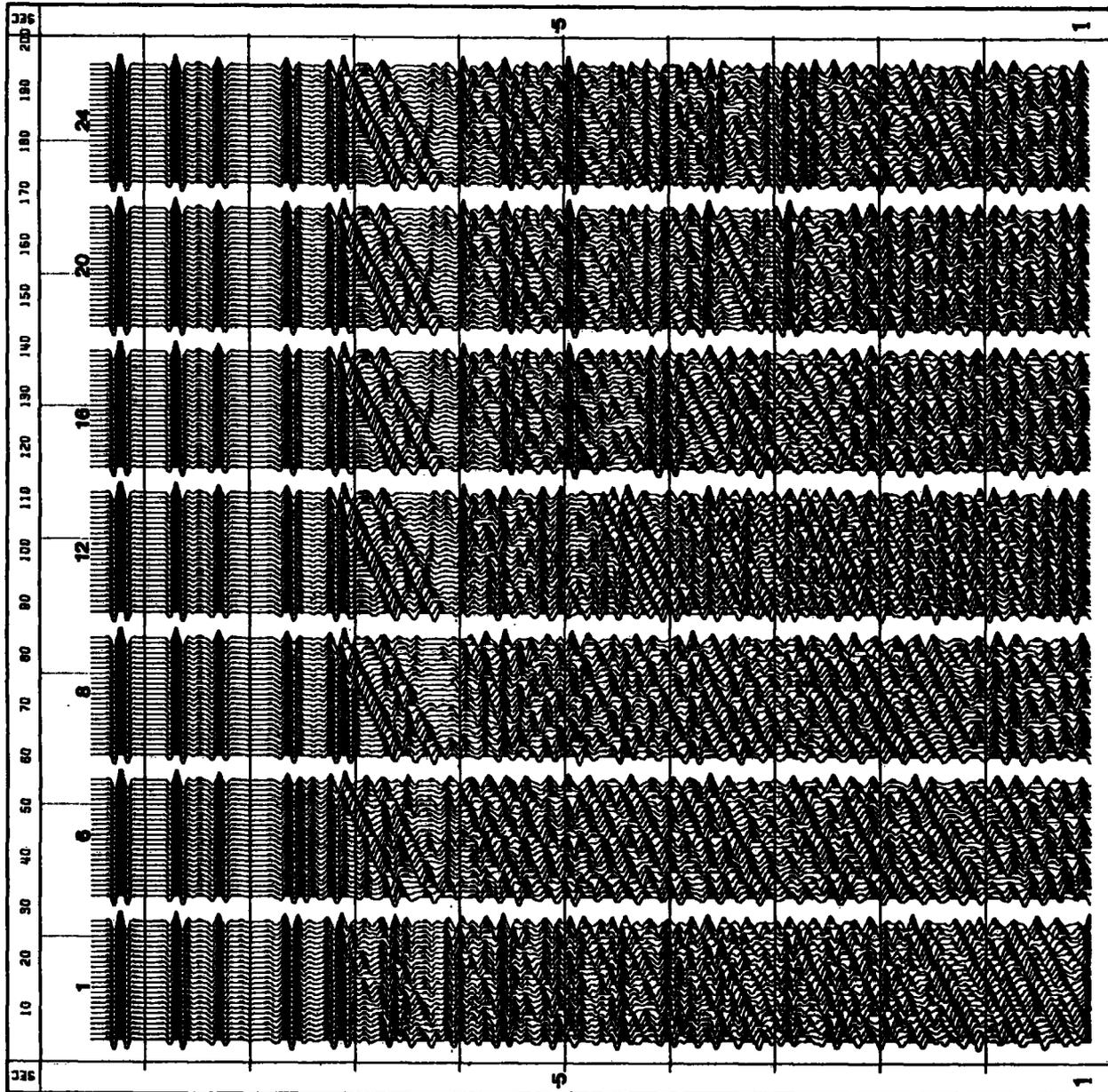
Figure 5.15 (b). Panels of autocorrelograms for corresponding sections
of Figure 5.15 (a).
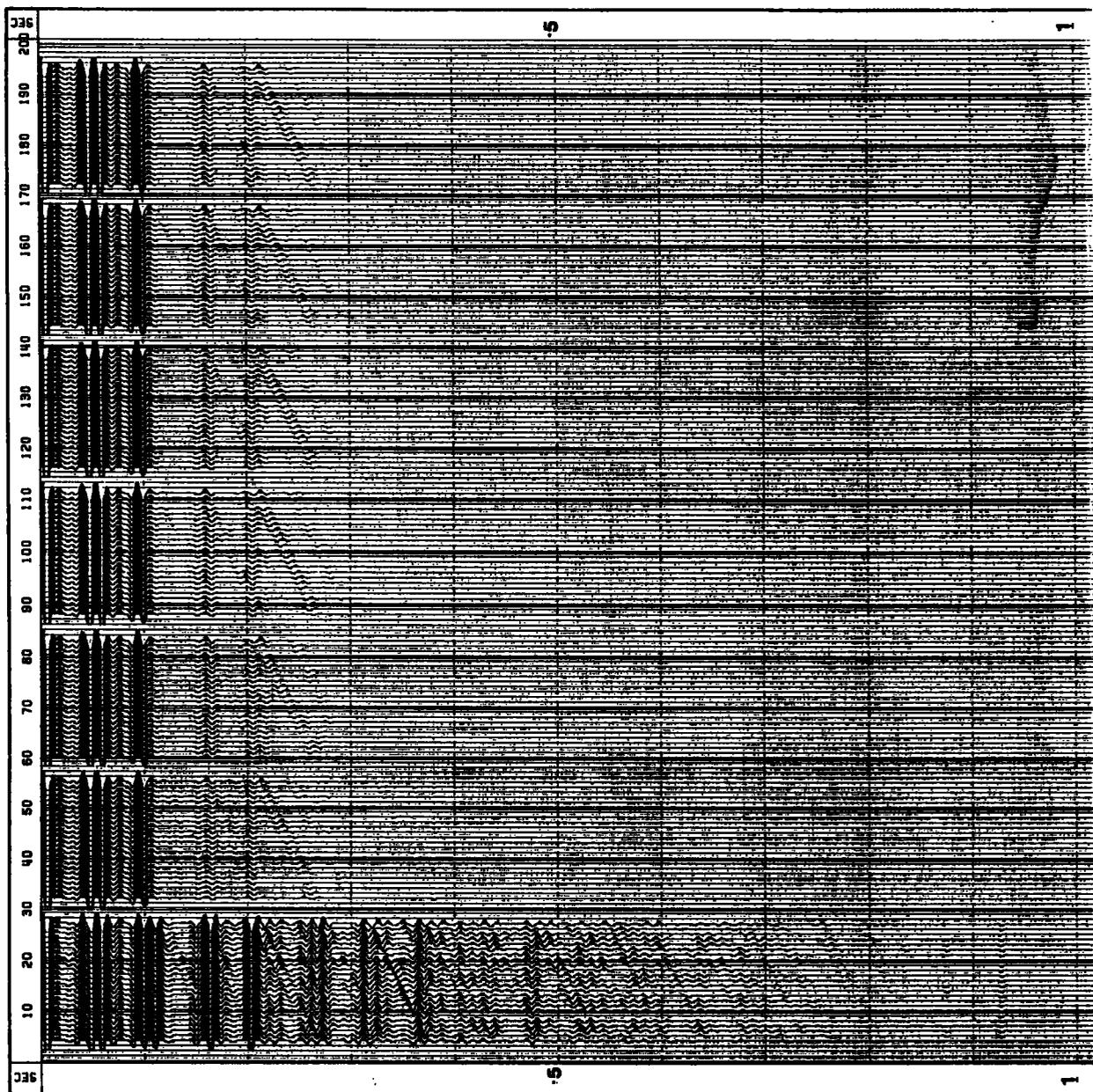
Figure 5.16 (a) Stacked sections of the synthetic data set. DBS is applied (gap=20 ms; filter length = 130 ms). High-cut frequency is 70 Hz.
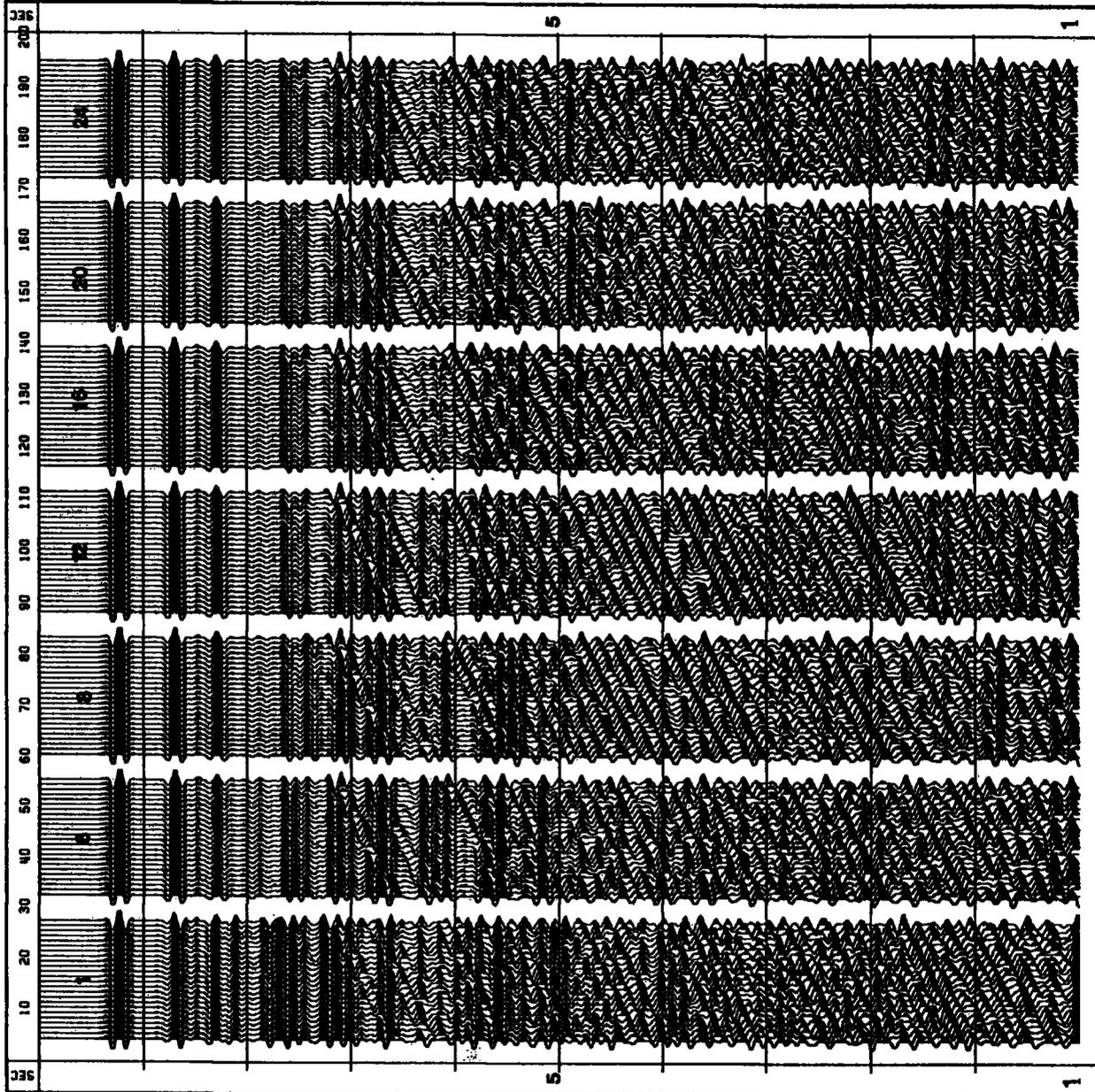
Figure 5.16 (b). Panels of autocorrelograms for corresponding sections
on Figure 5.16 (a).
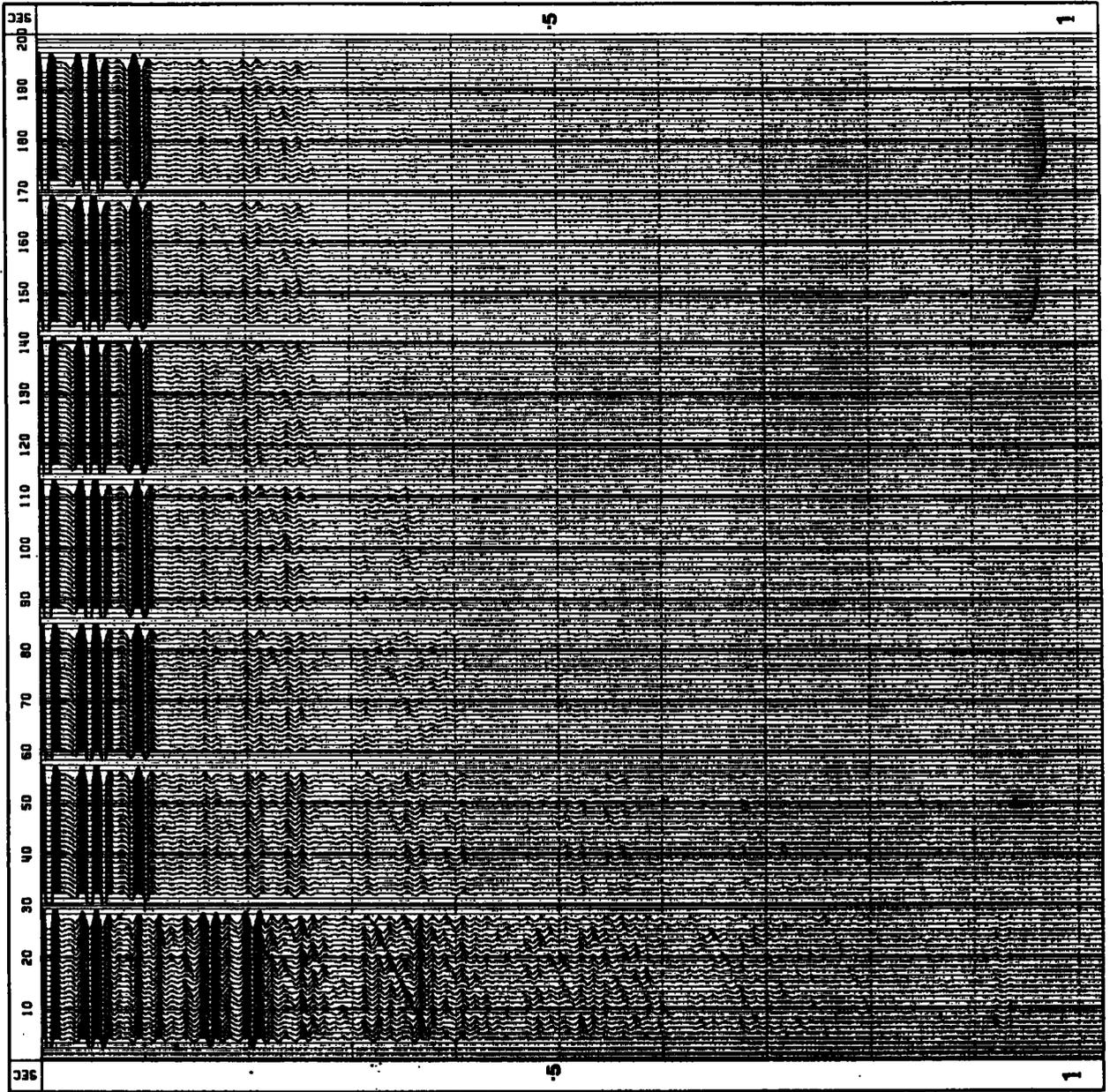
Figure 5.17 (a). Stacked sections of the Synthetic data set with
velocity filtering with an 11X11 point operator
applied before stack. High-cut frequency is 70 HZ.
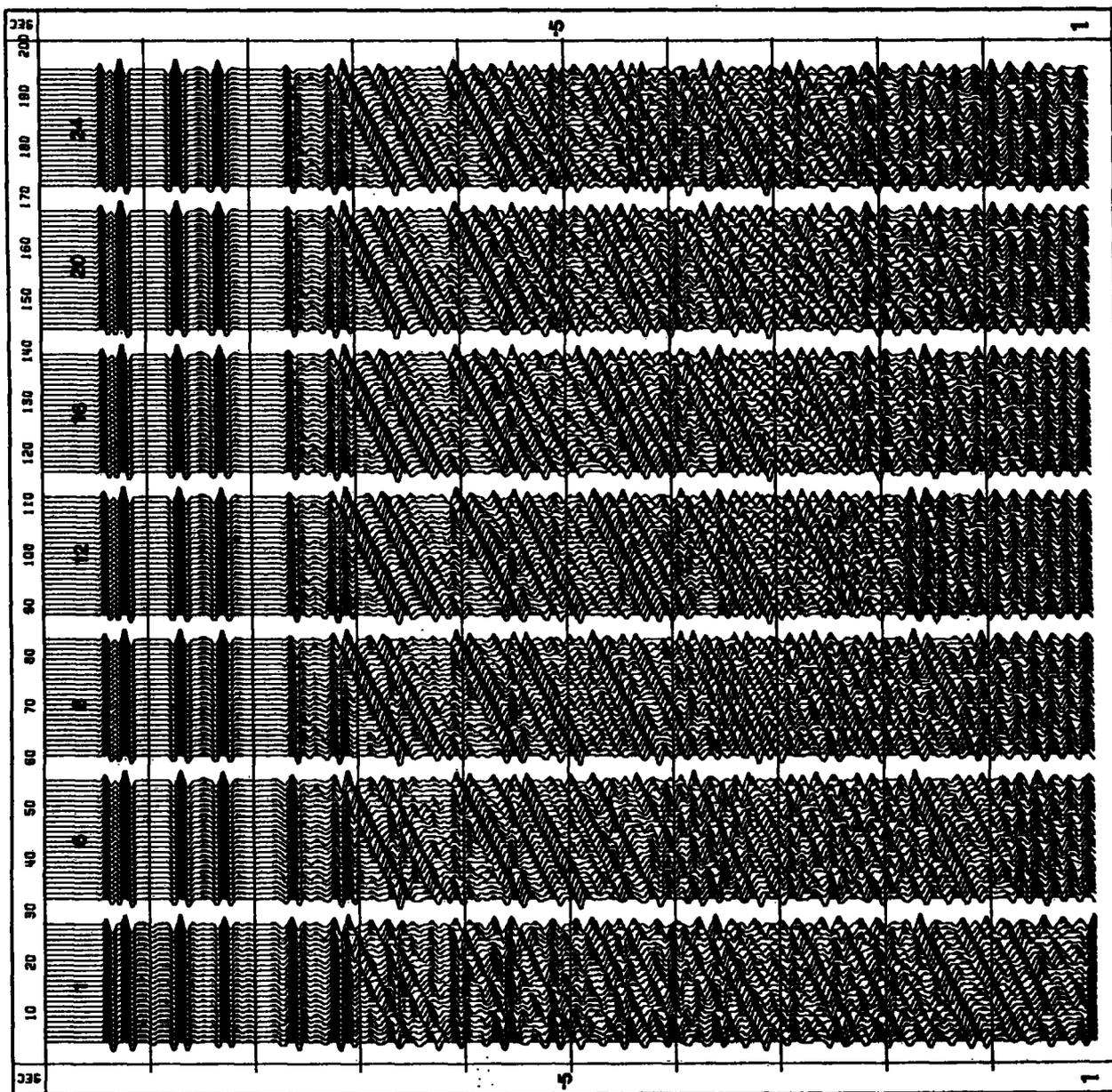
Figure 5.17 (b). Panels of autocorrelograms for the corresponding
sections on Figure 5.17 (a).
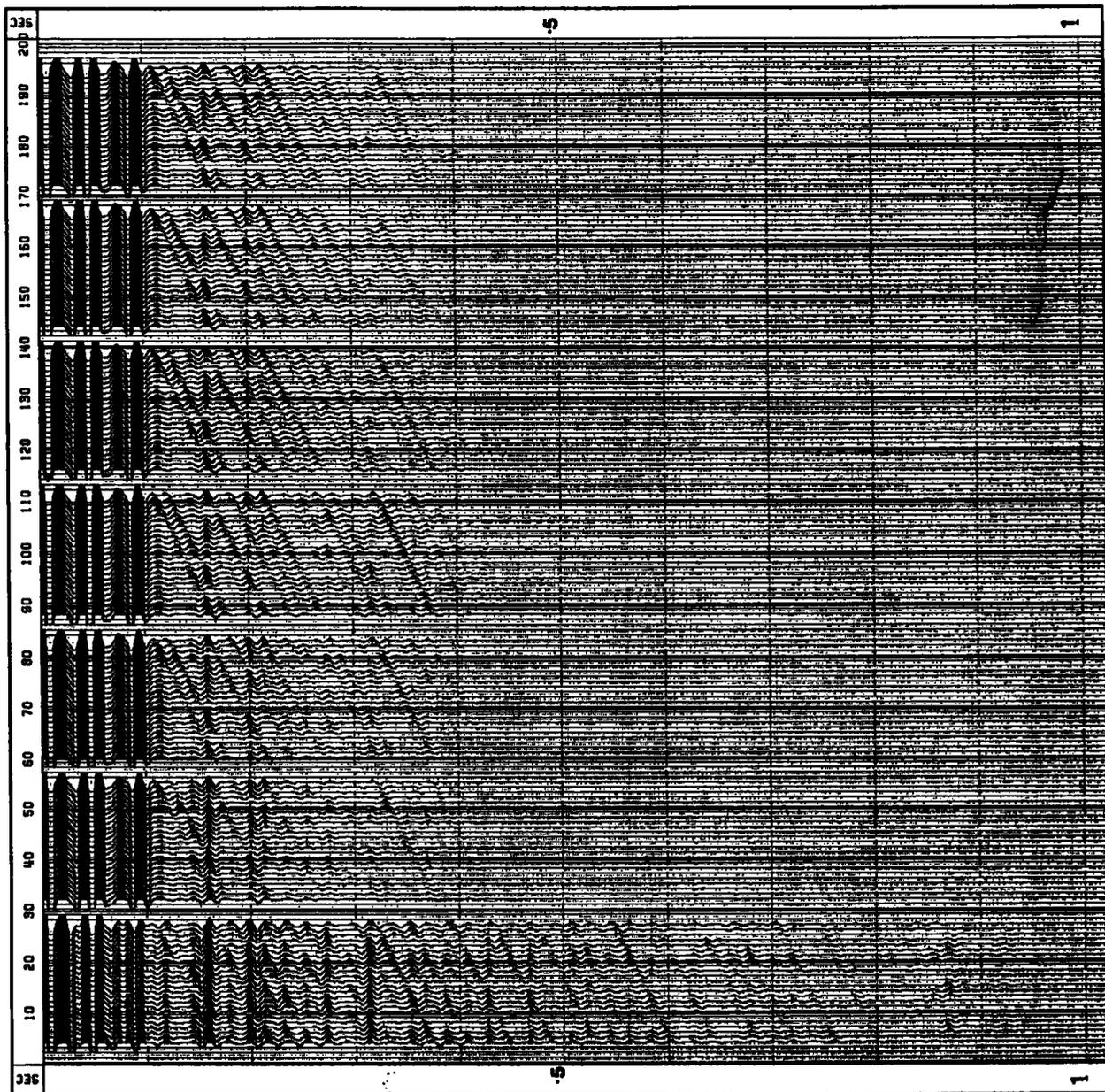
adequate. The near-trace spacing was 45 m and the group interval was 25 m, giving the 16-fold multiplicity for a shot interval of 12.5m. With this streamer length and near-channel spacing, an alternative group interval and shot interval can be chosen in order to increase the level of stack. A 400m streamer with 12.5 m group spacing will produce a 32-fold stack if the shot interval of 6.25 m is maintained. Alternatively, a 15 m near-trace spacing can be maintained and 48 channels at 8.25 m may be arranged to form a cable of about 396 m and if the shot interval is maintained as 8.25m, then 24-fold coverage is obtained. Any suitable combination can be chosen so long as the maximum offset does not exceed 420 m. Such a data set will need the same mute pattern as the 1979 data, but the increased level of stack within the p-wave penetration window will improve the S/N ratio and the resolution of the Coal Measures. In particular, velocity filtering can be applied to eliminate the seabed multiples. Spatial aliasing should not be a problem with these shorter hydrophone groups at frequencies of interest.

5.6   Summary.

An outline of the results for the models used in this chapter can be given in the following points.

The effect of frequency-dependent attenuation is significant only above a frequency of about 150 Hz and the banded structure (Coal Measures or anhydrite bands) do not affect the overall bandwidth, although spectral nulls are expected at frequency

intervals that correspond to the inverse of the average 2-way time within the bands.

The erosion of the surface of the limestone and/or the presence of 'fissures' or karst development within it, causes a decrease in the seismic resolution of Coal Measures. Focusing effects at the top of the limestone as well as the scattering of the seismic waves by these irregularities also lead to lower amplitudes of the reflections from the Coal Measures. Scattering affects the high frequencies more, and this, limits the potential resolution of data from the area. Having chosen an appropriate streamer, a broadband source with significant energy at the low frequency end as well is preferable.

When the prediction-error technique is applied to the reflectivity sequence for this area which is not white and not stationary, the suppression of the strong primary reflections is not severe. This was observed for a 32-point synthetic reflectivity sequence. The real reflectivity sequence would be more complicated, but in general, the technique should not be harmful.

Finally, stacked responses for different simulations of the seismic streamer length suitable for this area suggest that the geometry for the data acquisition in the region can have about 420 m of maximum offset. Coventional data processing may then be applied to the data that are acquired. In particular, velocity filtering is useful in eliminating the water-bottom multiple reflections.

C H A P T E R 6

SUMMARY AND CONCLUSIONS.

In this chapter, a summary of the present work is given and the main conclusions are outlined. Some of the problems that were faced in the course of the study are mentioned and suggestions for future approaches are included.

6.1 Summary of the Present Study.

Following an outline of the geology of the region off the coast of Durham, the application of offshore surface seismic surveying for the delineation of Coal Measures' geological structure in this area has been examined and the problems highlighted. A high proportion of the energy from the source returns as refractions and wide-angle reflections off the top of the Permian limestone, and also as reverberations within the Permian formations. The multiples have almost the same stacking velocities as the primary reflections within the Coal Measures because the limestone has a relatively high seismic velocity. Consequently, straight (standard) CMP stacking does not suppress them efficiently. Also, care must be taken during the acquisition of data from this region to ensure that data is not wastefully recorded at large offsets. Scattering from irregularities within the Permian strata will be more at high frequencies so that there is the need to use a broadband source rather than lay emphasis on

a high-frequency source which will have lower penetration consequent to these effects.

A theoretical study of the use of deterministic filters (3-point and 4-point filters) to suppress a 2-layer reverberatory wavelet was carried out for the earth models derived from a simplified geological section off the coast of Durham. The study was done before samples of the real data from this region were obtained and their application to these data produced poor results because of the errors in the estimation of the filter paramaters and because of the high levels of random noise in the input data. The advantages of such filters were outlined but it was shown that they are too simplistic to be applied to real data.

Standard and non-standard processing algorithms for multiple and random noise suppression were summarized and three of them were reviewed in greater detail for the purpose of applying them in the processing sequences for the real data samples. Prediction-error deconvolution and two alternative stacking techniques were considered. These are weighted stacking and iterative stacking. The advantages of the application of prediction-error deconvolution before and after stacking were summarized and its limitations were outlined. Velocity filtering of CMP data before stacking was also applied to some of the real data and an outline of the method was given in chapter 4.

The results of the processing of the real data sets by using these methods in alternative processing sequences and their discussions and interpretation were outlined in chapter 4.

The problems caused by the Permian overburden and faced during seismic surveying were modelled in chapter 5 by using AIMS and the layer-matrix method to compute synthetic seismograms. Mainly the effects of transmission, spreading and attenuation were considered for a typical reflectivity sequence of the geological section expected for this region. The alternative acquisition geometry was also modelled by using the reflectivity method and a version of the program SYNSEI. The conclusions that have been derived during the present study are outlined below.

6.2   Outline of Conclusions.

In chapter 2, it was shown that optimum weighted stacking results in a stacked trace that has a S/N power ratio which is equal to the sum of the S/N power ratios of traces that contribute to the stack and that an improvement of a factor of M (fold of stack) is possible when the traces have identical S/N power ratios. Only in rare circumstances when the amplitude scales and S/N power ratios of the traces of the NMO corrected CMP gather are respectively identical, can the straight stack have an optimum S/N ratio. However, in conditions where the input gathers have got low S/N power ratios, the implementation of the optimum weighted stacking technique is difficult and simplified versions must be conceived. The iterative stacking algorithm is easier to apply in theory and it was shown to produce a good eradication of strong seabed multiple reflections as well as random noise. Its main disadvantage was shown to be that it

creates more signal distortion than the other stacking techniques.

In chapter 3, deterministic filters for dereverberating a 2-layer multiple wavetrain were considered for ideal noise-free, normal incidence situations. Their simplicity of design and successful use in such conditions was confirmed. However, statistical methods of approach (mainly prediction-error deconvolution) are more suitable for real data because thay treat statistically random noise more efficiently. Deterministic filters are applicable in a variety of situations including the dereverberation of synthetic seismograms prior to matching them with field records and for theoretical problems of the inversion of seismograms to equivalent impedance logs. Current inversion methods assume a dereverberated input trace (Bambeger et al., 1979, Lailly 1981, and Mendel et al. 1980).

In chapter 4, the results of the processing of the real seismic reflection data were presented and discussed. It was concluded that the acquisition parameters for line 7940 achieved some penetration because the final sections showed Coal Measures reflections but their lateral continuity was poor. A comparison of the final sections and the field records showed that the segments of the data that fail to indicate the Coal Measures reflections are associated with the presence of a high velocity near-surface refractor which is evident on the corresponding field records. This refractor was considered to be a band of evaporite (mainly anhydrite) within the limestone. The 1979 mute pattern had to be severe because a relatively long streamer

(about 600 m) was used in the survey and the refractions and wide-angle reflections from the top of the limestone merge at large offsets (greater than the critical distance of 200 m) with the primary reflections. Besides the hampered penetration achieved in this 1979 survey, the poor quality of the sections is partly explained by the fact that the erosion of the limestone's surface and/or the presence of fissures within the limestone give rise to the scattering of the seismic energy, resulting in an overall poorer seismic efficiency of the source and poorer S/N power ratio within the Coal Measures.

Line 8201A was processed by using two processing sequences that differed in the stacking method. Although a better result was achieved with iterative stacking in suppressing both categories of noise, the final sections did not show Coal Measures reflections at all. A comparison of the streamer lengths in the 1979 and 1982 surveys (displayed on Figure 4.10) showed that the former was too long while the latter was too short. The choice of a streamer with an intermediate length would;

(a) improve the proportion of the seismic energy that is received in the pressure-wave penetration window relative to the 1979 data, and

(b) improve the level of stack within the p-wave penetration window relative to the 1982 data.

Such a streamer will result in shorter hydrophone groups (than in 1979) if a high multiplicity of coverage is to be obtained for the application of more efficient data processing techniques.

In chapter 5, examples of the seismic modelling of the

geological section of the region were presented. It was shown that a moderate attenuation profile for the post-Carboniferous succession affects frequencies above 150 Hz more. It was also shown that erosion of the limestone would diminish the resolution within the Coal Measures because of the focusing effects at its top surface. Because of the likely presence of fissures and karst development within the limestone, scattering especially at high frequencies should be considered in the choice of a source type. Although the best possible reflectivity sequence of the area that could be efficiently modelled as being non-white and non-stationary was used, it was clear from the examples displayed, that prediction-error deconvolution suppresses the very weak primary reflections only, along with the multiples. Synthetic seismograms with offset were stacked and processed for different streamer lengths and it was shown that a length of about 375m to 420m was adequate when the optimum muting pattern applied to the 1979 data was used.

Finally, the watergun source at a depth of about 5m applied in the 1979 survey is recommended for future trials. A tuned array of airguns or steam bubbles (STARJET) are other alternatives. A streamer of length of 400m would be adequate for a minimum of refractions and wide-angle reflections interfering with the Coal Mesures primaries, to be recorded. It can be towed at a depth of 5 - 7.5 m in order to avoid the effect of the free surface on the frequencies of interest. A hydrophone group spacing of 12.5 m and a shot interval of 6.25m would provide 32-fold coverage, and the following standard equations for CMP

spreads are applicable;

$$Y = n \Delta X / 2 m$$

and

$$T \, U = 1.95 \, Y$$

where

Y = distance in meters covered between records,

n = number of channels,

ΔX = channel spacing in meters,

m = multiplicity of coverage for CDP spacing of $\Delta X/2$,

U = ship's ground speed in knots (1 knot=1.852 km/hr),

T = time interval between shots in sec.

In this situation, we have

$\Delta X = 12.5$ m, $n=32$, $m=32$, and $Y=6.25$ m

so that a record length of about 1.5 sec, a record repetition interval of 3 sec and a ship speed of approximately 4.1 knots (7.5 km/hr) may be selected. The near-channel spacing of 20m can be maintained so that the maximum source to receiver offset is about 420 m. Alternative combinations can be chosen as long as the ship speed, maximum data length recorded and the maximum offset available are compatible with these guidelines.

6.3   Problems Faced and Suggestions for

Future Approaches.

One of the difficulties faced during the course of this study was the lack of detailed data on both the lithology and the seismic parameters of the formations in the region. A sonic log was run in the well BH. (figure 1.2) from the depth of 340m below the seabed so that the sonic velocity data for the geological succession above the Coal Measures were not available except for the estimates that were obtained from the seismic reference survey in the well. Density logs for both the Carboniferous and post-Carboniferous formations were not available either. Complete sonic and density logs from a well in the region would provide the data for more precise modelling.

The other problems were related with the computer programs that were used for the modelling. It was originally anticipated that the AIMS modelling package could be used for all the modelling requirements during this project but it cannot efficiently compute complete synthetic seismograms with offset. The inclusion of all multiple reflections is difficult because all the conceivable raypaths must be given in the data file. Even if this were possible, the CPU time required to generate such a gather would be prohibitively long. The reflectivity method and the program SYNSEI were used for generating synthetic data with offset but velocity windowing is necessary to reduce computing time. This, coupled with the problems of wrap-round that are encountered in the computations (a maximum of 1024 data points is allowed for each trace) introduces numerical errors in the final

results. With the program SYNSEI which allowed a more useful approximation of the response, it took approximately 800 CPU sec to generate a 24-fold gather with traces of 1.024 sec long sampled at intervals of 1 msec, but with the AIMS program it required more than 2500 CPU sec to compute the same gather with only about 25 multiple raypaths specified. Both computations were performed on the NUMAC IBM 370/168 machine. A good alternative method of generating synthetic seismograms with offset from a point source over a horizontally layered structure would be that developed by Kennett (1979). The method also uses Fourier synthesis followed by plane wave superposition. Although it is not expected to be computationaly faster than the reflectivity method, it has the advantage of allowing the direct computation of the complete reflection layer matrix. Also, aliasing effects can be reduced by a choice of a higher number of time points per record (4096 in this case instead of 1024). Velocity windowing is also required to reduce the computing time. As for the reflectivity method, its effect is to faithfully reproduce only the low-frequency part of the shallow reflections and it leads to a distortion of the propagation characteristics in the surface layer. However the fine discretization in space required for this study (Δ X is 6.25m to 25m) together with the damping introduced in the method would reduce both the effects of aliasing in the wavenumber domain (and consequent ringing after inverse transformation) and of numerical arrivals associated with velocity windowing.

Finally, the problem of scattering in general and that of

the roughness of the limestone's surface in particular could not be studied with AIMS. This is because AIMS superposes diffracted events on the seismic section of specular reflections. This is useful for studying the appearance of the section after the introduction of point scatterers into the model but not the cumulative effect of such points along a propagation path, on the amplitude and frequency content of deeper reflections.

Despite the above stated limitations, the present modelling has probably reproduced the main features. The modelling of the source type and the effect on the high frequencies of the scattering process are difficult to tackle. The real geological problems of this area mean that although the parameters suggested above will result in better data, the final sections will still be difficult to interpret.

References.

Anstey, N. A.,1964
 Correlation techniques - A Review.
  Geophys. Prosp. vol. 12, pp. 355-382

Anstey, N. A.,1966
 The sectional auto-correlogram and the sectional retro-cor-
 relogram - Part 1.
  Geophys. Prosp. vol. 14, pp.389-411

Anstey, N. A., and Newman P.,1966
 The sectional auto-correlogram and the sectional retro-cor-
 relogram - Part 2.
  Geophys. Prosp. vol. 14, pp.411-426

Backus, M. M.,1959
 Water reverberations - their nature and elimination.
  Geophysics vol. 24, pp.233-261.

Bamberger, A.,Chavent, G.,and Lailly P., 1979
  About the stability of the Inverse problem in 1-D
  wave equation - Application to the interpretation of
  seismic profiles.
   Journal of Applied Mathematics and Optimisation,

  No. 5, pp. 1-47.
Brandsaeter, H.,Farestveit, A.,and Ursin, B.,1979
  A new high-resolution or deep penetration airgun array.
   Geophysics vol. 44, pp. 865-879.

Burg, J. P.,1967
  Maximum Entropy Spectral Analysis.
   Society of Exploration Geophysicists, 37th annual
   International Meeting, Oklahoma City, Oklahoma.
Claerbout, J.,1976
  Fundamentals of Geophysical data processing.

  New York; McGraw-Hill.
Christie, P. A. F.,Hughes, V. J.,and Kennett, B. L. N.,1983
  Velocity Filtering of Seismic Reflection Data.
   First Break, vol. 1, No 3, pp. 9-24, March 1983.

Clarke, A. M.,Chambers, R. E.,Allonby, R. H.,and Magraw, D.,1961
  A marine geophysical survey of the undersea coalfields of
  Northumberland, Cumberland and Durham.
   The Min Engr., No. 15, pp. 197-215.

Davies, E. B.,and Mercado, E. J.,1968
  Multichannel Deconvolution filtering of field recorded
  seismic data.
   Geophysics vol. 33, pp. 711-722.

133

Davies, W., and Rees, W. J.,1944
British resources of steel moulding sands, Part 5. The Permian
Yellow Sands of Durham and Yorkshire.
J. Iron and Steel Inst., No. II for 1943, 104P-111P

Dix, C. H.,1955
Seismic velocities from surface measurements.
Geophysics vol. 20, pp. 68-86

Dobrin, M. B.,1976
Introduction to Geophysical Prospecting.

New York; McGraw - Hill, Inc.
Dunkin, J. W.,and Levin, F. K.,1973
Effects of normal moveout on the seismic pulse.
Geophysics vol. 38, pp. 635-642.

Embree, P.,Burg, J. P., and Backus, M. M.,1963
Wide-Band Velocity Filtering - The Pie-Slice Process.
Geophysics vol. 28, pp. 948-974.

Fail, M. P.,and Grau, G.,1963
Les filtres en eventail.
Geophys. Prosp. vol. 11, pp. 131-163.

Fuchs, K., 1968
The reflection of spherical waves from transition zones with
arbitrary depth dependent elastic moduli and density.
J. Phys. Earth, vol. 16, Special Issue, 27

Fuchs, K., 1970
On the determination of velocity depth distributions of
elastic waves from the dynamic characteristics of the
reflected wavefield.
Z. Geophys. vol 36, pp 531

Fuchs, K., and Muller, G., 1971
Computations of Synthetic Seismograms with the Reflectivity
Method and Comparison with Observations.
Geophys. J. R. astr. Soc., vol 23, pp. 417-433.

Griffiths, L. J.,Smolka, F. R., and Trembly, L. D.,1977
Adaptive deconvolution : a new technique for processing
time-varying seismic data.
Geophysics vol. 42, pp. 742-759.

Habibi-Ashrafi, F.,1978
Estimation of parameters in lossless layered media.
PhD. Dissertation, Univ. Southern California, Los Angeles,1978.

Hale, D.,and Claerbout, J. F.,1983
Butterworth dip filters.
Geophysics vol. 48, pp. 1033-1038.

Hodge, M. B.,1932
The Permian Yellow Sands of north-east England.
Proc. Univ. Durham Phil. Soc., 8, pp. 410-458.

Hughes, V. J.,1980
  Seismic Reflections from Coal Seams.
  PhD. thesis, University of Cambridge,1980.

Hughes, V. J.,and Kennett, B. L. N.,1983
  Seismic Reflections from Coal Seams.
  First Break vol. 1, pp. 9-18.

Jury, E. I.,1972
  Theory and application of the z-transform method.

  New York, John Wiley and Sons. Inc.
Kamal, C. J., and deFigueiredo, R. J. P.,1982
  Concepts and Techniques in Oil and Gas Exploration.

  Society of Exploration Geophysicists, Tulsa Oklahoma, 1982.
Kanasewich, E. R.,1981
  Time Sequence Analysis in Geophysics.

  The University of Alberta Press.
Kennett, B. L. N., 1979
  Theoretical Reflection Seismograms for Elastic Media.
  Geophys. Prosp. vol 27, pp. 301-321.

Kennett, B. L. N., 1983
  Seismic Wave Propagation in Stratified Media.

  Cambridge University Press
Kennett, B. L. N., 1984 (personal communication)
Koehler, F.,1964
  Deterministic deringing of seismic traces.
  Seismic Computing Corp., Internal Report.

Kunetz, G.,1964
  Generalisation des operateurs d'antiresonance a nombre quel-
  conque des reflecteurs.
  Geophys. Prosp. vol. 12, pp. 283-289.

Lailly, P., 1981
  The Inverse Problem in 1-D Reflection Seismics, in
  The Solution of the Inverse Problem in Geophysical

  Interpretation, edited by R. Cassinis, Plenum Press,

  New York.
Le Boulch, H.,1983
  Starjet - a new implosive marine source.
  First Break vol. 1, No 2, pp. 25-29, Feb. 1983.

Lines, L. R., and Treitel, S.,1983
  Digital filtering with the second moment norm.
  Geophysics vol. 48, pp. 505-514.

Longhurst, R. S., 1968,
  Geometrical and Physical Optics.

  Longmans, Green and CO LTD.
Loveridge, M. M.,1981

Residual Static Corrections
MSc. Dissertation, University of Durham, 1981.

Lu, C. H.,and Gupta, S. C.,1978
A multirate digital filtering approach to inter-
polation - application to common depth point stacking.
Geophysics vol. 43, pp. 877-885

Lucas, A. L.,1974
A High Resolution Marine Seismic Survey.
Geophys. Prosp. vol. 22, pp. 667-682.

Magraw, D.,Clarke, A. M.,and Smith, D. B.,1963.
The stratigraphy and structure of part of the south-east
Durham coalfield.
Proc. Yorks. geol. Soc. vol. 34, pp. 153-

Magraw, D.,1975
Permian beds of the offshore and adjacent coastal area of
Durham and south-eastern Northumberland.
Jl. geol. Soc. Lond. vol. 131, pp. 397-414.

Magraw, D.,1978
New boreholes into Permian beds off Northumberland and
Durham.
Proc. Yorks. geol. Soc. vol. 42, pp. 157-183.

May, B. T.,and Hron, F.,1978
Synthetic seismic sections of typical petroleum traps.
Geophysics vol. 43, pp. 1119-1147.

Mayne, W. H.,1962
Common reflection point horizontal data stacking techniques
Geophysics vol. 27, pp. 927-938.

McQuillin, R., Bacon, M., and Barclay, W., 1979
An Introduction to Seismic Interpretation.

Graham and Trotman, London, 1979.
Meyerhoff, J. H.,1966
Horizontal stacking and multichannel filtering applied to
common-depth point seismic data.
Geophys. Prosp. vol. 14, pp 441-454.

Mendel, J. M.,and Habibi-Ashrafi, F.,1980
A survey of approaches to solving inverse problems for
lossless layered media systems.
IEEE Transactions on Geoscience and Remote Sensing.

GE-18, pp. 320-330.
Mendel, J. M.,1984
Simultaneous Correction for Spherical Divergence and
Deconvolution without changing industrial practice.
Geophysics vol. 49, pp. 584-585.

Michon, D.,Wlodarczak, R.,and Merland, J.,1971
A new method of cancelling multiple reflections 'SOUSTON'.
Geophysics vol. 19, pp. 615-625.

136

Morley, L.,and Claerbout, J.,1983
  Predictive deconvolution in shot-receiver space
  Geophysics vol. 48, pp. 515-531.

Naess, O. E.,1979
  SuperStack : an iterative stacking algorithm
  Geophys. Prosp. vol. 27, pp. 16-28.

Naess, O. E.,and Bruland, L.,1981
  Velocity analysis using iterative stacking
  Geophys. Prosp. vol. 29, pp. 1-20.

Naess, O. E.,1982
  Single trace processing using Iterative CDP-stacking.
  Geophys. Prosp. vol. 30, pp.641-652.

Neidel, N. S.,1972
  Deterministic deconvolution operators, 3 point or 4 point?
  Geophysics vol. 47, pp.1039-1042.

Nunns, A. G.,1980
  Marine Geophysical Investigations in the Norwegian-Greenland sea
  between the latitudes of 62N and 74N.
  PhD thesis, University of Durham.

Peacock, K. L.,and Treitel, S.,1969
  Predictive deconvolution : theory and practice.
  Geophysics vol. 34, pp. 155-169.

Pflueger, J.,1972
  Spectra of water reverberations for primary and multiple
  reflections.
  Geophysics vol. 37, pp. 788-796.

Poulter, M. J.,1982
  The Design and Implementation of the Durham University
  Seismic Computing System.
  PhD. thesis, University of Durham.

Rietsch, E.,1980
  Estimation of the signal-to-noise ratio of seismic data
  with an application to stacking.
  Geophys. Prosp. vol. 28, pp. 531-550.

Robinson, E. A.,1957
  Predictive decomposition of time series with application
  to seismic exploration
  Geophysics vol. 32, pp. 418-484.

Robinson, E. A.,1967
  Multichannel Time Series Analysis with Digital Computer

  Programs.

  298pp, Holden-Day Incorporated, San Francisco.
Robinson, E. A.,and Treitel S.,1978
  The fine structure of the normal incidence synthetic

seismogram.
  Geophy. J. R. astr. Soc. vol. 53, pp. 289-309.

Robinson, E. A.,1979
  Predictive Deconvolution.
  in Developments in geophysical exploration methods,

  London Applied Science Publishers. pp. 77-106
Robinson, E. A.,1980
  Physical applications of stationary time-series

  London, Charles Griffin & Company Ltd.
Robinson, J. C.,1970
  Statistically optimal stacking of seismic data.
  Geophysics vol. 35, pp. 436-446.

Ruter, H.,and Schepers, R., 1978
  Investigation of the seismic response of cyclically
  layered carboniferous rock by means of synthetic seismograms
  Geophys. Prosp. vol. 26, pp. 26-47.

Ryu, V. J.,1982
  Decomposition (DECOM) approach applied to wave field analysis
  with seismic reflection records.
  Geophysics vol. 47, pp. 869-883.

Schneider, W. A.,Larner, K. L.,Burg, J. P.,and Backus, M. M.,1964
  A new data processing technique for the elimination of
  ghost arrivals on reflection seismograms.
  Geophysics vol. 29, pp. 783-805.

Schneider, W. A.,Prince, E. K. jr.,and Gibs, F. B.,1965
  A new data processing technique for multiple attenuation
  exploiting differential normal moveout.
  Geophysics vol. 30, pp. 348-362.

Schultz, P. S.,and Claerbout, J. K.,1978
  Velocity estimation and downward continuation by wavefront
  synthesis
  Geophysics vol. 42, pp. 939-949.

Sheriff, R. E.,1973
  Encyclopaedic Dictionary of Geophysics

  Society of Exploration Geophysics, Tulsa, Oklahoma.
Sheriff, R. E., 1975
  Factors Affecting Seismic Amplitudes
  Geophys. Prosp. vol. 23, pp. 125-138

Sheriff, R. E., and Geldart, L. P., 1982
  Exploration Seismology Volume 1
  History, theory and data acquisition
  Cambridge University Press.

Smith, D. B.,and Francis, E. A.,1967
  The geology of the country between Durham and West Hartlepool
  mem. geol. surv. U. K.

Smith, D. B.,1970
   Permian and Trias. in : Geology of Durham County
   (Hickling, G. (ed.)),
      Trans. nat. Hist. Soc. Northumb. 41, 66-91.

Smith, D. B.,1971
   The stratigraphy of the Upper Magnesian Limestone in Durham
   a revision based on the Seaham Borehole of the Institute of
   Geological Sciences.
      Rep. Inst. geol. Sci. 71/3, 1-12

Taner, M. T., 1980
   Long period sea-floor Multiples and their Suppression.
   Geophys. Prosp. vol. 28, pp. 30-48.

Taner, M. T.,and Koehler, F.,1969
   Velocity spectra - Digital computer derivation and
   application of velocity functions.
   Geophysics vol. 34, pp. 859-881.

Taner, M. T.,Cook, E. E.,and Neidel, N. S.,1970
   Limitations of the reflection seismic method : Lessons
   from computer simulations.
   Geophysics vol. 35, pp. 551-573.

Telford, W. M.,Geldart, L. P.,Sheriff, R. E.,and Keys, D. A.,1976
   Applied Geophysics.

   Cambridge University Press.
Treitel, S.,and Lines, L. R.,1982
   Linear inverse theory and deconvolution
   Geophysics vol.47, pp. 1153-1159.

Treitel, S.,Shanks, J. L.,and Frasier, C. W.,1967
   Some aspects of fan filtering
   Geophysics vol. 32, pp. 789-800.

Treitel, S.,1970
   Principles of digital multichannel filtering
   Geophysics vol. 35, pp. 785-811.

Trenchmann, C. T.,1925
   The Permian formation in Durham.
   Proc. Geol. Ass. Lond. 36,   135

Ulrych, T. J.,1971
   Application of homomorphic deconvolution to seismology.
   Geophysics vol. 36, pp. 650-660

Van Riel, W. J.,1965
   Synthetic seismograms applied to the seismic investigation
   of a coal basin.
   Geophys. Prosp. vol. 13, pp.105-121

Wadsworth, G. P.,Robinson, E. A.,Bryan, J. G.,and Hurley, P.
   M.,1953
   Detection of reflections on seismic records by linear
   operators.

Geophysics vol. 18, pp. 539-586.

Warren, R. D.,1981
  Signal procesing techniques applied to seismic refraction
  data.
  MSc. thesis - University of Durham.

White, R. E.,1973
  The estimation of signal spectra and related quantities
  by means of the multiple coherence function.
  Geophys. Prosp. vol. 21, pp. 660-703.

White, R. E.,1977
  The performance of optimum stacking filters in suppressing
  uncorrelated noise.
  Geophys. Prosp. vol. 25, pp. 166-178.

White, R. E.,1978
  Differential NMO filters
  BP Geophysical Symposium - Dec. 1978.
White, R. E.,1980
  Frequency-wavenumber Processing and attenuation of
  Long-Period multiples.
    Report no. TN472, Exploration and Production Department,
    Geophysical Division. The British Petroleum Company Limited.
Wiener, N.,1942
  The Interpolation, Extrapolation, and Smoothing of Stationary

  Time Series.

  John Wiley, New York.
Wiggins, R. A.,and Robinson, E. A.,1965
  Recursive solution to the multichannel filtering problem
    J. Geophys. Res. vol. 70, pp. 1885-1891.

Wiggins, R. A.,1966
  w-k filter design.
    Geophys. Prosp. vol. 14, pp.427-440.

Wood, L. C.,1982
  'Imaging the subsurface' in
    Concepts and Techniques in Oil and Gas Exploration;

    edited by Kamal C. Jain and deFigueiredo,
    SEG,1982, pp.45-90
Woolacott, D.,1912
  The stratigraphy and tectonics of the Permian of Durham
  (northern area).
    Proc. Univ. Durh. Phil. Soc. 4, 241.

Ziolkowski, A.,1979
  Seismic profiling for coal on land. pp. 271-306 in
  Developments in Geophysical Exploration Methods - 1,

  ed. by Fitch, A. A. Applied Science Publishers,
  Barking, England.
Ziolkowski, A.,1980
  Basic ideas behind the concept of deconvolution

and

Least-squares prediction of stationary linear processes.
Unpublished manuscripts.
Ziolkowski, A.,and Lerwill, W. E.,1979
A simple approach to high resolution seismic profiling
for coal.
Geophys. Prosp. vol. 27, pp. 360-393.

Ziolkowski, A., 1984
Deconvolution
IHRDC, Boston, USA.

Walker, C. D. T., 1980
Marine Seismic Exploration for Coal
in Seismic Techniques in offshore exploration.
London Geological Society Group Meeting.

APPENDIX A

Derivation of equation (15) of Chapter 2

The S/N ratio of the weighted stack (equation (11) of chapter 2) is

$$\gamma^{(M)} = S / N_0$$

where

$$N_0 = N \, E\left\{ \left(\sum_{i=1}^{M} (w_i a_i / C) n_{ij} \right)^2 \right\}$$

$$= \sum_{i=1}^{M} \sum_{k=1}^{M} (a_i a_k w_i w_k / C^2) N_i \, \delta_{ik}$$

$$= \sum_{i=1}^{M} (w_i/C)^2 N_i$$

and

$$\delta_{ik} = 0 \quad \text{if } i \neq k$$
$$= 1 \quad \text{if } i = K$$

is the Kronecker delta function. This gives

$$\gamma^{(M)} = S / \sum_{i=1}^{M} (w_i/C)^2 N_i \qquad \qquad \text{.. (A-1)}$$

which is to be maximized subject to the constraint that

$$\sum_{i=1}^{M} (w_i a_i / C) = 1 \qquad \qquad .. \ (A-2)$$

By the method of Lagrange Multipliers, the maximisation of the new function

$$\gamma' = \ (M) + \lambda (\sum_{i=1}^{M} (w_i a_i / C) - 1 \ ) \qquad .. \ (A-3)$$

with respect to the w_k, is equivalent to the constrained optimization of $\gamma^{(M)}$; λ is the Lagrange Multiplier. Hence

$$\gamma' = S/N_0 + \lambda (\sum_{i=1}^{M} (w_i a_i / C) - 1 \ ) \qquad .. \ (A-4)$$

and

$$(\partial \gamma' / \partial w_k) = 0 \qquad \text{for all } k=1,2,.. \quad M \qquad .. \ (A-5)$$

for γ' to be stationary.

$$(\partial \gamma' / \partial w_k) = -(S/N_0^2)(\partial N_0 / \partial w_k) + \sum_{i=1}^{M} (a_i / C) \delta_{ik}$$

and δ_{ik} has been defined above.

Since

$$(\partial N_0 / \partial w_k) = \sum_{i=1}^{M} (2w_i N_i / C^2) \delta_{ik}, \qquad .. \ (A-6)$$

it follows that

$$\sum_{i=1}^{M} (\lambda (a_i/C) - 2Sw_iN_i/N_0^2) \delta_{ik} = 0 \qquad \qquad .. \ (A-7)$$

for all k=1,2,....M . This is a system of M equations with M+1 unknowns from which

$$w_k = \lambda a_k N_0^2/(N_k 2SC) \qquad \qquad .. \ (A-8)$$

and the multiplier λ can be obtained from the constraint equation (A-2) as

$$\lambda = 1 \ / \ ((N_0^2/2SC^2)\sum_{k=1}^{M} a_k^2/N_k) \qquad \qquad .. \ (A-9)$$

and

$$w_k/C = (a_k^2 S/N_k).(1/a_k).(\sum_{k=1}^{M} a_k^2 S/N_k)^{-1}$$

and since

$$\gamma_k = (a_k^2 S/N_k),$$

the result becomes

$$w_k/C = \gamma_k/(a_k.R) \qquad \qquad .. \ (A-10)$$

where

$$R = \sum_{k=1}^{M} \gamma_k$$

Equations (A-10) give the required weights for equation (15), Chapter 2 if an optimum weighted stack is desired.

The optimum S/N ratio is given by

$$\gamma_{opt}^{(M)} = S \Big/ \sum_{k=1}^{M} (\gamma_k^2/a_k^2 R^2) N_k$$

$$= R \qquad\qquad .. \ (A-11)$$

as stated in equation (16) of chapter 2.

Equations for the Estimation of Signal Parameters.

Consider a normal-moveout corrected CMP gather and assume that there are at least three traces available which satisfy the assumptions given in section 2.3 . The signal has the same form but not necessarily the same amplitude.

Rietsch (1980) showed that the signal amplitudes can be estimated by a systematic exploitation of the cross-correlation of the traces as described by Robinson (1970). If each trace is represented by

$$\bar{s}_j = a_j \bar{s} + \bar{n}_j$$

then, to uniquely determine the amplitude factors a_j we assume that $\bar{s}$ has got a unit variance and then take the $M(M-1)/2$ different cross-correlations of the M traces in the gather as

$$\bar{s}_j \bar{s}_k = a_j a_k + \bar{s}(a_j \bar{n}_k + a_k \bar{n}_j) + \bar{n}_j \bar{n}_k \quad j < k$$

Since the signal and noise do not correlate, the equation simplifies to

$$\bar{s}_j \bar{s}_k = a_j a_k + \bar{n}_j \bar{n}_k \quad j < k$$

145

which can be solved by weighted least-squares techniques (Rietsch, 1980) to get

$$a_j = \alpha \left[\prod_{k \neq j} \bar{s}_j \bar{s}_k \right]^{(1/(M-2))}$$

where

$$\alpha = \left[\prod_{j=1}^{M} \prod_{k > j} \bar{s}_j \bar{s}_k \right]^{(-1/(M-1)(M-2))}$$

Having obtained the amplitude factors a_j, the original traces can be normalized so that the signal has the same amplitude on all of them, that is

$$\bar{s}_j = \bar{s} + \bar{n}_j \quad \text{for } j=1,2\ldots M \quad 3$$

for which the M(M-1) noise difference traces can be evaluated as

$$\bar{n}_{jk} = \bar{s}_j - \bar{s}_k$$

$$= \bar{n}_j - \bar{n}_k \qquad j < k$$

Their energy is approximately given by

$$n_{jk}^2 = n_j^2 - n_k^2 \qquad j < k$$

which is in a form that can be solved for the noise energy n_j^2 by the weighted least-squares techniques (Rietsch, 1980) to obtain

$$n_j^2 = (s_j^2 - 2\bar{s}_j\bar{s} + \beta) / (1 - 2w_j)$$

where

$$\beta = (\overline{s^2} - \overline{\sigma^2} + 2\bar{s}\bar{\sigma}) / (1 + U)$$

146

$$\tilde{s} = \sum_{k=1}^{M} w_k s_k$$

$$s^2 = \sum_{k=1}^{M} w_k s_k^2$$

$$\overline{\sigma} = \sum_{k=1}^{M} w_k \overline{s}_k \, / \, (1 - 2w_k)$$

$$\overline{\sigma^2} = \sum_{k=1}^{M} w_k s_k^2 \, / \, (1 - 2w_k)$$

$$U = \sum_{k=1}^{M} w_k \, / \, (1 - 2w_k)$$

and

$$w_k \simeq 1 \, / \, s_k^2 \neq 1/2 \ .$$

If $w_k = 1/2$ then the equations for β and n_j^2 are slightly modified.

APPENDIX B.

Pre-Deconvolution and Post-Deconvolution Amplitude Scaling.

The amplitudes of the seismic events that arrive at later times on a seismic trace are unduly low because of spreading losses and frequency dependent attenuation. This is often approximately compensated for by applying a time-ramp function to the data before processing is carried out. After such scaling, the late arrivals then contribute more to the autocorrelation function of the trace. The trace becomes more stationary.

If the seismic trace is represented by the time sequence x_t and an exponential scale factor $a^{\alpha t}$ is applied to it, then the resulting sequence is

$$y_t = a^{\alpha t} x_t \qquad \qquad .. \ (B-1)$$

The effect of the scaling can be expressed in terms of the ratio of the new amplitude to that of the old value at each time, i. e.

$$(y_t/x_t) = a^{\alpha t}$$

This ratio can be expressed in decibels by

$$\Omega \, dB = 20 \, \log_{10}(y_t/x_t) \qquad \qquad .. \ (B-2)$$

The trace amplitude changes during every second by a factor of

$$(\Omega/t) \ dB/sec = 20 \, \alpha \, \log_{10} a \qquad \qquad .. \ (B-3)$$

148

because of the application of the ramp.

The application of an exponential ramp of the form $e^{0.6t}$ to a seismic trace gives rise to an amplitude scaling of +5.2 dB/sec of the trace. The autocorrelogram function of the new trace is also an exponentially weighted version of that of the original trace.

APPENDIX C

COMPUTER PROGRAMS

This appendix gives a listing of the computer programs that were written during the course of this study for use on NUMAC (Northumbrian Universities Multiple Access Computer).

These programs have to be used together with a library FLOBYA of Time Sequence Analysis SUBROUTINES that was developed during this study. The library cannot be listed in this thesis but a summary of the routines that are available in it and their sources is outlined at the end of this appendix. The main programs, their listings and how they are run are given below. GPT9:MTHSIMLIB is the Array Processor maths FORTRAN simulator available on the departmental archives.

(1)

YIBEA1 is a time sequence analysis program used for pre-stack and/or post-stack signal analysis. The run command is

$RUN *FTNX SCARDS=YIBEA1 SPUNCH=YIB1.OBJ

$RUN YIB1.OBJ+FLOBYA+GPT9:MTHSIMLIB 5=DATAFILE 7=INPUT 8=OUTPUT

10=AUTOCORR 13=WAVELET

Unit 13 is supplied only if option 11 is requested (see subroutine INPUT of the listing). Here, LIN=7, LOUT=8, LAU=10 (See INPUT)

(2)

YIBEA2 is a stack program that was used for the study of various stacking algorithms in chapter 2. The run command is

$RUN *FTNX SCARDS=YIBEA2 SPUNCH=YIB2.OBJ

$RUN YIB2.OBJ+FLOBYA+GPT9:MTHSIMLIB 5=DATAFILE 7=INPUT 8=OUTPUT

150

(3)

YIBEA3 computes the complete Normal Incidence synthetic seismograms by the transfer matrix method as in chapters 3 and 5. It calls the routines MODEL, TRACE, and REFSER (Claerbout, 1976, pp. 160) The run command is

$RUN *FTNX SCARDS=YIBEA3

$RUN -LOAD+FLOBYA+GPT9:MTHSIMLIB+*GHOST 5=DATAFILE 15=-O 16=-AU

9=-PLOT

AIMS

The AIMS (Advanced Interpretive Modelling System, version 3, supplied by GeoQuest International Incorporated) program was used in this study for computing Normal Incidence traces (primaries only) and CMP gathers. The run command is

$RUN GPT9:AIMS.OBJ2+*PLOTSYS 5=DATAFILE 8=-A 10=-B 9=-P 12=-X 13=-Y

14=-Z 15=-R 16=-S 18=OUT 2=AIMSHED

This version (GPT9:AIMS.OBJ2) must be run if the AIMS time series data is desired in standard SEG'Y'. This data is written on the file OUT (unit 18). The header blocks AIMSHED must be supplied.

SYNSEI

The program SYNSEI (Fuchs and Muller, 1971, and Kennett, 1974) was used for generating complete synthetic seismograms with offset. It was altered to SYNSEIP and the run command is

$RUN *FTNX SCARDS=SYNSEIP

$RUN -LOAD+*GHOST 5=DATA 10=-A 12=-B 9=-PLOT 18=SYNTHETIC

15=-R 17=HEADERS

The program SYNSEIP includes the free surface effect and
writes the time series in a format for transfer to the
PDP11/34 computer system.

PROGRAMS USED ON THE PDP11/34

The programs that were used on the PDP11/34 computer were

DK1:SORT to translate data from standard SEG'Y' to DSEGY,

DK1:PROC for time sequence analysis,

DK1:STACK for stacking of CMP data,

DK1:VELAN suite for velocity analysis (semblance analysis),

DK1:VFILT for velocity filtering of CMP data,

DK1:WSTACK for weighted or iterative stacking of CMP data,

and the plotting software (see the documentation in the Seismic

Data Processing Laboratory for the details).

SUBROUTINES IN FLOBYA.

From Robinson (1967)
****

AUTOCR(X,N,M,AUT)
CROSS(LX,X,LY,Y,LG,G)
CROSST(N,X,M,Y,C)
DOT(L,X,Y,P)
DOTR(L,X,Y,ANS)
EUREKA(LR,R,G,F,A)
IMPULS(LX,X,K)
MINSN(LX,X,XMIN,INDEX)
NLOGN(N,LX,X,SIGN)
NORMAG(LX,X)
NORM1(LX,X)
REVERS(N,X)
SHAPE(LB,B,LD,D,LA,A,LC,C,ASE,SPACE)
SIDE(G,LA,A,C,R,AP)
ZERO(LX,X)

From Warren (1981)
****

BANBOX(LF,DT,FL,FH,FILT,W)

```
CONVOL(LB,B,LF,F,LC,CON)
CRS123(AUT,M,ICR1,ICR2,ICR3)
OPSPIK(LB,B,LF,F,LS,PI,ERRORS,INDEX,SP1,SP2,SP3,SP4,SP5)
PEFILT(LB,B,LF,F,LS,SP1,SP2,PEF,AUT,LPEF,PI)
PREDIC(JS,JE,D,LF,LS,PI,LPEF,FIL,KALPH)
SPIKER(LB,B,LA,A,LC,C,INDEX,ERRORS,SPACE)
```

Written during this study (documentation included in the routines)
****

```
ABSARG(L,X,R,ARG)
ADAPT(N,ANS,Y,L,LG,ALFA,K)
AGC    (from R. W. Hobbs)
AMPHS(M,B,LS,S,DELT,X1,X2,Y1,Y2)
ARABS(LX,X)
COMTRA(LA,A,B)
FRECON(LW,W,LZ,Z,LQ,Q)
MAX(L,X,VMAX)
MAXIM(X,ISTRT,ISTOP,RMAX,L)
MAXT(LX,X,M,XMAX)
MODEL(RC,RS) Modified from Johnson G. (personnal communication)
PAWPLT(M,B,DELT)
PERIOD(LX,X,B,BAV,M,FLAG)
PLTPHS(M,S,DELT,XP1,XP2,YP1,YP2)
POWER(LX,N,NN)
REFSER(R,C,M,N)        (Claerbout, 1976, pp. 160)
SIG(L,X,EN)
SPCTRA(LX,X,IFORM)
TRACE(A,T,N,K,S,SR) Modified from Johnson G. (personnal communication)
ZPAD(N1,N2,X)
```

```
C*******************************************************
C                    PROGRAM YIBEA1
C                    +++++++++++++
C
C
C
C          A PROGRAM TO CARRY OUT TIME-SEQUENCE PROCESSING OF
C                         SEISMIC DATA.
C          INPUT DATA FILES SHOULD GENERALLY BE IN STANDARD SEGY
C     FORMAT, BUT IT ACCEPTS INPUT THAT HAS NOT GOT STANDARD
C     SEGY HEADER BLOCKS IF 'INFLG' IS  NOT EQUAL TO ONE.
C     I/O OF SEISMIC TRACES IS HANDLED THROUGH UNFORMATTED
C     READ/WRITE STATEMENTS ONLY.
C          YIBEA1 ACCEPTS A SET OF 'NFILES' DATA FILES FROM LO-
C     GICAL UNIT 'LIN', PROCESSES EACH TRACE OF EACH FILE AC-
C     CORDING TO THE OPTIONS CHOSEN BY THE USER FROM A MENU
C     OF TWELVE, AND WRITES THE OUTPUT SEQUENTIALLY ON UNIT
C     'LOUT'. IF AUTOCORRELOGRAMS ARE REQUESTED, THEY ARE OUT-
C     PUTTED SEQUENTIALLY ON UNIT 'LAU'. IF THE DATA IS INPUT
C     IN STANDARD SEGY, THE OUTPUT IS ALSO IN STANDARD SEGY.
C     IF IT IS NOT, THE OUTPUT IS NOT AS WELL. THE AUTOCORREL-
C     OGRAM FILE HAS NO HEADER BLOCKS BUT EACH CORRELOGRAM HAS
C     A 240 BYTE HEADER THAT IS IDENTICAL TO THE TRACE HEADER
C     OF THE RECORD FROM WHICH IT IS COMPUTED.
C          THIS PROGRAM HAS THE FOLLOWING OPTIONS.
C          ─────────────────────────────────────────────
C     FLAG     OPTION NAME      NO. OF TIMES IT CAN BE CALLED.
C     ....     ...........      ...........................
C       1     POLARITY REVERSAL      NO RESTRICTION
C       2     TRACE NORMALISATION    NO RESTRICTION
C       3     RAMP(S)                2
C       4     TRACE MUTING           1
C       5     AUTOCORRELOGRAM        1
C       6     PREDICTION ERROR FILTER 1
C       7     BANDPASS FILTER (S)    2
C       8     AUTOMATIC GAIN CONTROL 1
C       9     BACKUS OPERATOR        1
C      10     FOUR-POINT OPERATOR    1
C      11     WAVELET SHAPING        1
C      12     ADAPTIVE DECONVOLUTION 1
C      13     EXIT                   1 (NORMALLY)
C
C          THE INPUT TO YIBEA1 IS FREE-FORMATTED (SEE THE
C     SUBROUTINE 'INPUT').
C          YIBEA1 REQUIRES THE FOLLOWING PACKAGES
C     1.   GPT9:MTHSIMLIB - AP SIMULATION PACKAGE.
C     2.   FLOBYA         - PERSONAL SUBROUTINE LIBRARY.
C
C          FILES UNITS NEEDED
C          ─────────────────────────────────
C          5      INPUT  TO MAIN PROGRAM
C        LIN      SEISMIC DATA (MAG. TAPE OR DISKFILE)
C       LOUT      PROCESSED OUTPUT (SEISMIC DATA)
C        LAU      AUTOCORRELOGRAM
C
C          RUNNING YIBEA1 ON MTS.
C          ─────────────────────────────
C
C          $RUN  *FTNX SCARDS=YIBEA1
```

```
C         $RUN -LOAD+FLOBYA+*GPT9:MTHSIMLIB 5=DATAFILE  LIN=INPUT
C                              LOUT=OUTPUT LAU=AUTOCORR 13=WAVELET
C
C             where LIN,LOUT and LAU are the appropriate
C             numbers that are entered on unit 5 .
C
C
C
C             BY   F. JIFON   (OCTOBER, 1983)
C**********************************************************************
C       MAIN PROGRAM
C**********************************************************************
C
      DIMENSION PNTER(2), LINOUT(2), ALFA(2), CONST(4), RAM(2048,2)
      DIMENSION FL(2), FH(2), LBEF(2), BEF(200,2), W(200,2)
      DIMENSION W1(50), WA(50), A(50)
C
C     COMMON BLOCKS FOR THE OPTIONS
C
      COMMON /UNITS/ LIN, LOUT, LAU
      COMMON /GEN/ NFILES, NCHANS, LSAMPS, JSAMP, KOPT(15), JTEST
      COMMON /ONETWO/ JTYPE
      COMMON /THREE/ PNTER, LINOUT, ALFA, CONST, RAM, JAZZ(2)
      COMMON /FOUR/ MUTE(24), TAP(100), NTAP
      COMMON /FIVE/ LAUT, JST, JND
      COMMON /SIX/ JSTART, JEND, LENFIL, LGAP, WHITE
      COMMON /SEVEN/ FL, FH, LBEF, BEF, W          -
      COMMON /EIGHT/ LHWIN
      COMMON /NINE/ C0, C1, J1, BAC(512)
      COMMON /TEN/ CO, CC1, CC2, JI1, JI2, FPF(512)
      COMMON /ELEVEN/ LW, W1, LWP, WA, LW1, LA, A, LC, C, SPACE(4096)
      COMMON /TWELVE/ NADAPT, LENG, LOG, AFA, KIN
C
C
      CALL INPUT
      JAZZ(1) = 0
      JAZZ(2) = 0
      CALL MAINPR
C
C     END  OF PROCESSING
C
      STOP
      END
C
C
C
      SUBROUTINE INPUT
C
C**********************************************************************
C     ALL PARAMETERS ARE READ IN FREE FORMAT.
C
C         DATAFILE STRUCTURE
C         _____
C
C
C     NFILES,NCHANS,LSAMPS,JSAMP
C         NFILES = number of files to be processed.
C         NCHANS = number of traces per file.
C         LSAMPS = number of samples per trace.
C         JSAMP  = sampling interval in milliseconds (integer).
```

OPTIONS (Write the number of the option followed (in the
*******   next line) by the data)

1   POLARITY REVERSAL
2   NORMALISATION
JTYPE = 0   normalisation to unit energy.
      = 1   normalisation to unit amplitude.
3   TRACE SCALING
PNTER,LINOUT,ALFA
      PNTER   TYPE OF SCALING
         1.   t
         2.   exp(t)
         3.   t**2
         4.   t*exp(t)
         5.   (t**2)*(exp(t))
    LINOUT = 1 scaling (insertion of a ramp)
           = 0 removal of a ramp.
    ALFA   = scaling factor for exponential ramps.
4   MUTING OF A TRACE
(MUTE(K),K=1,NCHAN)
NTAP
      MUTE(K) = number of samples to be muted from zero time.
      NTAP   = number of samples over which the mute is tapered
                with a cos**2 function . (NTAP . LT . MUTE(K))
5   AUTOCORRELOGRAM
LAUT,JST,JND
      LAUT = maximum lag (in samples) of the autocorrelogram.
      JST = start of trace window to be autocorrelated.
      JND = end of trace window to be autocorrelated.
6   PREDICTION ERROR FILTER
JSTART,JEND,LENFIL,LGAP,WHITE
      JSTART = start of design window (sample number JSTART)
        JEND = end of design window (sample number JEND)
      LENFIL = length of prediction filter in samples.
        LGAP = predictive gap (in samples).
       WHITE = prewhitening parameter (fraction of 1.)
               e. g. 0.0 - no prewhitening.
                     0.02 - 2% prewhitening.
7   BANDPASS FILTER
FL,FH,LBEF
      FL = low frequency cut-off.
      FH = high frequency cut-off.
    LBEF = number of samples of the equivalent time-domain
           operator. Hanning tapers are applied at both
           cut-off frequencies. LBEF IS ODD.
8   AUTOMATIC GAIN CONTROL (AGC)
LHWIN = half-length (in samples of the AGC gate.)
9   BACKUS OPERATOR
C0,C1,J1
           C0 = reflection coeff. of sea-surface.
           C1 = reflection coeff. of sea-bed.
           J1 = two-way time in water layer.
10   FOUR-POINT FILTER
C0,CC1,CC2,J1,J2
           C0 = reflection coeff. of sea-surface.
           CC1 = reflection coeff. of sea-bed.
           CC2 = reflection coeff. of deeper interface.

```
C             J1 = two-way time in water layer.
C             J2 = two-way time between sea-bed and deeper interface.
C        11     WAVELET SHAPER
C          (ALL THE DATA FOR THIS OPTION ARE READ FROM UNIT 13
C         #)
C                        %%%NOT UNIT 5%%%
C                        @@@@@@@@@@
C     LW,LWP,LW1,LA
C             LW = length of the input wavelet in no. of samples.
C             LWP = length of the desired wavelet in no. of samples.
C             LW1 = dummy variable
C             LA = length of the shaping filter in no. of samples.
C     (W1(J),J=1,LW)
C             W1 = input wavelet (F10.6 - unit 13)
C     (WA(J),J=1,LW1)
C             WA = desired wavelet (F10.6  - unit 13)
C        12         ADAPTIVE DECONVOLUTION (Griffiths et al., 1977)
C     NADAPT,LENG,LOG,AFA
C          NADAPT = window of the trace (starting from sample 1) to be
C                    adaptively filtered.
C           LENG = length of the adaptive operator in no. of samples.
C           LOG = lag (= predictive gap)
C           AFA = adaptive constant (.01 - 2.0)
C        13     EXIT (NO FURTHER PROCESSING OF THE TRACE)
C     LIN,LOUT,LAU
C             LIN = logical unit number of the input device.
C             LOUT = logical unit number of output device.
C             LAU = logical unit number for output device
C                   (autocorrelogram).
C     JTEST     CONVOLUTION FLAG
C               =1  convolutions by the method of Fast-Fourier
C                   transforms.
C               =0  time domain convolutions (slow)
C     INFLG     HEADER BLOCKS FLAG
C               =1  Standard SEGY header blocks
C               =0  No header blocks.
C***********************************************************************
C
      DIMENSION PNTER(2), LINOUT(2), ALFA(2), RAM(2048,2), CONST(4)
      DIMENSION FL(2), BEF(200,2), W(200,2), FH(2), LBEF(2)
      DIMENSION W1(50), WA(50), A(50)
C
      COMMON /UNITS/ LIN, LOUT, LAU
      COMMON /GEN/ NFILES, NCHANS, LSAMPS, JSAMP, KOPT(15), JTEST
      COMMON /ONETWO/ JTYPE
      COMMON /THREE/ PNTER, LINOUT, ALFA, CONST, RAM, JAZZ(2)
      COMMON /FOUR/ MUTE(24), TAP(100), NTAP
      COMMON /FIVE/ LAUT, JST, JND
      COMMON /SIX/ JSTART, JEND, LENFIL, LGAP, WHITE
      COMMON /SEVEN/ FL, FH, LBEF, BEF, W
      COMMON /EIGHT/ LHWIN
      COMMON /NINE/ C0, C1, J1, BAC(512)
      COMMON /TEN/ CO, CC1, CC2, JI1, JI2, FPF(512)
      COMMON /ELEVEN/ LW, W1, LWP, WA, LW1, LA, A, LC, C, SPACE(4096)
      COMMON /TWELVE/ NADAPT, LENG, LOG, AFA, KIN
C
C
      READ (5,*) NFILES, NCHANS, LSAMPS, JSAMP
```

```
      WRITE (6,*) NFILES, NCHANS, LSAMPS, JSAMP
C
      CONST(3) = JSAMP / 1000.0
      NUM = 0
      JR = 0
      JB = 0
   10 NUM = NUM + 1
C
      READ (5,*) NOM
      WRITE (6,*) NOM
      KOPT(NUM) = NOM
      GO TO (20, 30, 40, 50, 70, 80, 90, 100, 110, 120, 130, 150, 160),
     1NOM
C
   20 GO TO 10
C
   30 READ (5,*) JTYPE
      WRITE (6,*) JTYPE
      GO TO 10
C
   40 JR = JR + 1
      READ (5,*) PNTER(JR), LINOUT(JR), ALFA(JR)
      WRITE (6,*) JR, PNTER(JR), LINOUT(JR), ALFA(JR)
      GO TO 10
C
   50 READ (5,*) (MUTE(K),K=1,NCHANS)
      WRITE (6,*) (MUTE(K),K=1,NCHANS)
      READ (5,*) NTAP
      WRITE (6,*) NTAP
      PI = 4.0 * ATAN(1.0)
      DO 60 K = 1, NTAP
        ANG = (K - 1) * PI / (2.0*NTAP)
   60 TAP(K) = COS(ANG) * COS(ANG)
      GO TO 10
C
   70 READ (5,*) LAUT, JST, JND
      WRITE (6,*) LAUT, JST, JND
      GO TO 10
C
   80 READ (5,*) JSTART, JEND, LENFIL, LGAP, WHITE
      WRITE (6,*) JSTART, JEND, LENFIL, LGAP, WHITE
      WHITE = WHITE + 1.
      GO TO 10
C
   90 JB = JB + 1
      READ (5,*) FL(JB), FH(JB), LBEF(JB)
      WRITE (6,*) JB, FL(JB), FH(JB), LBEF(JB)
      CALL BANBOX(LBEF(JB), CONST(3), FL(JB), FH(JB), BEF(1,JB),
     1     W(1,JB))
      GO TO 10
C
  100 READ (5,*) LHWIN
      WRITE (6,*) LHWIN
      GO TO 10
C
  110 READ (5,*) C0, C1, J1
      WRITE (6,*) C0, C1, J1
      CALL IMPULS(512, BAC, 1)
```

158

```
      BAC(J1) = 2.0 * C1 * C0
      BAC(2*J1) = C1 * C0 * C0 * C1
      GO TO 10
 120  READ (5,*) CO, CC1, CC2, JI1, JI2
      WRITE (6,*) CO, CC1, CC2, JI1, JI2
      CALL IMPULS(512, FPF, 1)
      FPF(JI1) = CO * CC1
      FPF(JI2) = CC1 * CC2
      FPF(JI1 + JI2) = CO * CC2
      GO TO 10
C
 130  READ (13,*) LW, LWP, LW1, LA
      WRITE (6,*) LW, LWP, LW1, LA
      READ (13,140) (W1(J),J=1,LW)
      READ (13,140) (WA(L),L=1,LW1)
 140  FORMAT (8F10.6)
      GO TO 10
C
 150  READ (5,*) NADAPT, LENG, LOG, AFA
      WRITE (6,*) NADAPT, LENG, LOG, AFA
      GO TO 10
C
 160  CONTINUE
C
C     READ IN FILE UNIT NUMBERS
C
      READ (5,*) LIN, LOUT, LAU
C
C     CHOOSE BETWEEN FREQUENCY DOMAIN MULTIPLICATION
C     (JTEST.NE.0) AND TIME DOMAIN CONVOLUTIONS (JTEST=0)
C
      READ (5,*) JTEST
C
C     TRANSFER HEADER BLOCK INFORMATION IF REQUIRED
C
      READ (5,*) INFLG
      IF (INFLG .EQ. 1) CALL HEDA(LIN, LOUT)
C
      RETURN
      END
C
C
      SUBROUTINE MAINPR
C
C     MAIN SUBROUTINE OF YIBEA1.
C
      IMPLICIT INTEGER*2(I)
      DIMENSION PNTER(2), LINOUT(2), ALFA(2), RAM(2048,2), CONST(4)
      DIMENSION FL(2), FH(2), LBEF(2), BEF(200,2), W(200,2)
      DIMENSION AUT(2048), FF(512), P(512)
      DIMENSION CANS(4096), W1(50), WA(50), A(50)
      DIMENSION SEIS(2048), ANS(2560), TRACEA(2109)
C
C     COMMON BLOCKS FOR MAINPR
C
      COMMON /UNITS/ LIN, LOUT, LAU
      COMMON /GEN/ NFILES, NCHANS, LSAMPS, JSAMP, KOPT(15), JTEST
      COMMON /ONETWO/ JTYPE
```

159

```
      COMMON /THREE/ PNTER, LINOUT, ALFA, CONST, RAM, JAZZ(2)
      COMMON /FOUR/ MUTE(24), TAP(100), NTAP
      COMMON /FIVE/ LAUT, JST, JND
      COMMON /SIX/ JSTART, JEND, LENFIL, LGAP, WHITE
      COMMON /EIGHT/ LHWIN
      COMMON /SEVEN/ FL, FH, LBEF, BEF, W
      COMMON /NINE/ C0, C1, J1, BAC(512)
      COMMON /TEN/ CO, CC1, CC2, JI1, JI2, FPF(512)
      COMMON /ELEVEN/ LW, W1, LWP, WA, LW1, LA, A, LC, C, SPACE(4096)
      COMMON /TWELVE/ NADAPT, LENG, LOG, AFA, KIN
C
      EQUIVALENCE (TRACEA(61),SEIS(1)), (SEIS(1),AUT(1))
      DATA I0, I1, I2, ILONG /0, 1, 2, 8191/
      DATA IP, IWHITE /7500, 8191/
      DATA IA, IB, IC /0, 2048, 4096/
C
C     PROCESSING BEGINS . INITIALIZE AND CLEAR AP.
C
      CALL ZERO(2048, SEIS)
      CALL ZERO(2109, TRACEA)
      IDUM = 0
      CALL APINIT(IDUM, IDUM, IDUM)
      CALL APWAIT
      CALL APPUT(WHITE, IWHITE, I1, I2)
      CALL APWD
      CALL VCLR(I0, I1, ILONG)
      CALL APWR
C
C     SET UP CONSTANTS
C
      ONE = 1.0
      IPIN = LSAMPS
      IZ = 8192 - LSAMPS
      IS = LSAMPS - 1
C
C
      KING = 1
      NUN = 10
C
C     MAIN LOOP OVER NFILES
C
      DO 320 JFILES = 1, NFILES
        JINX = JFILES
C
C     LOOP OVER CHANNELS OF EACH FILE
C
        DO 280 JCHAN = 1, NCHANS
          JT = JCHAN
          JR = 0
          JB = 0
C
C     READ IN A TRACE
C
          ILEN = 4 * LSAMPS + 240
          CALL READ(TRACEA, ILEN, 0, LNUM, LIN, &340)
C
  10      CALL APWAIT
C
```

```
              CALL APPUT(SEIS, IA, IPIN, I2)
              CALL APWD

C
       20     NUM = 0
              NUM = NUM + 1
              JINDEX = KOPT(NUM)

C
              GO TO (30, 40, 70, 100, 110, 140, 160, 180, 190, 200, 210,
        1     260, 270), JINDEX

C
C          POLARITY REVERSAL
C
       30     CALL VNEG(I0, I1, I0, I1, IPIN)
              GO TO 20

C
C          TRACE NORMALISATION - UNIT ENERGY (JTYPE=0) OR UNIT AMPLITUDE
C  (JTYPE.NE.0)
C
       40     CONTINUE
              IF (JTYPE .EQ. 0) GO TO 50
              CALL MAXMGV(I0, I1, ILONG, IPIN)
              GO TO 60
       50     CALL SVESQ(I0, I1, ILONG, IPIN)
              CALL VSQRT(ILONG, I1, ILONG, I1, I1)
       60     CALL VDIV(ILONG, I0, I0, I1, I0, I1, IPIN)
              CALL APWR
              GO TO 20

C
C          PROCESS RAMP
C
       70     JR = JR + 1
              JAP = LINOUT(JR)
              CALL RAMP(JR)
              CALL APPUT(RAM(1,JR), IB, IB, I2)
              CALL APWD
              IF (JAP .EQ. 1) GO TO 80
              CALL VDIV(IB, I1, I0, I1, I0, I1, IPIN)
              GO TO 90
       80     CALL VMUL(IB, I1, I0, I1, I0, I1, IPIN)
       90     CALL VCLR(IB, I1, IB)
              GO TO 20

C
C          MUTE THE TRACE (COS**2 TAPERED OVER JCHAN SAMPLES)
C
      100     CALL MU(JCHAN)
              GO TO 20

C
C          AUTOCORRELATION
C
      110     ILAUT = LAUT
              ILENG = JND - JST + 1
              IBAUT = JST
              IB2 = 1024
              IB1 = 7167
              CALL VCLR(IB1, I1, IB2)
              CALL ACORT(IBAUT, IB1, ILAUT, ILENG)
              CALL ZERO(2048, SEIS)
              CALL APGET(AUT, IB1, ILAUT, I2)
```

```
          CALL APWD
C
C   CHECK THE AUTOCORRELOGRAM FUNCTION.
C
          CALL MAXIM(AUT, 1, LAUT, AUTMAX, LAM)
          DO 120 LET = 1, LAUT
            AUT(LET) = AUT(LET) / AUTMAX
120       CONTINUE
          IF (LAM .NE. 1) WRITE (6,130) LAM
130       FORMAT (10X, '***THE MAXIMUM VALUE OF THE AUTOCORRELATION
     1    FUNCTION', /, 10X,
     2
     3'***IS NOT AT ZERO LAG BUT AT A                 LAG OF', I5,
     4         '*JSAMP MSECS.', //)
C
          ILEN = (LAUT + 60) * 4
          CALL WRITE(TRACEA, ILEN, 0, LNUM, LAU)
          CALL VCLR(IB1, I1, IB2)
          GO TO 20
C
C   PREDICTION ERROR DECONVOLUTION
C
140       IBEG = JSTART
          IFIL = LENFIL
          ILA = LGAP + LENFIL + 5
          IR = 4096 + LGAP
          ILIN = JEND - JSTART + 1
          CALL ACORT(IBEG, IC, ILA, ILIN)
          CALL APWR
          CALL VMUL(IC, I1, IWHITE, I1, IC, I1, I1)
          CALL WIENER(IFIL, IC, IR, IB, IP, I1)
          CALL APWR
          CALL IMPULS(512, FF, 1)
C
C   GET PREDICTION FILTER
C
          CALL APGET(P, IB, IFIL, I2)
          CALL APWD
C
C   FORM PREDICTION ERROR FILTER
C
          DO 150 J = 1, LENFIL
150       FF(LGAP + J) = -P(J)
C
C   APPLY THE OPERATOR
C
          CALL APGET(SEIS, IA, IPIN, I2)
          CALL APWD
          CALL APPLY(JTEST, 512, FF, LSAMPS, SEIS, LANS, CANS)

          CALL APWR
          CALL APPUT(CANS, IA, IPIN, I2)
          CALL APWD
          CALL VCLR(IB, I1, IB)

          GO TO 20
C
C   BANDPASS
```

162

```
C
160      JB = JB + 1
         CALL APGET(SEIS, IA, IPIN, I2)
         CALL APWD
C
         CALL APPLY(JTEST, LBEF(JB), BEF(1,JB), 2048, SEIS, LANS, ANS)
C
         LH2 = LBEF(JB) / 2
         DO 170 J = 1, LSAMPS
170      SEIS(J) = ANS(J + LH2)
         CALL APWR
         CALL APPUT(SEIS, IA, IPIN, I2)
         CALL APWD
         GO TO 20
C
C    AUTOMATIC GAIN CONTROL
C
180      CALL AGC
         GO TO 20
C
C    BACKUS FILTER
C
190      CALL APGET(SEIS, IA, IPIN, I2)
         CALL APWD
C
         CALL APPLY(JTEST, 512, BAC, 2048, SEIS, LANS, CANS)
C
         CALL APWR
         CALL APPUT(CANS, IA, IPIN, I2)
         CALL APWD
         GO TO 20
C
C    FOUR POINT OPERATOR
C
200      CALL APGET(SEIS, IA, IPIN, I2)
         CALL APWD
C
         CALL APPLY(JTEST, 512, FPF, 2048, SEIS, LANS, CANS)
C
         CALL APWR
         CALL APPUT(CANS, IA, IPIN, I2)
         CALL APWD
         GO TO 20
C
C    WAVELET SHAPING FILTER
C
210      CALL APGET(SEIS, IA, IPIN, I2)
         CALL APWD
         IF (JFILES .GE. 2 .OR. JCHAN .GE. 2) GO TO 250
         CALL SHAPE(LW1, WA, LW, W1, LA, A, LC, C, ASE, SPACE)
         WRITE (6,220) LA
         WRITE (6,230) (A(K),K=1,LA)
         WRITE (6,240) ASE
220      FORMAT (10X, '***LENGTH OF SHAPING FILTER IS', I6, /, 10X,
     1           '***THE FILTER COEFFICIENTS ARE', /)
230      FORMAT (5(1X,F10.2,1X))
240      FORMAT (//, 10X, '***THE AVERAGE SQUARED ERROR IS', /, 10X,
     1           '***EQUAL TO', F15.6, ' UNITS', /)
```

163

```
250       CALL APPLY(JTEST, IA, A, 2048, SEIS, IANS, CANS)
          CALL APWR
          CALL APPUT(CANS, IA, IPIN, I2)
          CALL APWD
          GO TO 20

C
C     ADAPTIVE DECONVOLUTION.
C
260       CALL APGET(SEIS, IA, IPIN, I2)
          CALL APWD
          KIN = JFILES
          CALL ZERO(4096, CANS)
          CALL ADAPT(NADAPT, SEIS, CANS, LENG, LOG, AFA, KIN)
          CALL APWAIT
          CALL APPUT(CANS, IA, IPIN, I2)
          CALL APWD
          GO TO 20

C
C     EXIT
C
270       CONTINUE

C
C     RETRIEVE THE PROCESSED TRACE AND WRITE IT OUT
C
          CALL APGET(SEIS, IO, IPIN, I2)
          CALL APWD
          ILEN = 4 * LSAMPS + 240
          CALL WRITE(TRACEA, ILEN, 0, LNUM, LOUT, &340)

C
C     GET THE NEXT TRACE.
C
280       CONTINUE

          IF (JINX .EQ. KING*NUN) GO TO 290
          GO TO 310
290       WRITE (6,300) JINX
300       FORMAT (10X, '***', I6, '  FILES HAVE BEEN PROCESSED')
          KING = KING + 1
310       CONTINUE

C
C     START PROCESSING THE NEXT FILE.
C
320   CONTINUE
      JFILES = JFILES - 1
      WRITE (6,330) JFILES
330   FORMAT (/, 10X, '***NORMAL END OF EXECUTION', /, /, 10X, '***',
     1       I5, ' FILES WERE PROCESSED', //)
      GO TO 360

C
340   WRITE (6,350)
350   FORMAT (/, 10X, '***EOT ENCOUNTER OR I/O ERROR - STOPS EXECUTION',
     1       //)

C
360   CONTINUE

C
      RETURN
      END
C
```

```fortran
C
C
C     SUBROUTINE MU(JCHAN)
C
C     MUTES THE JCHAN'TH CHANNEL OVER MUTE(JCHAN) SAMPLES
C        USING AN NTAP COS**2 TAPER
C
      IMPLICIT INTEGER*2(I)
      DIMENSION DUM(1024)
C
      COMMON /FOUR/ MUTE(24), TAP(100), NTAP
      DATA IA /0/
C
      IMUTE = MUTE(JCHAN)
      CALL APGET(DUM, IA, IMUTE, I2)
      CALL APWD
      JJ = MUTE(JCHAN) - NTAP
      CALL ZERO(JJ, DUM)
      DO 10 K = 1, NTAP
10    DUM(JJ + K) = DUM(JJ + K) * TAP(NTAP - K + 1)
      CALL APPUT(DUM, IA, IMUTE, I2)
      CALL APWD
      RETURN
      END
C
C
C
      SUBROUTINE RAMP(JUG)
C
C     RAMP ROUTINE
C     THE USER CHOOSES ONE OF FIVE FUNCTIONS (SEE TEXT)
C
      IMPLICIT INTEGER*2(I)
      DIMENSION PNTER(2), LINOUT(2), ALFA(2), CONST(4), A(2048,2)
C
      COMMON /GEN/ JAG(3), JSAMP, KOPT(15), JTEST
      COMMON /THREE/ PNTER, LINOUT, ALFA, CONST, A, JAZZ(2)
C
      CONST(1) = ALFA(JUG)
      CONST(2) = 0.000
      CONST(3) = JSAMP / 1000.0
      CONST(4) = 1.
      JUMP = PNTER(JUG)
      IF (JAZZ(JUG) .EQ. 1) RETURN
      T = CONST(2)
      DO 70 J = 1, 2048
         GO TO (10, 20, 30, 40, 50), JUMP
10       A(J,JUG) = T
         GO TO 60
20       A(J,JUG) = EXP(CONST(1)*T)
         GO TO 60
30       A(J,JUG) = T * T
         GO TO 60
40       A(J,JUG) = T * EXP(CONST(1)*T)
         GO TO 60
50       A(J,JUG) = T * T * EXP(CONST(1)*T)
60       IF (A(J,JUG) .EQ. 0.0) A(J,JUG) = CONST(4)
         T = T + CONST(3)
70    CONTINUE
      JAZZ(JUG) = JAZZ(JUG) + 1
```

```
C

      RETURN
      END


C
C
C

      SUBROUTINE HEDA(NIN, NOUT)

C
C     HEADER BLOCK TRANSFERS
C

      IMPLICIT INTEGER*2(I)
      DIMENSION TPHEDA(800)
      INTEGER TPHEDB(100)

C
C     READ THE EBCDIC HEADER
C

      ILEN = 3200
      CALL READ(TPHEDA, ILEN, 0, LNUM, NIN)

C
C     READ BINARY HEADER
C

      ILEN = 400
      CALL READ(TPHEDB, ILEN, 0, LNUM, NIN)

C
C     WRITE EBCDIC HEADER
C

      ILEN = 3200
      CALL WRITE(TPHEDA, ILEN, 0, LNUM, NOUT)

C
C     WRITE BINARY HEADER
C

      ILEN = 400
      CALL WRITE(TPHEDB, ILEN, 0, LNUM, NOUT)

C
      RETURN
      END


C
C

      SUBROUTINE APPLY(JTEST, LZ, Z, LW, W, LQ, Q)

C
C     PROCESSING FILTER APPLICATION
C

      DIMENSION Z(2048), W(2048), Q(2048)

C
      IF (JTEST .EQ. 0) GO TO 10
      CALL FRECON(LZ, Z, LW, W, LQ, Q)
      RETURN

C
   10 CALL CONVOL(LZ, Z, LW, W, LQ, Q)

C
      RETURN
      END
```

```
C****************************************************************
C                    PROGRAM YIBEA2
C                    ------------
C
C      YIBEA2 IS A STACK PROGRAM USED FOR THE STUDY OF VARIOUS
C   STACKING ALGORITHMS  (CHAPTER 2). THE FOLLOWING STACKS CAN
C   BE CARRIED OUT ACCORDING TO THE VALUE CHOSEN FOR THE PARA-
C   METER 'STACKO':
C           STACKO                 STACK TYPE
C           ------                 ----------
C
C             1          STRAIGHT STACK (NORMALIZED BY 1/NCHAN(t)
C                            (MAYNE, 1962).
C             2          ITERATIVE (SUPER) STACK (NAESS,1979).
C             3          WEIGHTED STACK (ROBINSON,1970,NUNNS,1980).
C             4          WEIGHTED ITERATIVE STACK.
C             5          SLANT (CONSTANT RAY-PARAMETER) STACK
C                            (SMITH,1980).
C
C      YIBEA2 READS AND WRITES SEISMIC TRACES BY UNFORMATTED
C   READ/WRITE STATEMENTS. THE I/O DATA MAY BE FROM/ONTO
C   TAPE OR DISK. THE DATA MUST BE IN STD. SEGY FORMAT BUT
C   YIBEA2 WILL ACCEPT SEGY DATA WITH OR WITHOUT THE EBCDIC
C   AND BINARY HEADER BLOCKS ACCORDING TO THE VALUE OF 'INF-
C   LAG' THAT IS SUPPLIED.
C      THE DATA FILE HAS TO BE REORGANIZED FOR EACH NEW TAPE
C   BEING MOUNTED TO BE PROCESSED.
C
C                A VERSION BY F. JIFON (FEB. 1984)
C
C****************************************************************
C
C
C                    MAIN PROG
C                    ---------
C
C
      INTEGER*2 ILEN
      INTEGER STACKO
      DIMENSION TOSQ(2048), VINSQ(2048), XSQ(24)
      DIMENSION GATHER(2048,24)
C
C   COMMON BLOCKS
C
      COMMON /LAYER/ TOLYR(99), VLYR(99)
      COMMON /IN/ NFILES, NCHAN, L, NSTART, NLYR, M, FSAMP
      COMMON /PUT/ JNTSW, NVEL, MUT, JINDEN, MUTE(24), XSTART, XSTEP
      COMMON /VALUES/ L2INT, TOSQ, XSQ, VINSQ, STACKO, ITERAT, ITY, FAC,
     1    P
      COMMON /OPT/ KSTART, KSTOP, KST, KEN, NFLAG
C
C****************************************************************
C
C
C                    DATA INPUT  (FREE-FORMAT)
C                    -------------------------
C
C
C      NFILES,NCHAN,L,NSTART,NLYR,M
C               NFILES = number of files to be stacked.
C               NCHAN  = number of traces per record.
C                   L  = number of samples per trace.
C               NSTART = delay (in samples) to be applied before NMO.
C                 NLYR = number of points (layers) in each
```

```
C                           time-velocity function.
C                     M = interpolation level.
C     JNTSW,NVEL,MUT,JINDEN
C               JNTSW   = 1 for lateral interpolation of velocity
C                         functions.
C                       = 0 for no lateral interpolation.
C                 NVEL  = number of velocity functions.
C                 MUT   = 1 if muting is to be carried out.
C                       = -1 for no muting.
C
C
C     IF(MUT.EQ.1) (MUTE(K),K=1,NCHAN)
C               MUTE(K) = number of samples to be muted off
C                         trace number K of any file being stacked.
C     XSTART,XSTEP,FSAMP,INFLAG
C               XSTART  = near-trace offset.
C               XSTEP   = offset increment.
C               FSAMP   = sampling frequency in hertz.
C               INFLAG  = 1 for STD. SEGY header blocks on the input
C                         device (logical unit - 7) which are read
C                         and then written at the beginning of the
C                         output device (logical unit - 8) .
C     STACKO
C               STACKO  = stack type (see above)
C     IF(STACKO=2 OR STACKO=4) ITERAT,ITY,FAC
C               ITERAT  = number of iterations for an iterative stack.
C                 ITY   = -1  if normalisation is performed with the
C                             number of positive and negative amplitudes
C                             at the given time-point respectively.
C                       = +1  if normalisation is performed with a
C                             fraction FAC times the fold of cover at
C                             given  time-point.
C                 FAC   = fraction of the fold of cover (at a given
C                         time-point) to be used for the normalisation
C                         in the iterative algorithm.
C     IF(STACKO=3 OR STACKO=4) KSTART,KSTOP,KST,KEN,NLFAG
C               KSTART  = beginning of the window to be used for
C                         estimating the weights for a weighted stack.
C               KSTOP   = end of the window.
C                 KST   = beginning of the window to which the
C                         estimated weights are applied.
C                 KEN   = end of the above window.
C               NFLAG   = 0  for an optimally weighted stack.
C                       = 1  for a constant energy stack.
C                       = 2  for a diversity stack.
C     IF(STACKO=5) P
C                 P = ray-parameter (p=sin(i)/v) (See Shultz et al.,1978)
C      INSERT NVEL time(in seconds)-velocity(in meters/sec) functions
C               each preceeded by the CMP number of its location
C               and the number of layers (NLYR) for that function.
C               e.g. if NVEL=2 and NLYR=2 , insert
C                    135,2
C                    .070,1500.          first velocity function.
C                    .156,2800.
C                    235,2           )
C                    .060,1450.      ) second velocity function.
C                    .200,3000.      )
C                         where the CMP numbers for the location
C
```

168

```
C          of the velocity functions are respectively
C          135 and 235 (in increasing order).
C
C
C    ***************************************************************
C
C
      READ (5,*) NFILES, NCHAN, L, NSTART, NLYR, M
      READ (5,*) JNTSW, NVEL, MUT, JINDEN
      IF (MUT .EQ. 1) READ (5,*) (MUTE(K),K=1,NCHAN)
      READ (5,*) XSTART, XSTEP, FSAMP, INFLAG
      READ (5,*) STACKO
      IF (STACKO .EQ. 2 .OR. STACKO .EQ. 4) READ (5,*) ITERAT, ITY, FAC
      IF (STACKO .EQ. 3 .OR. STACKO .EQ. 4) READ (5,*) KSTART, KSTOP,
     1     KST, KEN, NFLAG
      IF (STACKO .EQ. 5) READ (5,*) P
C
C    INSERT THE VELOCITY FUNCTIONS IN ORDER OF INCREASING  CMP NUMBER
C    AFTER THE LAST LINE ABOVE.
C
C
C    ***************************************************************
C
C
C
C    GET THE NEXT POWER OF 2 THAT IS GREATER THAN L.
C
      L2INT = 2
      DO 10 K = 1, 1000
         IF (L2INT .GE. L) GO TO 20
         L2INT = 2 * L2INT
   10 CONTINUE
C
C    SET UP X**2 OR X
C
   20 X = XSTART
      DO 30 JCHAN = 1, NCHAN
         XSQ(JCHAN) = X ** 2
         IF (STACKO .EQ. 5) XSQ(JCHAN) = X
         X = X + XSTEP
   30 CONTINUE
C
      TSAMP = 1.0 / FSAMP
      T0 = NSTART * TSAMP
C
C    SET UP T0**2   (OR T0)
C
      DO 40 J = 1, L
         T0SQ(J) = T0 ** 2
         IF (STACKO .EQ. 5) T0SQ(J) = T0
         T0 = T0 + TSAMP
   40 CONTINUE
C
      L21NT = L2INT
      CALL SETAP(L21NT, M)
C
C    TRANSFER HEADER BLOCKS
C
      IF (INFLAG .EQ. 1) CALL HEDA(7, 8)
C
      L1 = L
```

169

```fortran
      NN = NCHAN
      CALL MAINPR(L1, NN, GATHER)
C
C     END OF PROGRAM.  BYE!
C
      STOP
      END



C
C
C
      SUBROUTINE SETAP(L2INT, M)
C
C     THIS ROUTINE SETS UP A COMPLEX EXPONENTIAL ARRAY IN THE AP
C     AT THE SPECIFIED LOCATION AND STORES A 1. AT 6144
C
      IMPLICIT INTEGER*2(I,K)
      COMMON /CCONST/ KIM, K0, K1, K2, K3, K4, K5, K6, K7, K8, K9, K10,
     1        K11, IA, IB, IC, ID, ITOP
C
C     INITIALIZE THE AP
C
      IDUM = 0
      CALL APINIT(IDUM, IDUM, IDUM)
      CALL APWR
C
      FIRST = 1.0
      ID1 = ID + K1
      ID2 = ID + K2
      IL2I21 = L2INT / 2 - 1
      Z = L2INT * M
      CONST = 1.0 / Z
      TWOPI = 8.0 * ATAN(1.0)
      CONST = CONST * TWOPI
C
      CALL APPUT(CONST, K0, K1, K2)
      CALL APWD
C
      CALL VRAMP(K0, K0, IB, K1, IL2I21)
      CALL APWR
      CALL VCOS(IB, K1, ID1, K2, IL2I21)
      CALL APWR
      CALL VSIN(IB, K1, ID2, K2, IL2I21)
      CALL APWR
      CALL VCLR(ID, K1, K1)
      CALL APWR
C
C     STORE 1. AT ID
C
      CALL APPUT(FIRST, ID, K1, K2)
      CALL APWD
C
      RETURN
      END
C
C
C
      BLOCK DATA
C
```

```
C      INITIALIZE ALL THE I*2 VARIABLES TO BE USED FOR
C      INDEXING IN AP
C
       IMPLICIT INTEGER*2(I - N)
       COMMON /CCONST/ KIM, K0, K1, K2, K3, K4, K5, K6, K7, K8, K9, K10,
      1        K11, IA, IB, IC, ID, ITOP
       DATA KIM, K0, K1, K2, K3, K4, K5, K6, K7, K8, K9, K10, K11, IA,
      1      IB, IC, ID, ITOP /-1, 0, 1, 2, 3, 4, 5, 6, 7, 8, 9, 10, 11,
      2      0, 2048, 4096, 6144, 8191/
C
       END
C
C
C
       SUBROUTINE MAINPR(L1, NN, GATHER)
C
C      MAIN SUBROUTINE  OF YIBEA2.
C
C
       IMPLICIT INTEGER*2(I,K)
       INTEGER*2 MSTOR, MCHAN, IONS
       INTEGER INDEX, ITERAT, STACKO, IND, TRH(60)
C
       DIMENSION GATHER(L1,NN), CHAN(2048), SEISM(32767)
       DIMENSION MSTOR(2048), MCHAN(2048), INDEX(2048), IONS(2048)
       DIMENSION TO2LYR(2048), V2LYR(99), TOINT(99), VELINT(99)
       DIMENSION TOSQ(2048), VINSQ(2048), XSQ(24)
       DIMENSION CONST(11), DUM(11), W(48)
       DIMENSION TRACEA(2108), SIG(2108), R(2048), STACK(2048)
C
C      COMMON BLOCKS
C
       COMMON /CCONST/ KIM, K0, K1, K2, K3, K4, K5, K6, K7, K8, K9, K10,
      1        K11, IA, IB, IC, ID, ITOP
       COMMON /IN/ NFILES, NCHAN, L, NSTART, NLYR, M, FSAMP
       COMMON /PUT/ JNTSW, NVEL, MUT, JINDEN, MUTE(24), XSTART, XSTEP
       COMMON /VALUES/ L2INT, TOSQ, XSQ, VINSQ, STACKO, ITERAT, MY, FAC,
      1        P
       COMMON /LAYER/ TOLYR(99), VLYR(99)
C
C      SHARED STORES
C
       EQUIVALENCE (TRACEA(61),SEISM(1)), (STACK(1),R(1))
       EQUIVALENCE (SIG(61),STACK(1)), (SIG(1),TRH(1))
C
C      CLEAR THE WORKING ARRAY SEISM
C
       CALL ZERO(32767, SEISM)
C
C      SET UP REQUIRED ADDRESSES AND CONSTANTS
C
       IC2 = IC + K2
       IC1 = IC + K1
       ID1 = ID + K1
       L1 = L + 1
       IL2I21 = (L2INT/2) - 1
       IL = L
       IL2INT = L2INT
       CONST(2) = M * FSAMP
```

```
        CONST(3)  =  0.5
        CONST(4)  =  -M * NSTART
        CONST(5)  =  0.0
        CONST(6)  =  L * M
        CONST(7)  =  L + 1
        CONST(8)  =  1.0
        CONST(9)  =  1.0 / M
        CONST(10) =  (L + 1) * M - 1
C
C       IGNORE VELOCITY INFORMATION IF STACKO IS 5
C
        IF (STACKO .EQ. 5) GO TO 20
C
        JVEL = 1
C
C               A N2LYR-POINT VELOCITY FUNCTION FOR CMP N2VAN
C
        READ (5,*) N2VAN, N2LYR
        READ (5,*)  (TO2LYR(J),V2LYR(J),J=1,N2LYR)
C
C       STORE THE VALUES JUST READ IN.
C
        NLYR = N2LYR
        NVAN = N2VAN
        DO 10 J = 1, NLYR
          TOLYR(J)  = TO2LYR(J)
          VLYR(J)   = V2LYR(J)
          TOINT(J)  = 0.0
          VELINT(J) = 0.0
   10 CONTINUE
C
   20 CONTINUE
C
C       MAIN LOOP OVER THE FILES TO BE STACKED
C
        DO 350 JFILES = 1, NFILES
C
          JSUM = 0
          JDIFF = 0
          JFIL = JFILES
C
C SET SEISM(L+1)=0.0 TO COPE WITH OVERFLOW IN TIME AND CLEAR AP
C
          SEISM(L1) = 0.0
          CALL VCLR(IA, K1, IL)
          CALL APWR
C
C         STORE ZEROS IN THE VECTOR MCHAN
C
          CALL APGET(MCHAN, K0, IL, K1)
          CALL APWD
C
C         ITERATE THROUGH CHANNELS
C
          DO 240 JCHAN = 1, NCHAN
C
            JTR = JCHAN
C
```

172

```
C       READ AN L*4 BYTE TRACE
C
        ILEN = 4 * L + 240
        CALL READ(TRACEA, ILEN, 0, LNUM, 7, &360)
C
C       TRANSFER TRACE HEADERS
C
        DO 30 J = 1, 60
30      SIG(J) = TRACEA(J)
        JCDPNO = TRH(6)
C
C       IF SLANT STACK IS DESIRED, IGNORE ALL ABOUT VELOCITY
C       INTERPOLATION.
C
        IF (STACKO .EQ. 5) GO TO 110
C
C       NOW CHECK THE CHANNEL NUMBER AND DO NOTHING IF IT IS .GE. 2
C
        IF (JCHAN .GE. 2) GO TO 110
C
C       CHECK IF CURRENT CMP NO IS .LT. N2VAN. IF YES, DO A LATERAL
C       INTERPOLATION OF THE VELOCITY FUNCTION.
C
        IF (JCDPNO .LT. N2VAN) GO TO 70
40      NLYR = N2LYR
        NVAN = N2VAN
        DO 50 J = 1, NLYR
          TOLYR(J) = TO2LYR(J)
50      VLYR(J) = V2LYR(J)
        IF (JVEL .EQ. NVEL) GO TO 100
        JVEL = JVEL + 1
C
C       READ THE NEXT VELOCITY FUNCTION
C
        READ (5,*) N2VAN, N2LYR
        READ (5,*) (TO2LYR(J),V2LYR(J),J=1,N2LYR)
C
        IF (JCDPNO .GE. N2VAN) GO TO 40
C
C       LATERAL INTERPOLATION OF STACKING VELOCITY.
C
        IF (JNTSW .EQ. 0) GO TO 100
        JINT = N2VAN - NVAN
        IF (JINT .LE. 1) GO TO 100
        RINT = FLOAT(JINT)
        DO 60 J = 1, NLYR
          TOINT(J) = (TO2LYR(J) - TOLYR(J)) / RINT
60      VELINT(J) = (V2LYR(J) - VLYR(J)) / RINT
        IF (JCDPNO .LE. NVAN) GO TO 100
        JDIFF = JCDPNO - NVAN
70      IF (JNTSW .EQ. 0) GO TO 100
80      DO 90 J = 1, NLYR
          TOLYR(J) = TOLYR(J) + TOINT(J)
90      VLYR(J) = VLYR(J) + VELINT(J)
        IF (JDIFF .LE. 1) GO TO 100
        JDIFF = JDIFF - 1
        GO TO 80
C
```

```
C      COMPUTE   (1/V**2) FOR USE IN T0**2 + X**2/(V**2)
C
100      CALL INVSQ(FSAMP, NSTART, NLYR, L, VINSQ)
C
C
110      JSUM = JSUM + 1
C
C     CHECK IF A MUTE IS NEEDED
C
         IF (MUT .NE. 1) MUTE(JCHAN) = 0
         CONST(11) = FLOAT((MUTE(JCHAN)*M) - 1)
C
C     IF SLANT STACK, FOLLOW ANOTHER PATH.
C
         IF (STACKO .EQ. 5) GO TO 120
         CONST(1) = XSQ(JCHAN)
C
C     COMPUTE INDEX ARRAY
C
         CALL APWR
C
C     TRANSFER CONTENTS OF ADDRESSES (K1,K11) TO HOST   ARRAY
C     DUM AND OVERWRITE THOSE LOCATIONS WITH CONST.
C
         CALL APGET(DUM, K1, K11, K2)
         CALL APWD
         CALL APPUT(CONST, K1, K11, K2)
         CALL APWD
C
C     TRANSFER T0SQ TO IB AND VINSQ TO IC1
C
         CALL APPUT(T0SQ, IB, IL, K2)
         CALL APWD
         CALL APPUT(VINSQ, IC1, IL, K2)
         CALL APWD
C
C     FORM IFIX(FSAMP*M*SQRT(T0SQ+XSQ(JCHAN)*VINSQ)+0.5)-NSTART*M
C
         CALL VSMUL(IC1, K1, K1, IC1, K1, IL)
         CALL APWR
         CALL VADD(IB, K1, IC1, K1, IB, K1, IL)
         CALL APWR
         CALL VSQRT(IB, K1, IB, K1, IL)
         CALL APWR
         CALL VSMSA(IB, K1, K2, K3, IB, K1, IL)
         CALL APWR
         CALL VINT(IB, K1, IB, K1, IL)
         CALL APWR
         CALL VSADD(IB, K1, K4, IB, K1, IL)
         CALL APWR
C
C        GO FOR CLIPPING
C
         GO TO 130
C
C        SLANT STACK
C
120      CONST(1) = P * XSQ(JCHAN)
```

174

```
        CALL APWR

C
C       TRANSFER K1-K11 TO DUM AND REPLACE WITH CONST.
C
        CALL APGET(DUM, K1, K11, K2)
        CALL APWD
        CALL APPUT(CONST, K1, K11, K2)
        CALL APWD

C
C       TRANSFER T0SQ (IN FACT T0) TO IB
C
        CALL APPUT(T0SQ, IB, IL, K2)
        CALL APWD

C
C       FORM IFIX(FSAMP*M(T0+P*X)+.5)-M*NSTART
C
        CALL VSADD(IB, K1, K1, IB, K1, IL)
        CALL APWR
        CALL VSMSA(IB, K1, K2, K3, IB, K1, IL)
        CALL APWR
        CALL VINT(IB, K1, IB, K1, IL)
        CALL APWR
        CALL VSADD(IB, K1, K4, IB, K1, IL)
        CALL APWR

C
C       NOW CLIP THE RESULT.
C
130     CALL VCLIP(IB, K1, K5, K6, IB, K1, IL)
        CALL APWR

C
C       CHECK FOR MUTED SAMPLES
C
        CALL LVGT(IB, K1, K11, K0, IC, K1, IL)
        CALL APWR
        CALL VFIX(IC, K1, IC, K1, IL)
        CALL APWR
        CALL APGET(MSTOR, IC, IL, K1)
        CALL APWD

C
C       UPDATE MCHAN
C
        DO 140 J = 1, L
140     MCHAN(J) = MCHAN(J) + MSTOR(J)
C
        CALL VSMSA(IB, K1, K7, K8, IC1, K1, IL)
        CALL APWR
        CALL VSMUL(IB, K1, K9, IB, K1, IL)
        CALL APWR
        CALL VINT(IB, K1, IB, K1, IL)
        CALL APWR
        CALL VSMUL(IB, K1, K10, IB, K1, IL)
        CALL APWR
        CALL VSUB(IB, K1, IC1, K1, IB, K1, IL)
        CALL APWR
        CALL VFIX(IB, K1, IB, K1, IL)
        CALL APWR

C
        CALL APGET(IONS, IB, IL, K1)
```

```
        CALL APWD
        DO 150 J = 1, L
          INDEX(J) = IONS(J)
150     CONTINUE

C
C     TRANSFER DUM BACK TO Kl
C
        CALL APPUT(DUM, Kl, K11, K2)
        CALL APWD

C
C     HAVING COMPUTED THE INDEX ARRAY, PREPARE FOR INTERPOLATION NOW.
C     CLEAR B IN AP.
C
        CALL VCLR(IB, Kl, IL2INT)
        CALL APWR

C
C     TRANSFER TRACE TO B
C
        CALL APPUT(SEISM, IB, IL, K2)
        CALL APWD

C
C     FIND TRACE MEAN AND STORE IT IN ITOP
C
        CALL MEANV(IB, Kl, ITOP, IL)

C
C     SUBTRACT MEAN FROM TRACE
C
        CALL VNEG(ITOP, Kl, ITOP, Kl, Kl)
        CALL VSADD(IB, Kl, ITOP, IB, Kl, IL)

C
C     SCALE THE TRACE
C
        IF (JINDEN .LT. 0) GO TO 160
        CALL SVESQ(IB, Kl, ITOP, IL)
        IF (JINDEN .EQ. 0) CALL VSQRT(ITOP, Kl, ITOP, Kl, Kl)
        CALL VDIV(ITOP, K0, IB, Kl, IB, Kl, IL)
160     CONTINUE

C
C     MUTE THE TRACE IF REQUIRED
C
        IF (MUT .NE. 1) GO TO 170
        IMUTE = MUTE(JCHAN)
        CALL VCLR(IB, Kl, IMUTE)
        CALL APWR

C
C     TRANSFER MODIFIED TRACE BACK TO SEISM
C
170     LP = 1
        CALL APGET(SEISM(LP), IB, IL, K2)
        CALL APWD

C
C     INTERPOLATE NOW IF NECESSARY
C
        IF (M .EQ. 1) GO TO 190

C
C     TAKE THE FOURIER TRANSFORM OF THE TRACE AND PUT IT IN C
C
        CALL RFFTB(IB, IC, IL2INT, Kl)
```

176

```
              CALL RFFTSC(IC, IL2INT, K0, K1)
              CALL VCLR(IC, K1, K2)
              CALL APWR
C
C     ITERATE FROM 2 TO M
C
              DO 180 J = 2, M
C
C     MULTIPLY TRANSFORM BY COMPLEX EXPONENTIAL ARRAY
C
                  CALL CVMUL(IC2, K2, ID1, K2, IC2, K2, IL2I21, K1)
                  CALL APWR
C
C     MOVE C TO B AND TAKE THE IN PLACE TRANSFORM
C
                  CALL VMOV(IC, K1, IB, K1, IL2INT)
                  CALL APWR
                  CALL RFFT(IB, IL2INT, KIM)
C
C     TRANSFER SHIFTED TRACE BACK TO SEISM
C
                  LP = LP + L
                  CALL APWR
                  CALL APGET(SEISM(LP), IB, IL, K2)
                  CALL APWD
  180         CONTINUE
C
C     SORT OUT CORRECT SAMPLES FROM SEISM AND STORE THEM IN STACK
C
  190         DO 200 JJ = 1, L
                  IND = INDEX(JJ)
                  STACK(JJ) = SEISM(IND)
  200         CONTINUE
              WRITE (6,210)
  210         FORMAT (10X, '***STACK RETRIEVED', //)
C
C     IF A STRAIGHT OR SLANT STACK IS DESIRED, ADD THE NMO CORRECTED
C TRACE
C     TO THE ACCUMULATING ARRAY. IF NOT, STORE IT AS THE NEXT COLUMN
C     OF THE NOTIONAL MATRIX 'GATHER'.
C
              IF (STACKO .EQ. 1 .OR. STACKO .EQ. 5) GO TO 230
              DO 220 JI = 1, L
                  GATHER(JI,JCHAN) = STACK(JI)
  220         CONTINUE
              GO TO 240
C
C     TRANSFER STACK INTO B1 AND ADD STACK TO A
C
  230         CONTINUE
              CALL APWR
              CALL APPUT(STACK, IB, IL, K2)
              CALL APWD
              CALL VADD(IA, K1, IB, K1, IA, K1, IL)
              CALL APWR
C
C     END OF FILE LOOP
C
```

177

```
240   CONTINUE
      DO 250 J = 1, L
        IF (MCHAN(J) .EQ. 0) MCHAN(J) = 1
        CHAN(J) = MCHAN(J)
250   CONTINUE

C
C
C     CHOOSE A STACK OR NORMALIZE THE STRAIGHT OR SLANT STACK.
C
C     GO TO (260, 280, 290, 320, 260), STACKO
C
C
260   IF (JSUM .EQ. 0) GO TO 270
C
      CALL APWR
      CALL APPUT(CHAN, IB, IL, K2)
      CALL APWD
      CALL VDIV(IB, K1, K0, K1, K0, K1, IL)
C
C     TRANSFER SCALED STACK BACK TO STACK
C
270   CALL APWR
      CALL APGET(STACK, IA, IL, K2)
      CALL APWD
      GO TO 330
C
C     ITERATIVE STACK
C
280   CALL SUPER(L, NCHAN, GATHER, R, CHAN)
      GO TO 330
C
C     OPTIMUM WEIGHT STACK.
C
290   CALL OPTWGT(L, NCHAN, GATHER, W)
C
      DO 300 K = 1, L
        R(K) = 0.0
        DO 300 J = 1, NCHAN
300   R(K) = R(K) + GATHER(K,J)
C
      IF (NCHAN .GE. 3) GO TO 330
      CALL APPUT(R, IA, IL, K2)
      CALL APWD
      IF (JSUM .EQ. 0) GO TO 310
      CALL APWR

      CALL APPUT(CHAN, IB, IL, K2)
      CALL APWD
      CALL VDIV(IB, K1, K0, K1, K0, K1, IL)
310   CALL APWR

      CALL APGET(STACK, IA, IL, K2)
      CALL APWD
      GO TO 330
C
C     OPTIMUM WEIGHTED SUPER STACK.
C
320   CALL OPTWGT(L, NCHAN, GATHER, W)
      CALL SUPER(L, NCHAN, GATHER, R, CHAN)
```

178

```fortran
C
C        WRITE A 4*L BYTE STACKED TRACE
C
 330     CONTINUE
         ILEN = 4 * L + 240
         CALL WRITE(SIG, ILEN, 0, LNUM, 8, &360)
C
C
         IF (MOD(JFIL,10) .EQ. 0) WRITE (6,340) JFIL
 340     FORMAT (10X, '***', I5, ' FILES HAVE BEEN PROCESSED')
C
C     STACK THE NEXT FILE.
C
 350 CONTINUE
C
C     PROCESSING FINISHED!
C
      GO TO 380
 360 WRITE (6,370)
 370 FORMAT (10X, '***END OF TAPE ENCOUNTERED! --STOP!', /)
C
C
 380 RETURN
     END
C
C
C
     SUBROUTINE INVSQ(FSAMP, NSTART, NLYR, L, VINSQ)
C
C     SUBROUTINE TO GENERATE INVERSE SQUARES OF STACKING VELOCITY
C
     DIMENSION VINSQ(2048)
     COMMON /LAYER/ TOLYR(99), VLYR(99)
C
     N1 = 1
     N2 = IFIX(FSAMP*TOLYR(1)) - NSTART
     VINSQ1 = 1.0 / VLYR(1) ** 2
     DO 10 I = N1, N2
       VINSQ(I) = VINSQ1
 10  CONTINUE
C
     IF (NLYR .EQ. 1) GO TO 40
     DO 30 J = 2, NLYR
       N1 = N2 + 1
       N2 = IFIX(FSAMP*TOLYR(J)) - NSTART
       DELV = (VLYR(J) - VLYR(J - 1)) / (N2 - N1 + 2)
       V = VLYR(J - 1)
       DO 20 I = N1, N2
         VINSQ(I) = 1.0 / V ** 2
         V = V + DELV
 20    CONTINUE
 30  CONTINUE
 40  N1 = N2 + 1
     N2 = L
     VINSQN = 1.0 / VLYR(NLYR) ** 2
     DO 50 I = N1, N2
       VINSQ(I) = VINSQN
 50  CONTINUE
```

```fortran
C
      RETURN
      END
C
C
C
      SUBROUTINE SUPER(LSAMP, M, X, R, CHAN)
C
C     THIS SUBROUTINE PERFORMS THE ITERATIVE STACKING
C     ALGORITHM (NAESS, 1979).
C     M1=NUMBER OF + AMPLITUDES AT GIVEN TIME-POINT.
C     N1=NUMBER OF - AMPLITUDES AT GIVEN TIME-POINT.
C     THEY MAY BE USED FOR NORMALISATION INSTEAD OF
C     (CHAN(I)*FAC).
C
      COMMON /VALUES/ DUM(4121), STACKO, ITERAT, ITYPE, FAC, P
      DIMENSION X(LSAMP,M), CHAN(1), R(2048)
      INTEGER*2 ILEN
      INTEGER STACKO
C
C
C
      K = 0
   10 CONTINUE
C
      K = K + 1
      IF (K .GT. ITERAT) GO TO 100
C
      DO 90 I = 1, LSAMP
        M1 = 0
        N1 = 0
        SP = 0.0
        SM = 0.0
C
C   GET SP AND SM
C
        DO 40 J = 1, M
          IF (X(I,J) .GT. 0.0) GO TO 30
          IF (X(I,J) .EQ. 0) GO TO 20
          N1 = N1 + 1
   20     SM = SM + X(I,J)
          GO TO 40
   30     M1 = M1 + 1
          SP = SP + X(I,J)
   40   CONTINUE
        IF (ITYPE .LT. 0) GO TO 50
        CHAMY = FAC * CHAN(I)
        CHAPY = FAC * CHAN(I)
        GO TO 60
   50   CHAMY = FLOAT(M1)
        CHAPY = FLOAT(N1)
   60   CONTINUE
        SM = SM / CHAMY
        SP = SP / CHAPY
C
C   GET NEW VALUES OF X(I,J)
C
        DO 80 I1 = 1, M
```

180

```
           IF (X(I,I1) .GT. 0.0) GO TO 70
           IF (ABS(X(I,I1)) .GT. ABS(SM)) X(I,I1) = SM
           GO TO 80
 70        IF (X(I,I1) .GT. SP) X(I,I1) = SP
 80     CONTINUE
        IF (K .NE. ITERAT) GO TO 90
        R(I) = SP + SM
 90 CONTINUE
     GO TO 10
C
C    END OF STACK
C
100 CONTINUE
C
C    EXIT
C
     RETURN
     END
C
C
C
     SUBROUTINE OPTWGT(N, M, SS, W)
C
C    COMPUTES THE OPTIMUM, CONSTANT ENERGY, OR DIVERSITY
C    STACKING WEIGHTS FOR AN NMO-CORRECTED GATHER STORED
C    IN SS(N,M). M IS THE NUMBER OF CHANNELS AND IS GREATER
C    OR EQUAL TO 3 AND LESS OR EQUAL TO 24. (SEE RIETSCH, 1980).
C
     DIMENSION SS(N,M), S(2048,24), W(M), Y(500), X(500)
     DIMENSION W1(48), WIN(48), DDOT(48), WIM(48), E(48)
     DIMENSION A(48), NOISE(48), R(48), SVB(1024), SIGVB(1024)
C
     COMMON /OPT/ KSTART, KSTOP, KST, KEN, NFLAG
     REAL*4 NOISE
C
C
C
     IF (M .LT. 3) WRITE (17,10)
 10 FORMAT (10X, '***THE NUMBER OF CHANNELS IS LESS THAN 3', //)
     IF (M .LT. 3) RETURN
C
C    CLEAR THE WORKING ARRAYS AND GET THE LENGTH OF THE WINDOW.
C
     CALL ZERO(500, X)
     CALL ZERO(500, Y)
     IV = KSTOP - KSTART + 1
     WRITE (17,*) IV, KSTART, KSTOP, INDIC, KST, KEN, NFLAG
C
C
C
     DO 20 J = 1, M
       DO 20 I = 1, IV
         S(I,J) = SS(KSTART + I - 1,J)
 20 CONTINUE
C
C    DO THE CONSTANT ENERGY OR DIVERSITY STACK
C
     IF (NFLAG .NE. 0) GO TO 180
```

```
C
C      CALCULATION OF SIGNAL SCALES
C
       MM = M - 1
       P1 = 1.0
       DO 40 I = 1, MM
         JP = I + 1
         DO 40 J = JP, M
           DO 30 L = 1, IV
             X(L) = S(L,I)
30         Y(L) = S(L,J)
           CALL DOT(IV, X, Y, P1P)
           P1 = P1 * ABS(P1P)
40 CONTINUE
C
       PD = P1 ** (1.0/FLOAT((M - 2)*(M - 1)))
C
       DO 70 J1 = 1, M
         P2 = 1.0
         DO 60 J2 = 1, M
           IF (J1 .EQ. J2) GO TO 60
           DO 50 L = 1, IV
             X(L) = S(L,J1)
50         Y(L) = S(L,J2)
           CALL DOT(IV, X, Y, P2P)
           CALL ZERO(500, X)
           CALL ZERO(500, Y)
           P2 = P2 * ABS(P2P)
C
60     CONTINUE
C
       PN = P2 ** (1.0/FLOAT(M - 2))
C
       A(J1) = PN / PD
C
70 CONTINUE
C
C      GET A TRACE SEGMENT
C
       KKEN = KEN
       KKST = KST
       IT = KKEN - KKST + 1
C
C
C
       CONTINUE
C
       DO 80 J = 1, M
         DO 80 I = 1, IT
80 S(I,J) = SS(KKST + I - 1,J) / A(J)
C
C      COMPUTE THE ENERGY IN EACH CHANNEL
C
       DO 100 J = 1, M
         DO 90 L = 1, IT
90     X(L) = S(L,J)
       CALL SIG(IT, X, E(J))
       CALL ZERO(500, X)
```

```
100 CONTINUE
C
C
C

      U = 0.0
      SQB = 0.0
      SIGMA = 0.0
      DO 110 J = 1, M
        W1(J) = 1.0 / E(J)
        IF (W1(J) .EQ. .5) W1(J) = W1(J) - 1.
        WIN(J) = W1(J) / (1.0 - 2.0*W1(J))
        U = U + WIN(J)
        SQB = SQB + W1(J) * E(J)
        SIGMA = SIGMA + WIN(J) * E(J)
        WIM(J) = 1.0 / (1.0 - 2.0*W1(J))
110 CONTINUE
C
C   COMPUTE   ,      . THE VECTORS SIGMA AND S
C
      DO 130 I = 1, IT
        SIGVB(I) = 0.0
        SVB(I) = 0.0
        DO 120 J = 1, M
          SVB(I) = SVB(I) + W1(J) * S(I,J)
          SIGVB(I) = SIGVB(I) + WIN(J) * S(I,J)
120     CONTINUE
130 CONTINUE
C
C   GET BETA.
C
      CALL DOT(IT, SVB, SIGVB, PDP)
      PDP = 2.0 * PDP
      BETA = (SQB - SIGMA + PDP) / (1.0 + U)
C
C   GET THE NOISE VECTOR.
C
      DO 150 J = 1, M
        DO 140 L = 1, IT
140     X(L) = S(L,J)
        CALL DOT(IT, X, SVB, DDOT(J))
        DDOT(J) = 2.0 * DDOT(J)
        NOISE(J) = (E(J) - DDOT(J) + BETA) * WIM(J)
        CALL ZERO(500, X)
150 CONTINUE
C
C   GET THE S/N RATIO
C
      RS = 0.0
      DO 160 J = 1, M
        R(J) = (A(J)**2) * (1.) / NOISE(J)
        IF (R(J) .LT. 0.) GO TO 160
        RS = RS + R(J)
160 CONTINUE
C
C   GET THE WEIGHTS (EQUATION 15 -APPENDIX A)
C
      DO 170 J = 1, M
170 W(J) = R(J) / (A(J)*RS)
```

183

```fortran
C
C      APPLY THE WEIGHTS.
C
       GO TO 210
C
C      CONSTANT ENERGY OR DIVERSITY STACKING.
C
  180 DO 200 J = 1, M
       DO 190 L = 1, IV
  190    X(L) = S(L,J)
         CALL SIG(IV, X, E(J))
         CALL ZERO(500, X)
         IF (NFLAG .EQ. 1) W(J) = 1. / SQRT(E(J))
  200 IF (NFLAG .EQ. 2) W(J) = 1. / (E(J)*E(J))
C
C      APPLY THE WEIGHTS NOW.
C
  210 DO 230 J = 1, M
       IF (J .EQ. 1) WRITE (17,220)
  220    FORMAT (10X, 'APPLYING WEIGHTS TO GATHER ', /)
         FC = W(J)
         IF (W(J) .LT. 0.) FC = 0.
         DO 230 I = 1, IT
           SS(KKST + I - 1,J) = FC * S(I,J)
  230 CONTINUE
C
C      LOG.
C
  240 WRITE (17,250) (E(I),A(I),NOISE(I),R(I),W(I),I=1,M)
      WRITE (17,260) RS
  250 FORMAT (1X, 5(1X,F12.6,1X), /)
  260 FORMAT (/, 10X, '***THE OPTIMUM S/N OF THE DATA WINDOW IS', F12.6,
     1        //)
C
C      EXIT
C
      RETURN
      END
```

```
C**********************************************************
C          PROGRAM YIBEA3
C          ────────────────
C
C
C          YIBEA3 IS USED FOR STUDIES OF NORMAL INCIDENCE
C       RESPONSES OF A FEW MODELS WRT DEREVERBERATION PROBLEMS
C
C**********************************************************
C
C
C                 DATAFILE    (UNIT 5)
C                 ─────────────
C
C       *         N,K,NWL,DELTA,SAMPR,(ANOM(I),I=1,K)
C                 (3I4,F5.2,F5.0,/,(10A4))
C       *         (VEL(I),I=1,N+1)
C                 (8F6.0)
C       *         (DEN(I),I=1,N+1)
C                 (10F5.2)
C       *         (DIP(I),I=1,N)
C                 (8F6.0)
C       *         (THICK(I),I=1,N)
C                 (8F6.0)
C       *         FLAP0,FLAP1                   )       ALL THESE LINES
C       *         LENWAV   (IF FLAP0=1 )        )          ARE
C       *         FLAG0                         )          IN
C       *         NSAMP,JSAMP,LHWIN,LSAMPS,LAUT )       FREE-FORMAT.
C       *         C0,C1,C2,JIF1,JIF2            )
C       *         AGC,FSPK0
C
C                 UNIT 13
C                 ────────
C
C       LENWAV SAMPLES OF THE WAVELET IN FREE-FORMAT.
C                (REQUIRED IF FLAP0=1)
C
C                 OUTPUT FILES
C                 ─────────────
C
C       UNIT 15 - SEISMIC TRACES (UNFORMATTED)
C       UNIT 16 - AUTOCORRELOGRAMS (UNFORMATTED)
C
C       ──────────────────────────────────────────────────
C
C       N = number of layers.
C       K = number of normal incidence shots to generate.
C       NVEL = 1 (always set NVEL = 1 to avoid convolution within
C                   the subprogram MODEL)
C       DELTA = interval between shots in KM.
C       SAMPR = sampling rate in hertz (1/(DEL(t)) DEL(t)=sampling
C                   interval.
C       (ANOM(I),I=1,K) = names of the K shots to be calculated.
C       (VEL(I),I=1,N+1) = p-wave velocities up to layer N+1.
C       (DEN(I),I=1,N+1) = layer densities up to layer N+1.
C       (DIP(I),I=1,N)    = dips of the interfaces up to layer N.
C       FLAP0  = flag to indicate if the impulse response is to
C                   be convolved with a wavelet. If YES, FLAP0=1.
C
C       FLAP1 = flag to indicate if the result of the convolution
C                   is to be advanced for correction of a delay as is
C                   the case if the wavelet is a symmetrical
C                   bandpassed waveform.
C                   If yes, FLAP1=1. The result of the
```

185

```
C                        convolution is shifted by LENWAV/2 samples.
C            LENWAV = number of samples of wavelet to be read from
C                     unit   13. Inserted only when FLAP0=1 .
C            FLAG0 = flag to indicate if an AGC is to be applied to
C                     the final result. If yes, FLAG0=1 .
C            NSAMP = number of samples of the trace to be written on
C                     unit  5 .
C            JSAMP = sampling interval in milliseconds.
C            LHWIN = length of half-window for AGC (may be dummy if
C                     FLAG0 is not unity.
C            LSAMPS = number of samples to autocorrelate (starting
C                     from the-first sample).
C            LAUT   = number of LAGS of the autocorrelation to be
C                     computed starting from the zero LAG.
C            C0     = reflection coefficient of surface interface.
C            C1     = reflection coefficient of the seabed.
C            C2     = reflection coefficient of deeper interface.
C            JIF1   = two-way time in water layer.
C            JIF2   = two-way time between the seabed and the strongly
C                     reflecting interface.
C            AGC    = annotation flag. AGC=1 if FLAG0=1 .
C            FSPK0  = annotation flag. FSPK0=1 if FLAP0=1 .
C
C            LIBRARIES REQUIRED.
C            ──────────────────
C
C            1. GPT9:MTHSIMLIB (AP SIMULATION PACKAGE)
C            2. *GHOST
C            3. FLOBYA (PERSONAL SUBROUTINE LIBRARY)
C
C            RUNNING YIBEA3 ON MTS.
C            ─────────────────────
C
C            $RUN *FTNX SCARDS=YIBEA3
C            $R -LOAD+FLOBYA+GPT9:MTHSIMLIB+*GHOST 5=DATAFILE
C                13=WAVELET 15=-A 16=-B 9=PLOTFILE
C
C            BY  F.  JIFON  (DECEMBER, 1982)
C
C ******************************************************************
C
C
      INTEGER FLAG0, FLAP0, FLAP1
C
C     COMMON BLOCKS
C
      INTEGER*2 ILEN
      COMMON /MASTER/ D(2048)
      COMMON /MOD1/ ANS(2048), AUT(2048)
      COMMON /MOD2/ C0, C1, C2, JIF1, JIF2
      COMMON /GEN/ L(2), NSAMP, JSAMP, KK(15)
      COMMON /EIGHT/ LHWIN
C
      REAL WL(100), FTT(256), EQ(2048), S(2048)
      EQUIVALENCE (D(1),EQ(1))
      DIMENSION RS(2048), RC(2048), SEIS(2048)
C
C
```

186

```
C
      CALL ZERO(2048, SEIS)
      CALL ZERO(2048, EQ)
      CALL ZERO(2048, AUT)
      M = 1024
      CALL IMPULS(256, FIT, 1)
C
C*******GENERATE THE IMPULSE RESPONSE AND ZERO INITIAL IMPULSE
C
      CALL MODEL(RC, RS)
      RS(1) = 0.0
C
C******READ IN DATA NOW AND SAVE RS
C
      READ (5,*) FLAP0, FLAP1
      IF (FLAP0 .EQ. 1) READ (5,*) LENWAV
      IF (FLAP0 .EQ. 1) GO TO 20
      DO 10 J = 1, 1024
         S(J) = RS(J)
   10 CONTINUE
   20 CONTINUE
      READ (5,*) FLAG0
      READ (5,*) NSAMP, JSAMP, LHWIN, LSAMPS, LAUT
      READ (5,*) C0, C1, C2, JIF1, JIF2
C
C*******IF CONVOLUTION IS TO BE DONE , READ WAVELET FROM UNIT 13
C
      IF (FLAP0 .NE. 1) GO TO 60
C
C
C
      READ (13,*) (WL(K),K=1,LENWAV)
C
C*******DO THE CONVOLUTION
C
      CALL CONVOL(LENWAV, WL, M, RS, LS, SEIS)
C
C*******IS TIME SHIFT NEEDED?
C
      IF (FLAP1 .NE. 1) GO TO 40
      LAND = LENWAV / 2
      LS = LS - LAND
      DO 30 J = 1, LS
         S(J) = SEIS(J + LAND)
   30 CONTINUE
      GO TO 60
   40 DO 50 J = 1, LS
         S(J) = SEIS(J)
   50 CONTINUE
   60 CONTINUE
      LS = 1024
C
C*******AUTOCORRELATE NOW
C
      CALL AUTOCR(S, LSAMPS, 500, AUT)
C
C
C
```

```fortran
      DO 70 J = 1, LS
   70 D(J) = S(J)
C
C
      IF (FLAG0 .NE. 1) GO TO 90
      CALL AGCDET
      WRITE (6,80)
   80 FORMAT (10X, '***AGC HAS BEEN APPLIED', /)
   90 CONTINUE
C
C*******WRITE OUT TRACE AND AUTOCORRELATION
C
      ILEN = 4 * LSAMPS
      CALL WRITE(EQ, ILEN, 0, LNUM, 15)
      ILEN = 4 * LAUT
      CALL WRITE(AUT, ILEN, 0, LNUM, 16)
C
C*******DECONVOLUTION
C
      FIT(JIF1) = C0 * C1
      FIT(JIF2) = C2 * C1
      FIT(JIF1 + JIF2) = C0 * C2
      CALL CONVOL(256, FIT, LS, S, LANS, ANS)
      CALL AUTOCR(ANS, LSAMPS, 500, AUT)
C
      DO 100 J = 1, LS
  100 D(J) = ANS(J)
C
C
      IF (FLAG0 .NE. 1) GO TO 110
      CALL AGCDET
  110 CONTINUE
C
C*******WRITE OUT DECONVOLVED TRACE AND ITS AUTOCORRELATION
C
      ILEN = 4 * LSAMPS
      CALL WRITE(EQ, ILEN, 0, LNUM, 15)
      ILEN = 4 * LAUT
      CALL WRITE(AUT, ILEN, 0, LNUM, 16)
C
C*******PLOTTING
C
      REWIND 15
      REWIND 16
      CALL MODPLT(LSAMPS, LAUT)
C
C*******END OF PROGRAM
C
      STOP
      END
C
C
      SUBROUTINE MODPLT(LX0, LAUT)
C
C   SUBROUTINE TO PLOT RESULTS OF DETERMINISTIC FILTERING
C
      INTEGER*2 ILEN
      DIMENSION X(1024), DPOS(1024)
```

188

```
      INTEGER AGC, FLAPO
C
      CALL ZERO(1024, X)
C
C** INITIALIZE PLOT
C
      DO 10 J = 1, 1000
         DPOS(J) = J
   10 CONTINUE
C
C** READ IN THE ANNOTATION FLAGS.
C
      READ (5,*) AGC, FSPKO
   20 FORMAT (4I4)
C
C**C
C
      CALL PAPER(1)
      CALL PSPACE(0.0, 1.0, 0.0, 1.08)
      CALL BOX(0.0, 0.61, 0.04, 1.06)
      CALL POSITN(0.02, 1.055)
      CALL JOIN(0.36, 1.055)
C
C** DRAW THE TIME GRID
C
      T = 0.0
      YINC = (1.055 - 0.045) / 10.0
      YPOS = 1.055
      DO 30 J = 1, 10
         YPOS = YPOS - YINC
         T = T + .1
         YPOSI = YPOS + 0.005
         CALL CTRMAG(10)
         CALL PLOTNF(0.036, YPOSI, T, 1)
         CALL POSITN(0.02, YPOS)
         CALL JOIN(0.36, YPOS)
   30 CONTINUE
C
C** LABEL THE TIME AXIS
C
      CALL CTRORI(1.0)
      CALL PLOTCS(0.012, 0.45, 'TWO-WAY TRAVEL TIME IN S', 24)
      CALL CTRORI(0.0)
C
C
      DX = 0.08
      CALL CTRSET(6)
      CALL CTRMAG(40)
      CALL PLOTCS(0.38, 0.95, 'FIG', 3)
      IF (AGC .NE. 1) GO TO 40
      CALL CTRSET(5)
      CALL PLOTCS(0.38, 0.40, 'AGC ON', 6)
      CALL PLOTCS(0.40, 0.30, 'A/ AND ', 7)
      CALL PLOTCS(0.40, 0.20, 'C/', 2)
   40 CONTINUE
      CALL CTRMAG(10)
      CALL CTRSET(5)
      IF (FSPKO .EQ. 1) GO TO 50
```

189

```
      CALL PLOTCS(.38, .85, 'A/ SYNTHETIC TRACE', 18)
      GO TO 60
 50 CALL PLOTCS(0.38, 0.85, 'A/ IMPULSE RESPONSE (I.R.)', 26)
 60 CONTINUE


      CALL PLOTCS(0.39, 0.80, '(TRANSFER MATRIX SOLUTION)', 26)
      CALL PLOTCS(0.38, 0.75, 'B/ AUTOCORRELATION OF', 21)
      CALL PLOTCS(0.40, 0.70, ' A/', 3)

      IF (FSPK0 .EQ. 1) GO TO 70
      CALL PLOTCS(0.38, 0.65, 'C/ FILTERED TRACE', 17)
      GO TO 80
 70 CALL PLOTCS(.38, .65, 'C/ FILTERED I.R.', 16)
 80 CONTINUE


      CALL PLOTCS(0.40, 0.60, '(FOUR-POINT FILTER)', 19)
      CALL PLOTCS(0.38, 0.55, 'D/ AUTOCORRELATION OF', 21)
      CALL PLOTCS(0.40, 0.50, ' C/', 3)

      X3 = 0.13
      DO 140 K = 1, 4
        GO TO (90, 100, 110, 120), K
 90     CALL PLOTCS(X3, 1.0, 'A', 1)
        GO TO 130
.00     CALL PLOTCS(X3, 1.0, 'B', 1)
        GO TO 130
110     CALL PLOTCS(X3, 1.0, 'C', 1)
        GO TO 130
120     CALL PLOTCS(X3, 1.0, 'D', 1)
130     X3 = X3 + DX
140 CONTINUE
      X1 = 0.06
      X2 = 0.13
      CALL MAP(-100.0, 100.0, 1000.0, 1.0)
      DO 220 K = 1, 4


      IF (K .EQ. 2 .OR. K .EQ. 4) GO TO 150
      LX = LX0
      ILEN = 4 * LX
      CALL READ(X, ILEN, 0, LNUM, 15)
      GO TO 170
150     LX = LAUT
      ILEN = 4 * LX
      CALL READ(X, ILEN, 0, LNUM, 16)
160     FORMAT (8(1X,F15.6,1X))
170     CONTINUE
      CALL MAXT(LX, X, M, XMAX)

      DO 180 J = 1, LX
        X(J) = (X(J)*90.0) / XMAX
180     CONTINUE
      CALL PSPACE(X1, X2, 0.045, 1.055)

      IF (FSPK0 .NE. 1) GO TO 200
      DO 190 J = 1, LX
```

```
          CALL POSITN(0.0, DPOS(J))
190   CALL JOIN(X(J), DPOS(J))
      GO TO 210
200   CALL PTPLOT(X, DPOS, 1, LX, -5)
210   CALL POSITN(0.0, 1000.0)
      CALL JOIN(0.0, 1.0)
      X1 = X1 + DX
      X2 = X2 + DX
      CALL ZERO(1024, X)
220 CONTINUE

      CALL PSPACE(0.0, 1.0, 0.0, 1.08)
      CALL GREND

      STOP
      END
```

```
******************************************************
                PROGRAM SECTPLOT
                _____


        SECTION PLOTTING PROGRAM


            INPUT   (UNIT 5)
            _____

                LENG,LAUT,NCDPS,LUNIT,IFLAP,DX,SCALE,ITL,DT
                INDIC,LUX

        LENG = number of samples per trace.
        LAUT = length (in samples) of the trace to be plotted.
       NCDPS = number of traces to be plotted.
       LUNIT = logical unit number of the device on which
               the seismic data are stored in trace mode.
       IFLAP = annotation flag  (IFLAP.GE.1.AND.LE.11) TRY 1
          DX = sets the number of traces per cm of the
               horizontal (X) axis. (try 20.0 to 40.0)
       SCALE = amplitude scale relative to 100.0 .
         ITL = 0 if a baseline is desired for each trace.
          DT = sampling interval in sec.
       INDIC = 1 if the input file has got STD SEGY header blocks.
         LUX = scratchfile on which the header blocks may be
               written.

     ********SUPPLY UNIT 9 FOR THE PLOT.***********
             ____

   NB.
       **THE PROGRAM ASSUMES THAT THE DATA ARE SAMPLED AT 1000HZ***


       BY  F. JIFON    ( MARCH 1984)

******************************************************

     READ (5,*) LENG, LAUT, NCDPS, LUNIT, IFLAP, DX, SCALE, ITL, DT
     READ (5,*) INDIC, LUX

     IF (INDIC .EQ. 1) CALL HEDA(LUNIT, LUX)

     CALL PLOTAD(LENG, LAUT, NCDPS, LUNIT, IFLAP, DX, SCALE, ITL, DT)


     STOP
     END




     SUBROUTINE PLOTAD(LENG, LAUT, NCDPS, LUNIT, IFLAP, DX, SCALE,
    1           ITL, DT)

     SUBROUTINE   TO GENERATE THE PLOT FILE

     INTEGER*2 ILEN, LEN
     DIMENSION AUT(2200), TRACEA(2260), DPOS(2200)
```

```
      EQUIVALENCE (TRACEA(61),AUT(1))

C     INITIALIZE THE  PLOT.
C
C     DO 10 J = 1, LAUT
        DPOS(J)  = J
10    CONTINUE
C
C
      CALL PAPER(1)
      CALL PSPACE(0.0, 4.0, 0.04, 1.06)
      CALL CSPACE(0.0, 4.0, 0.04, 1.06)
C
C
      X1 = 0.04
      X2 = 0.34
      DX0 = 0.001 * DX
C
C     PLOT THE  TRACES
C
      DO 40 J = 1, NCDPS
        ILEN = 4 * LENG + 240
        CALL READ(TRACEA, ILEN, 0, LNUM, LUNIT)
C
        AMAX = 0.1E+02
C
        DO 20 K = 1, LAUT
          AUT(K) = (AUT(K)*SCALE) / (AMAX)
20        CONTINUE
C
        CALL PSPACE(X1, X2, 0.045, 1.035)
        CALL MAP(-100.0, 100.0, FLOAT(LAUT), 1.0)
        CALL PTPLOT(AUT, DPOS, 1, LAUT, -5)
        IF (ITL .NE. 0) GO TO 30
        CALL POSITN(0.0, FLOAT(LAUT))
        CALL JOIN(0.0, 1.0)
30      CONTINUE
        CALL CTRMAG(10)
        CALL PLOTCS(X1 + 0.04, 1.035, '+', 1)
        X1 = X1 + DX0
        X2 = X2 + DX0
40    CONTINUE
C
      L = LAUT / 100
      T = 0.0
      YINC = (1.035 - 0.045) / L
      YPOS = 1.035
      X3 = X2 + 0.005
      CALL MAP(0.0, 4.0, 0.04, 1.06)
      CALL PSPACE(0.0, 4.0, 0.04, 1.06)
      CALL CTRMAG(20)
      CALL CTRORI(3.0)
C
C     ANNOTATION OF SECTION.
C
      GO TO (50, 60, 70, 80, 90, 100, 110, 120, 130, 140, 150), IFLAP
50    CALL PLOTCS(X3 + 0.02, 0.9, 'LINE        (CMP    -CMP    )', 27)
      GO TO 160
```

193

```
 60 CALL PLOTCS(X3 + 0.02, .9, 'AUTOCORRELOGRAM      ', 19)
    GO TO 160
 70 CALL PLOTCS(X3 + 0.02, .9, 'BACKUS FILTER. C =          =    ', 32)
    GO TO 160
 80 CALL PLOTCS(X3 + .02, .9, 'PREDICTIVE DECONVOLUTION.', 25)
    CALL CTRSET(2)
    CALL PLOTCS(X3 - .02, .9, 'LENGTH OF FILTER=   MS;GAP=   MS', 32)
    CALL PLOTCS(X3 - .06, .9, 'DESIGN WINDOW (        );LAMBDA=   ',
   1    35)
    GO TO 160
 90 CALL PLOTCS(X3 + .02, .9, 'FOUR-POINT FILTER.              ',
   1    33)
    CALL PLOTCS(X3 - .02, .9, 'C =      ; C =      ;   =   MS;   =   MS'
   1    , 38)
    GO TO 160
100 CALL PLOTCS(X3 + .02, .9, 'COMMON MID-POINT GATHER', 23)
    GO TO 160
110 CALL PLOTCS(X3 + .02, .9, 'HORIZONTAL STACK', 16)
    GO TO 160
120 CALL PLOTCS(X3 + .02, .9, 'ITERATIVE STACK', 15)
    GO TO 160
130 CALL PLOTCS(X3 + .02, .9, 'OPTIMUM WEIGHTED STACK', 22)
    GO TO 160
140 CALL PLOTCS(X3 + .02, .9, 'CONSTANT ENERGY STACK', 21)
    GO TO 160
150 CALL PLOTCS(X3 + .02, .9, '   DIVERSITY STACK', 18)
C
160 CALL CTRORI(0.0)
    CALL POSITN(0.02, 1.035)
    CALL JOIN(X3, 1.035)
    CALL CTRMAG(10)
C
C
    DO 170 J = 1, L
      YPOS = YPOS - YINC
      T = T + (FLOAT(LAUT)/10.) * DT
      YPOS1 = YPOS + 0.005
      CALL PLOTNF(0.036, YPOS1, T, 3)
      CALL POSITN(0.02, YPOS)
      CALL JOIN(X3 - .1, YPOS)
170 CONTINUE
C
    CALL CTRORI(1.0)
    CALL CTRSET(2)
    CALL PLOTCS(0.012, 0.44, 'TWO-WAY TRAVELTIME IN SECS', 26)
    CALL CTRORI(0.0)
C
    X4 = X3 + .040
    CALL PSPACE(.003, X4, .039, 1.061)
    CALL MAP(0., 1., 0., 1.)
    CALL BORDER
    CALL GREND
C
    RETURN
    END
C
C

    SUBROUTINE HEDA(NIN, NOUT)
```

```
C
C      TRANSFER HEADER BLOCKS
C
       IMPLICIT INTEGER*2(I)
       DIMENSION TPHEDA(800)
       INTEGER TPHEDB(100)
C
C      READ THE EBCDIC HEADER
C
       ILEN = 3200
       CALL READ(TPHEDA, ILEN, 0, LNUM, NIN)
C
C      READ BINARY HEADER
C
       ILEN = 400
       CALL READ(TPHEDB, ILEN, 0, LNUM, NIN)
C
C      WRITE EBCDIC HEADER
C
       ILEN = 3200
       CALL WRITE(TPHEDA, ILEN, 0, LNUM, NOUT)
C
C      WRITE BINARY HEADER
C
       ILEN = 400
       CALL WRITE(TPHEDB, ILEN, 0, LNUM, NOUT)
C
       RETURN
       END
```